Age-associated changes to calcium handling proteins across the whole heart

being a thesis submitted for the Degree of Doctor of Philosophy

in the University of Hull

by

Fiona Sara Hatch BSc (Hons)

December 2012

Abstract

Age is a major risk factor for the development of cardiac problems. The ageing process causes significant changes to cardiac structure and function. These are linked with the elderly heart's diminished ability to respond to cardiac demand and associated with the increased frequency of myocardial dysfunction and arrhythmias. A key factor involved in such problems is the regulation of intracellular calcium ions (Ca^{2+}) which is involved in contraction of the heart and the upstroke of the sinoatrial (SA) node pacemaker. Dysfunction in the regulation of intracellular Ca^{2+} increases the probability of an arrhythmogenic episode and would be indicative of progressive SA node, atrial and ventricular dysfunction.

The current study sought to investigate the effects of ageing on the expression of Ca^{2+} handling proteins. The ageing process was analysed in rats at 6 (young-adult), 12 (adult) and 24 months old (elderly). Heart samples were assessed by western blot, qPCR, immunocytochemistry and electrophysiology. The expression of L-type calcium channels ($Ca_v1.2$), ryanodine receptors (RYRs), sarcoendoplasmic reticulum ATPase (SERCA), phospholamban (PLB), sodium-calcium exchangers (NCX) and plasma membrane Ca^{2+} ATPase pumps (PMCA) were analysed in the SA node, right atrium, left atrium, left ventricle and right ventricle.

The effect of ageing of the SA node was assessed via recordings of intrinsic heart rate in response to isoprenaline, a β-adrenergic stimulator, and nifedipine. With age response to isoprenaline was diminished and SR Ca^{2+} cycling was established as crucial for pacemaker activity. Application of cylopiazonic acid profoundly reduced the response to isoprenaline in the younger age groups but had no effect in the elderly, elucidating the age-associated reduced role of SERCA2a. The decline in protein expression of SERCA2a, RYR2 and $Ca_v1.2$ supported dysfunctional spontaneous activity in the elderly SA node. In addition there was an age related increase in sensitivity to nifedipine which highlighted the importance of $Ca_v1.2$ channels and the compensatory up-regulation of NCX1.

Age-associated changes in the crista terminalis (CT) and right atrium (RA) muscle were investigated to determine whether the relationship between SA node dysfunction and age can be marked by alterations to surrounding tissue. With advancing age, CT tissue exhibited increased $Ca_v1.2$ and RYR2 expression and decreased SERCA2a expression. These are considered key components in generating arrhythmogenic episodes. The LA contained significantly higher levels of Ca^{2+} transport proteins compared with the RA. The combined increase of $Ca_v1.2$, RYR2 and SERCA2a activity in the LA, greatly augments SR Ca^{2+} content and the probability of SR 'leakage' leading

to an arrhythmia. In contrast the RA exhibited dramatic Ca^{2+} remodelling with decreased expression of all Ca^{2+} handling proteins.

The expression of Ca^{2+} handling proteins were assessed in the left ventricle (LV) and right ventricle (RV); the former was further distinguished into the LV endocardium and epicardium. SERCA2a activity was significantly lower in the RV compared with the LV. Within the elderly age group RYR2, SERCA2a, PMCA4a all decreased in expression, whist NCX1 had elevated levels in the LV and RV. The changes in the LV were further investigated across the myocardial wall and found RYR2, $Ca_V1.2$ and NCX1 PLB to be elevated in the young endocardium. Heterogeneity varied with age; SERCA2a activity and RYR2 protein was increased in the endocardium, but overall disparity across the myocardium was reduced. This emphasised the effect of ageing across the LV wall which may contribute to the endocardium's increased susceptibility to arrhythmias.

Overall this study reported age-associated changes to the expression of Ca^{2+} handling proteins which will alter the Ca^{2+} transient and AP propagation in the ventricles, atria and spontaneous activity in the SA node. Although these changes may be adaptive mechanisms to maintain contractile function, increased SR Ca^{2+} content or inadequate Ca^{2+} removal would predispose to arrhythmias. Therefore, although ageing is not considered a disease, it remains the most prevalent risk factor as a predisposition to disease. Data in this study has clearly linked 'ageing' with altered intracellular Ca^{2+} regulation in all regions of the heart.

Acknowledgements

I would like to thank my supervisor Dr Sandra Jones and also Dr Matthew Lancaster for continuous help in obtaining the electrophysiology data. I am also grateful to my secondary supervisor Dr Anne-Marie Seymour for her guidance and support.

I would also like to thank Mrs Kathleen Bulmer for her invaluable teachings and general technical support in the lab.

My sincere gratitude goes to my family who have supported me throughout my PhD, especially during the 'writing up' phase. I should also like to thank my colleagues and friends at the University, Sam Drennan, David Taylor, Amy Dawson and Thomas Butler.

Finally, I am grateful to the University of Hull 80th Anniversary scholarship for funding this PhD.

Contents

Abstract ii
Acknowledgements iv
Contents v
List of figures xii
List of tables xiv
List of abbreviations xv
Chapter 1 General introduction 1
1.1 Elderly population 2
1.2 Structure and function of the heart 3
1.2.1 Building blocks of the heart 4
1.2.2 Excitation-Contraction Coupling 5
1.2.3 Ions contributing to normal cardiac function 7
1.2.3.1 Cardiac calcium channels 8
1.2.3.2 Cardiac sodium channels 9
1.2.3.3 Cardiac potassium channels 9
1.2.3.4 Resting membrane potential 10
1.2.4 Basic cardiac action potential configuration 11
1.2.5 Regional tissue specific action potentials 13
1.2.5.1 SA node - pacemaker tissue 13
1.2.5.2 Atria action potentials. 14
1.2.5.3 Ventricular action potentials 14
1.3 Calcium handling within the heart 15
1.3.1 Rise of Ca^{2+} during diastolic depolarisation 15
1.3.1.1 Intracellular mechanisms involved in Ca^{2+} transient 15
1.3.1.2 Sarcolemma bound proteins involved in Ca^{2+} influx 16
1.3.2 Removal of intracellular Ca^{2+} 17
1.3.2.1 Extrusion of Ca^{2+} via the SR-Ca^{2+} pump 17
1.3.2.2 Additional mechanisms in the reduction of $[Ca^{2+}]_i$ 17
1.4 Pacemaker activity 19
1.4.1 Sinoatrial node 19
1.5 Ca^{2+} mismanagement within the heart 20
1.5.1 Cardiac arrhythmias 20
1.5.1.1 Pathophysiology of cardiac arrhythmias 21
1.5.1.2 Consequences of cardiac arrhythmias 22
1.6 The effect of ageing on the heart 22

1.6.1 Animal models of ageing 22
1.6.2 Structural and functional changes 23
1.6.3 Ageing effects on Ca^{2+} transient 24
1.6.4 Effect of ageing on the SA node 25
1.7 Aims of study 26
Chapter 2 Materials and methods 27
2.1 Heart sample acquisition 28
2.1.1 Acquisition of hearts 29
2.1.2 Dissection of the whole heart 29
2.1.3 Dissection of Sinoatrial Node 31
2.2 Western Blotting 32
2.2.1 Sample Preparation 32
2.2.2 Bicinchoninic Acid (BCA) method of determining protein concentration 33
2.2.3 Preparations of samples for western blot 35
2.2.4 SDS-Polyacrylamide Gel (SDS-PAGE) 35
2.2.5 Electrophoresis 36
2.2.6 Electroblotting 37
2.2.7 Probing the nitrocellulose membrane 38
2.2.8 Visualisation of nitrocellulose membrane 40
2.2.9 Image analysis 40
2.3 Immunocytochemistry 42
2.3.1 Frozen sections 42
2.3.2 Slide Processing 42
2.3.3 Probing of the tissue section 43
2.3.4 Confocal imaging of sections 43
2.3.5 Analysis of immunocytochemistry sections 44
2.4 Mapping of the sinoatrial node region 46
2.4.1 Preparation of the sinoatrial node 46
2.4.2 Optical mapping of the sinoatrial node 46
2.5 Sinoatrial node mapping 49
2.5.1 Bi-polar electrode mapping of the SA node 49
2.5.2 Analysis of electrophysiological recordings 52
2.6 RNA and real-time PCR 54
2.6.1 Total RNA Extraction 54
2.6.2 RNA Concentration Analysis- NanoDrop 1000 55
2.6.3 Reverse Transcription (cDNA Synthesis) 56
2.6.4 qPCR - Test amplification of cDNA 57

2.6.5 qPCR – StepOne Plus Applied Biosystems 59

Chapter 3 Effect of ageing on Ca^{2+} regulation involved in spontaneous activity of the sinoatrial node 62

3.1 Introduction 63

3.1.1 Sinoatrial node 63

3.1.2 Calcium handling within the SA node 63

3.1.2.1 Mechanisms behind SA node spontaneous beating 63

3.1.3 Effect of ageing on spontaneous SA node activity 65

3.1.3.1 Effect of ageing on proteins key to pacemaker activity 65

3.1.3.2 Effect of ageing on AP propagation across the SA node 66

3.1.4 Effect of ageing on exercise and β-adrenergic stimulation on mammalian intrinsic heart rate 67

3.1.5 Effect of age on the sensitivity to nifedipine 67

3.1.6 Objectives 68

3.1.7 Hypothesis 68

3.2 Methods 69

3.2.1 Dissection of right atrium to use in western blotting 69

3.2.2 Western blotting 69

3.2.2.1 Antibody detection and peptide controls 70

3.2.2.2 Immunoblotting method using methanol-free transfer 71

3.2.3 Bi-polar electrode mapping of the SA node 71

3.2.3.1 Pacemaker shift analysis 72

3.2.4 Immunocytochemistry 73

3.2.5 Statistical analysis 73

3.3 Results 74

3.3.1 Confirmation of protein localisation 74

3.3.2 Optical mapping of Ca^{2+} transients 77

3.3.3 Age-dependent physiological changes 77

3.3.3.1 Body-weight to heart-weight ratio 77

3.3.3.2 Intrinsic heart rate 77

3.3.4 Adrenergic response 78

3.3.4.1 Effect of increasing age on the response to isoprenaline as a β-adrenergic stimulator 78

3.3.4.2 Investigation into the role of the SR in β-adrenergic response. 80

3.3.5 Effect of ageing on conduction velocity 80

3.3.5.1 Effect of ageing on the conduction velocity in the presence of isoprenaline 80

3.3.5.2 Role of the SR in conduction velocity and its response to β-adrenergic stimulation. 81
3.3.5.3 Effect of β-adrenergic stimulation on pacemaker shift 82
3.3.5.4 Age-associated variations in AP propagation. 82
3.3.6 Age-associated changes in SR associated proteins 87
3.3.6.1 Effect of ageing on SERCA2a activity within the SA node 87
3.3.7 Age-associated changes in sensitivity and expression of proteins involved in CICR - Cav1.2 and RYR2 92
3.3.7.1 Effect of ageing on the sensitivity of the SA node to nifedipine 92
3.3.7.2 Age-associated changes to RYR2 protein expression 93
3.3.7.3 Variations in $Ca_v1.2$ protein expression in the SA node with increasing age. 94
3.3.8 Age-associated changes in sarcolemma membrane associated proteins within the SA node. 97
3.4 Discussion 101
3.4.1 Summary of Chapter 3 101
3.4.2 Age-associated physiological differences 101
3.4.3 β-adrenergic response 102
3.4.3.1 Effect of ageing on sensitivity to isoprenaline 102
3.4.3.2 Role of SERCA in β-adrenergic response 102
3.4.3.3 Effect of ageing on conduction velocity in the SA node 104
3.4.3.4 Effect of isoprenaline on other protein targets further explains the age-associated decline in β-adrenergic response 105
3.4.3.5 Effect of isoprenaline and CPA on pacemaker shift 107
3.4.4 Effect of ageing on the sensitivity to nifedipine 108
3.4.4.1 Age-associated affect on the influx of Ca^{2+} via $Ca_v1.2$ 108
3.4.5 Age-associated changes in calcium handling proteins and their effect on SA node function/activity. 110
3.4.6 Limitations 111
3.4.7 Conclusions 112
Chapter 4 Age-associated changes in Ca^{2+} handling proteins within atrial tissue 113
4.1 Introduction 114
4.1.1 RA heterogeneity 114
4.1.1.1 Structure of the RA 114
4.1.1.2 Crista terminalis 114
4.1.1.3 Ageing and CT tissue 115
4.1.2 Right and left atria 115
4.1.2.1 Role of the atria in the heart 115

4.1.2.2 Cardiac arrhythmias originating outside of the SA node 115
4.1.2.3 Effect of ageing on calcium regulation within the atria 116
4.1.3 Objectives 117
4.1.4 Hypothesis 117
4.2 Methods 118
4.2.1 Further dissection of the RA 118
4.2.2 RA tissue sections for immunocytochemistry 118
4.2.3 Statistical analysis 118
4.3 Results 119
4.3.1 Characterisation of qPCR technique 119
4.3.1.1 Test for positive and negative reverse transcriptase controls using actin primer 119
4.3.1.2 Selection of endogenous control 120
4.3.2 Calcium handling in the RA differs with age 121
4.3.2.1 Age-associated differences in SERCA2a activity and expression across the RA 121
4.3.2.2 Effect of ageing on the protein expression of RYR2 128
4.3.2.3 Expression of $Ca_v1.2$ channels within RA regions changes with increasing age 131
4.3.2.4 Age-associated changes in cell membrane calcium handling proteins across the RA 134
4.3.3 Age-associated comparison of alterations in calcium regulation in the left and right atria 140
4.3.3.1 Age-associated changes in SERCA2a activity across the left and right atria 140
4.3.3.2 Age-associated changes in CICR release proteins, RYR2 and $Ca_v1.2$ 149
4.3.3.3 Age associated changes in cell membrane calcium handling proteins NCX1 and PMCA4a 152
4.4 Discussion 157
4.4.1 Summary of Chapter 4 157
4.4.2 Heterogeneity of the tissue surrounding the SA node 160
4.4.2.1 Effect of age and region on SERCA2a activity; its role in the generation of arrhythmias 160
4.4.2.2 Effect of ageing on the spontaneous activity of the CT: a cause for concern 160
4.4.2.3 Age-associated changes in protein expression: comparing the RA muscle and CT 161
4.4.3 Overall comparison of atria 161
4.4.3.1 Age-associated changes across the atria 161

4.4.3.2 Changes in SERCA2a activity across the atria and its role in atrial fibrillation 162
4.4.3.3 Protein and mRNA data disparity: age-associated changes in mRNA translation 163
4.4.4 Limitations 164
4.4.5 Conclusion 164
Chapter 5 Effect of age on Ca^{2+} handing proteins in the ventricles 165
5.1 Introduction 166
5.1.1 Consequences of advancing age on the ventricles 166
5.1.1.1 Calcium remodelling within the left and right ventricles 166
5.1.1.2 Age-associated changes in the removal of Ca^{2+} from the cytosol 167
5.1.2 Comparison of the left and right ventricles 168
5.1.3 Variations in calcium handling protein expression across the LV myocardium wall 168
5.1.4 Objectives 170
5.1.5 Hypothesis 170
5.2 Methods 171
5.2.1 Western blotting 171
5.2.2 qPCR actin and endogenous control 171
5.2.3 Immunocytochemistry 171
5.2.3.1 Transmural gradient across the LV myocardium 171
5.2.4 Statistical analysis 172
5.3 Results 173
5.3.1 Effect of ageing on left and right ventricular tissue 173
5.3.1.1 Age-associated changes in SERCA2a activity across the ventricles 173
5.3.1.2 Age associated changes to proteins involved in CICR within the ventricles 180
5.3.1.3 Effect of ageing on calcium extrusion within the ventricles 186
5.3.2 Effect of ageing on transmural changes across the left ventricular wall 191
5.3.2.1 Age-associated changes to SERCA2a activity between the epicardium and endocardium of the LV wall 191
5.3.2.2 Analysis of ageing on the effect of CICR associated proteins across the LV 198
5.3.2.3 Investigation into the effect of ageing on NCX1 and PMCA4a across the LV myocardium 204
5.4 Discussion 209
5.4.1 Summary of Chapter 5 209
5.4.2 Implications of ageing on calcium regulation within the LV 212
5.4.2.1 Effect of age on SERCA2a activity in the left ventricle 212

5.4.2.2 SERCA2a activity across the left ventricular wall and its response to ageing 213
5.4.2.3 Effect of ageing on EC coupling with focus on proteins involved in CICR 214
5.4.2.4 Heterogeneity in calcium handling proteins across the left ventricular myocardium 215
5.4.3 Calcium handling protein expression across the left and right ventricles is affected by age and region 216
5.4.3.1 Variation in SERCA activity across the ventricles 216
5.4.3.2 Variations in calcium handling proteins across the ventricles 216
5.4.4 Limitations 216
5.4.5 Conclusion 217
Chapter 6 Discussion 218
6.1 Overall summary of study 219
6.2 Ca^{2+} handling in the atria versus ventricles 220
6.2.1 Cardio myocytes structural differences with consequences on Ca^{2+} handling 220
6.2.1.1 Propagation of Ca^{2+} in atrial myocytes 222
6.2.2 Altered AP properties linked to variations in Ca^{2+} handing proteins and changes with age 223
6.2.3 Ca^{2+} handling protein differences and similarities across the heart 224
6.2.4 Culprits in the generation of arrhythmias in the atria and ventricles 225
6.3 Alternative mechanisms involved in Ca^{2+} influx 226
6.3.1 Alternative pathways for Ca^{2+} influx 226
6.3.1.1 Stretch activated channels 226
6.3.1.2 Store-operated calcium channels and depletion of SR Ca^{2+} content 227
6.3.1.3 T type calcium channels in the SA node 228
6.4 Future work 228
6.5 Clinical implications 229
6.6 Conclusion 230
Publications 232
References 233

List of figures

Figure 1.2 Schematic diagram of the mammalian heart. 3
Figure 1.3 The movement of Ca^{2+} and the channels, pumps and receptors involved in Ca^{2+} homeostasis within a mammalian cardiac myocyte. 7
Figure 1.4 Profile of a typical cardiac AP from a ventricular cell. 11
Figure 1.5 Typical AP profile from the SA node 13
Figure 1.6 Typical AP profile from the atria 14
Figure 1.7 Schematic of typical AP profiles from the LV. 14
Figure 2.1 Rat Heart: 30
Figure 2.2 Right Atrium. 31
Figure 2.3 Protein standard curve. 34
Figure 2.4 Components of semi-dry discontinuous blotting. 38
Figure 2.5 Optical mapping and BigJ Software: 48
Figure 2.6 Earthing of the electrophysiology equipment: 50
Figure 2.7 Electrophysiology Rig setup: 51
Figure 2.8 SA node map: 52
Figure 3.1 Right atrium. 69
Figure 3.2 Dot blot testing $Ca_v1.2$ antibodies. 70
Figure 3.3 Protein loading for $Ca_v1.2$ and the corresponding peptide control. 70
Figure 3.4 Fast semi-dry methanol-free transfer method (A) versus methanol transfer (B). 71
Figure 3.5 Example map of the SA node preparation with labelled LPS. 72
Figure 3.6 Example of immunolabelling of each antibody (page 73 and 74) 75
Figure 3.7 Separated channels of immunolabelling of PLB in LV sections. 76
Figure 3.8 Changes in intrinsic heart rate with age under control conditions (blue) and in the presence of 3µM CPA (red). 78
Figure 3.9 Dose response of isoprenaline versus intrinsic heart rate. 79
Figure 3.10 The affect of CPA on conduction velocity in aged SA node. 81
Figure 3.11 Activation map of the SA node at 6 months 84
Figure 3.12 Activation map of the SA node at 12 months 85
Figure 3.13 Activation velocity map of the SA node at 24 months 86
Figure 3.14 SERCA2a protein expression in the SA node with increasing age 88
Figure 3.15 PLB protein expression in the SA node with increasing age 89
Figure 3.16 Localised PLB protein in the SA node with increasing age 90
Figure 3.17 SERCA2a activity in the SA node with increasing age. 91
Figure 3.18 Nifedipine dose response curves for rats aged at 6 and 24 months. 93
Figure 3.19 RYR2 protein expression in the SA node with increasing age 95
Figure 3.20 $Ca_v1.2$ protein expression in the SA node with increasing age 96
Figure 3.21 NCX1 protein expression in the SA node with increasing age 98
Figure 3.22 $Na_v1.5$ protein expression in the SA node with increasing age 99
Figure 3.23 PMCA4a protein expression in the SA node with increasing age 100
Figure 4.1 Right atrium. 118
Figure 4.2 118
Figure 4.3 Actin transcript test amplification gel. 119
Figure 4.4 Profile of SERCA2a protein expression across the RA with increasing age 122
Figure 4.5 Localisation of SERCA2a protein expression within regions of the RA 123
Figure 4.6 Profile of PLB protein expression across the RA with increasing age. 125
Figure 4.7 Localisation of PLB protein expression within regions of the RA. 126
Figure 4.8 SERCA2a activity in the RA with advancing age. 127
Figure 4.9 Profile of RYR2 protein expression across the RA with increasing age 129
Figure 4.10 Localisation of RYR2 protein expression within regions of the RA 130
Figure 4.11 Profile of $Ca_v1.2$ protein expression across the RA with increasing age 132

Figure 4.12 Localisation of $Ca_v1.2$ protein expression within regions of the RA 133
Figure 4.13 Profile of NCX1 protein expression across the RA with increasing age 135
Figure 4.14 Localisation of NCX1 protein expression within regions of the RA 136
Figure 4.15 Profile of PMCA4a protein expression across the RA with increasing age ..138
Figure 4.16 Localisation of PMCA4a protein expression within regions of the RA 139
Figure 4.17 Profile of SERCA2a protein expression across the atria with increasing age 141
Figure 4.18 Localisation of SERCA2a protein expression across the atria.....142
Figure 4.19 Profile of PLB expression in the LA and RA.....144
Figure 4.20 Localisation of PLB protein expression across the atria.....145
Figure 4.21 SERCA2a activity across the atria with advancing age. 146
Figure 4.22 Profile of RYR2 protein expression across the atria with increasing age.....147
Figure 4.23 Localisation of RYR2 protein expression across the atria.....148
Figure 4.24 Profile of $Ca_v1.2$ protein expression across the atria with increasing age....150
Figure 4.25 Localisation of $Ca_v1.2$ protein expression across the atria 151
Figure 4.26 Profile of NCX1 protein expression across the atria with increasing age.....153
Figure 4.27 Localisation of NCX1 protein expression across the atria.....154
Figure 4.28 Profile of PMCA4a protein expression across the atria with increasing age 155
Figure 4.29 Localisation of PMCA4a protein expression across the atria.....156
Figure 5.1 Example profile of a LV wall tile scan. 172
Figure 5.2 Profile of SERCA2a protein expression across the ventricles with increasing age.....174
Figure 5.3 Localisation of SERCA2a protein expression across the ventricles.....175
Figure 5.4 Profile of PLB protein expression across the ventricles with increasing age. 177
Figure 5.5 Localisation of PLB protein expression across the ventricles.....178
Figure 5.6 SERCA2a activity in the LV and RV with advancing age. 179
Figure 5.7 Profile of RYR2 protein expression across the ventricles with increasing age 181
Figure 5.8 Localisation of RYR2 protein expression across the ventricles.....182
Figure 5.9 Profile of $Ca_v1.2$ protein expression across the ventricles with increasing age 184
Figure 5.10 Localisation of $Ca_v1.2$ protein expression across the ventricles 185
Figure 5.11 Profile of NCX1 protein expression across the ventricles with increasing age 187
Figure 5.12 Localisation of NCX1 protein expression across the ventricles.....188
Figure 5.13 PMCA4a protein expression across the ventricles with increasing age 189
Figure 5.14 Localisation of PMCA4a protein expression across the ventricles.....190
Figure 5.15 SERCA2a protein expression across the LV wall with increasing age 192
Figure 5.16 Localisation of SERCA2a protein expression across the LV wall 193
Figure 5.17 PLB protein expression across the LV wall with increasing age.....195
Figure 5.18 Location of PLB protein expression across the LV wall 196
Figure 5.19 SERCA2a activity in the LV wall with advancing age. 197
Figure 5.20 RYR2 protein expression across the LV wall with increasing age 199
Figure 5.21 Location of RYR2 protein expression across the LV wall.....200
Figure 5.22 $Ca_v1.2$ protein expression across the LV wall with increasing age.....202
Figure 5.23 Location of $Ca_v1.2$ protein expression across the LV wall 203
Figure 5.24 NCX1 protein expression across the LV wall with increasing age 205
Figure 5.25 Location of NCX1 protein expression across the LV wall.....206
Figure 5.26 PMCA4a protein expression across the LV wall with increasing age 207
Figure 5.27 Location of PMCA4a protein expression across the LV wall.....208

List of tables

Table 1.1 Hierarchy of pacemakers in the order of highest firing frequency in humans. ..19
Table 2.1 Western blotting: Primary and secondary antibodies, suppliers and dilutions. 41
Table 2.2 Immunocytochemistry: Primary and secondary antibodies, suppliers and dilutions. ..45
Table 2.3 qPCR 96-well plate layout: ..60
.Table 2.4 qPCR: Primers, reference codes, fluorescent labels and suppliers. ..61
Table 3.1 Drugs application and their concentrations..71
Table 3.2 Tested antibody dilutions for immunocytochemistry..73
Table 3.4 EC50 of isoprenaline and CPA..79
Table 3.5 Pacemaker shift associated with CPA or isoprenaline. ..82
Table 3.6 EC50 and Hill slope coefficient data of nifedipine with increased age. ..92
Table 4.1 C_T values for atrial tissue with desmin as an endogenous control..120
Table 4.2 C_T values for atrial tissue with GADPH as an endogenous control ..120
Table 4.3 Profile of expression of Ca^{2+} handling proteins across the right atria and impact of age. ..158
Table 4.4 Profile of expression of Ca^{2+} handling proteins and mRNA across the left and right atria and the impact of age. ..159
Table 5.1 Profile of expression of Ca^{2+} handling proteins and mRNA across the left and right ventricle and the impact of age. ..210
Table 5.2 Profile of expression of Ca^{2+} handling proteins and mRNA across the LV myocardial wall and the impact of age. ..211

List of abbreviations

AC – Adenylyl Cyclase

AP – Action potential

ATP – adenosine triphosphate

AV node – Atrioventricular node

BPM – Beats per Minute

Ca^{2+} – Calcium ions

cAMP – cyclic adenosine monophosphate

CaMKII – Calmodulin dependent kinase II

$Ca_v1.2$ – L-type calcium channel

$Ca_v3.1$ – T-type calcium channel

CICR – Calcium Induced Calcium Release

CPA –- Cyclopiazonic acid

CT –- Crista terminalis

DNA –- Deoxyribonucleic Acid

E-C coupling – Excitation Contraction coupling

ENDO – Endocardium

EPI – Epicardium

HF – Heart Failure

LA – Left Atrium

LCR – Local Calcium Release

LPS – Leading Pacemaker Site

LV – Left Ventricle

mRNA –- messenger Ribonucleic Acid

NCX – Sodium Calcium Exchange

PKA - Protein kinase A

PLB –- Phospholamban

PMCA – Plasma Membrane Calcium ATPase

qPCR–- Quantitative polymerase chain reaction

RA - Right Atrium

RV – Right Ventricle

RYR – Ryanodine Receptor

SA node – Sinoatrial node

SERCA – Sarcoendoplasmic recticulum Ca^{2+} ATPase

SR – Sarcoendoplasmic recticulum

Chapter 1 General introduction

1.1 Elderly population

"Everyone is the age of their heart" is a Guatemalan proverb which emphasises the link between age and the cardiovascular system (Crowe, 2006). As health care technology improves the size of the elderly population is increasing due to extending average lifespan (Fries, 2002). The elderly population, those aged 65 and over, is predicted to grow so that by 2035 it will constitute 23% of the UK population (Figure 1.1) an increase of 1.7 million people compared with 1985. This increase in elderly population will not only affect the UK, but the rest of the EU with Germany predicted to have the greatest increase by 2035, marked at a 31% elderly population.

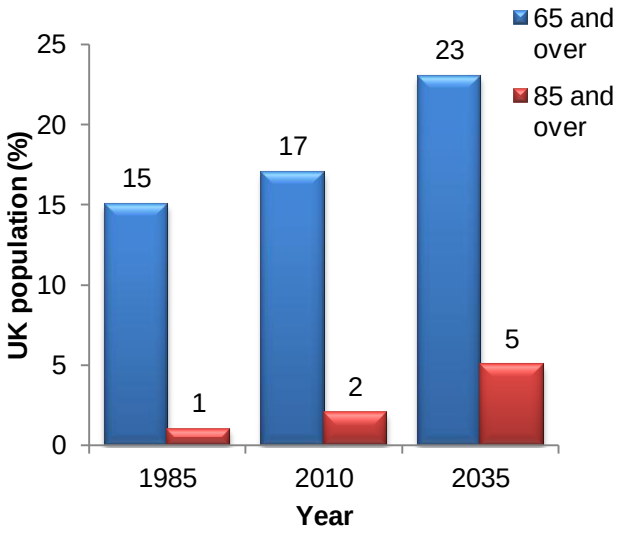

Figure 1.1 Percentage of the UK population considered elderly.

2035 projected values based on data up to 2010. Data sourced from: Office for National Statistics, national records of Scotland, Northern Ireland Statistics and Research Agency.

This data has increased interest in the physiology of ageing and the onset of age-associated diseases. The cardiovascular system is one of many body systems that deteriorates in function with age, but failure of the cardiovascular system is responsible for the highest percentage of deaths throughout the UK; in 2007 circulatory diseases was the leading cause of death in both sexes with approximately 530 deaths each day (Office for National Statistics UK, 2008). Consequently with the rising elderly population this will put the National Health Service under greater strain and the demand for treatment increased as the frequency of age-associated diseases rises alongside the ageing population.

Ageing itself cannot be considered a disease, however, it is a process of accumulation of damage and pathology; therefore ageing can be a predisposition to disease. The onset of cardiovascular disease will alter cardiac function it (Lakatta and Sollott, 2002), in particular an age-associated predisposition to irregular heartbeats, or an arrhythmia, is dually linked to altered functionality of the heart. In order to investigate these alterations with age the physiology of a young healthy heart must firstly be examined.

1.2 Structure and function of the heart

The cardiovascular system is a vital transport system for delivering oxygenated blood, nutrients and chemical signals to organs and tissues. It also aids the removal of waste by trafficking carbon dioxide to the lungs, as well as other waste products such as urea and uric acid to the kidneys. These all revolve around the heart pumping blood to all areas of the body, emphasising its uniqueness and importance as an organ. It is an autonomous organ that will beat up to 2.52 billion times in an average lifetime of a 70 year old human (Levine, 1997). The mammalian heart has four main chambers, the right atrium (RA) and left atrium (LA) at the top of the heart, the left ventricle (LV) and right ventricle (RV) at the bottom, which is separated by the septum (Figure 1.3). The heart is surrounded by an extensive blood supplying system, the coronary arteries, which provide oxygenated blood to the cardiac tissue.

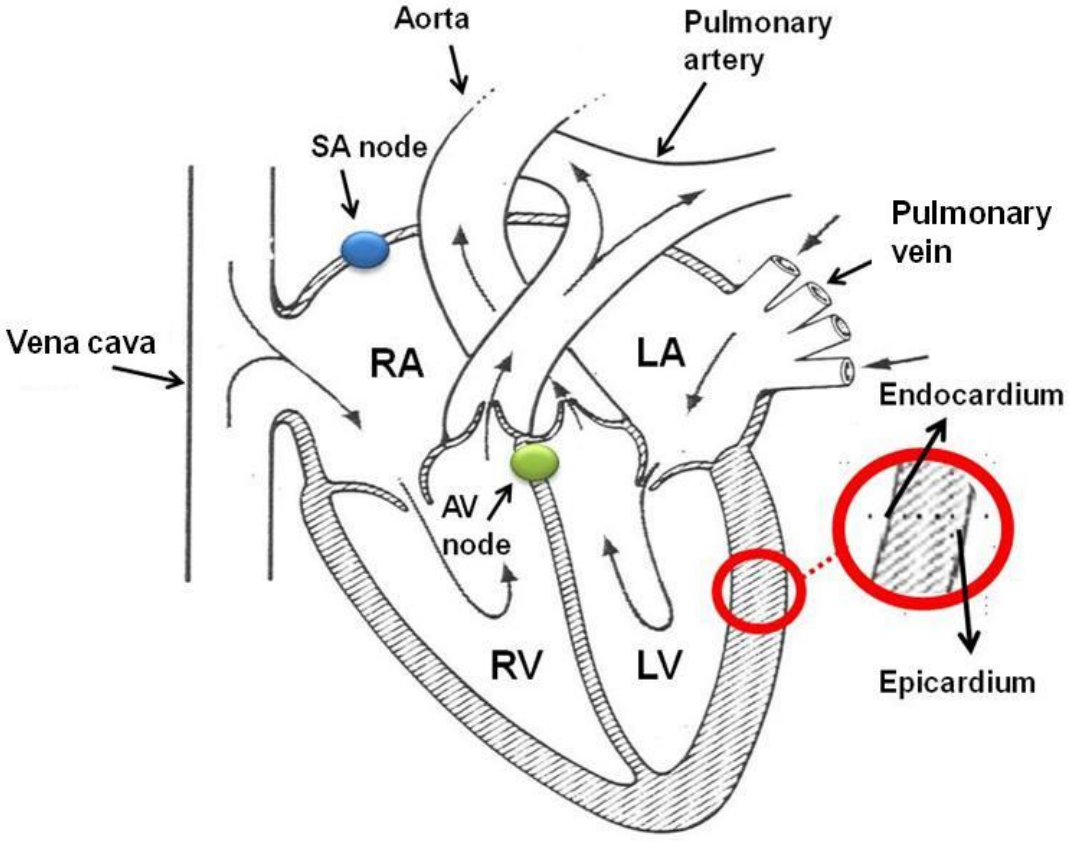

Figure 1.2 Schematic diagram of the mammalian heart.

Chambers of the heart are shown, with the LV myocardium illustrated in greater detail, alongside the vascular system associated to each chamber. The locations of the sinoatrial node and atrioventricular node are shown in blue and green respectively.

There are two anatomically separate vascular circuits. Pulmonary circulation of deoxygenated venous blood travels to the RA followed by the RV and then through the

pulmonary arteries to the lungs, where the blood is oxygenated and enters the left hand side of the heart via the pulmonary veins. Systemic circulation is where oxygenated blood enters the LA to the LV then pumped to the rest of the body via the aorta. Valves prevent blood flowing back between the chambers; the mitral bicuspid valve is, found between the LA and LV, and the tricuspid valve, which separates the RA and RV, preventing regurgitation of blood. The vessels carrying oxygenated blood known as the arteries have thicker walls of smooth muscle allowing them to withstand more pressure than veins. It is important that arteries have the plasticity to dilate and contract back to it's original shape again according to blood flow (Martini et al., 2006).

As the LV is required to pump blood to the rest of the body, high pressure is required to ensure all tissues are reached; consequently the LV has the thickest wall of muscle allowing it to generate high pressure (Greenbaum et al., 1981). The LV wall, as with the rest of the heart, is made up of three layers, the endocardium which lines the inner side of the heart and has an extensive capillary network, followed by the myocardium and the outer region which is known as the epicardium (Figure 1.2) (Antzelevitch et al., 1991). In contrast, the RV is thinner as the muscle is only required to pump blood to the lungs.

1.2.1 Building blocks of the heart

The heart is composed of cells known as myocytes, conduction tissue, blood vessels, fibrous tissue and adipose tissue. Myocytes are the principle component, composing approximately 75% of the total volume of the myocardium (Brilla et al., 1991). Each myocyte is bound to the next via an intercalated disc, made up of desmosomes, along with a gap junctional area that serves as low resistance electrical pathways. Ventricular myocytes account for greater than half of the heart weight measuring between 10-25µm in diameter and 50-100µm in length (Laks et al., 1967). In contrast to atria cells that are fewer in number and comparatively smaller; less than 10µm in diameter and approximately 20µm in length (McNutt and Fawcett, 1969).

Each myocyte is bound by an external membrane known as the sarcolemma, which separates the intracellular and extracellular spaces. Within the sarcolemma all the organelles and contractile apparatus are contained in the cytoplasm, which is a fluid microenvironment. Surrounded by this fluid are contractile proteins located within the myofibrils; thick myosin filaments and the thin actin filaments. During cellular contraction the filaments slide over each other and pulls together the two ends of the

contractile unit known as the sarcomere, resulting in shortening of the myofibril (Solaro and Rarick, 1998).

Apart from the contractile apparatus, mitochondria occupy a large proportion of each myocyte; wedged between the myofibrils these organelles provide the main source of energy supply close to the main site of use (Schaper et al., 1985). Mitochondria produce ATP required for myofibrils to contract. Mitochondria also accumulate calcium to prevent cytosolic levels from becoming too high (Hirano et al., 2001).

Cardiac myocytes can be isolated as individual cells as they are the building blocks of cardiac tissue. It is vital that myocytes are able to communicate between themselves to allow the continuation of electrical excitation. When two cardiac myocytes make contact the sarcolemma becomes highly specialised to form an intercalated disk; these are also present longitudinally to provide lateral contact between myocytes. The intercalated disks contain three main specialised components: the gap junctions, the fascia adherens junctions and the desmosomes. Adherens junctions and desmosomes provide the mechanical coupling of one cell to another, and ensures the electrical activityis transmitted throughout the myocardium (Severs, 1990). Gap junctions are large pores that serve as low resistant electrical pathways, where physical communication of molecules or ions less than1 kDa takes place between the cytosol of two neighbouring cells (Yeager and Gilula, 1992). Gap junctions are comprised of two connexons, one for each neighbouring cell, and each connexion is composed of six proteins known as ‘connexins’ (Delmar, 2002).

1.2.2 Excitation-Contraction Coupling

Transverse tubules (T-tubules) are an extension of the sarcolemma and have the same ultrastructure as the cell surface; these act to bring the intra- and extracellular domains extremely close together and increase the cell surface area to facilitate the spread of excitatory stimulus to within the cell. Caveolae are present at the surface of both the t-tubules and sarcolemma contributing further to an increased surface area (Schlegel et al., 1998). T-tubules are vital in E-C coupling, due to the presence of L-type calcium channels ($Ca_v1.2$) which are embedded in the bilayer. These channels are activated during depolarisation permitting the entry of Ca^{2+} which increases the concentration of Ca^{2+} within the cell ([100nm]); in turn this activates the sarcoplasmic reticulum (SR) via ryanodine receptors (RYRs), to then release comparatively more Ca^{2+} resulting in an overall 10-100 fold increase. Throughout the extreme mechanical forces during systole

(contraction) and diastole (relaxation) the T-tubules lumen always remain open allowing the entry of oxygen and nutrients (Kostin et al., 1998).

Calcium (Ca^{2+}) is required to bind to troponin C, and this in turn induces the conformational change required for contraction. The major facilitator of Ca^{2+} control around the cardiomyocytes is the sarcolemma, a lipid bilayer that possesses pumps and channels to aid maintenance of the cellular environment. Additionally the sarcolemma plays a vital role in excitation-contraction coupling (E-C coupling) (Bers, 2002) as it does not just line the outer surface of the cardiac myocytes, but also penetrates into the intracellular space to form a series of tube-like invaginations (Soeller and Cannell, 1999).

The SR takes on the appearance of small vesicles or granules, which contains the Ca^{2+} binding protein calsequestrin (Gyorke et al., 2009). As Ca^{2+} enter through the t-tubules, the SR store of Ca^{2+} is released rapidly (Bassani and Bers, 1995). This interaction is facilitated by the close contact between the T-tubules and the RYRs present on the SR which detect the influx of Ca^{2+} (Figure 1.3). Consequently when the wave of depolarisation reaches the t-tubules, it has only to send the Ca^{2+} a very short distance to the SR resulting in an extremely short delays in the release of calcium ions. Reuptake of Ca^{2+} is also conducted by the SR via the sarcoplasmic reticulum Ca-ATPase (SERCA) pumps which results in relaxation (Stewart and MacLennan, 1974, Haghighi et al., 2004).

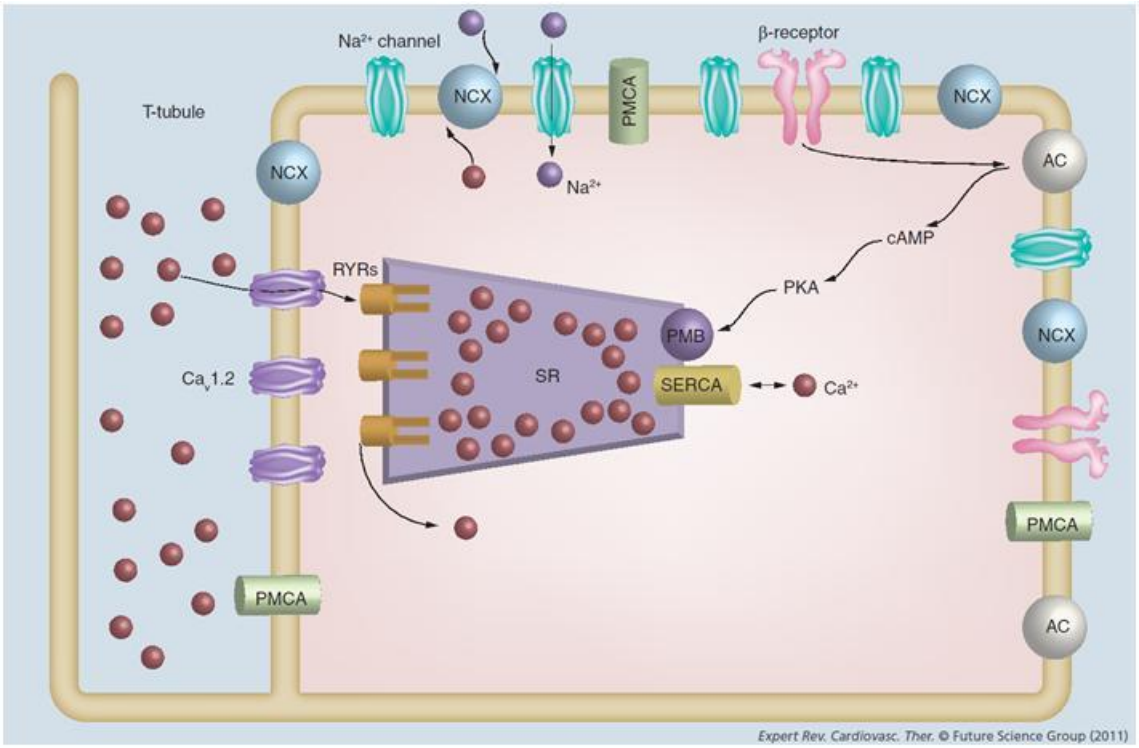

Figure 1.3 The movement of Ca^{2+} and the channels, pumps and receptors involved in Ca^{2+} homeostasis within a mammalian cardiac myocyte.

The T-tubule invagination shows the link between the $Ca_V1.2$ channels, ryanodine receptors (RYRs) and the sarcoplasmic reticulum (SR). The sarcoendoplasmic reticulum Ca^{2+} ATPase (SERCA) pump, shown here with its regulator PLB, transports Ca^{2+} back into the store after an action potential. Ca^{2+} is also removed via the sodium calcium exchanges (NCXs) and the plasma membrane Ca^{2+} ATPase (PMCA) pumps. SERCA is also affected by adenylyl cyclase and cAMP, which can increase activity. Reproduced from Expert review of Cardiovascular Therapy 9(8), 1059-1067 (2011) with permission of Expert Reviews Ltd (Hatch et al., 2011).

1.2.3 Ions contributing to normal cardiac function

To understand the delay between repolarisation and the onset of a new action potential (AP) it is important to know the sequence of channel opening and closing. The Hodgkin-Huxley hypothesis has three phases; resting, activated and inactivated (Katz, 1993). This model is a simplified version of how channels gate the flux of ions; however, more complex models for specific ion channels may provide a more accurate picture (Bennett et al., 1995).

1.2.3.1 Cardiac calcium channels

Calcium is an important ion for myocytes as it is needed to bind to the troponin C on the myofilaments to enable contraction. The most abundant of channels includes L-type calcium channels with the sub-groups of $Ca_v1.2$ and $Ca_v1.3$. The former is found throughout the heart and is the main channel which functions in letting in the majority of calcium within the myocyte.

The channels are referred to as 'L-type' meaning long-lasting due to the depolarisation being an extended plateau that can last up to 200ms. There are four known members of the L-type calcium channel family ($Ca_v1.1$, 1.2, 1.3 and 1.4) of which the $Ca_V1.2$ gene encodes for the typical L-type calcium channel found in cardiac tissue. There are two molecular weight forms of the $Ca_v1.2$ channel, 240 and 210 kDa, which differ due to truncation of the C-terminus. The latter of which can regulate transcription of $Ca_v1.2$ channels (Schroder et al 2009).

The activity of a single $Ca_v1.2$ channel can switch between three different gating modes: Mode 0 where the channel is unable to open; Mode 1 is referred to as normal activity with brief openings that occur in rapid succession; and Mode 2 where there is a high open probability which results in a long opening time interrupted by quick closings (Benitah et al 2009; McDonald et al 1994). Regulation of the density of $Ca_v1.2$ channels is key to determining the flux of calcium into the cell. Consequently there are multiple mechanisms involved in controlling the density of calcium channels, some are more understood than others with mechanisms still being uncovered.

Kinase modulations are the best understood mechanisms; phosphorylation of Ca^{2+} channel-forming proteins by protein kinase A (PKA) is the main and mostly investigated process for Ca^{2+} channel activation. PKA can phosphorylate the $Ca_v1.2$ channels directly increasing the probability and the duration of the open state of the channels and thus the amount of Ca^{2+} influx. The PKA pathway begins with an agonist binding to its receptor which causes receptor stimulation resulting in activation of GTP-binding proteins and consequently stimulates adenylyl cyclase (AC). The stimulated AC feeds on ATP to produce cAMP, increased cAMP concentration causes PKA to be activated resulting in positive feedback. Activated PKA phosphorylates several proteins related to excitation-contraction coupling, including the $Ca_v1.2$ channels (Bers DM 2002). β-adrenergic stimulation affects I_{Ca} at the level of a single channel, where the main effect is an increase in the channel's probability of opening (Mode 2) (van der Heyden MA et al 2005).

Previous methods have focused on how signalling may affect existing calcium channels, however, channels can also be regulated at the level of protein expression. Alterations in the density of $Ca_v1.2$ channels have been associated with changes in physiological conditions such as the onset of cardiovascular diseases including atrial fibrillation and heart failure (Kamp and He, 2002). Recent studies (Zhao et al., 2009) have shown that chronic stress can be associated with increases in α_{1c} subunit expression which in turn causes self-upregulation of $Ca_v1.2$ channels and thus an increase in L-type calcium channel current.

1.2.3.2 Cardiac sodium channels

The predominant type of sodium channel protein present in cardiac tissue is $Na_v1.5$ which is expressed by the SCN5A gene (Gellens et al., 1992). Sodium channels are widely distributed through most of the heart and respond to the onset of depolarisation of phase 0 of an AP (Figure 1.4); the opening of the $Na_v1.5$ channels occurs when the membrane potential reaches between -70 to -60mV. Regulation of sodium channels is by cAMP-dependent protein kinase A and C (PKA and PKC) (Cukierman, 1996). But changes in phosphorylation can also result in a shift of activation or availability so that fewer $Na_v1.5$ channels may contribute to the AP. Furthermore depending on the specific receptors PKC activity can also modulate the activation of Na^+ channels (Ono et al., 1993).

1.2.3.3 Cardiac potassium channels

Potassium channels can be simplified by dividing them into two distinct molecular families, voltage operated channels (K_v) and inward rectifier channels (K_{ir}) (Deal et al., 1996). The main role of potassium channels is to control the outward flow of K^+ particularly during repolarisation (K_v) and the maintenance of the resting membrane potential (K_{ir}). There are two voltage-operated potassium channels known as delayed rectifier potassium channels (Sanguinetti and Jurkiewicz, 1991) present in cardiac myocytes; the slow and fast repolarisation currents but an even more rapid component has been found in human and rat atrium (Wang et al., 1993). The slow repolarising potassium channel (I_{Ks}) is a slow activating current and does not show any form of inactivation (Kurokawa et al., 2001). As with sodium channels, I_{Ks} is regulated by PKA and PKC (Walsh and Kass, 1988) and responds to β-adrenergic stimulation resulting in an acceleration of the AP via shortening its duration. The faster repolarisation current

(I_{Kr}) activates slowly, but is rapidly inactivated and particularly affects ventricular repolarisation (Sanguinetti et al., 1995).

Another important potassium channel is the transient outward potassium current (I_{TO}), which is a voltage-gated potassium channel and accounts for the very early repolarisation just after the peak of the upstroke in an AP (Figure 1.4; phase 0 and 1). This current is prevalent in atrial, Purkinje and ventricular cells (Schram et al., 2002) and helps reset the AP to the early phase of the plateau. Apart from the initial repolarisation, I_{TO} continues to contribute to repolarisation throughout phase 2.

1.2.3.4 Resting membrane potential

The resting cardiomyocyte maintains a polarised negative potential varied from -85mv to -60mV, region dependent. A resting potential is maintained primarily by the preferential permeability of the membrane to K^+. The inward rectifier family of potassium channels maintains the resting membrane potential of cardiac myocytes (Hume and Uehara, 1985) via the $K_{ir}2.1$ channel proteins (Lopatin and Nichols, 2001). When the membrane potential shifts above the potassium equilibrium potential the channel activates to pass an outward current to attempt to balance the shift; similarly this channel contributes to the repolarisation phase of the AP to help regain the resting membrane potential (Kurachi, 1985). Furthermore this channel may pass an inward potassium current if the cell is hyperpolarised to aid the maintenance of the high internal K^+ activity, consequently stabilising the membrane polarity.

1.2.4 Basic cardiac action potential configuration

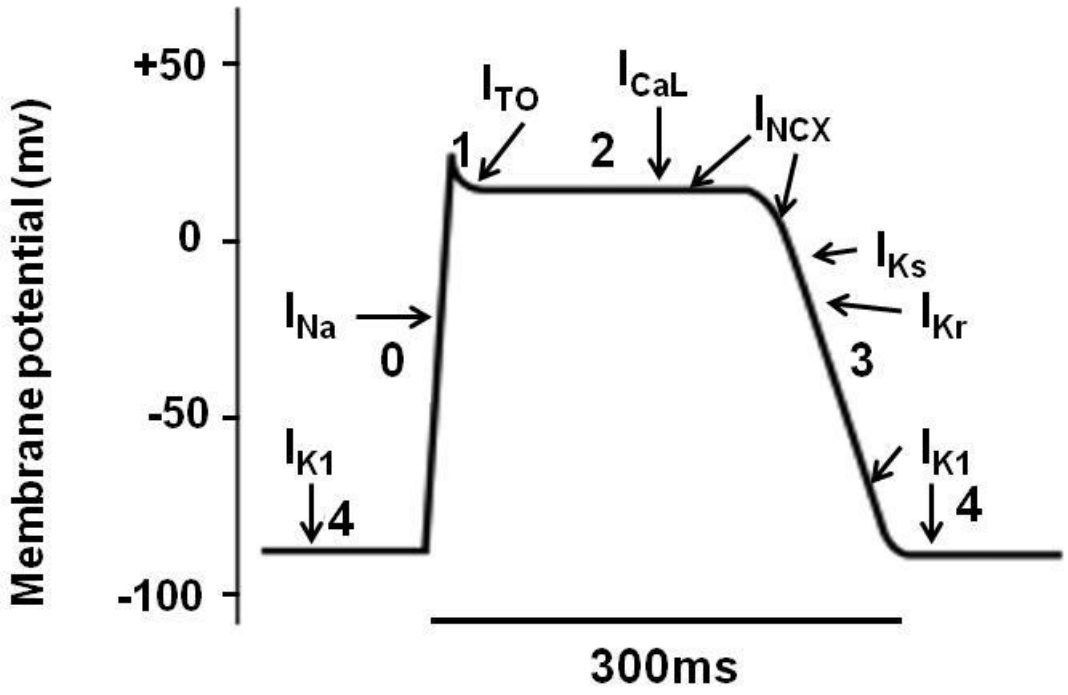

Figure 1.4 Profile of a typical cardiac AP from a ventricular cell.

Each phase is numbered from 0 to 4 with contributing currents shown. The resting potential is illustrated at -80mv with a peak of +30mv and time in ms shown on the x axis.

Cardiac myocytes, like other excitable cells, maintain electrochemical gradients of ions across their membrane establishing a trans-membrane voltage difference. An AP describes the change in voltage across a membrane due to the movement of K^+, Na^+ and Ca^{2+} ions across the membrane, down their concentration gradients (Figure 1.4). APs are the result of membrane depolarisation followed by repolarisation as instigated by alterations to ion channel gating. These APs can vary in shape and duration depending on species and cardiac tissue type (see section 1.2.5).

The first phase of the AP is phase 0 which is a rapid upstroke of the membrane potential due to the rapid influx of Na^+. The large and brief inward I_{Na} is accomplished by the $Na_v1.5$ channels which activate at approximately -70mV. Activation of these channels allows Na^+ to flow into the cell along the electrochemical gradient. Voltage-gated $Na_v1.5$ channels have very brief openings and short latency (Roden and George,

1997). Recovery of I_{Na} occurs at a negative membrane potential ensuring sufficient refractory period and protection from multiple impulses.

A dip in the membrane potential occurs immediately after the initial upstroke of Na^+ producing early repolarisation, which is labelled as phase 1. This early repolarisation occurs as a combination of the inactivation of I_{Na} and the activation of a transient outward current, I_{TO}, which is independent of Ca^{2+} and is mediated by potassium channels. The components of the current I_{TO} have fast activation kinetics and combine both slow and fast inactivation (Xu et al., 1999).

During phase 2 the membrane potential remains relatively depolarised resulting in a plateau phase of the AP. This plateau is due to the inward Ca^{2+} current (I_{Ca}) carried by voltage-gated Ca^{2+} channels. The predominant I_{CaL}, due to $Ca_v1.2$ channels, is activated at -40mV during the early depolarisation (phase 0) and is due to the trigger of Ca^{2+} from the SR causing a transient rise in intracellular Ca^{2+} concentration. This rise in Ca^{2+} activates the Na^+-Ca^{2+} exchanger (NCX) protein which causes a positive shift of the NCX current (I_{NCX}) to promote a net inward current of $3Na^+$ for Ca^{2+}.

Inward Ca^{2+} currents are reduced by voltage and Ca^{2+}- dependent inactivation causing the final repolarisation at phase 3. Coupled with this is the decline in I_{NCX} as the decay in Ca^{2+} transient removes the drive of the exchanger. Nevertheless the main contributor to phase 3 repolarisation is the outward K^+ ions labelled as the I_{Kr} and I_{Ks} for the rapid and slow currents respectively. Lastly the underlying I_{K1} works to repolarise the cell.

Phase 4 is the resting membrane potential maintained in between AP. The resting cardiomyocyte is preferentially permeable to K^+ due to I_{K1} which maintains a membrane potential of approximately -80mV. The resting potential is based on the combination of Nernst equilibrium potential and conductance of ions; this potential can be determined from the Goldman-Hodgkin-Katz equation (Campbell et al., 1988).

1.2.5 Regional tissue specific action potentials

1.2.5.1 SA node - pacemaker tissue

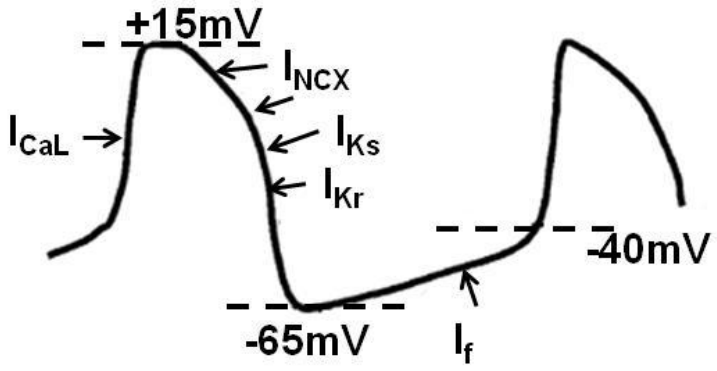

Figure 1.5 Typical AP profile from the SA node

SA node tissue has a more positive resting membrane potential of -65mV compared with other cardiac tissue. Nor is the potential maintained at a steady voltage, instead the membrane potential gradually increases, primarily via I_f (see 3.1.2.1) until it reaches -40mV threshold (Figure 1.5). The upstroke of the AP is instigated by $Ca_v1.2$ channels and therefore is more gradual. The density of K_{ir} is generally very low in pacemaker cells and absent in SA node cells (Irisawa et al., 1993); but also has a lower density in Purkinje fibres in comparison to ventricular myocytes (Cordeiro et al., 1998). The low density of potassium channels explains the more positive resting potential of +15mV found in pacemaker cells. Inactivation of $Ca_v1.2$ channels plus SR Ca^{2+} uptake via SERCA returns the membrane back to its resting state.

1.2.5.2 Atria action potentials.

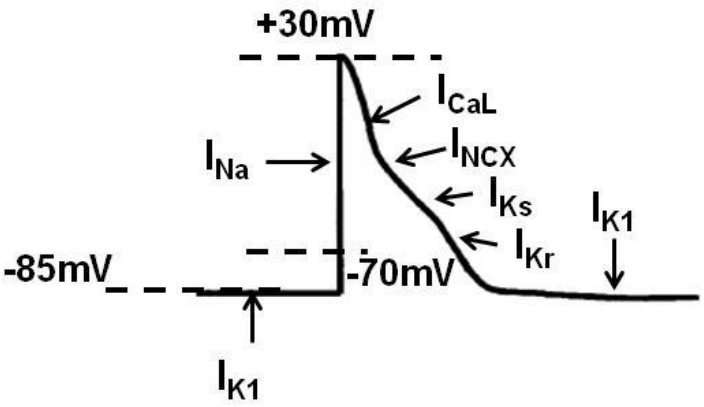

Figure 1.6 Typical AP profile from the atria

The membrane resting potential of atrial myocytes are -85mV with a threshold potential of -70mV and peak potential of +30mV (Figure 1.6). Atrial myocytes have a lower resting membrane potential similar to ventricular myocytes, but shortened AP duration as found in pacemaker tissue. The upstroke of the AP is instigated by I_{Na} with prolongation of the AP maintained by I_{CaL}, however, the comparatively lower density of Cav1.2 channels in atrial myocytes explains the decreased amplitude of I_{CaL}.

1.2.5.3 Ventricular action potentials

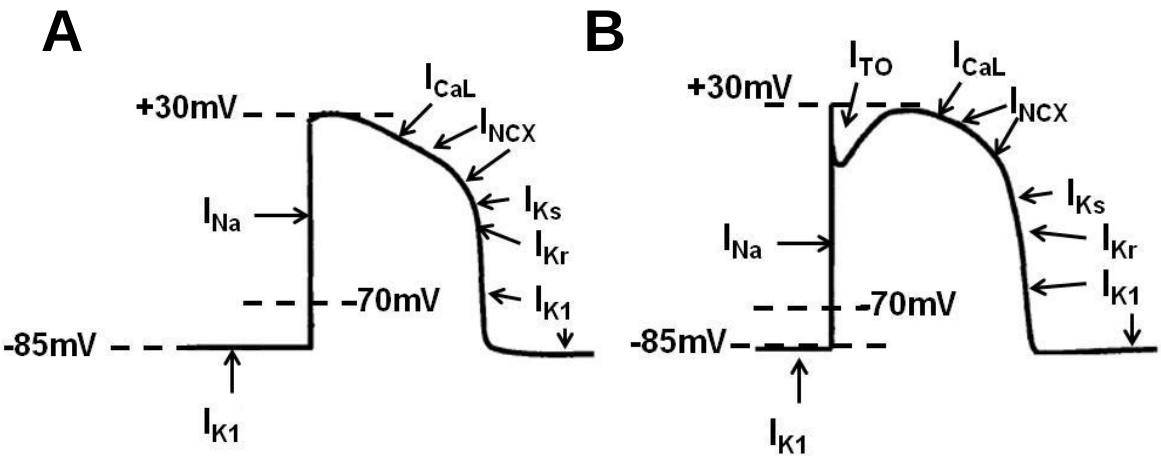

Figure 1.7 Schematic of typical AP profiles from the LV.

(A) endocardium and (B) epicardium.

The resting potential is illustrated at -85mV with a threshold potential of -70mV and peak potential of +30mV (Figure 1.7). The main noticeable difference is that phase 1, the early repolarisation caused by I_{TO}, is not present in the endocardium and AP

duration is longer (Figure 1.7A). The fast I_{TO} is expressed primarily in the epicardium whilst the slow I_{TO} inactivation is predominantly expressed in the endocardium (Nabauer et al. 1996). Similarly this translates to a greater current in the epicardium reflecting a brief AP compared with the endocardium (Liu et al. 1993). The density of Kir2.1, responsible for I_{K1}, varies across the LV wall and between species, contributing further to the shorter AP duration in the epicardium (Nerbonne, 2000).

1.3 Calcium handling within the heart

1.3.1 Rise of Ca^{2+} during diastolic depolarisation

Cell depolarisation, though initially triggered by I_{Na}, or I_{CaL} in the case of pacemaker tissue, is prolonged due to Ca^{2+} which also activates cellular contraction. The mechanisms involved in the rise of intracellular Ca^{2+} concentration ($[Ca^{2+}]_i$) via E-C coupling have been previously introduced, however, due to the cardiomyocyte's high sensitivity to Ca^{2+}, regulation of Ca^{2+} is tightly controlled by multiple proteins.

1.3.1.1 Intracellular mechanisms involved in Ca^{2+} transient

An extracellular source of Ca^{2+} influx are the L-type calcium channels ($Ca_v1.2$), and are characteristically sensitive to dihydropyridines such as nifedipine or nitrendipine. Also present in cardiac muscle are T-type Ca channels but in comparison the amount of current generated (I_{CaT}) in ventricular myocytes is undetectable in multiple species (Yuan et al., 1996), suggesting a role in the atria or pacemaking activity (Hagiwara et al., 1988). This suggests different functional roles, with $Ca_v1.2$ channels being vital in SR Ca^{2+} release and the refilling of the SR Ca^{2+} stores. The amount of Ca^{2+} entry via $Ca_v1.2$ channels is important for the contractile force of the myocyte. $Ca_v1.2$ channel density can be calculated based on the relationship between open probability, whole cell and single channel current (McDonald et al., 1986). The number of $Ca_v1.2$ channels directly affects I_{CaL} with evidence in the rabbit and rat ventricular myocytes of which the former has increased density, peak I_{CaL} and AP duration compared with the rat (Yuan et al., 1996). In addition there is a clear link between I_{CaL} inactivation and SR Ca^{2+} release, so that as the SR Ca^{2+} release gets larger alongside contractile force, $Ca_v1.2$ channels inactivatd more rapidly preventing SR Ca^{2+} overload (Adachi-Akahane et al., 1996). Conversely in the opposite scenario, enhanced I_{CaL} via prolonged $Ca_v1.2$

inactivation plus reduced Ca^{2+} efflux will restore SR Ca^{2+} content after depletion (Trafford et al., 1997).

Another mechanism for Ca^{2+} influx apart from the SR and $Ca_v1.2$ channels, are the sodium-calcium exchangers. During the early phase of an AP, due to the high intracellular Na^+ concentration, NCX enters 'reverse mode' (see 1.3.2) which extrudes Na^+ in exchange for Ca^{2+} that directly contributes to calcium indicuated calcium release (CICR) (Bers et al., 1988). Additionally outward I_{NCX} has been reported to activate during SR Ca^{2+} release and this intracellular Ca^{2+} caused activation state can vary dynamically during the Ca^{2+} transient (Weber et al., 2001). Nevertheless the qualitative contribution of NCX to Ca^{2+} influx during an AP is relatively small compared with that of I_{CaL}. During a typical rabbit ventricular twitch I_{CaL} was estimated to be responsible for 23% of total $[Ca^{2+}]_i$ whilst SR Ca^{2+} release responsible for the remaining 77% (Bassani et al., 1995a, Bassani et al., 1992).

1.3.1.2 Sarcolemma bound proteins involved in Ca^{2+} influx

Ryanodine receptor (RYR) opens the SR Ca^{2+} release channel. Three RYR isoforms have been identified, RYR1 found in skeletal muscle (Imagawa et al., 1987), RYR2 located in cardiac tissue (Otsu et al., 1990) and RYR3 identified in the brain (Hakamata et al., 1992). RYR2 has a high single channel conductance with relatively low Ca^{2+} selectivity (Smith et al., 1988b) but is involved in Ca^{2+} sparks which occur at rest at a very low frequency (Cheng et al., 1993). The normal AP Ca^{2+} transient is composed of the summation of numerous Ca^{2+} sparks synchronising to produce the prolonged Ca^{2+} transient via CICR and the release of Ca^{2+} from the SR store (Lopez-Lopez et al., 1995). The sensitivity of RYR2 declines in a time-dependent manner after the local release of Ca^{2+} (Schiefer et al., 1995) which correlates to the involvement in pacemaker activity (see section 1.4.1). The SR, to which the RYR proteins are attached , is entirely intracellular and contains 1mM high concentration of Ca^{2+}. During an AP the majority of Ca^{2+} responsible for increases in $[Ca^{2+}]_i$ originates from the SR. Physiologically intracellular SR $[Ca^{2+}]$ is buffered by calsequestrin (MacLennan and Wong, 1971). Calsequestrin in cardiac SR is highly acidic and each molecule can bind approximately 35-40 Ca^{2+} (Mitchell et al., 1988). Though calsequestrin is used to buffer Ca^{2+}, evidence of over expression, reported increased SR Ca^{2+} content with marked reduction in Ca^{2+} transients and contractions (Jones et al., 1998). Overall the SR acts like a sink for Ca^{2+} which on release is responsible for the majority of Ca^{2+} during a Ca^{2+} transient.

1.3.2 Removal of intracellular Ca^{2+}

Relaxation is facilitated by SERCA which pumps Ca2+ back into the SR and is the main contributor to the decay of the $[Ca^{2+}]_i$ transient. Additional routes include the NCXs, which is a constant sarcolemma pump, PMCA, a membrane protein that pumps Ca^{2+} out of the cell using ATP and the mitochondrial Ca^{2+} uniporter.

1.3.2.1 Extrusion of Ca^{2+} via the SR-Ca^{2+} pump

Removal of Ca^{2+} is mainly conducted by the SERCA pump which is attached to the SR; when fractionated SERCA makes up 90% of the protein in a typical cardiomyocyte (Saito et al., 1984). Two SERCA proteins have been identified, SERCA1 located in skeletal muscle (MacLennan et al., 1985) and SERCA2a found in cardiac muscle (Brandl et al., 1986). The SR-Ca^{2+}-pump transportes two Ca^{2+} for each ATP molecule (Reddy et al., 1996). A major difference between skeletal and cardiac muscle SR-Ca pump is that SERCA2a in cardiac muscle contains the regulatory protein phospholamban (PLB) (Tada et al., 1982) which exists as a homopentamer and monomer. To increase activity of the SR-Ca pump, PLB is phosphorylated by cAMP-dependent PKA at Ser-16 amino acid site and by CaMKII at Thr-17; both producing increases in the Ca^{2+} affinity of SERCA2a by 2-3 fold (Sham et al., 1991, Simmerman et al., 1986). In contrast using a heterologous coexpression study, maximal inhibition was observed as 3 PLB monomers per SR-Ca ATPase (Reddy et al., 1996). A comparison within the heart indicates that PLB expression is approximately ten fold less in the atria compared with the ventricles (Briggs et al., 1992). An alternative study investigating over expression of PLB indicated approximately 40% of the SERCA2a pumps are normally regulated by PLB, and for comparative maximum pump inhibition to occur, 2.6 fold over expression was required (Brittsan et al., 2000).

1.3.2.2 Additional mechanisms in the reduction of $[Ca^{2+}]_i$

Apart from the SR-Ca pump, two further mechanisms are responsible for Ca^{2+} extrusion, the plasma membrane Ca-ATPase pump (PMCA) and the NCX. Four human isogenes exist of the PMCA pumps (Shull et al., 1985) and further splice variants (Carafoli and Stauffer, 1994). PMCA4 plays a vital role in cardiac AP relaxation (Hammes et al., 1998). The activity of PMCA can be increased by cAMP-dependent phosphorylation and calmodulin (Caroni and Carafoli, 1981). The rate of extrusion of PMCA has been estimated to be relatively low (<1µM/sec) thus it is comparatively less important than SERCA (200µM/sec). Consequently while PMCA has a high affinity for

Ca^{2+} the transport rate is too gradual to be the major factor for relaxation, but may be important in Ca^{2+} efflux during rest (Bassani et al., 1995b).

Early work proposed a site that both Na^{+} and Ca^{2+} compete and could also bring Ca^{2+} into the cell (Luttgau and Niedergerke, 1958); this was later identified in the heart (Reuter and Seitz, 1968). Studies have shown that the NCX is both sensitive to membrane potential and is able to generate a voltage gradient (Bers et al., 1980, Caroni et al., 1980) with a stoichiometry of 3Na:1Ca (Reeves and Hale, 1984). There are two modes to the NCX, a forward mode by which Na^{+} enters the cell generating an inward current, and a reverse mode causing Ca^{2+} influx or an outward current. The direction of net current can be determined by the electrochemical gradient of both Ca^{2+} and Na^{+} (Kimura et al., 1986). During an AP, NCX transports Ca^{2+} into the myocyte as previously mentioned, however, the upstroke of I_{Na} is very rapid and the intake of Ca^{2+} via $Ca_v1.2$ channels and SR Ca^{2+} release, drives the NCX into forward mode causing Ca^{2+} efflux, thus aiding relaxation. Though the NCX is not as fast at extruding Ca^{2+} compared with SERCA, the rate of Ca^{2+} removal is estimated to be approximately 25µM/sec (Li et al., 1991) which is substantially greater than PMCA pumps or the mitochondrial Ca^{2+} uniporter.

Mitochondria can accumulate large amounts of Ca^{2+} but physiologically would be relatively low compared with the SR (Bassani et al., 1992). Ca^{2+} can enter the mitochrondia via the uniporter which only occurs during a large electrochemical gradient (Fry et al., 1984). Consequently during a typical cardiac cycle the rate of Ca^{2+} uptake is relatively low (Bassani et al., 1992).

Overall relaxation is aided by multiple mechanisms that vary in their level of contribution. In rabbit ventricular myocytes the pathways for Ca^{2+} removal has been estimated and quantified producing a percentage of Ca^{2+} efflux for each transporter: PMCA, 0.86%; mitochondrial Ca^{+2} uniporter, 0.62%; NCX, 30% and SERCA 68.5% (Bers and Bridge, 1989, Bassani et al., 1994a, Bassani et al., 1995b, Bassani et al., 1994b). Nevertheless these values are varied depending on the cell type, conditions of experiment and species.

1.4 Pacemaker activity

Pacemaker regions are a congregation of myocytes that are spontaneously active. These pacemaker cells are a crucial component for the heart to be an autonomous organ; there are three main regions with the sinoatrial (SA) node considered the primary pacemaker due to the highest frequency of activity, followed by the atrioventricular (AV) node and then the Purkinje fibres (see table 1.1). The SA node is a region of heterogeneous spontaneous tissue located in the top of the right atrium (Figure 1.2) and is the site of origin for an impulse. These pacemaker cells are unique due to the fact that calcium ions provide the initial upstroke in the action potential (see section 1.2.5.1). Electrical excitation originates from the SA node and spreads across the right and left atria, to be collected at the AV node. The AV node is a second area of congregated pacemaker cells located at the top of the ventricles at the Koch's triangle. After a brief delay at the AV node, the AP propagation speeds up as it travels along a specialised bundle of His conducting fibres. These Purkinje fibres, which are also spontaneously active, then divide into two major branches, so the electrical impulses can spread through both ventricles.

Table 1.1 Hierarchy of pacemakers in the order of highest firing frequency in humans.

Pacemaker tissue	Intrinsic frequency	Classification
SA node	100beats/min	Primary
AV node	40 beats/min	Secondary
Purkinje fibers	20 beats/min	Tertiary

1.4.1 Sinoatrial node

The SA node was discovered over 100 years ago (Keith and Flack, 1907) located in the right atrium (Figure 1.2). SA nodal cells are relatively smaller than both ventricle and atrial cells, with measurements in the rabbit indicating 25-30µm long and less than 8µm in diameter (Bleeker et al., 1980). Furthermore these cells are characteristically 'empty' containing few myofilaments that are poorly organised and contain numerous caveolae on the sarcolemma membrane, which would increase surface area much akin to t-tubules (Bleeker et al., 1980). In the rabbit there is a gradual transition in cell type in all directions from the centre of the SA node, highlighting no distinct border between the pacemaker tissue and the beginning of the CT and atrial muscle (Masson-Pevet et al., 1984).

It was not until the 1970s that voltage clamp studies were conducted on whole preparations or isolated nodal cells, to determine the mechanism of pacemaking

(Irisawa et al., 1993). During this time it was hypothesised that pacemaking was a result of the decay of the delayed rectifier K^+ current combined with the activation of I_F and Ca^{2+} channels. On the other hand, at the same time it was known that spontaneous Ca^{2+} release from the SR could activate an I_{NCX} producing depolarisation (Tsien et al., 1979). It was then considered that maybe a combination of the two produced pacemaker activity sparking an ongoing debate (Lakatta and Difrancesco, 2009), for an up-to-date comparison see chapter 3.

The propagation of an AP in the SA node is relatively complex, with duration greatest at or near the leading pacemaker site (centre) which tapers off at a similar rate in all directions (periphery) (Yamamoto et al., 1998). This creates a downward gradient in AP duration along the conduction pathway which also results in repolarisation of the SA node occurring in the opposite direction to that of depolarisation (Boyett et al., 1999).

1.5 Ca^{2+} mismanagement within the heart

1.5.1 Cardiac arrhythmias

Cardiac arrhythmias, which are irregular rhythms of the heart, increase in severity with age and remain a leading cause of morbidity and mortality in the Western world (Goonasekara et al., 2010, Hatch et al., 2011). The symptoms of cardiac arrhythmias can include chest pains, palpitations, breathlessness, dizziness and syncope. The most common type of sustained arrhythmia is atrial arrhythmias, predominantly atrial fibrillation (AF), which affects an estimated 4.5 million individuals in Europe (Fuster et al., 2006). These arrhythmias are responsible for 15% of strokes in the general population (Chamorro, 2010) and, due to the increasing age-associated prevalence of this problem, 25% of strokes in individuals are over the age of 80 years (Hopps and Marcy, 2009). Atrial arrhythmias can frequently be tolerated but generally more acute and serious are ventricular arrhythmias which include ventricular fibrillation (VF) and ventricular tachycardia (VT); these are the most common cause for sudden cardiac death (SCD) and implicated in 20% of annual deaths in the USA (Lopshire and Zipes, 2006).

There are numerous reasons for the development of cardiac arrhythmias; however all are based on disruption of normal electrical conduction throughout the heart. Instability in the fluxes of ions and conduction of the cardiac action potential can result in spontaneous unregulated depolarisation in areas of the cardiac tissue thus initiating an arrhythmia. One of the leading ion fluxes that can trigger the initiation of an arrhythmia is the movement of Ca^{2+}. Whether initiating the heart beat or simply modulating activity

of the cardiac pacemaker the role of intracellular Ca^{2+} is without doubt important for normal cardiac pacemaker function. Studies have shown that intracellular calcium regulation in cells from the sinoatrial node region is changing with progressive ageing associating with slowed spontaneous pacemaking, depressed dynamic response of the heart rate and an increased incidence of pacemaker problems seen in the elderly (Brown, 1982). Consequently those over 65 years of age account for the majority of individuals requiring artificial pacemaker implants to support a failing sinoatrial node. Such dysfunction of the sinoatrial node is also likely to increase the probability of developing atrial arrhythmias (Hartel and Talvensaari, 1975).

1.5.1.1 Pathophysiology of cardiac arrhythmias

A cardiac arrhythmia essentially causes the electricity of the heart to be out of control and consequently the beats are no longer succinct, the result being inefficient activation of the heart muscle (Podrid and Kowey, 2001). Most atrial and ventricular arrhythmias can be divided into either fast 'tachyarrythmias' or slow 'bradyarrhythmias'. Ventricular arrhythmias are mainly subsequent to ischemic episodes when sections of the heart are no longer electrically activated in the normal manner potentially resulting in electrically semi-isolated sections capable of producing their own action potential or only slowly responding to an existing action potential. Three arrhythmogenic mechanisms are common to atrial and ventricular arrhythmias; ectopic automaticity, after-depolarisations, and re-entry circuits (Zipes, 2003).

Ectopic automaticity is the development of a new site of spontaneous depolarization in a region that is not within the SA node, ectopic being the Greek word for 'out of place'. It is often called an '*ectopic beat*', though atrial ectopic excitation may not progress to produce a ventricular beat. (Pumir et al., 2005). The severity of ectopic automaticity can vary from being relatively harmless, perhaps simply substituting for normal SA node activity but still initiating close to normal recruitment of the heart muscle, to significantly hindering diastolic or systolic function of the heart (Keating and Sanguinetti, 2001). Ventricular tachyarrhythmias for example are often serious since the very rapid excitation pattern observed with some ventricular ectopic foci can limit ventricular filling time and coupled with a disrupted muscle recruitment drastically reduce cardiac output.

Re-entry circuit arrhythmias normally arise when the normal conduction of the action potential becomes slowed in a sub-region of the heart, often subsequent to localised ischemia. The slowed propagation means electrical excitation can potentially re-

encounter newly-repolarised tissue and cause further depolarisation before the arrival of a new excitatory impulse from the normal cardiac conduction pathway. Depending on the speed of propagation and action potential duration this process can continuously repeat to cause a sustained re-entry arrhythmia (Marine et al., 2001).

After-depolarisations are caused by spontaneous depolarising currents occurring either shortly after or during the repolarisation process. These can result in the spontaneous triggering of a further action potential which will then propagate to the surrounding tissue. Typically such depolarisations are the result of elevated intracellular Ca^{2+} overload triggering NCX current shuttling Ca^{2+} out and Na^{+} in (Zeng and Rudy, 1995).

1.5.1.2 Consequences of cardiac arrhythmias

As a consequence of an arrhythmia the patient may exhibit symptoms of dizziness, fatigue, palpitations, accompanied by the clinically observations of rhythm disturbance, bradycardia, sinus pauses, or in more severe cases sinus arrest, sinus exit block and re-entrant arrhythmias, which without treatment may result in sudden death. With the onset of AF, ventricular filling and therefore cardiac output is reduced, which can lead to further increases in left atrial pressure as compensation. As a result, the onset of AF may develop into acute heart failure, which is more likely in older people due to the additional burdens of elevated vascular and left ventricular stiffness (Ward and Witham, 2009). AF is present in up to 40% of patients hospitalised with heart failure and has a strong link with congestive heart failure (CHF) where CHF predisposes to AF (Ward and Witham, 2009). Patients having one of these disorders are at increased risk of developing the other (Wang et al., 2003). Therefore having an arrhythmia may not be fatal by its self, but places the sufferer at increased risk of other fatal illness/diseases, which escalate in propensity and severity with increasing age.

1.6 The effect of ageing on the heart

Each chapter (3, 4 and 5) highlights the detailed alterations in specific cardiac tissue with age, however, the overall notable differences will be mentioned briefly.

1.6.1 Animal models of ageing

To investigate ageing it must be deemed necessary to use an invasive process which ethically prevents the use of human tissue. Rodents have long been used to study age-associated cardiac changes, most commonly rats and mice (Lompre et al., 1991b,

Josephson et al., 2002, Allah et al., 2011). The lifespan of rodents are relatively short which is advantageous in ageing models, rats have a maximum lifespan of approximately 38 months, which is species and strain specific (Lipman et al., 1996), and mice up to 36 months (Blackwell et al., 1995). To define the term at which "old age" is reached, mortality rates would be considered 50%. Using previously determined survival curves (Bomhard et al., 1997) it can be estimated that 6 months of age rats are equivalent to young-adults and 24 months old rats are equivalent to approximately 70 year old humans.

1.6.2 Structural and functional changes

Apart from vascular changes there are numerous age-related cardiac tissue changes which affect both the structure and function. Structural changes are most noticeable with the continual change being the decrease in number of cardiomyocytes with age so that in a centenarian heart only approximately one-third of its original heart cell number remains (Olivetti et al., 1991). Similarly the number of pacemaker cells present in the SA node also decreases. Further changes include the increase in elastic and collagen tissue in all parts of the conduction system, with fat accumulation around the SA node which can sometimes produce a partial or complete separation of the node from the atrial cardiac tissue (Fraticelli et al., 1989, Song et al., 1999). Additionally there is an age-associated degree of calcification of the left side of the cardiac skeleton which involves the aortic and mitral annuli, the central fibrous body and the interventricular septum (Fornieri et al., 1992). Calcification of these regions may affect the AV node, Bundle of His and its branches at the bottom of the apex due to their proximity to the affected tissues (Lakatta and Sollott, 2002).

To overcome the previously mentioned reduction in arterial compliance the heart must compensate by pumping with a greater force. The heart would respond as any other muscle would when faced with increased load which is to enlarge, also known as ‘hypertrophy’. The LV is the most affected region, where the wall thickness can increase up to 30% between the ages of 20 to 80 and cardiac mass also increases (Docherty, 1990). Hypertrophy is associated with remodelling of various signalling circuits that would alter gene expression and directly coordinate hypertrophic growth (Heineke and Molkentin, 2006). In addition Ca^{2+} stores and pathways was shown to mediate hypertrophic signalling (Wu et al., 2006); consequently alterations to these pathways link together the relationship between ageing and hypertrophy development.

1.6.3 Ageing effects on Ca^{2+} transient

Further age-associated alterations in Ca^{2+} handling within the ventricles directly affects ventricular AP. The main reported finding was the prolongation of the AP (Wei et al., 1984). This was attributed to the inactivation kinetics of the I_{CaL} and I_{TO}. Due to the prolongation of the AP, the Ca^{2+} transient and contraction amplitudes in elderly cardiac muscle is preserved (Capasso et al., 1983). More recent work has debated that prolongation is an adaptation to sustain youthful $[Ca^{2+}]_i$ regulation (Janczewski et al., 2002). Overall the prolonged Ca^{2+} elevation is due to the reduced rate of Ca^{2+} being sequestered back into the SR via the SERCA pump (Froehlich et al., 1978). This reduction is due to the reduced expression of the SERCA2a protein (Lompre et al., 1991a). Perhaps to partially compensate for the reduced velocity of Ca^{2+} pumping into the SR some studies have shown an increased expression of NCX acting to remove Ca^{2+} across the sarcolemma (Wong et al., 1998). The longer period of elevated concentration of Ca^{2+} with each action potential allows the myocardium of aged hearts to generate force for a longer period of time during excitation enabling further ejection of blood during late systole, which is beneficial when confronted with increased vascular stiffness. However the trade-off is that the senescent myocardium is more susceptible to Ca^{2+} overload (Hano et al., 1995); a dysregulation of Ca^{2+} homeostasis can lead to impaired contraction, development of arrhythmias and cell death.

The extended action potential and calcium transient associated with ageing is potentially a problem since when the heart rate is fast there is a lack of time for the internal calcium to decrease back to resting levels, diastole is thus incomplete and cardiac filling and ejection limited (Morgan et al., 1990). This issue particularly arises during tachycardic arrhythmias where the high beating frequency can result in a precipitous fall in cardiac output. Furthermore with ageing, the number of β adrenergic receptors decreases and changes occur in adenylyl cyclase isoform expression (Roth et al., 1998) reducing the production of cAMP in response to adrenergic stimulation. This decline in the signalling pathways that normally activate SERCA and improve ventricular response can limit the dynamic range of cardiac performance in the elderly.

Alterations in Ca^{2+} regulation has been acknowledged in specific regions, primarily the LV, but is never compared to the remaining heart. Each chamber may undergo different degrees of remodelling, as such Ca^{2+} homeostasis may become dysfunctional. Mismanagement of Ca^{2+} has previously been associated with arrhythmogenesis, particularly in the SA node which as with the rest of the heart also shows signs of deterioration with age.

1.6.4 Effect of ageing on the SA node

Sinus dysfunction can result in rhythm disturbances, bradycardia, sinus pauses, sinus arrest and arrhythmias (Jones et al., 2007b). The relative accumulation of collagen in the human SA node increases with age, but past adulthood showed no further significant differences (Alings et al., 1995). Linked to the rise in the percentage of collagen, in the human atria, is the increased variability in atrial conduction (Spach and Dolber, 1986). Furthermore there is significant structural remodelling and fibrosis of the SA node (Segawa et al., 1996) which in combination may cause a conduction block and thus lead to an arrhythmogenic episode. This separation and suppression can initiate or perpetuate a cardiac arrhythmia as the disconnected areas can display intrinsic automaticity and the disrupted conductivity may be the foundation for a re-entrant atrial arrhythmia – such as atrial flutter; a potentially fatal problem due to the associated significant reduction in diastolic filling. A more recent study into atrial remodelling in elderly patients highlighted conduction slowing and voltage loss particularly around the crista terminalis region - instigating this region as a sight for arrhythmogenic activity (Kistler et al., 2004).

Ageing also induces molecular changes within the SA node; ranging from reduced expression of $Ca_v1.2$ channel protein (Jones et al., 2007b) to decreases in connexion expression and associated inter-cellular conduction (Jones et al., 2004). Alterations to calcium handling and shuttling within the SA node would result in changes to the regular impulses. Such a change will result in decreased excitability of the nodal tissue, a reduced action potential upstroke velocity and a consequent reduction in the reliability of propagation of the action potential. Such an alteration is likely to also lead to a reduction in intracellular calcium which may affect SR-dependent modes of pacemaking and pacemaker response limiting the dynamic range of SA node function (Vinogradova et al., 2010). A reduced maximal heart rate response with ageing is a conserved finding between studies but it is yet to be confirmed that intracellular calcium alterations are key to this fundamental change in cardiac response.

Such age-associated disruption of conduction is not unique to the atria. It has also been documented as a result of age-associated calcification at the aortic and mitral annuli, the central fibrous body or the inter-ventricular septum. These in turn can affect the functionality of the AV node, bundle of His and branches at the apex (Bhat et al., 1974). Again such disruption of conduction, this time through the ventricles, paves the way for uneven conduction of the cardiac action potential and increases the risk of re-entrant arrhythmias such as ventricular tachycardia (Mercando et al., 1995).

1.7 Aims of study

The process of ageing affects all regions of the heart; however, the differing function of each region may result in divergent Ca^{2+} regulation remodelling. The changes in the atria would vary to those of the ventricles based on output demand of each; furthermore within each area there is additional subdivision of the systemic to pulmonary system. Investigations into age-associated alterations to Ca^{2+} handling proteins across the whole heart will provide new insights in the ageing cardiovascular field. The initial aims of this study were therefore:

I. To identify the origins of age-associated diminished response to increased cardiovascular demand and the relationship between likelihood of an arrhythmogenic episode and age.
II. To define the effect of the ageing process on Ca^{2+} handling protein expression in each region of the heart.

Chapter 2 Materials and methods

2.1 Heart sample acquisition

General Reagents:

All reagents were purchased from Sigma Aldrich U.K. unless otherwise stated.

Principle:

Cardioplegic solution, which brings on asystole, was used to transfer the heart to the dissection dish. Tyrode's solution, an isotonic interstitial fluid, was used throughout dissection and electrophysiology techniques. GNI solution (glucose, sodium acetate and insulin) was added separately as an energy source, and calcium chloride as a source of calcium ions.

Reagents:

Cardioplegic Solution (4°C) (1L:	277.5mM Glucose
	30mM KCl
	25mM $NaHCO_3$
	34.2mM Mannitol
2x Strength Bicarbonate-buffered Tyrode Solution (10L):	
	187.5mM NaCl
	40mM $NaHCO_3$
	2mM Na_2HPO_4
	2mM $MgSO_4 \cdot 7H_2O$
	10mM KCl
Daily solution (4°C) (500ml):	1M Glucose
(dilute 1:100 in tyrode solution)	2M Na Acetate
	100U/ml Insulin
Extra Addition:	2mM $CaCl_2$
	ddH_2O

2.1.1 Acquisition of hearts

Protocol:

Male Han Wistar rats were aged to 6 months, 12 months and 24 months. In accordance with UK Home Office guidelines all animals were maintained until sacrificed by the Schedule one procedure of anaesthetic overdose, followed by exsanguination. Each animal was weighed, the heart removed and weighed. Hearts were rinsed in oxygenated bicarbonate-buffered Tyrode solution at 37°C then placed in cold cardioplegic solution. Hearts were dissected into regions of interest and tissue was either mounted for sectioning or stored in 1.5ml eppendorfs, initially frozen in liquid nitrogen and stored at -80^{o}C. Ethical permission was given by The University of Hull for the use of animal tissue within this study.

2.1.2 Dissection of the whole heart

Protocol:

Double-strength Tyrode solution (10L) was made in advance, stored at room temperature and used within 4 weeks. Single-strength Tyrode solution was made immediately before use, by diluting 1L of double-strength Tyrode solution with 1L dd$H_2$0. The daily solution was stored at 4°C for a month; 10 ml was added per litre of single strength Tyrode solution. $CaCl_2$ was added to the single strength Tyrode solution at a quantity specific to the species, for rat 2mM was used.

The heart was removed by cutting through the diaphragm and rib cage on either side of the thoracic cavity. The aorta and heart were gently lifted and an incision was made across the aorta, pulmonary vein and any other attached tissue then immersed in cold cardiologic solution. The heart was placed in a large petri dish with a silicone based plastic dish containing 37°C oxygenated bicarbonate-buffered Tyrode solution. Insect pins were used to impede the heart in the centre; smaller pins were used to pin out the atria to give clear access to the aorta (Figure 2.1A). The apex was held by tweezers and removed from left to right. An incision was made along the septum to dissect away the right ventricle. Cutting through the left ventricle wall on either side of the septum, it was stored as the ‘rest’ sample for other analyses. The left ventricle was trimmed and stored as multiple aliquots; the epicardium and endocardium were removed while the ‘middle’ myocardium was stored with the septum. To separate the epicardium and endocardium, the outer and inner wall respectively, was sheared off using small

dissection scissors, so that only the first layer was removed. The left and right atria were pinned (Figure 2.1B), the left atria cut to release from atrial septum.

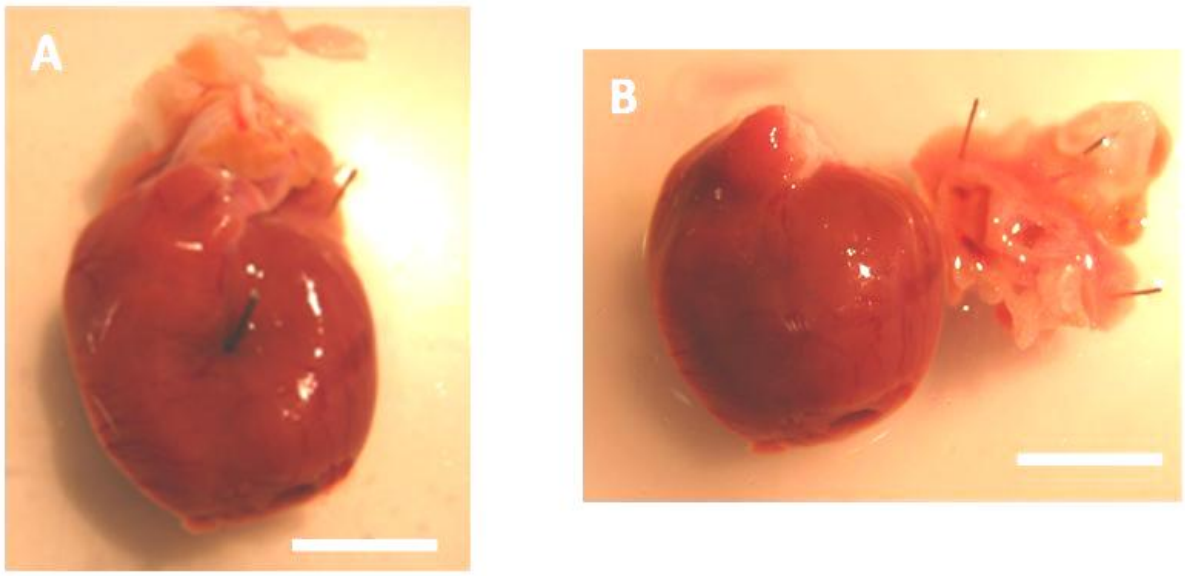

Figure 2.1 Rat Heart:

The heart was pinned in the centre to prevent movement (A) and the atria were cut at the base of the aorta separating them from the ventricles (B). Scale bar indicates 10mm.

2.1.3 Dissection of Sinoatrial Node

Protocol:

The right atrium includes the intercaval region, crista terminalis, superior vena cava, inferior vena cava and any remaining aorta. The superior and inferior vena cava were opened and pinned to expose the intercaval region, which contained the sinoatrial node (Figure 2.2). The right atrial muscle is located at the top left with the branching muscles visible. The crista terminalis (CT) located in the middle of the preparation runs from the top left of the superior vena cava (SVC) to the bottom near the inferior vena cava (IVC). The far right side of the preparation is the septum (S) which was originally attached to the left atrium. In the centre is labelled the sinoatrial (SA) node.

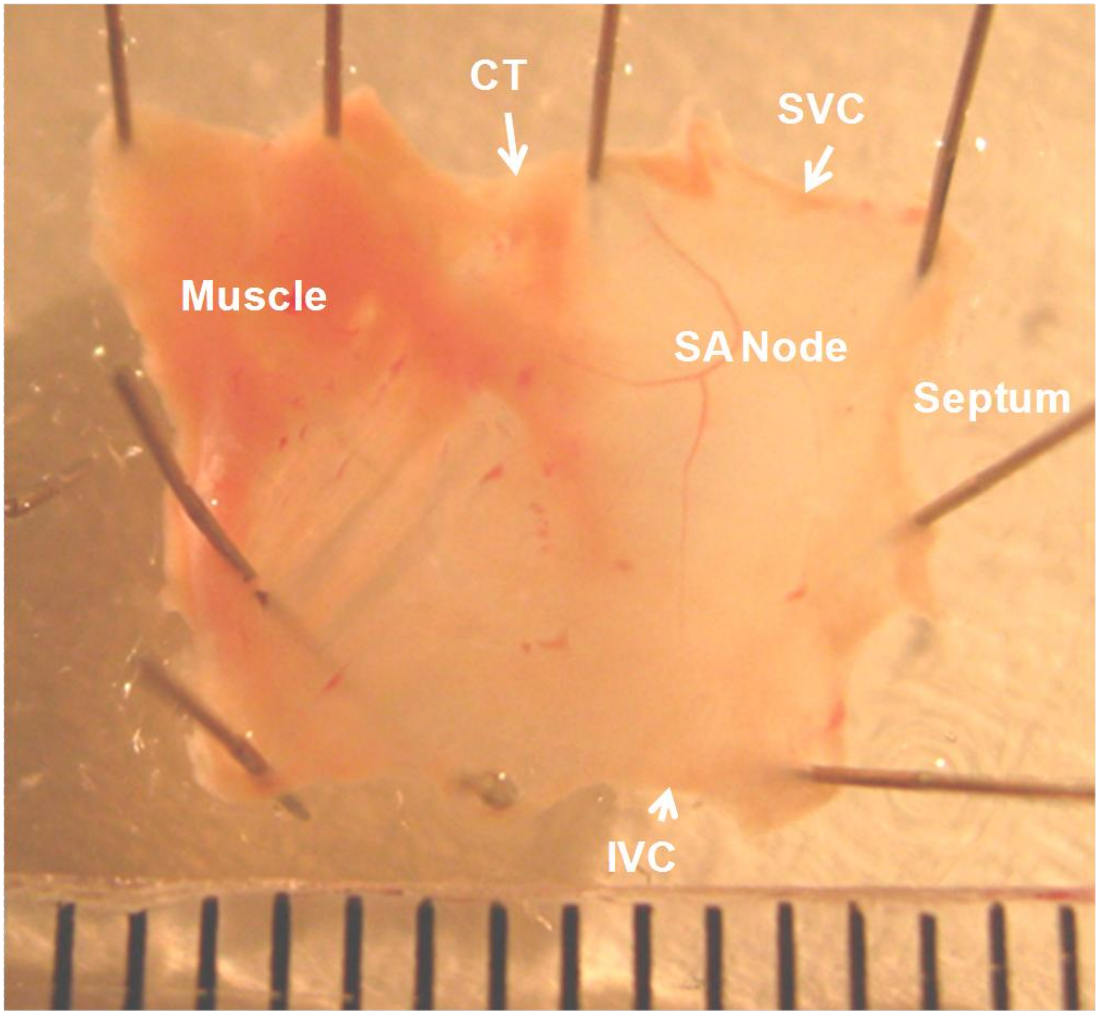

Figure 2.2 Right Atrium.

The right atrium encompassing the SA node is shown with a ruler indicating 1mm intervals. Structures are labelled: crista terminalis (CT), sinoatrial (SA) node, superior vena cava (SVC), inferior vena cava (IVC)

2.2 Western Blotting

Principle:

Proteins present in cell lysates are separated dependent on their molecular weight via a sodium dodecyl sulphate polyacrylamide gel electrophoresis (SDS-PAGE). Once the proteins separated, they were transferred to a nitrocellulose membrane by the process of discontinuous electrophoresis. The membrane was processed using complexes of antibodies to reveal quantities of specific proteins.

2.2.1 Sample Preparation

Reagents:

Protease inhibitors (5 ml):	1% SDS
(Stored in aliquots	1mM iodoacetimide
at –20^{o}C)	1mM benzathonium chloride
	5.7mM Phenylmethylsulfonylfluoride (PMSF)
	ddH_20
Homogenisation buffer (5ml):	500µl protease inhibitors
(freshly made as required)	10mM EDTA
	300mM sucrose
	0.35mM SDS
	Phosphate buffer saline pH 7.2 (4.5ml)

Protocol:

Using a pestle and mortar heart tissue was crushed under liquid nitrogen into a fine powder and suspended in homogenisation buffer. Each sample was subjected to one cycle of freeze-thaw, and then centrifuged at 5000g for 5 minutes at 4°C. The cell lysate was removed and stored at 80°C.

2.2.2 Bicinchoninic Acid (BCA) method of determining protein concentration

Principle:

Protein concentration was measured using the BCA protein assay kit (Pierce Scientific, U.K), based on a previously developed technique (Smith et al., 1985). In alkaline conditions present protein reduces Cu (II) to Cu (I); a chromogen specific to Cu I, bicinchoninic acid, forms a purple complex. Absorption of the complex formed was measured at 565nm and was deemed directly proportional to protein concentration.

Reagents:

Reagent A: Bicinchoninic acid (BSA) solution contains:

25mM BCA-Na_2, 160mM $NaCO_3.H_2O$

7.0mM Na_2tartrate, 0.1M NaOH

$NaHCO_3$; pH 11.25

Reagent B: 160mM $Cu_2O_4.5H_2O$

Protein standards were prepared from a stock solution of 1mg/ml Bovine Serum Albumin (BSA) in 0.15M NaCl with 7.7mM NaN_3, diluted to 250µg/ml.

Protocol:

Reagent B and Reagent A were combined in a ratio of 1:50, to produce Reagent C for immediate usage. A 96-well plate was used; 10µl of standard or sample per well (in triplicate) mixed with 190µl of Reagent C. Samples were routinely diluted by a factor of 15. The plate was incubated for a minimum of 30 minutes at room temp or overnight at 4°C. Absorbance was measured at 565nm using a Biotek plate reader (Biotek Instruments, U.S.A). The protein standard curve was plotted in Excel (Microsoft) and the protein concentration of each sample calculated (for example, see figure 2.3).

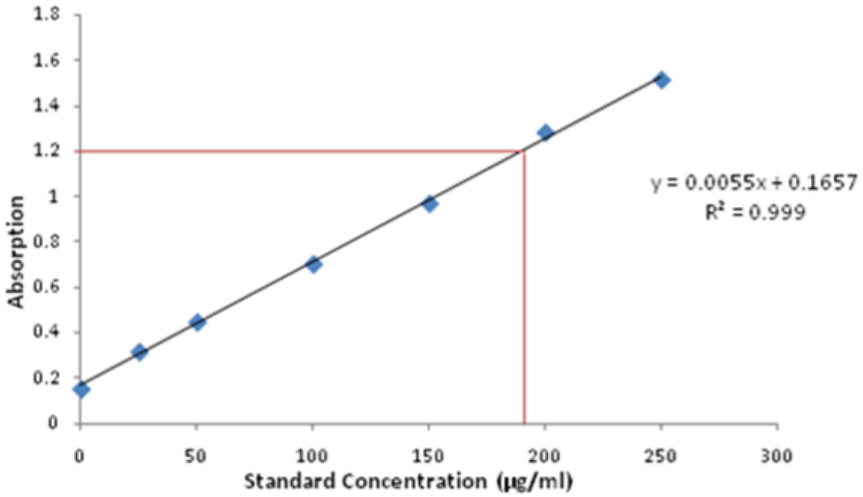

Figure 2.3 Protein standard curve.

Plotted values of absorption at standard concentrations of 0, 25, 50, 100, 150, 200 and 250µg/ml with a line of regression and r value.

Using the linear regression equation, the protein concentration for a mean absorbance of each sample triplicate was calculated. Ideal R^2 should be near to 1.0.

Example calculation for a protein sample:

Average absorption: 1.2 1.2 x 15 (dilution factor) = 18

Equation of gradient: y= 0.0055x + 0.1657

Use and rearrange the equation: (18 - 0.1657) ÷ 0.0055 = 3242.6 µg/ml

Divide to obtain protein per µl: 3242.6 ÷ 1000 = 3.2426 µg/µl

For 40µg of protein: 40 ÷ 3.2426 = 12.34µl.

Thus, 40ug of protein is contained within 12.34ul.

2.2.3 Preparations of samples for western blot

Reagents:

Laemmli Buffer:

0.125M Tris-HCl, pH6.8

0.2M glycerol

0.15M SDS

72mM bromophenol blue

0.6mM β2-mercaptoethanol

ddH_2O

Protocol:

An appropriate amount of protein was mixed with 5µl of laemmli buffer and then made-up to a final volume of 25µl with homogenisation buffer. All samples were heated at 80°C for 10 minutes and allowed to cool before loading on to the SDS-PAGE. SDS, an anionic detergent, was applied to generate negatively charged proteins. Binding of the SDS to the polypeptide chain resulted in an even distribution of charge per unit mass which allowed protein separation by approximate size (Weber and Osborn, 1969).

2.2.4 SDS-Polyacrylamide Gel (SDS-PAGE)

Principle:

SDS-PAGE technique to allow the separation of proteins according to their electrophoretic mobility.

Reagents:

Protogel: 30% ($^{w}/_{v}$) acrylamide

0.8% ($^{w}/_{v}$) bisacrylamide

Protogel buffer: 1.5M Tris-HCl, 0.384% SDS, pH 8.8

Protogel stacking buffer: 0.5M Tris-HCl, 0.4% SDS, pH 6.8

Ammonium persulphate: 0.44M in ddH_2O

TEMED: 6.7M in ddH_2O

Protocol:

Flat and spacer plates were cleaned with water, followed by ethanol to ensure no dust nor debris were present. A permanent marker and ruler were used to mark 1cm below the comb to allow easy estimation when pouring the running gel to ensure correct ratios of running to stacking gel. For a 10% running gel, 2ml of protogel, 2.6ml of protogel buffer and 5.3ml of dH_2O were mixed. Then 10µl of TEMED and 100µl of ammonium persulphate were added and the mixture was rapidly poured between the glass plates; a single vertical slab gel measuring 10cm x 8cm x 1.5mm one flat plate was prepared for use with the mini-protean (Bio-Rad Laboratories, U.K). A small amount of water-saturated butanol was added as on the top of the running gel to prevent oxidation and eliminate air bubbles.

The water-saturated butanol was removed, the top layer rinsed with pure water and dried with filter paper. The 4% stacking gel consisting of 0.65ml of protogel, 1.25ml of protogel stacking buffer and 3.05ml of dH_2O with an addition of 5µl of TEMED and 50µl of ammonium persulphate, was poured onto the running gel and a 15 well comb was inserted across the top.

2.2.5 Electrophoresis

Principle:

Electrophoresis is the process of movement of dispersed particles relative to the buffer under the influence of an electrically charged field. This was conducted using a BioRad electrophoresis tank with a power pack (BioRad Laboratories, U.K). Subsequently the gel was removed from the plates for electroimmunoblotting.

Reagents:

Electrophoresis buffer (10x concentration): 0.25M Tris

1.92M glycine

1% SDS

Protocol:

The set gel was placed in the electrophoresis tank and electrophoresis buffer (National Diagnostics, U.K) was diluted in 1L ddH_20, added to the tank and gel combs removed. The wells were washed with further electrophoresis buffer using a disposable plastic pipette. Samples and rainbow molecular weight marker (Amersham GE Healthcare; U.K) were loaded and electrophoresis was carried out. Initially 10mA ran the samples through the stacking gel; bromophenol blue in the laemmli buffer allowed visualisation of the sample and then the current was increased to 50mA per running gel for 2 hours.

2.2.6 Electroblotting

Principle:

A semi-dry discontinuous electroblotting method dictates the use of filter paper pre-soaked in buffers of varying ions and pH placed in between two plate electrodes. An electric current was passed through and the proteins transferred to a nitrocellulose membrane (Thermo Scentific, U.K); this achieved a fast, homogeneneous transfer.

Reagents:

Anode 1 buffer (A1): 80% 0.3M Tris, pH 10.4

20% methanol

Anode 2 buffer (A2): 80% 25mM Tris, pH 10.4

20% methanol

Cathode buffer (C): 80% 25mM 6-aminonhexanoic acid, pH 7.6

20% methanol

Methanol was purchased from Fisher Scientific, U.K.

Protocol:

Semi-dry method of discontinuous blotting used a TE 77, which (Amersham, Biosciences U.K) consisted of two graphite plate electrodes,;Whatman filter paper

(Fisher Scientific, U.K) was used to act as a reservoir to hold the buffers. On completion of electrophoresis, the gels were removed from the plates and placed on a piece of nitrocellulose membrane (0.45µm pore size) pre-cut to the pre-measured size. The sandwich of filter paper (reservoirs of buffers), gel and nitrocellulose membrane was compiled then placed between the anode and cathode plates as in Figure 2.4. A plastic roller was lightly applied to ensure there were no bubbles between the gel and the nitrocellulose membrane. A constant current density of 0.8mA/cm^2 was applied to the electrodes for 2 hours at room temperature, this equated to 50mA/mm^2 per gel undergoing transfer.

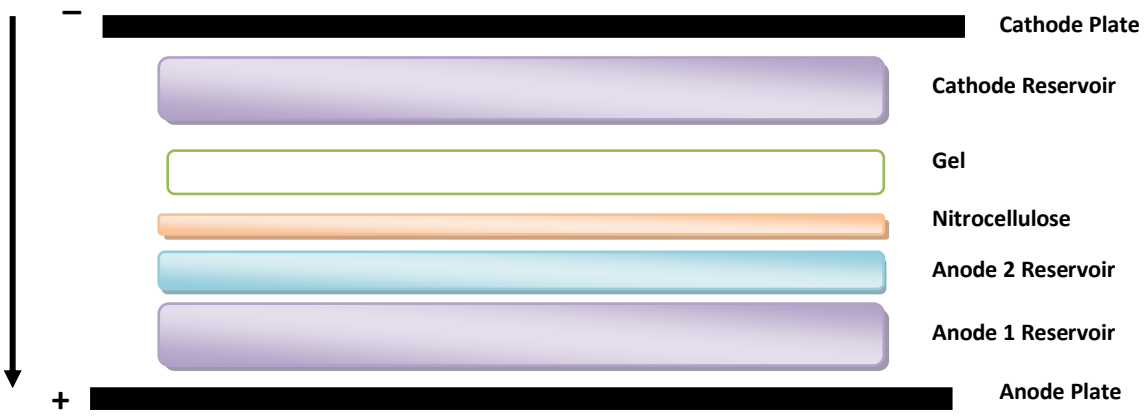

Figure 2.4 Components of semi-dry discontinuous blotting.

The filter paper , gel and nitrocellulose membrane were arranged to form the sandwich.

2.2.7 Probing the nitrocellulose membrane

Reagents:

PBS:	0.05M KH_2PO_4
(2L stock of 10x concentration)	0.05M Na_2HPO_4
	1.3M NaCl
Phosphate Buffer Saline (PBS)-TWEEN:	
	500µl of TWEEN 20 in 1 litre of PBS
Blocking Buffer:	5g dried milk (non-fat) in 100ml of PBS

Secondary buffer:	PBS SuperBlock© Buffer with primary or secondary antibody

Protocol:

Following electroimmunoblotting the nitrocellulose membrane was labelled using a Chinagraph pencil (Royal Sovergeign, U.K), transferred to a clean plastic dish and agitated in blocking buffer for 60 minutes at room temperature. Excess buffer was rinsed three to four times using PBS-TWEEN for at least 5 minutes whilst being agitated. The membrane was transferred to a new plastic dish. PBS superblock buffer (Thermo Scientific, UK) plus primary antibody solution (see Table 2.1) was added and incubated overnight at 4°C. Subsequently the membrane was allowed to reach room temperature whilst being agitated for around 30 minutes. The primary antibody was removed and retained, stored at 4°C for future use. The nitrocellulose membrane was washed three times in PBS-TWEEN for 5 minutes.

The membrane was incubated at room temperature for one hour with the secondary antibody solution (see Table 2.1) whilst being agitated. The PBS Blocking buffer solution contained a non-specific blocking agent. Finally, the membrane was rinsed three times in PBS-TWEEN, for periods of at least 5 minutes each, followed by a 15 minutes final wash.

2.2.8 Visualisation of nitrocellulose membrane

Reagents:

ECL system:	Western Blotting Substrate Kit of reagents 1 and 2 (Pierce Scientific, U.K.)
Film:	Hyperfilm (Amersham Life Sciences, U.K.)
Developer:	Paper Developer Ilford PQ (Harman Technology Ltd., U.K.)
Fixer:	Rapid Fixer Ilford Hypam (Harman Technology Ltd., U.K.)
Acetate:	Transparency Film for copiers (Impega, U.K.)

Equal quantities of reagent 1 and 2 were mixed, poured over the membrane for a short incubation period of 1-2 minutes and then placed between two sheets of acetate and exposed to film. Exposure time was 2 minutes initially. If bands were faint, exposure time was increased - up to 30 minutes. Films were developed using developer for 10-30 seconds until bands were visible and moved to fixer (30 seconds to 2 minutes) until developer was completely removed and films had a clear background.

Alternatively the Bio-Rad Molecular Imager Chemi Doc XRS+ was used to digitally acquire band densities and processed using Image Lab 3.0.

2.2.9 Image analysis

Protocol:

Image J (Version 1.43 Developed by Wayne Rasband, NIH, USA) was used to analyse the intensity of bands. This technique was conducted for all bands including samples and controls. Each band was highlighted using a manually drawn box which was dragged to each subsequent band ensuring the area was kept the same; the total density of the inner boxed area was subsequently calculated. All data were normalised to desmin expression. To compare two separate blots bands were normalised to a sample that was present on both blots. The determining factor was calculated and the sample densities were either multiplied or divided.

Table 2.1 Western blotting: Primary and secondary antibodies, suppliers and dilutions.

Antibody		Host/Type	Manufacturer	Dilution	Diluent	Blocking Buffer
Cav1.2	Primary	Rabbit/polyclonal	Alomone Labs, Israel	1:1000	PBS Superblock Thermo Scientific, U.K	0.25% Tween PBS + 5% milk
	Secondary	Swine Anti-rabbit	Dako, Denmark	1:1000	As above	
PMCA4a	Primary	Mouse/monoclonal	Thermo Scientific, U.S.A	1:1000	As above	As above
	Secondary	Rabbit Anti-mouse	Dako, Denmark	1:1000	As above	
SERCA2a	Primary	Mouse/monoclonal	Thermo Scientific, U.S.A	1:1000	As above	As above
	Secondary	Rabbit Anti-mouse	Dako, Denmark	1:1000	As above	
RYR2	Primary	Mouse/monoclonal	Thermo Scientific, U.S.A	1:1000	As above	As above
	Secondary	Rabbit Anti-mouse	Dako, Denmark	1:1000	As above	
NCX1	Primary	Mouse/monoclonal	Thermo Scientific, U.S.A	1:1000	As above	As above
	Secondary	Rabbit Anti-mouse	Dako, Denmark	1:1000	As above	
PLB	Primary	Mouse/monoclonal	Badrilla Ltd. U.K	1:1000	As above	As above
	Secondary	Rabbit Anti-mouse	Dako, Denmark	1:1000	As above	
Desmin	Primary	Mouse/monoclonal	Dako, Denmark	1:1000	As above	As above
	Secondary	Rabbit Anti-mouse	Dako, Denmark	1:1000	As above	

All secondary antibodies were HRP-conjugated.

2.3 Immunocytochemistry

Principle:

Immunocytochemistry was used to determine the location of proteins, to provide qualitative and quantitative data from frozen tissue sections from various regions of the heart.

2.3.1 Frozen sections

Heart regions were frozen in Tissue-Tek O.C.T (Sakura, NL) which provided a support matrix for cryostat section at temperatures below -10°C. To improve section adhesion to the slide, Poly-L-Lysine slides (Fisher Scientific, U.K) were used. A cryostat (HM505E Microm) was used slice tissue mounted in O.C.T at a thickness of 10µm, which were collected on poly-L-Lysine slide. Slides were labelled and stored at -80°C.

2.3.2 Slide Processing

Reagents:

Wash:	PBS pH 7.2
Fixative:	4% Paraformaldehyde
Detergent solution:	0.05% Triton X-100 in PBS 7.4
Blocking solution:	25% serum (fetal calf serum) (Hyclone, U.K)
	0.1% BSA (0.1g in 100ml of PBS 7.4) (Fluka, U.S.A)

Protocol:

Slides were defrosted and a resin ring was drawn around the tissue. Once the ring was dry (sections were kept moist by using a humidity chamber) the tissue was fixed in 4% Paraformaldehyde (PFA) for 30-40 minutes at room temperature whilst in a fume cupboard. The PFA was removed by washing the tissue section in PBS three times for 5 minutes each. The tissue was incubated for 15-30 minutes in Triton X-100, which perforated the membrane and improved antibody coverage. The slides were rinsed 3 times in PBS for periods of 5 minutes each. To block non-specific sites, blocking

solution was applied for 2 hours. The solution was removed and the slide carefully blotted.

2.3.3 Probing of the tissue section

The primary antibody was diluted in blocking solution (see Table 2.2), applied to the resin ring and was incubated overnight at 4ºC in a humidity chamber.

Following equilibration to room temperature the primary antibody was removed and each slide was washed four times with PBS for a period of 5 minutes each. The secondary antibody was diluted using blocking solution (see Table 2.2) and used to incubate slides for 2 hours in the dark. The secondary antibody was removed and the slides were rinsed with PBS four times for a period of 15 minutes each.

The sections were mounted in Vectashield (Vector Laboratories, CA U.S.A) to prevent photo bleaching. Two small drops of vectorshield, usually one drop per resin ring, were applied to a cover slip, which was placed adjacent to the slide and slowly pressed at an angle onto the cover slip to create a seal. The cover slip was firmly and gently pressed onto the slide to ensure any bubbles were removed and any excess Vectashield was dried and sealed with nail vanish. The slides were allowed to dry in the fridge overnight and stored at 4ºC in the dark until visualised.

2.3.4 Confocal imaging of sections

Reagents:

Immersion oil: Immersol 518F (Carl Zeiss Ltd., U.K)

Lens tissue: Whatman 105 (Whatman International, U.K)

Protocol:

Slides were viewed under a plan apochromat 40x/1.3 oil iris M27 lens using a LSM 710 confocal (Carl Zeiss Ltd.; U.K). ZEN 10 program was used to alter settings whilst LSM Image Browser (Carl Zeiss LSM, U.K) was used to compress, export and view the images.

2.3.5 Analysis of immunocytochemistry sections

Protocol:

Image J was used to analyse the fluorescence of the image. The image was converted to a RGB stack to separate out the fluorescent channels. Using ROI manager the image's threshold was altered so that the fluorescent tissue (channel Alex-Flur 488 only) was highlighted separate to the background and non-fluorescence tissue. This highlighted region was then selected using the 'select wizard wand' and then density of the region was measured. As a control the background was also measured and subtracted from the fluorescent region.

Table 2.2 Immunocytochemistry: Primary and secondary antibodies, suppliers and dilutions.

Antibody		Host/Type	Manufacturer	Dilution	Diluent	Blocking Buffer
Cav1.2	Primary	Rabbit/polyclonal	Alomone Labs, Israel	1:250	25% FCS + 0.1% BSA in PBS	25% FCS + 0.1% BSA in PBS
	Secondary	Goat Anti-rabbit	Invitrogen, U.K	1:1000	As above	
PMCA4a	Primary	Mouse/monoclonal	Thermo Scientific, U.S.A	1:250	As above	As above
	Secondary	Goat Anti-mouse	Invitrogen, U.K	1:1000	As above	
SERCA2a	Primary	Mouse/monoclonal	Thermo Scientific, U.S.A	1:250	As above	As above
	Secondary	Goat Anti-mouse	Invitrogen, U.K	1:1000	As above	
RYR2	Primary	Mouse/monoclonal	Thermo Scientific, U.S.A	1:250	As above	As above
	Secondary	Goat Anti-mouse	Invitrogen, U.K	1:1000	As above	
NCX1	Primary	Mouse/monoclonal	Thermo Scientific, U.S.A	1:250	As above	As above
	Secondary	Goat Anti-mouse	Invitrogen, U.K	1:1000	As above	
PLB	Primary	Mouse/monoclonal	Badrilla Ltd. U.K	1:100	As above	As above
	Secondary	Goat Anti-mouse	Invitrogen, U.K	1:1000	As above	
WGA	Primary			1:500	As above	As above
	Secondary	Goat Anti-mouse	Invitrogen, U.K	1:1000	As above	

All secondary antibodies were Alex-Flor 488 conjugated.

2.4 Mapping of the sinoatrial node region

Principle:

Optical mapping of the SA node provided a novel approach to investigating action potential propagation from the leading pacemaker site and across the CT into the atrial muscle. JPW-603 was used to visualise Ca^{2+} movement and consequently track action potential propagation.

2.4.1 Preparation of the sinoatrial node

The SA node was dissected as previously described (see section 3.0.3) and pinned onto a silicone-based temperature control bath. To improve signal to noise ratio as much fat was possible was removed from the tissue.

2.4.2 Optical mapping of the sinoatrial node

Reagents:

Dye (JPW-603) (12ml):	0.8g/ml of EtOH
Bicarbonate-buffered Tyrode Solution:	
	NaCl 130mM
	$NaHCO_3$ 24mM
	NaH_2PO_4 1.2mM
	$MgCl_2$ 1.0mM
	Glucose 5.6mM
	KCl 4mM
	$CaCl_2$ 1.8mM
Gas:	5% CO_2 95% O_2
Blebbistatin (stock):	0.3M DMSO (frozen)
	10µM per experiment
Isoprenaline:	25nM

Protocol:

Multiple pins were placed around the edge of the SA node tissue to minimise movement of tissue due to the flow of the buffer. The SA node was maintained in oxygenated bicarbonate-buffered Tyrode solution throughout the experiment at 37°C and constantly monitored (Figure 2.5A). Wires connecting the cameras and equipment were insulated and secured to minimise movement and improve signal to noise ratio (Figure 2.5A). Blebbistatin (Sigma Aldrich) was added to the solution to prevent muscle movement once the SA node tissue was in place under the optical camera. Flow was stopped and JPW-603 was added to the buffer, whilst incubated in the dark (Figure 2.5A). Light emitting diodes (LEDs) emitted a 488 wavelength of light and the depolarisation was recorded using the camera (1kHz CCD Hamamatsu 16x16 res). Data were analysed using BigJ software (Figure 2.5B) which showed images of fluorescence, wave depolarisation profiles and allowed manipulation of recordings. Isoprenaline (25nM) was added, to increase heart rate and incubated for 10 minutes before recordings were taken to observe changes in the rate of depolarisation peaks at intervals of 10 minutes for up to an hour.

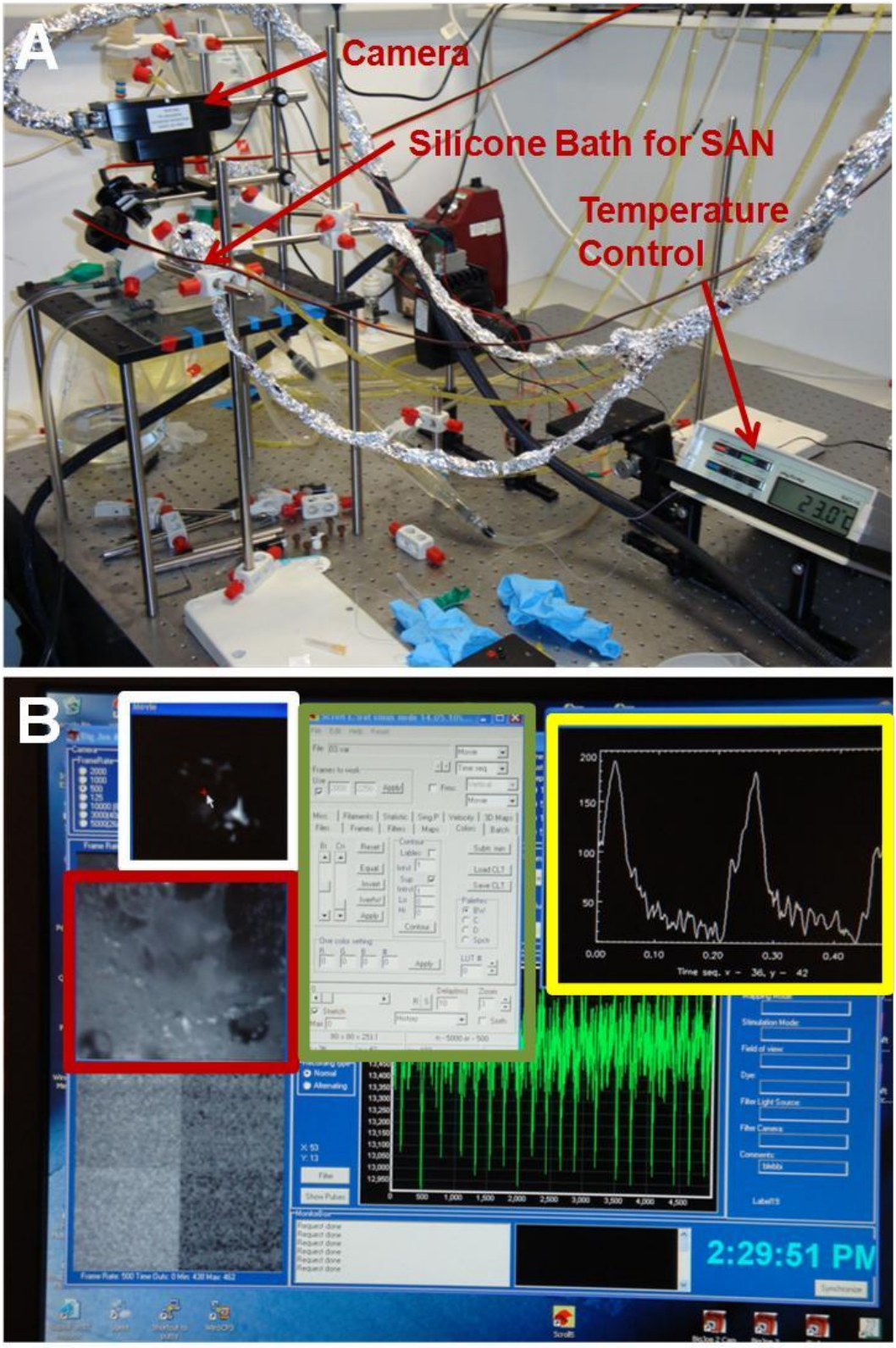

Figure 2.5 Optical mapping and BigJ Software:

A - SA node preparation was setup on a secured stand with a moveable clamp with the LED camera attached above. **B -** White panel was the fluorescent image of the SA node, red panel was the camera view. Yellow panel was the action potentials virtually recorded and the green panel allowed multiple alterations to the properties of how the voltage changes were optically recorded.

2.5 Sinoatrial node mapping

Principle:

SA node mapping was used to measure Ca^{2+} transients and their propagation across the SA node through the CT and into the atrial muscle.

2.5.1 Bi-polar electrode mapping of the SA node

Principle:

Rat SA node was prepared as described previously (see section 2.1.3) and pinned out onto the silicone-based water bath. All equipment was earthed to reduce noise (Figure 2.6).The internal water bath was filled with 168ml of oxygenated bicarbonate-buffered Tyrode solution, maintained at approximately 37°C (RS Temp Monitor 615-8212), and was re circulated at a flow rate of 45ml/min (Watson Marlow Sci 400; Masterflex Consol 77200-62) (Figure 2.7).

Reagents:

Cyclopiazonic acid (CPA):	PBS pH 7.2
	CPA
Isoprenaline disulphate:	PBS pH 7.2
	Isoprenaline disulphate
Nifedipine:	PBS pH 7.2
	Nifedipine
Bicarbonate-buffered Tyrode solution:	NaCl 130mM
	$NaHCO_3$ 24mM
	NaH_2PO_4 1.2mM
	$MgCl_2$ 1.0mM
	Glucose 5.6mM
	KCl 4mM
	$CaCl_2$ 1.8mM
Gas:	5% CO_2 95% O_2

Protocol:

Bipolar electrodes (Figure 2.7) were denoted as either the reference electrode or the leading pacemaker site electrode. Using a microscope (Leica, E.U) a full SA node map was created by fixing the RE on the right atrial muscle and moving the LPSE a millimetre each time (Figure 2.8) across the intercaval region, crista terminalis (CT) and part of the atrial muscle. The electrodes simultaneously recorded the action potential at the two points which was sent through an Axon CNS Digitiser (Digidata 1440A; Digitimer Hum Bug) and visualised using Clampex 10.1. The intrinsic heart rate was calculated based on the RE recordings; the number of APs occurring in 30 seconds was counted and then doubled to produce intrinsic heart rate data.

For CPA and isoprenaline studies the whole SA node was not mapped, instead the LPSE was used to mark the leading pacemaker site (LPS) and its shift according to chemical application noted. Throughout the dose response study the RE was not moved from its original site.

The preparation was washed in oxygenated bicarbonate-buffered Tyrode solution before being dissected into separate regions then frozen using liquid nitrogen and stored at -80°C.

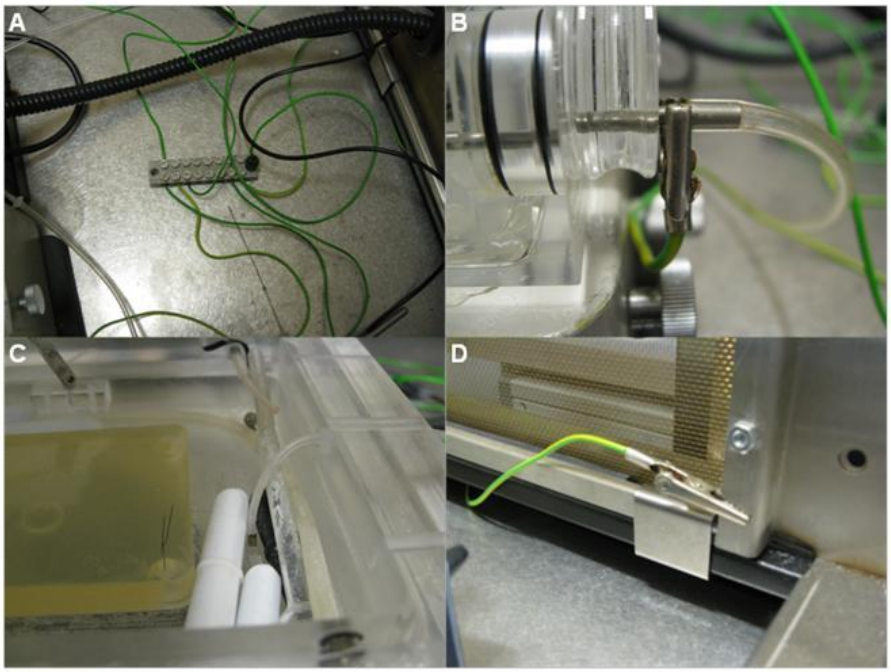

Figure 2.6 Earthing of the electrophysiology equipment:

To reduce noise all equipment was earthed (A) this included the water bath (B) the internal water (C) and the Faraday cage (D).

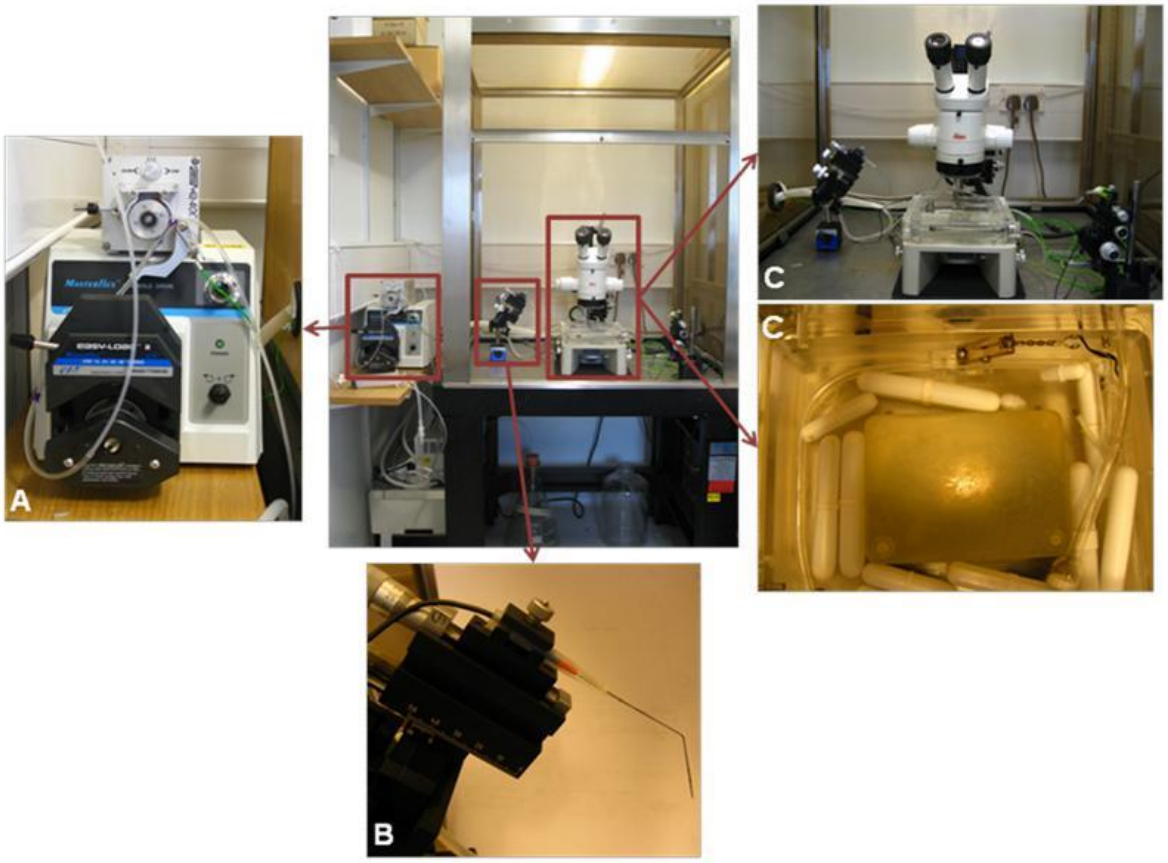

Figure 2.7 Electrophysiology Rig setup:

The flow was controlled by a Microflex pump (A). Electrodes were move manually across the SA node region (B). The SA node preparation was pinned to the silicone bath placed underneath the microscope (C).

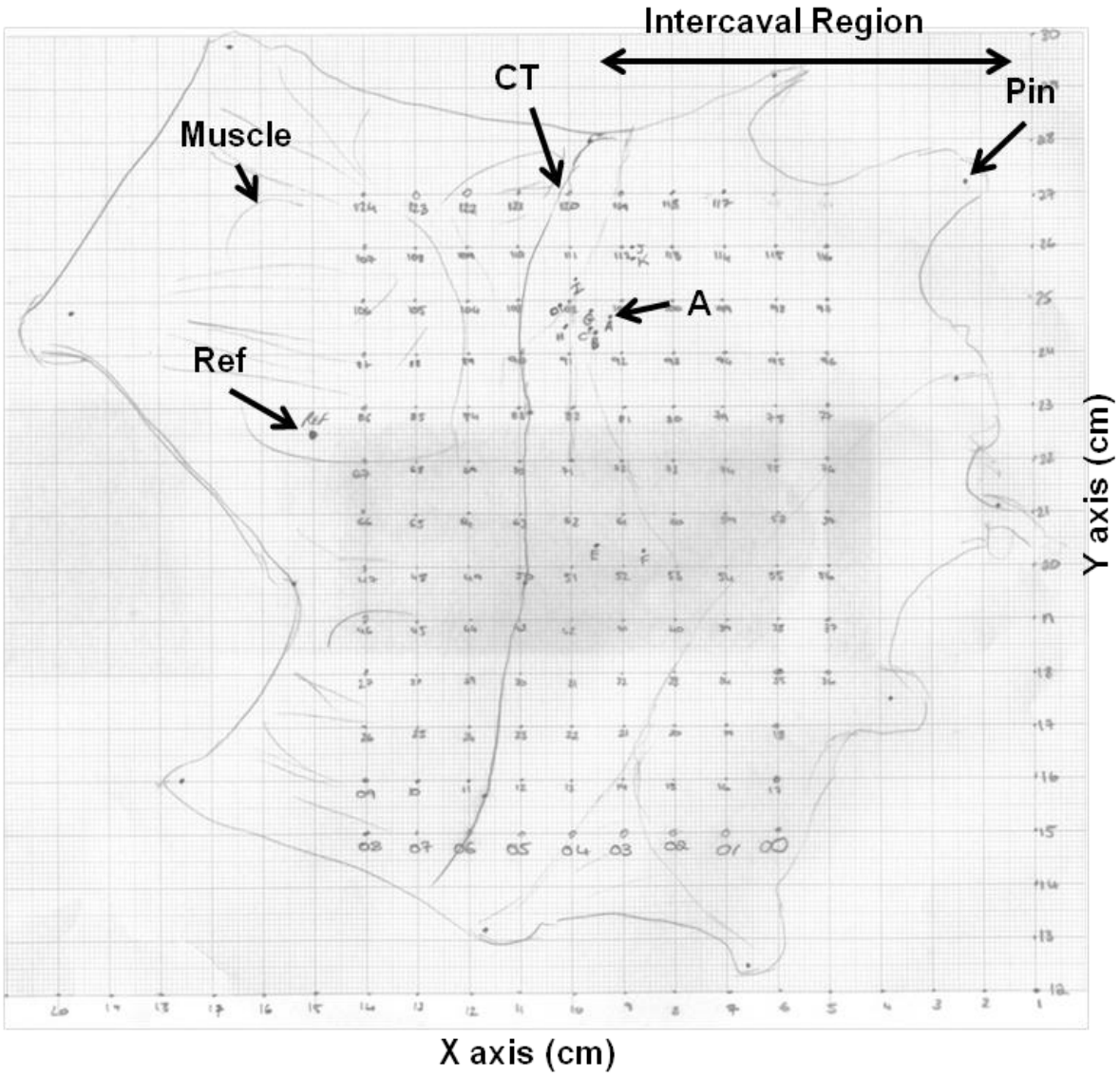

Figure 2.8 SA node map:

The map was drawn as viewed underneath the microscope, points were made for pin location and approximate tissue contours drawn such as the crista terminalis (CT). Location of the reference electrode was denoted as 'ref', the leading pacemaker site was recorded and denoted as letters A to H. Scale of the y and x axis is 1cm per large square which denoted 1mm on the preparation.

2.5.2 Analysis of electrophysiological recordings

Programs:

Clampex 10.1

Sigma Plot Version 12.0

Protocol:

The simultaneous recordings of the bipolar electrodes allowed the action potential propagation and velocity to be calculated. Clampex 10.1 was used to analyse action potential time points generated by the LPSE versus the RE. The difference was subtracted and divided by the distance between the electrodes to calculate the velocity.

The full SA node map was used to create 3D contour maps to analyse action potential propagation and velocity. Sigma plot (Version 12.0) was used to calculate the 3D contour of action potentials recorded at each cm point of the map.

2.6 RNA and real-time PCR

Tissue was harvested as described in section 2.1 and crushed using a mortar and pestle under DNAse and RNAse free conditions for RNA extraction.

2.6.1 Total RNA Extraction

Principle:

Column-based nucleic acid purification technique was used to obtain total RNA from crushed cardiac tissue. An RNeasy Fibrous Tissue Mini Kit (Qiagen) was used. The RNeasy mini spin column combined guanidine- isothiocyanate lysis of cells with a silica-membrane to quickly acquire high purity RNA.

Reagents:

B Mecaptoethanol – 10µl
RNase free ethanol – 500ml
RNAeasy Fibrous Tissue Mini Kit (Qiagen) containing:
- RPE Buffer
- Proteinase K (additional)
- RLT Buffer
- RNAse Free Water
- RW1 Buffer
- DNAse
- RDD Buffer

Protocol:

To 1 ml of buffer RLT, 10 µl of β-ME was added and 4:1 ratio of absolute Ethanol was added to the RPE buffer to obtain a working solution. The DNAse I stock was prepared by dissolving the lyophilised DNAse I in 550µl of RNAse-free water and mixed by gentle inversion and stored as 100µl aliquots at -20°C. Thawed aliquots were stored at 2-8°C for up to 6 weeks, but were not re-frozen. Tissue samples were weighed (30mg-60mg), transferred from a to 2ml cryovial (RNAse/DNAse-free) and 300µl of β-ME/buffer RLT was added followed by 590 µl of RNAse/DNAse-free water. Proteinase K solution was added, 10µl per sample, and mixed thoroughly by pipetting. Samples were incubated for 15 minutes at 55°C, and then centrifuged at 20-25°C for 3 minutes

at 10,000 × g. The supernatant (approx 900µl) was transferred to a new eppendorf and 500µl of ethanol (96-100%) was added and mixed by gentle inversion.

Approximately 700µl of the sample, including any precipitate that may have formed, was transferred to an RNAeasy Mini spin column placed in a 2 ml collection tube and centrifuged at 20–25°C for 15 s at ≥8000 x g (≥ 10,000 rpm). The flow-through was discarded. This step was repeated for the remaining sample using the same collection tube, the flow-through again being discarded. Subsequently 350µl of RW1 buffer was added to the RNAeasy spin column and centrifuged at 20–25°C for 15 s at ≥ 8000 x g (≥ 10,000 rpm) to wash the membrane. The flow-through was discarded. To 70 µl Buffer RDD, 10 µl of DNAse I stock solution was added (per sample) and centrifuged briefly to collect residual liquid from the sides of the tube. The DNAse solution (78µl to account for pipetting errors) was then directly added to the RNAeasy spin column membrane and incubated at room temperature for 15 minutes.

Samples were rinsed by adding 350µl RW1 buffer to the RNAeasy spin column and centrifuging for 15 s at ≥ 8000 × g (≥ 10,000 rpm) at 20-25°C, the flow-through was discarded. The membrane was rinsed twice using 500µl of RPE buffer (pre-mixed with ethanol). The sample was incubated at room temperature for 3 minutes before being centrifuged at 20–25°C for 15 seconds at ≥ 8000 x g (≥ 10,000 rpm).

After centrifugation the RNAeasy spin column was carefully removed from the collection tube. The RNAeasy spin column was transferred to a new 2ml eppendorf tube and centrifuged at approx 20,000 x g for 1 minute to ensure that all RPE buffer was removed. The RNAeasy spin-column was then transferred to a 1.5ml eppendorf and 36µl of RNAse-free water was added directly to the column membrane, incubated at room temperature for 10 minutes and centrifuged for 1 minute at 12,000 x g at 20-25°C. The membrane was rinsed a further two times using the same elute and centrifuged to ensure that all RNA has been transferred from the membrane to the water.

2.6.2 RNA Concentration Analysis- NanoDrop 1000

Reagents:

RNAse-free water (Ambion, U.S.A)

Lense wipes

Protocol:

For the machine to be calibrated and zeroed, 1.2µl of RNAse-free water was pipetted onto the reader and the lid closed. This was then repeated using 1.2µl of sample and the program (NanoDrop 1000) recorded the absorbance from which the concentration of each sample was calculated.

2.6.3 Reverse Transcription (cDNA Synthesis)

Principle:

Reverse transcriptase was used to reverse transcribe RNA into its DNA complement (complementary DNA or cDNA) which was then amplified using the polymerase chain reaction (PCR) technique.

Reagents (per 2µg sample):

Purchased from Invitrogen U.K unless otherwise stated

2µg total RNA sample (according to calculated concentration)

2µl DNase Buffer

2µl DNase

2µl EDTA 25nM

1µl Random Primers (Promega)

1µL Nuclease free water (Ambion, U.S A.) } MM1

2µl 10mM dNTP mix

8µl 5x First Strand Buffer

2µl DTT 0.1M } MM2

2µl RNAse OUT

2µl Supercript III

Protocol:

Two samples were made, a positive reverse transcription (RT) which would contain detectable cDNA and a negative RT used as a control to look at background fluorescence. The extracted tRNA concentrations (see section 2.6.1) were used to calculate the volume required for 2µg of mRNA. DNAse buffer (20000x concentration)

and DNase enzyme was added, made up to 20µl using RNAse/DNAse free water and incubated at room temperature for 15 minutes. EDTA was added and incubated for a further 10 minutes at 65°C. The sample was cooled on ice and centrifuged. Master mix 1 (MM1) was made by adding of random primers, nuclease free water and 10mM dNTP. 4µl of the MM1 was incubated with the sample for 5 minutes at 65°C, cooled on ice and centrifuged.

Master mix 2 (MM2) was made by adding 5x first strand buffer and DTT (0.1M); 10µl of MM2 was added to the sample. To each positive RT sample RNAse OUT and Superscript III was added. To each negative RT sample RNAse/DNAse free water was added instead of RNAse OUT and Superscript III. A Techne PCR machine was used to heat the sample for 5 minutes at 25°C followed by 60 minutes at 50°C and lastly 15 minutes at 70°C. cDNA samples were stored at 2-4°C for a maximum of 3 days and at -20°C for longer periods of time.

2.6.4 qPCR - Test amplification of cDNA

Principle:

To detect the cDNA within each sample, end point qPCR was used with forward and reverse actin primers (Sigma Aldrich, U.K) and SYBR safe (Life Technologies, U.K) was added to the agarose gel.

Reagents (per 1µl of cDNA sample):

1µl cDNA sample

10µl ReddyMix

1µl Forward Actin Primer

1µl Reverse Actin Primer

7µl RNAse/DNAse free water

} MM3

TAE Buffer (50x): 2.0M TRIS Acetate

100mM Na_2EDTA

Agarose Gel 2.5%:

2.5g Agarose Powder

5µl SYBR Safe DNA gel stain

5µl Hyperladder IV

Protocol:

Actin was used to test the positive RT samples. Master mix 3 (MM3) was made by adding Reddymix (Thermo Scientific, U.K), forward primers, reverse primers to RNase/DNase free water. To each 1µl of cDNA sample, 19µl of the MM3 was added and placed in a Techne PCR machine. Samples were heated at 95°C for 2 minutes followed by 25 cycles of 95°C for 25 seconds, 65°C for 35 seconds, 72°C for 65 seconds and lastly 72°C for 5 minutes.

A 2.5% agarose gel was made by dissolving agarose powder in 100ml of a 1 x concentration of TAE buffer (National Diagnostics, UK). The mixture was swirled then heated in the microwave. The agarose was cooled under cold tap water until warm to the touch whilst being continuously swirled to ensure the solution did not set. SYBR Safe (Life Technologies, U.K) was added to the gel which was poured into a mould with a 30 wells comb and left to set for 15 minutes.

The comb was removed and TAE buffer was added to the electrophoresis tank (Bio-Rad Laboratories, U.K). Hyperladder IV (Bioline, U.K) was used as a marker. Positive RT samples were loaded first (10-15µl), space was left (3-4 wells), followed by the remaining negative RT samples. The gel was run at 100V for a maximum of 45 minutes or until the samples were a third way down the gel. The gel was imaged using a Bio-Rad Molecular Imager Chemi Doc XRS+.

2.6.5 qPCR – StepOne Plus Applied Biosystems

Principle:

Real Time PCR or quantitative PCR (RT-PCR; qPCR) was used to detect and quantify sequence expression in a DNA sample. Gene expression assays were used to detect specific DNA sequences. Oligonucleotides labelled with a VIC/FAM fluorescent reporter hybridise to the DNA target sequence and fluoresce.

Reagents (per well):

Purchased from Applied Biosystems, U.S.A.

1µl cDNA Sample

10µl TaqMan Fast Master Mix

1µl TaqMan Gene Expression Assay

1µl TaqMan Endogenous Control

7µl DNAse/RNAse free water

} MM4

Equipment:

Purchased from Applied Biosystems, U.S

MicroAmp Fast Optical 96 Wells Plate

Optical Adhesive Cover

Applied Biosystems StepOne Plus

StepOne Software 2.2

Protocol:

Master mix 4 (MM4) was made by adding TaqMan Fast Master mix, TaqMan Gene Expression Assay (Table 2.4), TaqMan endogenous control and DNAse/RNAse free water. To each of the 96 wells 1µl of cDNA sample was added followed by 19µl of master mix. Negative controls in triplicates consisted either of 1µl of negative RT control (no cDNA) or a no template control (NTC) which was 1µl of DNAse and RNAse free water. Consequently this provided dual controls to test the background fluorescence of all chemicals excluding the presence of cDNA.

The plate was sealed using an optical adhesive cover and analysed on Applied Biosystems StepOne Plus qPCR machine. StepOne Software (Version 2.2) was used to initiate the program, setup the plate, and analyse the data.

Table 2.3 qPCR 96-well plate layout:

	Wells 1 2 3	Wells 4 5 6	Wells 7 8 9	Wells 10 11 12
A	No RT	Sample 7	Sample 15	Sample 23
B	NTC	Sample 8	Sample 16	Sample 24
C	Sample 1	Sample 9	Sample 17	Sample 25
D	Sample 2	Sample 10	Sample 18	Sample 26
E	Sample 3	Sample 11	Sample 19	Sample 27
F	Sample 4	Sample 12	Sample 20	Sample 28
G	Sample 5	Sample 13	Sample 21	Sample 29
H	Sample 6	Sample 14	Sample 22	Sample 30

Layout for 30 samples and controls: No RT represents a negative RT sample, whereas NTC represents a no template control which consisted of DNAse/RNAse free water.

In the qPCR assay, a positive reaction was determined by accumulation of fluorescent signal, all primers were labelled with FAM fluorescence except for desmin which was VIC labelled. The cycle threshold (C_T) was detected and recorded; the C_T is defined as the number of cycles required for the fluorescent signal to exceed the 'background fluorescence', known as the threshold. These C_T levels are inversely proportional to the amount of target nucleic acid in the sample, consequently the lower the C_T level the greater amount of target nucleic acid in the sample. All transcript primers were tested and optimised to insure a C_T value of 29 or less was achieved, as these are considered strong positive reactions indicative of abundant target nucleic acid.

Table 2.4 qPCR: Primers, reference codes, fluorescent labels and suppliers.

Primer	Host/Reference	Manufacturer	Fluorescence Tag
Actin Forward	Rat_ActB_F	Sigma Aldrich U.K. SY101204499-003	N/A
Actin Reverse	Rat_ACTB_R	Sigma Aldrich U.K. SY101204499-004	N/A
Cav1.2 Cacna1c	Rat NM_012517	Invitrogen, U.K. Rn00709287_m1	FAM
RYR2 Ryr2	Rat NM_001191043.1	Invitrogen, U.K. Rn01470303_m1	FAM
SERCA2a Atp2a2	Rat NM_001110139.2	Invitrogen, U.K. Rn00568762_m1	FAM
NCX1 Slc8a1	Rat NM_019268.2	Invitrogen, U.K Rn00570527_m1	FAM
Desmin Des	Rat NM_022531.1	Invitrogen, U.K Rn00574732_m1	VIC
GAPDH Gapdh	Rat NM_017008.3	Invitrogen, U.K. Rn01775763_g1	VIC
TaqMan Gene Expression Master Mix (5ml)	N/A	Invitrogen, U.K. Cat No. 4369016	ROX

All primers were used as part of the TaqMan Gene Expression Assay kits.

Chapter 3 Effect of ageing on Ca^{2+} regulation involved in spontaneous activity of the sinoatrial node

3.1 Introduction

3.1.1 Sinoatrial node

Visualised on the endocardial surface, the sinoatrial (SA) node is located in the right atrium between the crista terminalis (CT) and intercaval region (flanked by the superior and inferior vena) (Opthof, 1988) as shown in figure 3.1. It is a spontaneously active, heterogeneous region of tissue and is the primary pacemaker of the heart. Congregated nodal cells, also referred to as the leading pacemaker cells, often vary in location and size depending on species (Opthof et al., 1985, Opthof et al., 1986), but in all cases instigation of an impulse is driven by calcium ions (Ca^{2+}) and drives the upstroke of the action potential in the SA node (Verheijck et al., 1999).

3.1.2 Calcium handling within the SA node

3.1.2.1 Mechanisms behind SA node spontaneous beating

Multiple mechanisms revolving around calcium handling proteins are implicated in the spontaneous activity of the SA node (see section 1.4). There are two main debates, spontaneous SR release also called local calcium releases (LCR) or 'calcium clock' and the funny current (I_f) (Lakatta and Difrancesco, 2009).

Spontaneous rhythmic Ca^{2+} cycling involves the SERCA pump to replenish SR Ca^{2+} content and ryanodine receptors (RYRs) for sub-sarcolemmal local Ca^{2+} release. The plant alkaloid ryanodine, which causes RYRs to remain in a sub-conductance state was used to access RYR2 function. The application of ryanodine resulted in depletion of SR Ca^{2+} content, reduced AP amplitude in SA nodal cells (Satoh, 1997), impaired activation of NCX1 (Zhou and Lipsius, 1993) and overall caused slowing of the spontaneous beating rate (Li et al., 1997). Further evidence using voltage clamp of SA nodal cells, LCRs were observed to be spontaneous and rhythmic, which generated current fluctuations due to the NCX1 (Bogdanov et al., 2001). This led to further work which investigated the sub-sarcolemmal RYR-NCX interaction which showed that both transporters are co-localised at the microscopic level (Lyashkov et al., 2007).

The LCR period is determined by the speed at which SR cycles Ca^{2+} (Vinogradova et al., 2004). Factors that affect the kinetics of SR Ca^{2+} cycling include the available Ca^{2+} for pumping and activity of SERCA2a and RYR2 function (Vinogradova et al., 2010).

To determine the crucial role of SERCA2a function in spontaneous pacemaker firing Vinogradova *et al.* used cyclopiazonic acid (CPA), an inhibitor of Ca^{2+} ATP-ase (Goeger et al., 1988), to suppress SERCA activity and found decreases in spontaneous beating rate of up to 50% in rabbit SA nodal cells (Vinogradova et al., 2010). Furthermore the reduced spontaneous beating rate was observed to be a result of prolongation of the LCR period due to the diminished SR Ca^{2+} refilling time. The decline in LCR number and size, due to CPA, delays the occurrence of the LCR-activated NCX1, which in turn reduces I_{NCX} amplitude leading to a decrease in diastolic depolarisation (Vinogradova et al., 2010).

PLB regulates the speed at which Ca^{2+} is pumped into the SR; in its unphosphorylated state PLB binds to SERCA2a and inhibits its function (Colyer and Wang, 1991). Phosphorylation of PLB occurs via cAMP-mediated, PKA-dependent activation which increases SERCA2a activity and therefore speed of relaxation (Colyer and Wang, 1991). By increasing PKA-dependent phosphorylation of PLB via β-adrenergic stimulation LCR period can be decreased shortening spontaneous cycle length and thus increasing heart rate (Vinogradova et al., 2010). Though this can be attributed to enhanced SERCA2a activity, changes in PLB phosphorylation have also been shown to play an important role in cardiac pacemaker function (Zhai et al., 2000).

Alternatively I_f channels are also able to generate diastolic depolarisation phase of the AP and thus be responsible for spontaneous activity. I_f channels, first discovered in 1979, are activated by a hyperpolarised membrane resulting in the term 'funny current' (Brown et al., 1979). These I_f channels were shown to have a threshold of about -40 to -50mV with full activation at -100mV which correlates to the membrane voltage range of diastolic depolarisation (Baruscotti et al., 2005). I_f channels have also been shown to be directly affected by β adrenergic stimulation and thus could contribute to increasing spontaneous beating rate (DiFrancesco et al., 1986).The 'funny current' channels are expressed by the HCN gene of which there are 4 isoforms, HCN4 is the dominant isoform in SA node and other pacemaker tissue (Shi et al., 1999). Expression of HCN4 was noted to be highly concentrated in the central node, decreasing in the periphery and finally disappearing in the right atria (RA) muscle tissue (Liu et al., 2007). The role of I_f in pacemaker activity is being studied extensively by the use of genetic remodellingand over-expression of HCN with a previous study showing steepened diastolic depolarisation and doubling in rate of beating in ventricular myocytes (Qu et al., 2001).

Nevertheless ablation of the HCN4 gene via knock-out mice showed pacemaker activity was reduced only by approximately 50% (Stieber et al., 2003). In addition

inhibition of I_f channels, using the drug ivabradine, slowed the spontaneous firing rate but did not cease completely (Yaniv et al., 2012a). Both these studies indicate that I_f channels are important in generating spontaneous activity in pacemaker tissue but may not be the exclusive mechanism involved in spontaneous activity. Consequently it is possible that a combination of both LCR and I_f channels might explain the instigation of spontaneous activity within the SA node.

3.1.3 Effect of ageing on spontaneous SA node activity

Whether initiating the heart beat or simply modulating activity of the cardiac pacemaker, the role of intracellular Ca^{2+} is essential for normal cardiac pacemaker function. Studies have shown that intracellular calcium regulation in the SA nodal cells changes with progressive ageing and this has been associated with a slowing in spontaneous pacemaker activity (Jones et al., 2007a), depressed β-adrenergic response of the heart (Turner et al., 1999) and an increased incidence of pacemaker anomalies seen in those greater than 65 years old (Brown, 1982). Such dysfunction of the sinoatrial node is also likely to increase the probability of developing atrial arrhythmias (Hartel and Talvensaari, 1975). Consequently, the elderly account for the majority of individuals requiring artificial pacemaker implants to support a failing sinoatrial node with over 600,000 pacemakers implanted worldwide per year (Wood and Ellenbogen, 2002).

3.1.3.1 Effect of ageing on proteins key to pacemaker activity

Atrial arrhythmias have increased prevalence in the elderly population, thus many studies have focused on changes in calcium handling proteins/mRNA expression during such dysfunction. RYR2 mRNA investigated in the RA of patients suffering from AF and was found to not change with age, though no study of RYR2 protein was conducted (Lai et al., 1999). A more relevant ageing study investigated RYR2 mRNA and protein expression in the SA node of 25 months of age rats and was observed to both decrease with age (Tellez et al., 2011). RYRs role in controlling heart rate was previously made clear, but gain-of-function via knock-in mouse models has been associated with arrhythmia generation and sudden cardiac death (Chelu et al., 2009). In contrast RYR2 knockout mice did not have the opposite effect, lower levels of expression contributed to fatal arrhythmias (Bround et al., 2012). In association with RYR2, NCX1 mRNA was observed to not change significantly with age but investigation into protein levels were not performed (Tellez et al., 2011). Within the

same study investigation into HCN4 mRNA expression showed an up-regulation in the 25 months old rats in both the SA node and RA muscle (Tellez et al., 2011).

SERCA2a protein has not been investigated within the SA node, but within the RA muscle mRNA and protein levels were observed to not change significantly with age. However, calcium ATP-ase activity significantly decreased with age (Kaplan et al., 2007). To partially explain the decrease in activity a more recent study showed contradictory data with decreased mRNA levels in the SA node and atrial muscle of 25 months old rats (Tellez et al., 2011). Similarly in human patients suffering from AF SERCA2a mRNA was down-regulated (Lai et al., 1999).

$Ca_v1.2$ channels, responsible for the upstroke of the AP in the SA node and for the main influx of Ca^{2+}, were shown to decline in the ageing guinea pig; with drastic decreases noted from 18 months of age onwards (Jones et al., 2007a). Similarly in the rat, the decrease in $Ca_v1.2$ protein can be explained by Tellez *et al.* who showed decreased $Ca_v1.2$ mRNA expression within the SA node. In addition human patients affected by AF also showed decreased levels of $Ca_v1.2$ mRNA (Lai et al., 1999). Though protein or mRNA levels may not be the only change with age; a study in ageing ventricular cells showed that the properties of $Ca_v1.2$ channels gating were altered which included an increase in the average probability of being open (Josephson et al., 2002).

3.1.3.2 Effect of ageing on AP propagation across the SA node

Propagation across cardiac tissue is facilitated by gap junctions, which have been studied and located between nodal cells (Opthof, 1994). Within these gap junctions are connexins allowing movement of ions between cells (Harfst et al., 1990). Conduction velocity across the SA node is reliant on this movement. With age conduction velocity has been previously shown to increase (Alings and Bouman, 1993). In contrast a study by Jones *et al.* in 2004 investigated age-associated changes to connexin expression in the SA node. They reported a decline in connexin 43 protein, which is the most abundant form in cardiac tissue, within the centre of the SA node; this area of tissue lacking connexin 43 progressively increased across the animal's lifespan. No change was reported in connexin 40 or 45 but conduction maps showed AP conduction time and conduction distance increased proportionally with age whereas conduction velocity decreased, highlighting the importance of connexin 43 protein (Jones et al., 2004).

3.1.4 Effect of ageing on exercise and β-adrenergic stimulation on mammalian intrinsic heart rate

With age, the ability to respond to stress or exercise becomes diminished, this is partially attributed to the reduced ability to increase heart rate (Fleg et al., 2005). One of the most notable changes to the ageing cardiovascular system is the diminished responsiveness to β-adrenergic stimulation (Turner et al., 1999). Some studies have shown that the density of β-receptors is selectively decreased with ageing (Roth et al., 1998) and additional deficits in the protein kinase A signalling cascade (Liu et al., 2011) (Lakatta and Sollott, 2002). Evidence suggests reduced contractile force is due to the failure of β-adrenergic stimulation to increase intracellular calcium transients to the same extent in senescent hearts compared with younger hearts (Xiao et al., 1994). This may be attributed to reduced availability of $Ca_v1.2$ channels and thus diminished influx, or possibly to alterations in SR function.

3.1.5 Effect of age on the sensitivity to nifedipine

Nifedipine, and its analogues, are used to treat resistant hypertension (Zemancikova and Torok, 2009). Nifedipine is a dihydropyridine which selectively blocks the α1-subunit of $Ca_v1.2$ channels to shut down the channels preventing calcium ions from entering the cell. At low concentrations nifedipine lessens cellular Ca^{2+} influx and consequently SR Ca^{2+} content; this reduces the contractile force of the cardiac tissue, thus reducing hypertension.

With age, the sensitivity to nifedipine increases consequently doses should be reduced in patients in elderly patients (Maxwell et al., 2000). It is unknown whether the mechanics of $Ca_v1.2$ channel properties change with age, or if the decrease in $Ca_v1.2$ protein levels is responsible (Jones et al., 2007a). Therefore using an ageing model and incrementing concentration of nifedipine, altered sensitivity can be determined.

3.1.6 Objectives

i. To determine the role of the SR in the spontaneous activity of the SA node and how this changes with the impact of aging.
ii. To investigate the age-associated response to β-adrenergic stimulation and the role of the SERCA, RYR2 and $Ca_v1.2$ in aiding such a response.
iii. To elucidate age-associated changes in AP propagation and conduction velocity within the intercaval region under the influence of isoprenaline and CPA.
iv. To investigate the change in sensitivity to nifedipine with age and determine the potential mechanisms for variations in pacemaker activity on the removal of $Ca_v1.2$ using $Ca_v1.2$, RYR2, SERCA2a and NCX1 protein expression data to explain.

3.1.7 Hypothesis

1. SR calcium cycling is crucial for pacemaker activity and age-associated changes to calcium handling within the SA node will affect this spontaneous activity.

2. β-adrenergic response is reliant on efficient SR calcium cycling via SERCA2a pump activity; with age this decreases, thus β-adrenergic response is diminished.

3. With age Ca^{2+} remodelling occurs in the SA node and has a direct influence on sensitivity to nifedipine.

3.2 Methods

3.2.1 Dissection of right atrium to use in western blotting

Hearts were removed and RA dissected as previously described (see Chapter 2). The RA was pinned out and each region dissected (Figure 3.1) to be frozen, crushed and analysed on an SDS-page gel (see section 2.2).

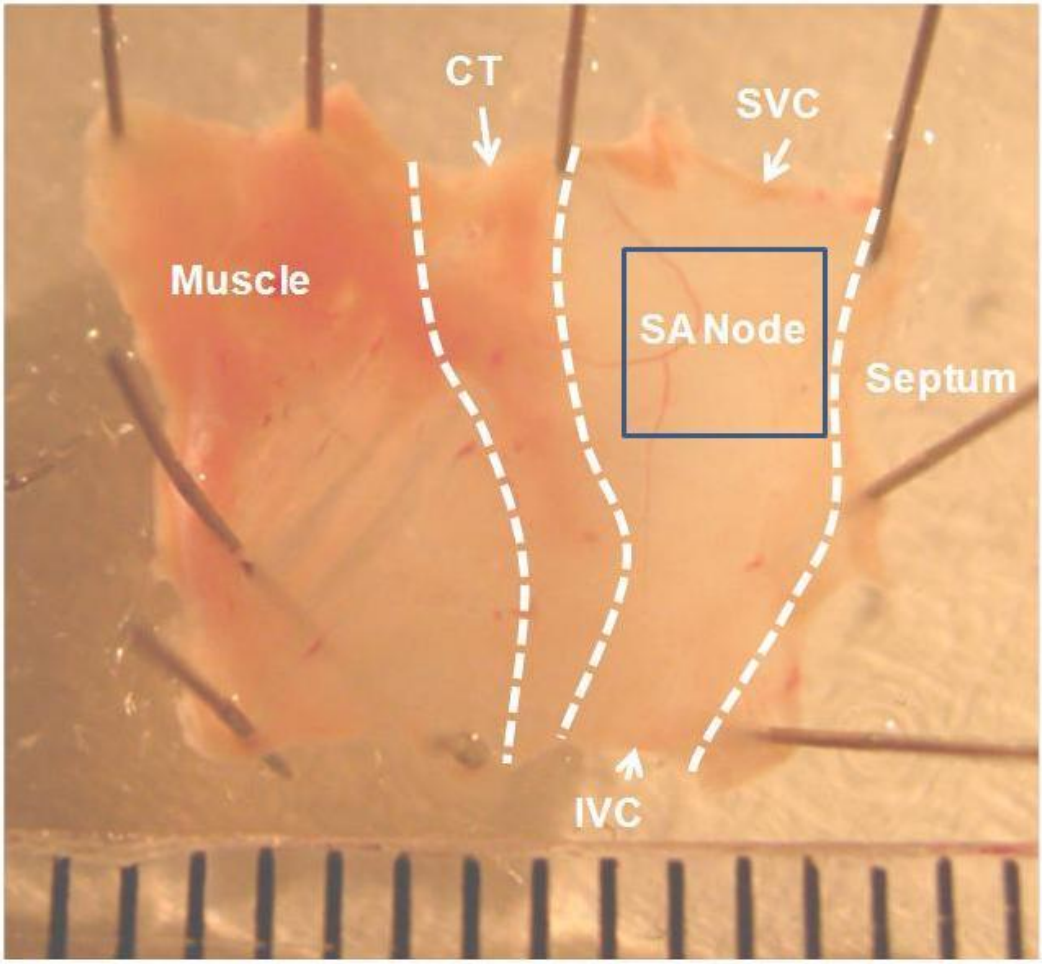

Figure 3.1 Right atrium.

Dashed lines indicate where the RA was dissected to identify each region prior to being frozen in liquid nitrogen and stored at -80°C. Solid square outline highlights centre of the SA node with remaining considered periphery.

3.2.2 Western blotting

Western blotting was performed using extracted protein from dissected region as described in 2.1.2 and protein expression analysed as in 2.2. For dilutions of primary and secondary antibodies for all western blots see Table 2.1.

3.2.2.1 Antibody detection and peptide controls

Optimal conditions for primary and secondary antibodies were determined by the use of dot blots (Figure 3.2). Non-specific binding was established via these dot blots and thus new lots were purchased and the process repeated. This tested the specificity of the antibodies and also allowed the deduction of appropriate dilutions.

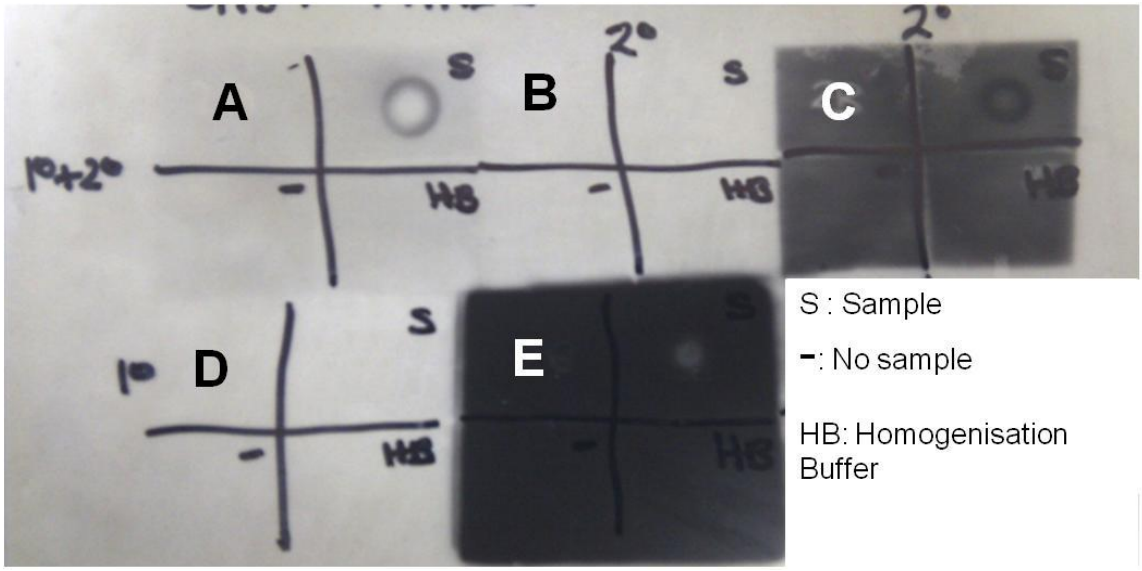

Figure 3.2 Dot blot testing $Ca_v1.2$ antibodies.

A) $Ca_v1.2$ and anti-rabbit secondary antibody B) anti-rabbit secondary only C) alternative anti-rabbit secondary antibody D) $Ca_v1.2$ antibody only E) third alternative anti-rabbit secondary There was clear non-specific binding from two of the anti-rabbit secondary antibodies (C+E).

Once the primary and secondary antibodies were tested to be specific, test western blots were conducted (Figure 3.3). Peptide controls were used to determine whether the band of interest disappeared in the presence of a control.

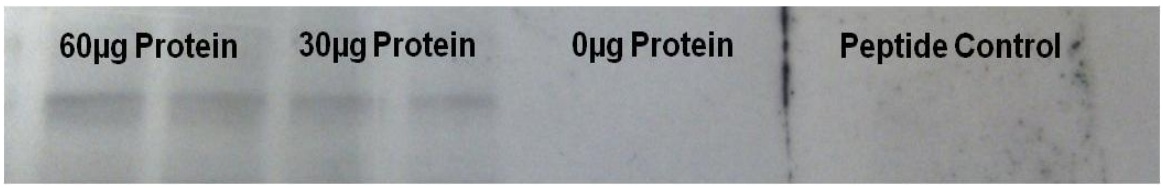

Figure 3.3 Protein loading for $Ca_v1.2$ and the corresponding peptide control.

$Ca_v1.2$ specific peptides bind to the antibody preventing it from binding to the protein. On the left are the bands from non-peptide bound Cav1.2 antibody and on the right is the blot with the peptide bound antibody. This confirms that the band shown is the Cav1.2 protein.

3.2.2.2 Immunoblotting method using methanol-free transfer

To reduce transfer time and remove the use of methanol, Pierce® Fast Semi-Dry transfer (Thermo Scientific, U.S.A) was tested which reduced transfer time to a maximum of 15 minutes (Figure 3.4). Consequently the semi-dry methanol electroblotting technique was conducted for all western blots (see section 2.2.6).

Figure 3.4 Fast semi-dry methanol-free transfer method (A) versus methanol transfer (B).

Bands were more succinct, visible and cleaner when using methanol, compared with the patchy, uneven transfer when using the fast semi-dry transfer.

3.2.3 Bi-polar electrode mapping of the SA node

The heart was removed from the animal, dissected (see section 2.1), the SA node pinned and maintained in 37°C oxygenated Tyrode solution (described in section 2.5.1). Cyclopiazonic acid (CPA), isoprenaline and nifedipine were added at varying concentrations (see table 3.1). These were initially added via direct application to the internal water bath but this produced fluctuations of temperature and heart rate. Therefore the buffer was continuously circulated at a flow of 45ml/min which provided sufficient perfusion of the tissue and a steady temperature. Consequently the drugs were added to the circulating buffer which produced consistent measurements. For intrinsic heart rate recordings a reference electrode was placed on the RA muscle whilst another electrode was located on the leading pacemaker site (LPS) within the SA node region for conduction velocity and pacemaker shift measurements.

Table 3.1 Drugs application and their concentrations

Drug	Concentrations
Cyclopiazonic acid (CPA)	3µM
Isoprenaline	1nM, 10nM, 100nM, 1µM
Nifedipine	0.1µM, 0.3µM, 1µM, 3µM, 10µM, 30µM

3.2.3.1 Pacemaker shift analysis

To analyse the shift in the LPS, locations were noted on drawn maps of the SA node preparation (Figure 3.5). The location of the LPS was calculated by measuring the time delay between the earliest AP noted within the SA node and the propagated AP recorded at the reference electrode. The LPS electrode was moved until the earliest AP impulse was detected, this was then labelled with an alphabetic letter. The LPS under control conditions, Tyrode solution, was pinpointed and in response to the addition of CPA and isoprenaline at each concentration, the new location of LPS was noted. To analyse the shift, the new LPS compared to the control LPS was noted to shift either downward, termed negative shift, and given a value of -1 or shifted upward, termed positive shift, and given a value of 1. If there was no shift in LPS location a value of 0 was allocated for that SA node preparation.

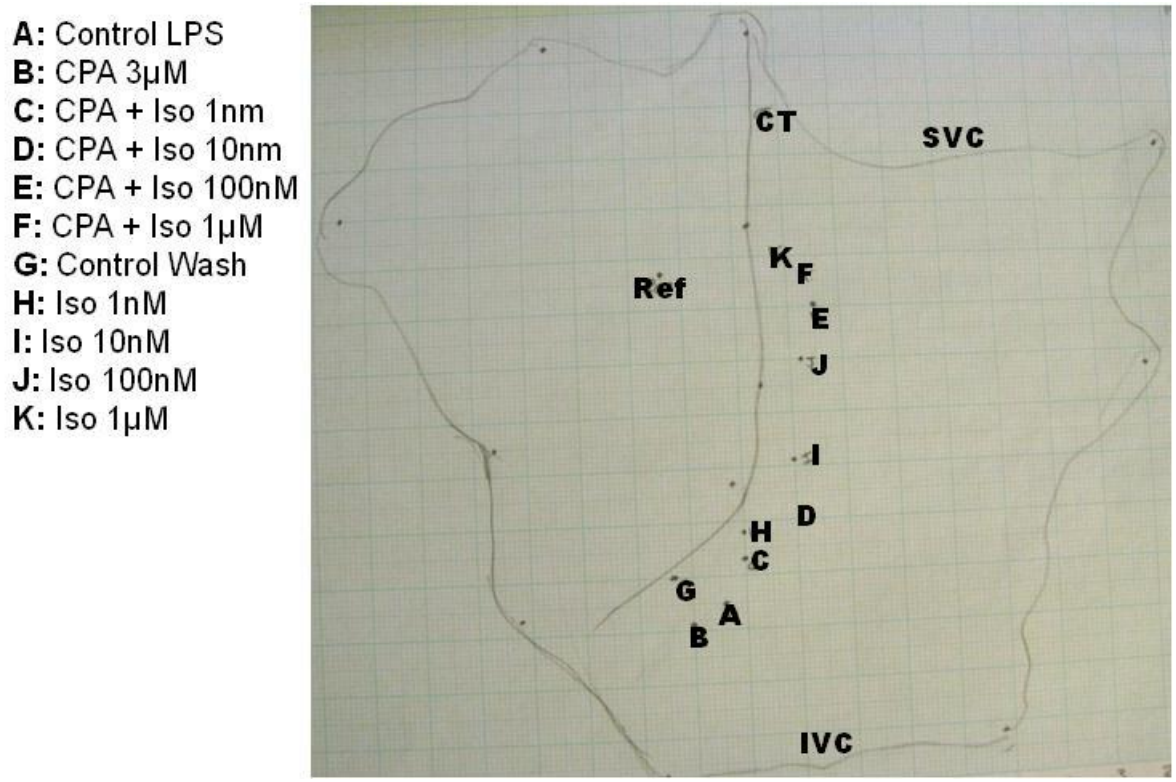

Figure 3.5 Example map of the SA node preparation with labelled LPS.

Labelled using alphabetic letters are the locations of leading pacemaker sites in the presence of isoprenaline (Iso) with and without CPA. Locations of the reference electrode (ref), crista terminalis (CT) and the superior and inferior vena cava (SVC, IVC) are labelled.

3.2.4 Immunocytochemistry

Immunocytochemistry was performed using SA node tissue as described in 2.1.3 and section 2.3. Primary and secondary antibody dilution was determined by testing various dilutions (see table 3.2). Once a good signal to noise ratio was optimised, the dilution was used for data collection (see table 2.2).

Table 3.2 Tested antibody dilutions for immunocytochemistry

Antibody	Dilutions tested
Cav1.2	1:1000; 1:500; 1:250; 1:100; 1:50
PMCA4a	1:1000; 1:500; 1:250; 1:100
SERCA2a	1:1000; 1:500; 1:250; 1:100
PLB	1:1000; 1:500; 1:250; 1:100; 1:50
NCX1	1:1000; 1:500; 1:250; 1:100
RYR2	1:1000; 1:500; 1:250; 1:100
Goat anti-rabbit (Alexa Fluor 488)	1:1000; 1:5000
Goat anti-mouse (Alexa Fluor 488)	1:1000; 1:5000

3.2.5 Statistical analysis

For all western blot and immunocytochemistry data statistical differences were determined using a one way ANOVA with Holm-Sidak comparisons. For each age group 6 (young-adult), 12 (adult) and 24 months (elderly) of age, n=5. Data are presented as means ± SEM.

3.3 Results

3.3.1 Confirmation of protein localisation

To determine positive immunolabelling of each antibody, high resolution scans using a x63 lens located binding of antibodies and was compared with previous studies (Figure 3.6). SERCA2a and PLB are example images from RV sections, arrows show binding of antibody at t-tubule sites. RYR2 binding in the LA is shown at the edges of the sarcolemma membrane with lesser binding at t-tubule sites shown. $Ca_V1.2$ is shown bound to t-tubules throughout the RV as well as the sarcolemma membrane. NCX1 and PMCA4a are shown bound to the majority of the sarcolemma membrane in the RV and LA respectively with some streak patterns of binding throughout the cell, both NCX1 and PMCA4a had more background noise compared to other antibodies. Control image shown is an illustrative RV section without primary or secondary labelling and WGA only image shows the binding of WGA to a RV tissue section (Figure 3.6).

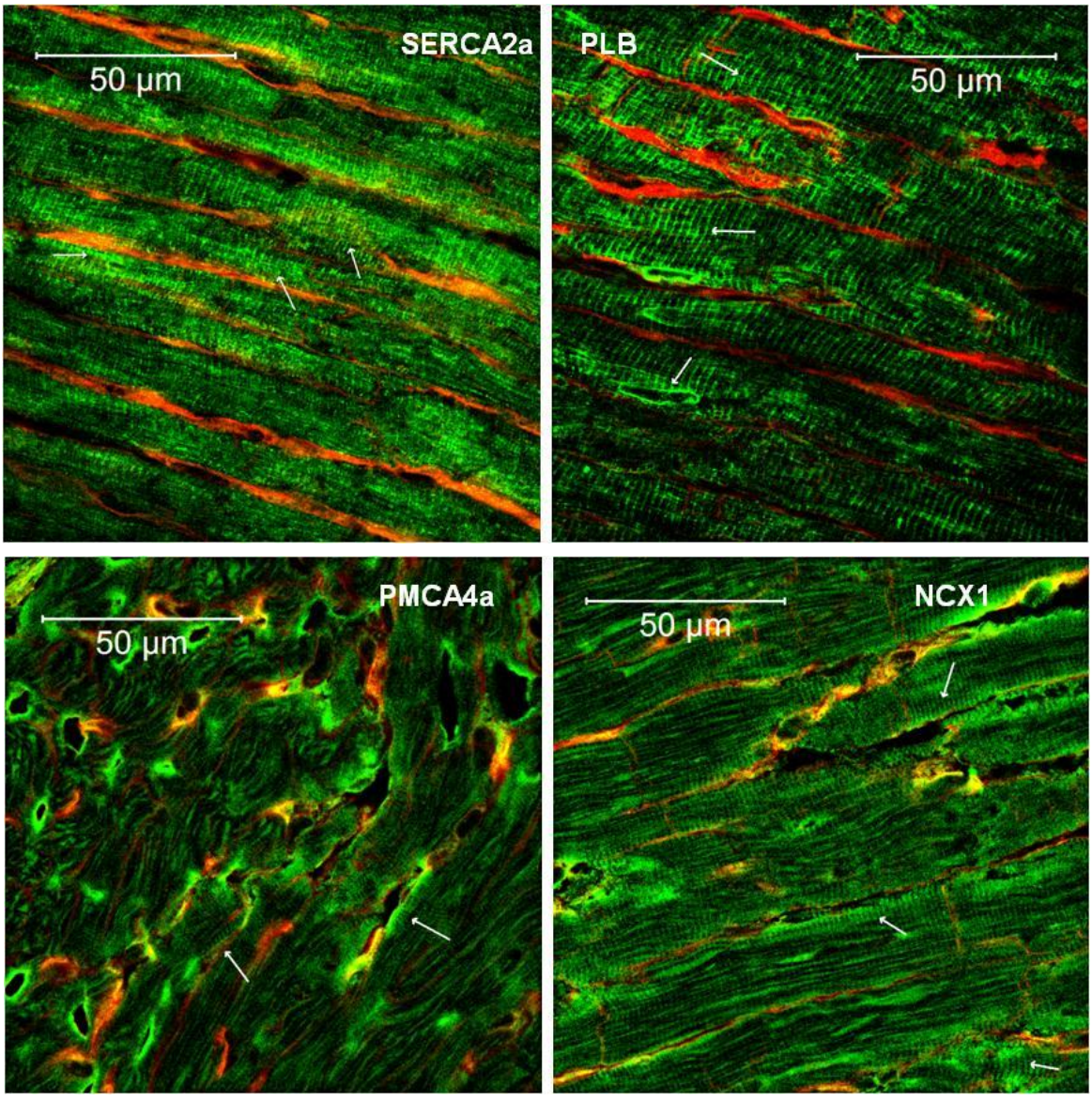

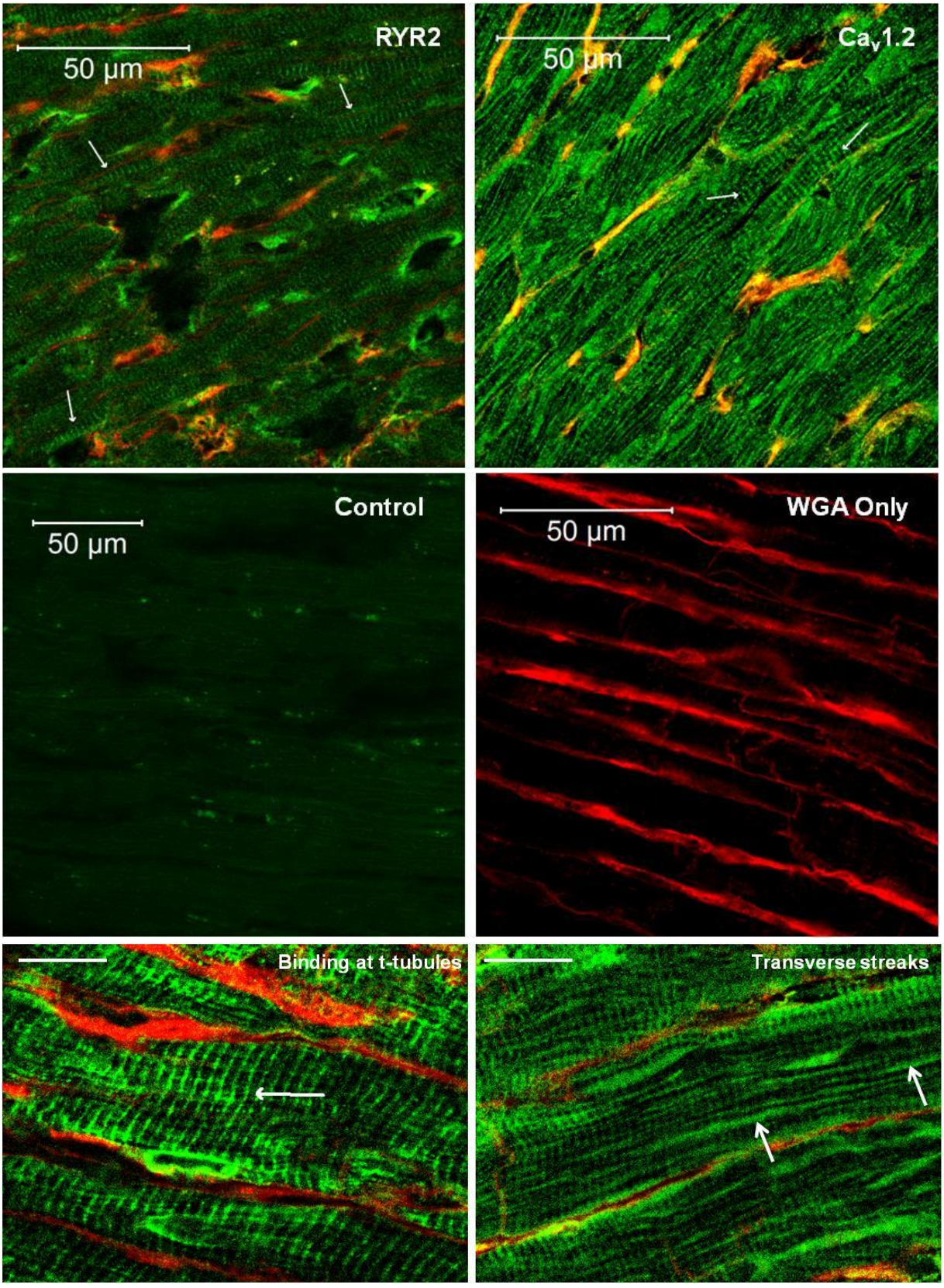

Figure 3.6 Example of immunolabelling of each antibody (page 73 and 74)

Images of RV sections, except PMCA4a which is from the LA. White arrows indicate specific binding. Lastly shown are specific structures at high zoom. Scale bars are shown in white indicating either 50µm as stated or 20µm.

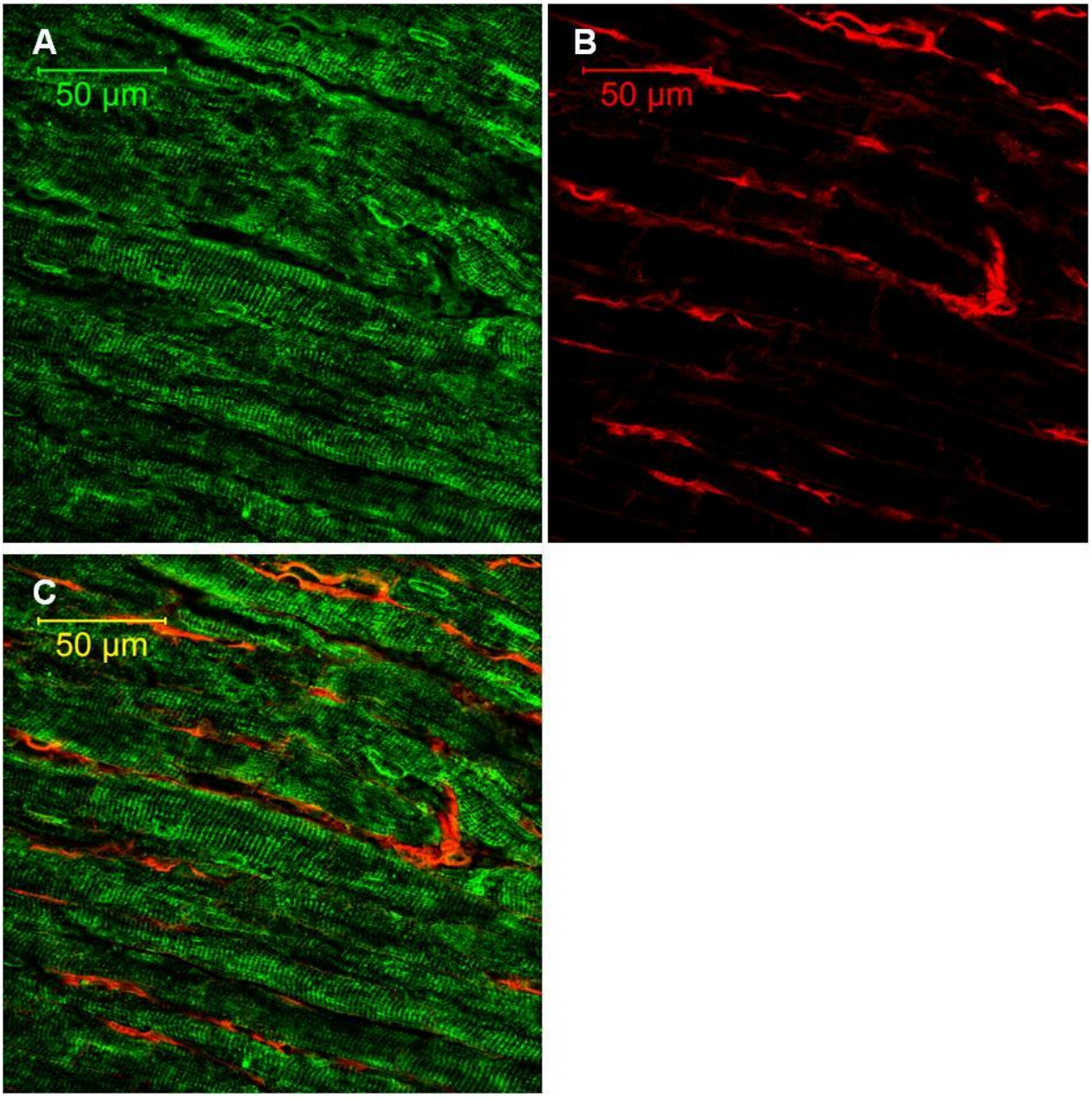

Figure 3.7 Separated channels of immunolabelling of PLB in LV sections.

Images of LV sections showing alexa flor-488 bound PLB antibody shown in green (A) and wheat germ agglutinin (WGA) (B) that binds to cell membranes shown in red, and the combined florescent channels (C).

Two channels were used for all images, and the wave lengths altered so that the best signal to noise ratio was achieved. This produced clear separate channel images (Figure 3.7) that allowed the visualisation of the cell membranes, but the analysis of the alexa-flor 488 fluorescence only.

3.3.2 Optical mapping of Ca^{2+} transients

Due to the slow perfusion rate, accumulation of debris and lack of nutrients resulted in the cessation of the SA node after 1 hour of experimentation. Therefore data from this technique was not recorded or analysed.

3.3.3 Age-dependent physiological changes

3.3.3.1 Body-weight to heart-weight ratio

The 24 months old rats were significantly heavier with larger hearts compared with the 6 months, but had a significantly lower heart to body weight ratio (Table 3.3).

Table 3.3 Age-associated changes to body and heart weight.

Age of animals	Body weight (g)	Heart weight (g)	Heart:Body weight ($x10^{-3}$)
6 months	517±10	1.55±0.06	3.9±0.09
12 months	556±16	1.64±0.03	2.9±0.04
24 months	661±37***#**	1.76±0.04*	2.4±0.08***#**

* denotes p <0.05 vs. 6 months and # denotes p<0.05 vs. 12 months. n=6 per age group. Data presented as mean ±SEM.

3.3.3.2 Intrinsic heart rate

Intrinsic heart rate under control conditions ranged from 276 beats per minute (bpm) at 6 months to 191 bpm in the elderly animals. There was no significant difference in the intrinsic heart rate between the 6 and 12 months of age. However, with advanced age there was a reduction in rate from 100±3.3% at 6 months of age to 78±3.1% in the 24 months of age animals (Figure 3.8).

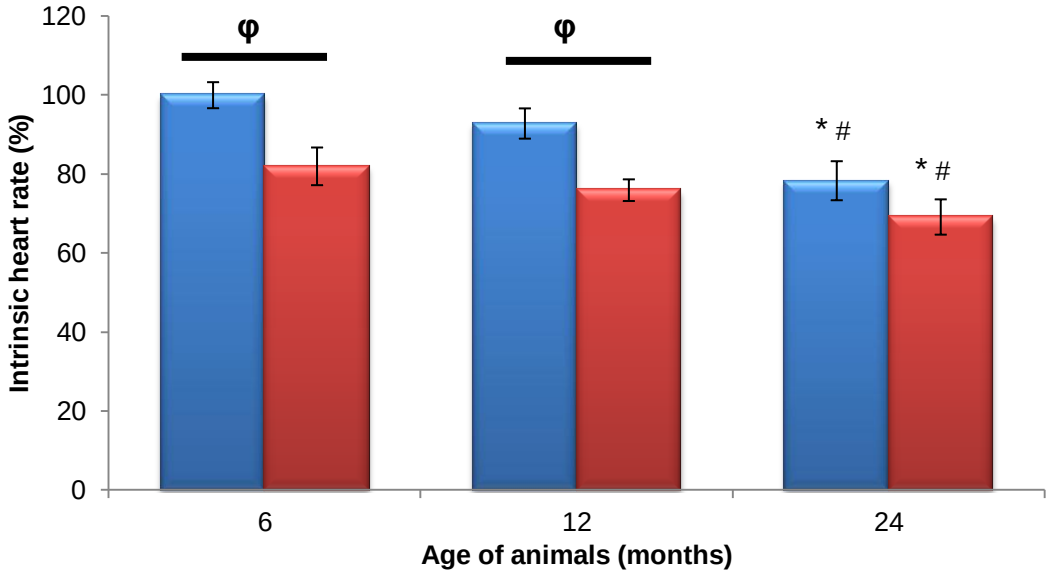

Figure 3.8 Changes in intrinsic heart rate with age under control conditions (blue) and in the presence of 3μM CPA (red).

* denotes p <0.05 vs. 6 months age group and # denotes p<0.05 vs. 12 months age group and φ p<0.05 within age group. Statistical differences were determined using a two way ANOVA with Holm-Sidak comparisons. For each age group 6, 12 and 24 months of age, n=6. Data are presented as means ± SEM.

3.3.4 Adrenergic response

3.3.4.1 Effect of increasing age on the response to isoprenaline as a β-adrenergic stimulator

There was an age-associated decline in the response to β-adrenergic stimulation via isoprenaline (Figure 3.9). There was a significant difference between the 6 and 12 months age groups on the addition of 10nM of isoprenaline. The 12 months old rats showed a more robust response from 117±4.9% at 6 months compared with 136±8.0%. Nevertheless at all other concentrations of isoprenaline there was no difference between the two age groups. By 24 months of age the lower concentrations of isoprenaline were less effective in increasing intrinsic heart rate as observed at 1nM (86±3.8%) and 10nM (103±5.8%) and even at 100nM (127±6.0%) was significant lower when compared with the 12 months age group (142±4.9%) but not with the 6 months age group (133±5.3%). Nevertheless with 1μM isoprenaline there was no significant difference across all age groups, indicating that a maximal response to the highest concentration of isoprenaline is still possible in the old rats, though whether there are

deleterious aftermath consequences are unknown. The change in sensitivity to isoprenaline with age can be explained further by the EC50 data shown in table 3.4; there was a significant increase in the EC50 at 24 months of age compared with the younger age groups.

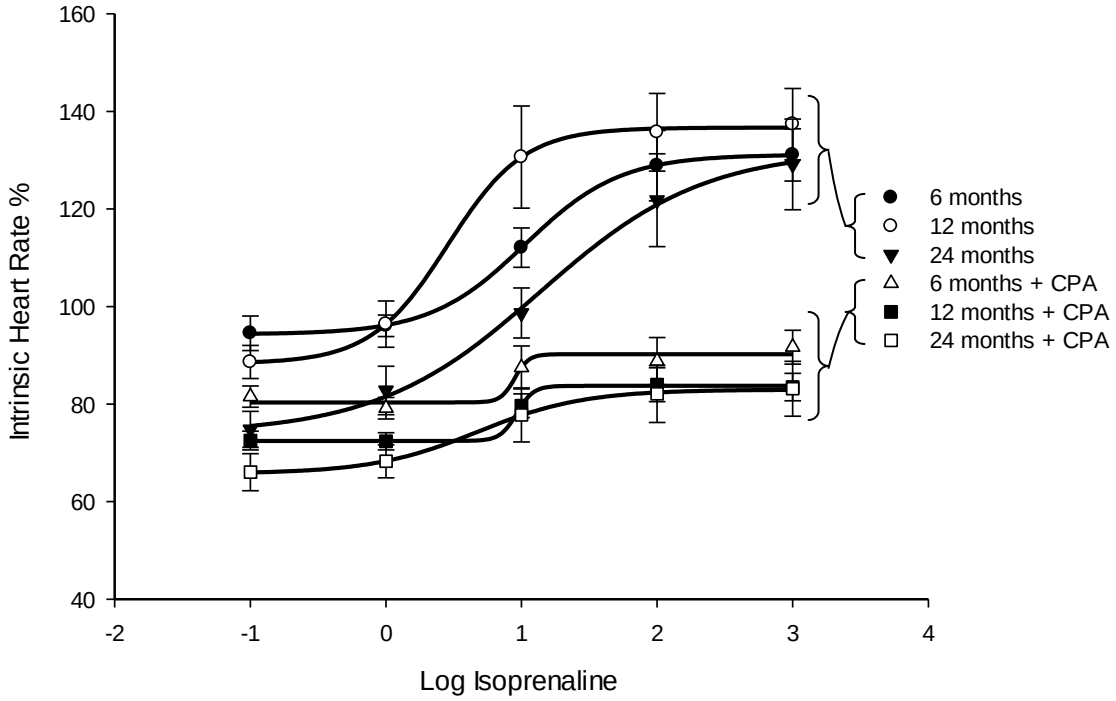

Figure 3.9 Dose response of isoprenaline versus intrinsic heart rate.

All data were compared with the average control 6 months data without CPA (3µM). Hill-slope was plotted and used to calculate the coefficients and EC50. n=6 per age group. Data presented as means ±SEM.

Table 3.4 EC50 of isoprenaline and CPA

Drugs/Age	6 months	12 months	24 months
Isoprenaline	3±2nM	10±4nM	24±3nM*#
Isoprenaline + CPA	18±4nM*#	18±4nM*#	18±4nM

* denotes p <0.05 vs. 6 months data and # denotes p<0.05 vs. 12 months data. Isoprenaline with CPA data was averaged EC50 data from across all age groups. n=6 per age group. Data presented as mean EC50±SEM.

3.3.4.2 Investigation into the role of the SR in β-adrenergic response.

To determine the role of SERCA2a in the response to isoprenaline, CPA was used to reduce and/or abolish SERCA2a activity from typical pacemaker activity. CPA significantly reduced intrinsic heart rate at both 6 (81±4.7%) and 12 months of age (75±2.7%) compared with the rates under control conditions (6 months 100±3.3%; and 12 months 93±2.1%) (Figure 3.9). However, although there was a small decrease in heart rate at 24 months in the presence of CPA from 78±3.1% to 69±4.4% this was non-significant. Furthermore in the presence of increment concentrations of isoprenaline, CPA significantly reduced the effect of the β-adrenergic stimulator at all concentrations (Figure 3.9). The 6 months age group showed small but significantly higher intrinsic heart rates at 1nM (81±4.8%) and 10nM (90±2.4%) isoprenaline with 3µM CPA when compared to the 24 months old age group (1nM 71±2.7% and 10nM 81±4.2%). Nevertheless at all other concentrations there was no significant difference in intrinsic heart rate between all age groups indicating that 3µM of CPA abolished the age-associated difference observed in the isoprenaline only studies. This is further confirmed by the EC50 data which was shown to be an average 18±4nM across all age groups (Table 3.4).

3.3.5 Effect of ageing on conduction velocity

3.3.5.1 Effect of ageing on the conduction velocity in the presence of isoprenaline

Under control conditions there was a significant age-associated decrease in conduction velocity across the CT to the reference electrode located in the RA muscle (Figure 3.10). There was no difference between 6 months (100±2.1%) and 12 months of age (99±5.3%), but a decline was observed in the 24 months old age group (82±1.8%). On the addition of isoprenaline there was no significant increase in conduction velocity at the lower concentrations (1nM and 10nM) across all age groups. At 100nM of isoprenaline faster conduction velocity was observed in the 6 months (138±7.6%), 12 months age group (134±2.4%) and a small but significant rise at 24 months of age (106±4.1%). The maximum dose of isoprenaline produced a minor increase in conduction velocity at 24 months of age (120±1.1%), this was not significantly different to data observed at 100nm, but was 38% faster compared to control conditions. At 1µM of isoprenaline SA node preparations showed dramatically enhanced conduction velocity at 6 months (205±9.1%) and 12 months old (183±6.0%) age groups (Figure 3.10).

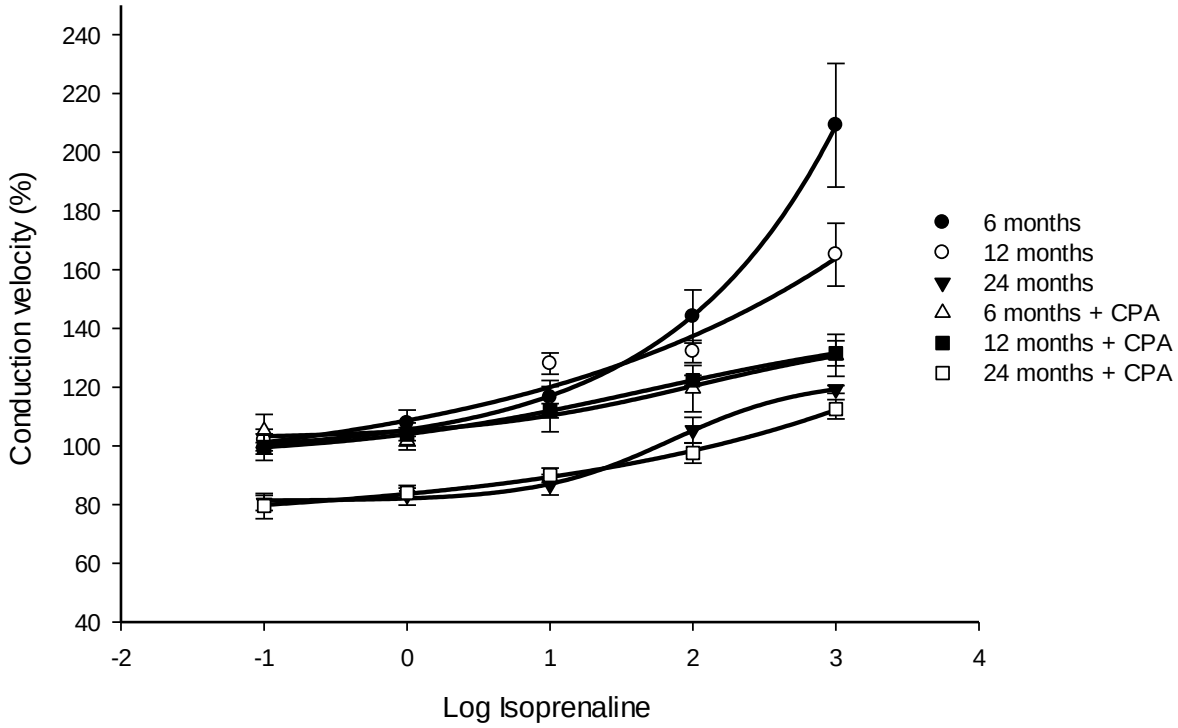

Figure 3.10 The affect of CPA on conduction velocity in aged SA node.

All data were compared with the average control 6 months data without CPA (3µM). n=6 per age group. Data presented as means ±SEM.

3.3.5.2 Role of the SR in conduction velocity and its response to β-adrenergic stimulation.

On the addition of CPA there was no significant differences in conduction velocity between control conditions across all age groups (Figure 3.10). The response to lower doses of isoprenaline was unaffected by the addition of 3µM of CPA. However, CPA significantly diminished the conduction velocity response to the maximum dose of isoprenaline in the 6 months age group (136±3.1%) and in the 12 months age group (133±2.7%). With age CPA did not affect the conduction velocity at any concentration of isoprenaline; 1µM of isoprenaline and 3µM CPA still resulted in a significant increase in conduction velocity (113±3.7%) when compared with the control CPA data (81±5.4%).

3.3.5.3 Effect of β-adrenergic stimulation on pacemaker shift

Isoprenaline caused positive pacemaker shift at all ages (Table 3.5). At 6 and 12 months of age, the addition of 3µM of CPA caused a negative shift in the LPS on the SA node preparation. Conversely in the 24 months age group there was an upward shift in the location of the LPS. After the addition of isoprenaline to the 3µM of CPA, the LPS continued to shift downward at 6 and 12 months age groups compared with the control location. Nevertheless at 24 months the effect CPA had at the younger age groups was not apparent with advanced age; on the addition of isoprenaline to 3µM of CPA there was a positive pacemaker shift similar to that observed with isoprenaline alone.

Table 3.5 Pacemaker shift associated with CPA or isoprenaline.

Drug/Age	6 months	12 months	24 months
Iso	3	5	5
CPA	-2	-2	3
CPA + Iso	-2	-2	3

Negative values indicate a shift lower than the control leading pacemaker site location whereas positive values indicate a shift higher. n=6 per age group. Data within each age group were summed to produce the final value.

3.3.5.4 Age-associated variations in AP propagation.

The AP is instigated from the LPS which was located under control conditions and is labelled as 'A' or 'LPS' on the manually drawn map (Figure 3.11). The conduction velocity map illustrates the propagation of the AP from the LPS (shown in red) and its spread across the SA node preparation and how this changed over the three age groups. At 6 months of age there is a clear LPS which propagates outwards in an even conduction velocity until it reaches further tissue (Figure 3.11A). Although the location of the LPS was seemingly lower than the drawn location on the manual map (Figure 3.11B), this location was derived after all recordings had been made, thus the LPS may have shifted in this time. In the 12 months age group there is a clear LPS at the top of the SA node preparation which propagated downwards (Figure 3.12) throughout the rest of the tissue. The location of the LPS is similar to the manually drawn site, interestingly in this preparation after addition of isoprenaline and CPA, the LPS seemed resilient to shifts in location.

With age there was a change in the propagation of the AP under control conditions (Figure 3.13). There appeared to be competition between two LPS. Using the manually

drawn map (Figure 3.13B) the LPS labelled 'A' resembles the large red region labelled with the number 1 in the conduction velocity map (Figure 3.13A), emphasising that this could be the main pacemaker site. Nevertheless the second LPS labelled 2 either prevents efficient propagation or is competing with the LPS for pacemaker control; if the latter is successful this may explain the subsequent shift of the LPS to location 'C'.

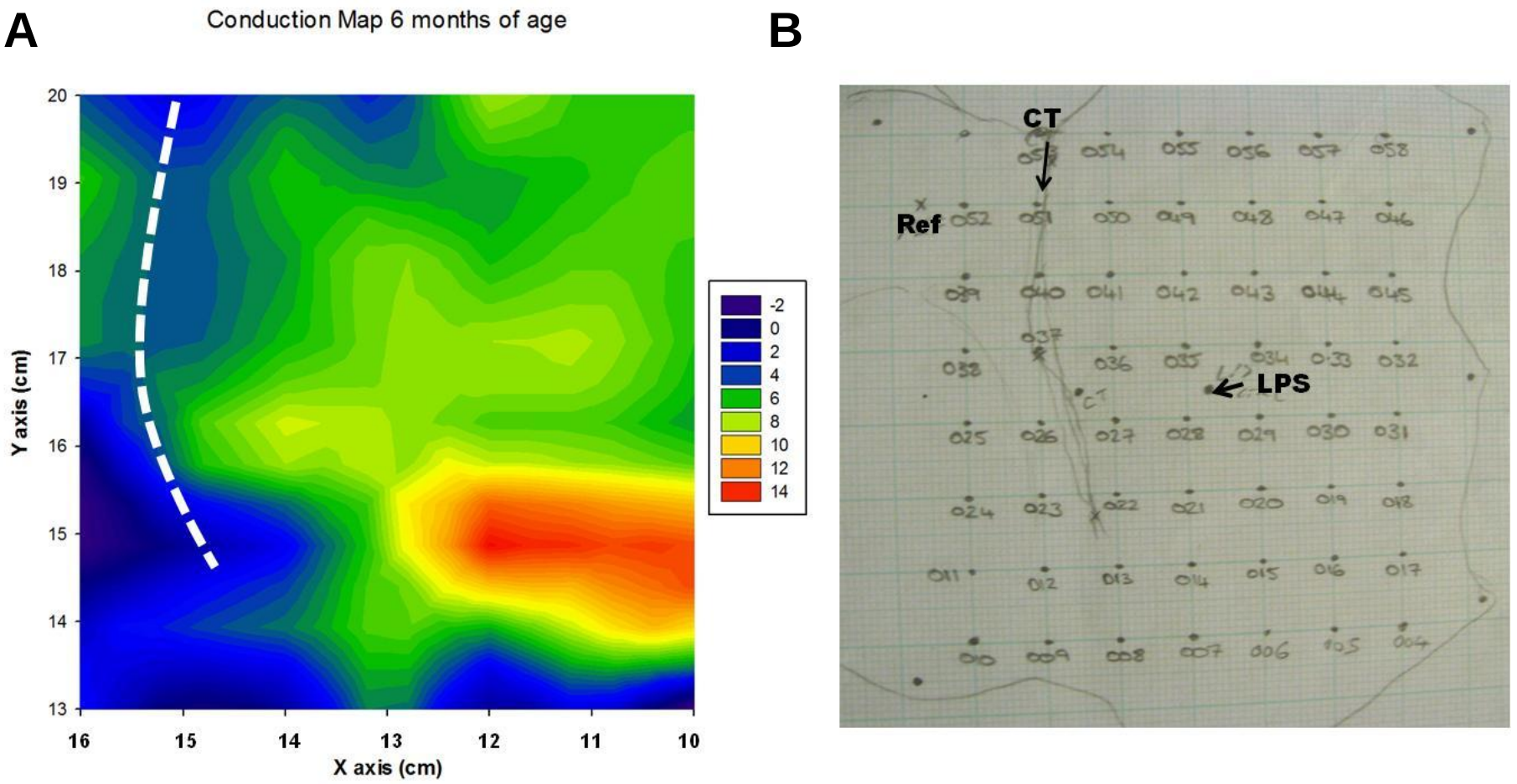

Figure 3.11 Activation map of the SA node at 6 months

A) Contour map of AP propagation plotted with smoothed data using tricube weighting and polynomial regression; white dotted line is the indication of the CT; B) Drawn map of the SA node tissue preparation with scale of 1 cm to 1 mm; labelled is the LPS under control conditions. (n=1)

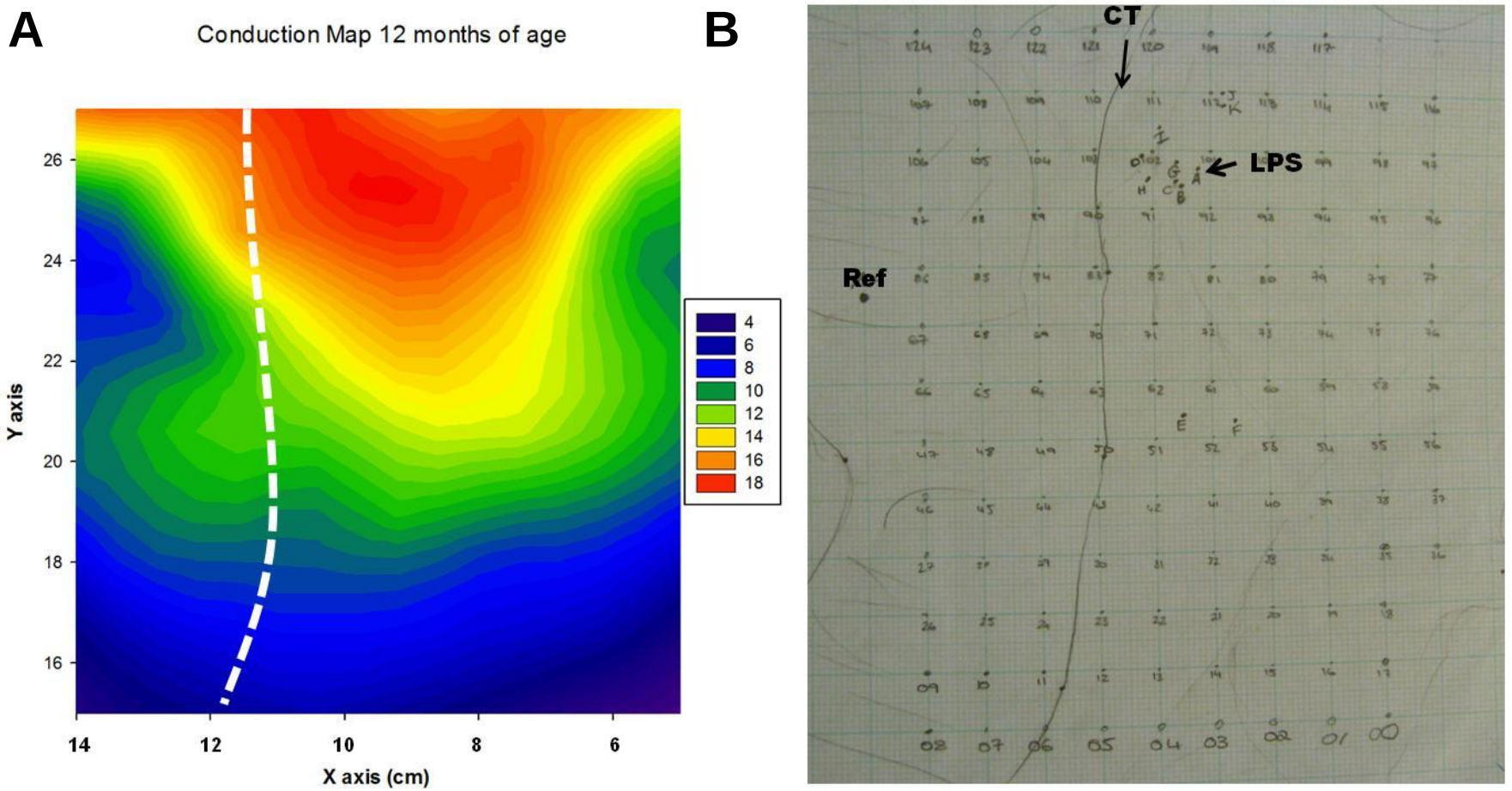

Figure 3.12 Activation map of the SA node at 12 months

A) Contour map of AP propagation plotted with smoothed data using tricube weighting and polynomial regression; white dotted line is the indication of the CT; B) Drawn map of the SA node tissue preparation with scale of 1 cm to 1 mm; labelled 'A' is the LPS under control conditions. (n=1)

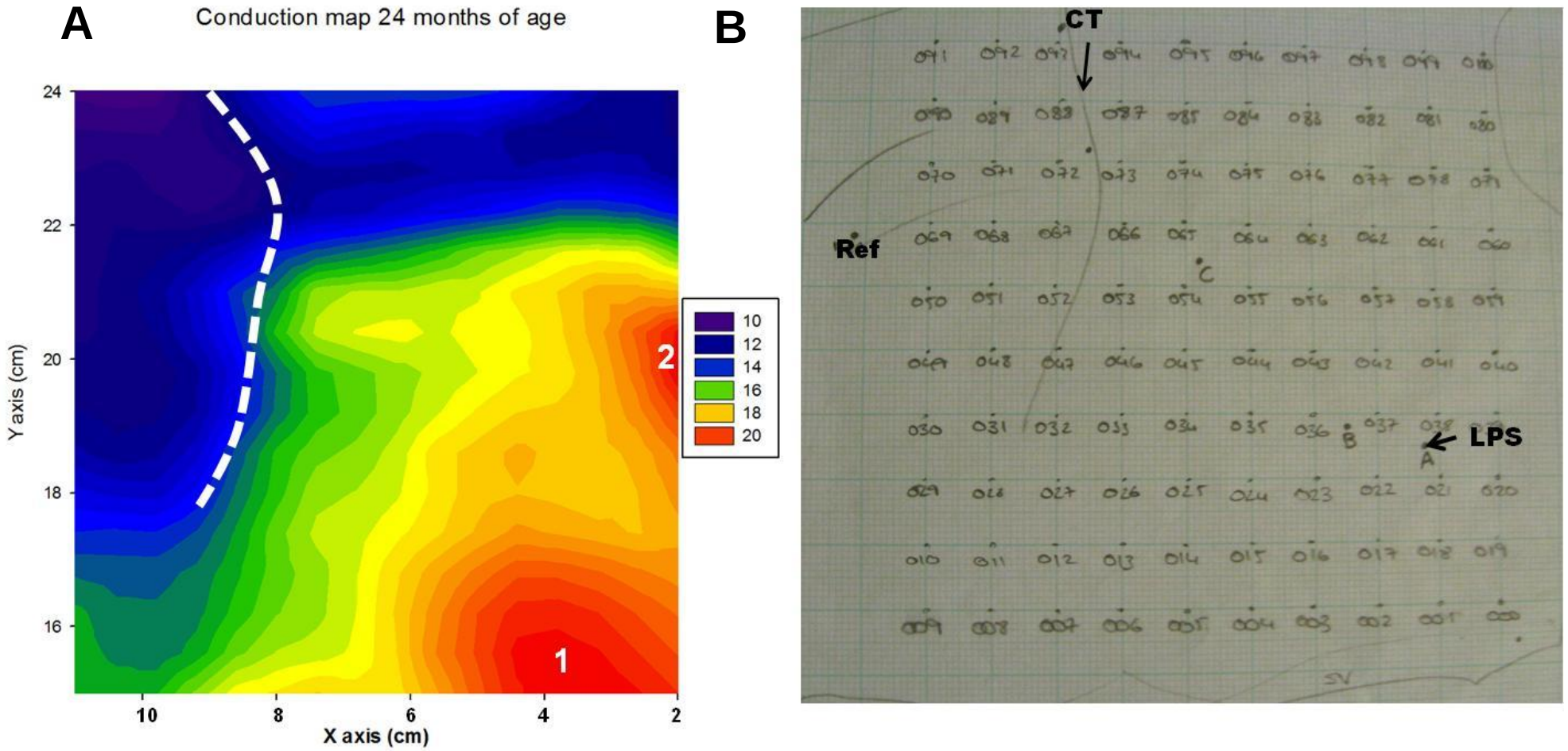

Figure 3.13 Activation velocity map of the SA node at 24 months

A) Contour map of AP propagation plotted with smoothed data using tricube weighting and polynomial regression; white dotted line is the indication of the CT; B) Drawn map of the SA node tissue preparation with scale of 1 cm to 1 mm; labelled 'A' is the LPS under control conditions. (n=3)

3.3.6 Age-associated changes in SR associated proteins

3.3.6.1 Effect of ageing on SERCA2a activity within the SA node

Illustrated by Figure 3.14B is the significant increase in SERCa2a protein expression, from 100±6.9% at 6 months to 150±9.2% at 12 months of age. However, with age there was a significant decline in SERCA2a expression to 67±7.1%. In addition with age there was clear decrease in the density of SERCA2a from 100±6.4% in the 6 months age group to 71±9.5% at 24 months of age (Figure 3.14C). Furthermore Figure 3.14D showed the densities of SERCA2a from the confocal microscopic sections of the SA node for 6 and 24 months of age as dense clumps erratically spaced within nodal cells; these dense clumps often formed flower petal patterns that radiated outwards, as shown by the white arrows.

There was a significant increase in total PLB protein levels at 12 months of age from 0.75±0.06 compared with 0.61±0.04 at 6 months (Figure 3.15). The separate isoforms, PLB monomer and pentamer, were analysed separately to determine which isoforms were responsible for the decline. Within the 12 months age group, there was a rise in PLB pentamer from 0.37±0.03 (6 months) to 0.52±0.04, however, PLB monomer levels remained equivalent between the two age groups. With age there was a reduced level of PLB total protein (0.39±0.05); both PLB pentamer and monomer halved in their protein expression levels. PLB protein showed t-tubular arrangement in a few of the nodal cells, as shown by the white arrows (Figure 3.16B), there were also dense clumps throughout. With age there was a significant decline from 100±7.4% in the 6 months age group to 78±8.9% at 24 months of age. Striations were no longer visible in the old nodal cells, with dense patches more irregular but mainly concentrated at the sarcolemma membrane (Figure 3.16C).

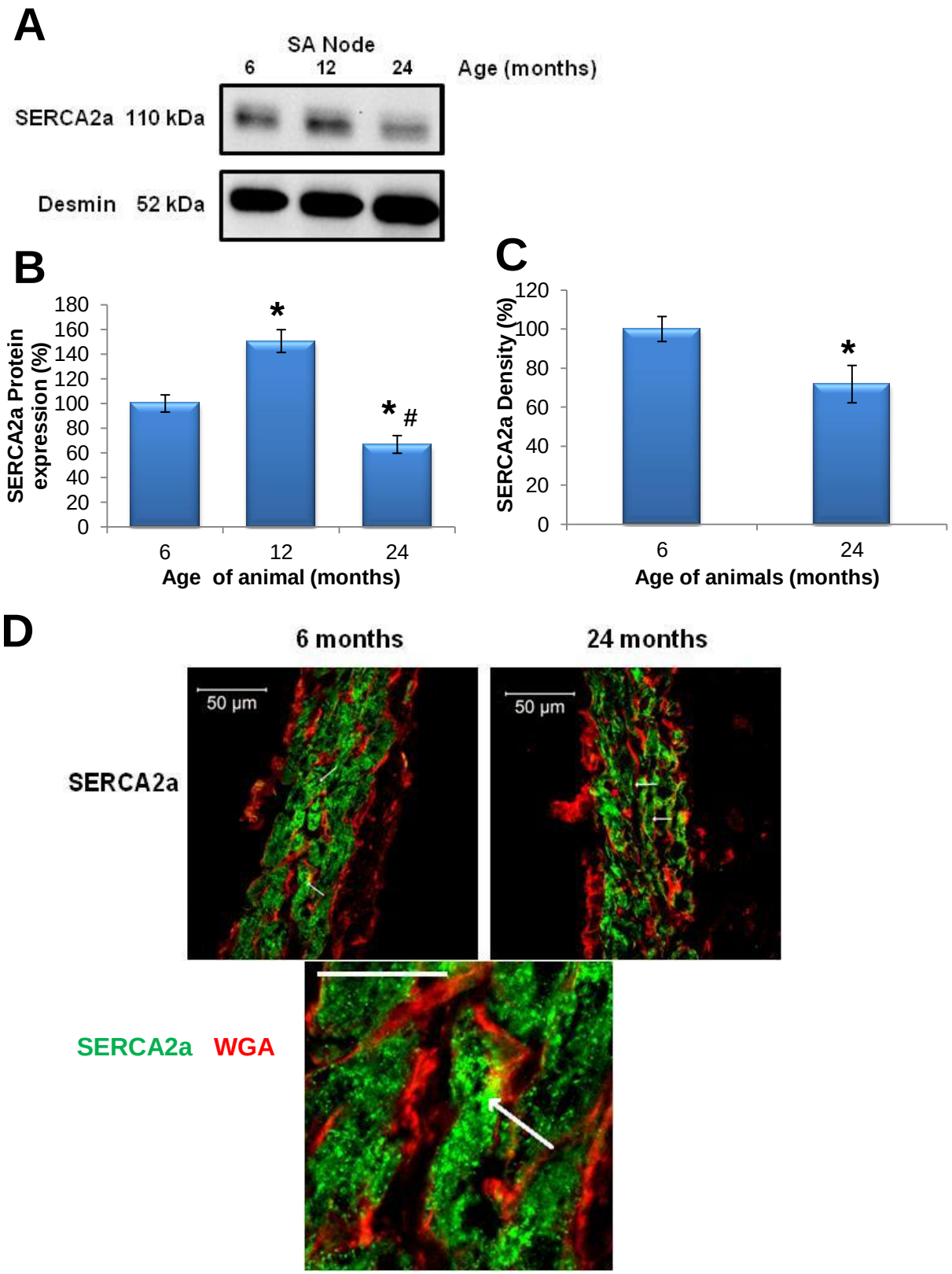

Figure 3.14 SERCA2a protein expression in the SA node with increasing age

A) illustrative blots of SERCA2a protein and desmin; B) SERCA2a protein expression normalised to desmin; C) density of SERCA2a label for SA node; D) illustrative images of the SA node are shown from rat hearts at 6 and 24 months of age; E) high resolution image with 15µm scale bar. * denotes $p<0.05$ vs. respective 6 months data; # denotes $p<0.05$ vs. respective 12 months data. n=5 per age group.

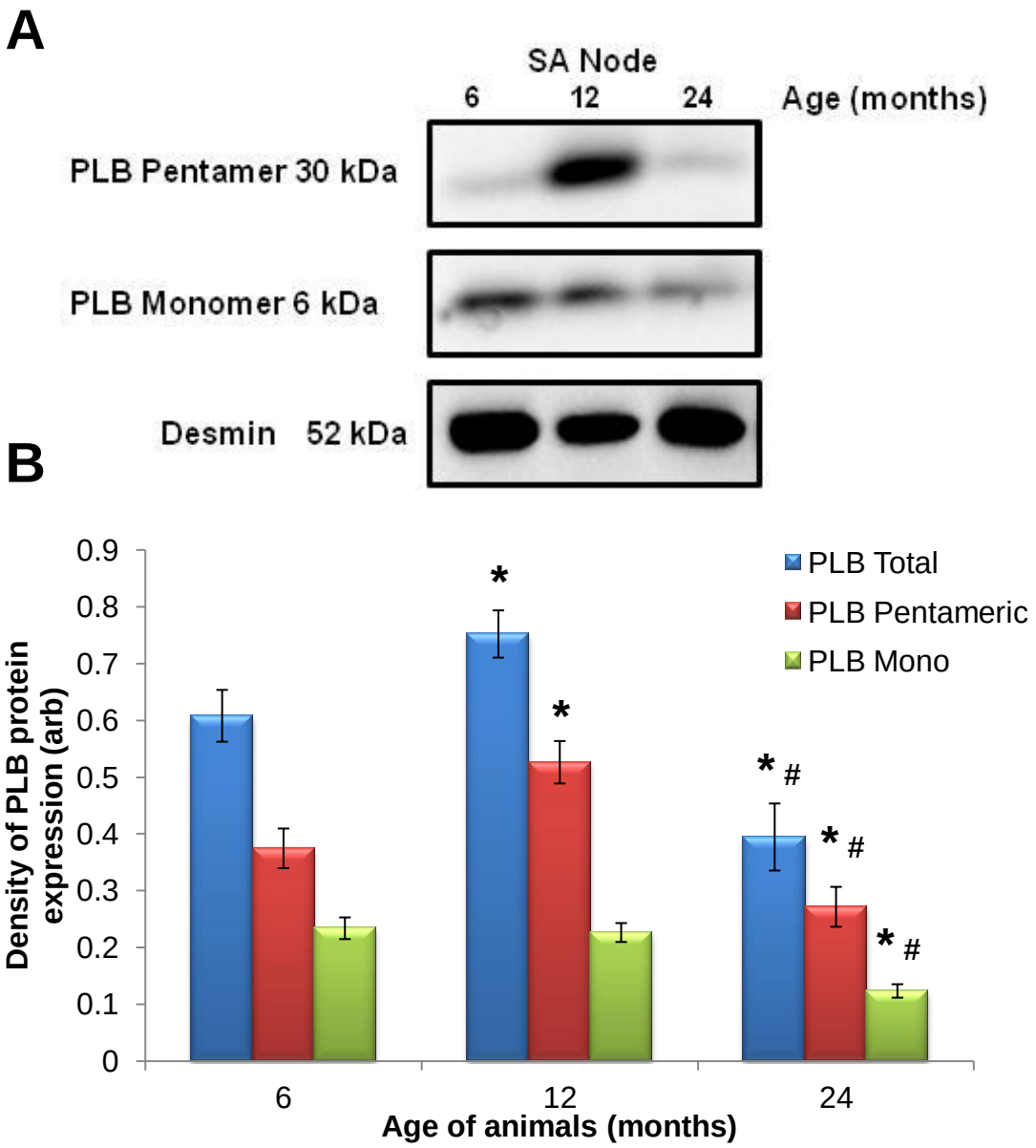

Figure 3.15 PLB protein expression in the SA node with increasing age

A) illustrative blots of PLB protein and desmin; B) analysis of raw PLB density data normalised to desmin. Data presented are mean ± SEM. Statistical differences were determined by two way ANOVA with Holm-Sidak comparisons; * denotes $p<0.05$ vs. 6 months SA node # denotes $p<0.05$ vs. respective 12 months data. n=5 per age group.

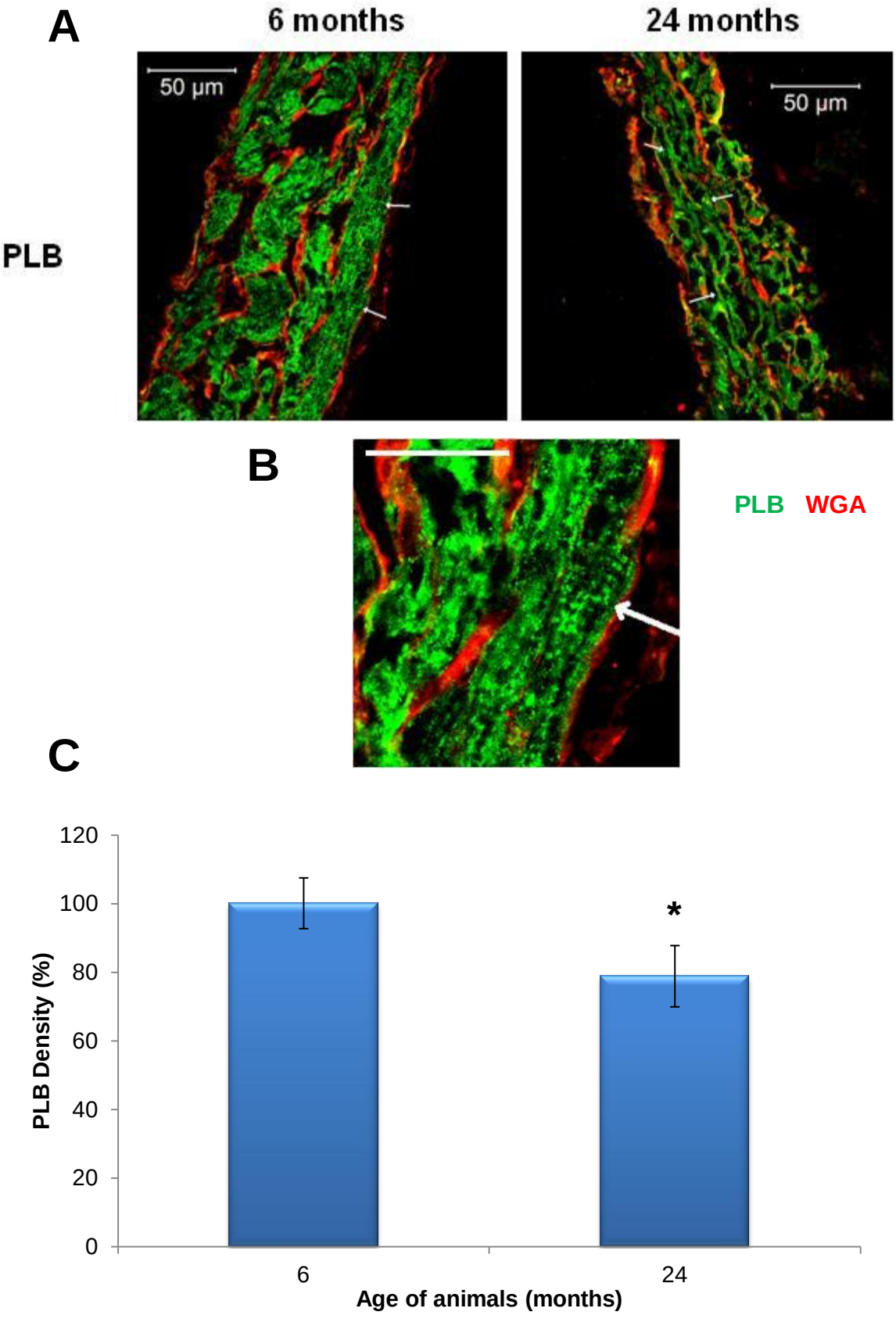

Figure 3.16 Localised PLB protein in the SA node with increasing age

A) illustrative images of the SA node are shown from rat hearts at 6 and 24 months of age; B) high resolution image with 15µm scale bar; C) density of PLB label for SA node. * denotes $p<0.05$ vs. respective 6 months data. n=5 per age group.

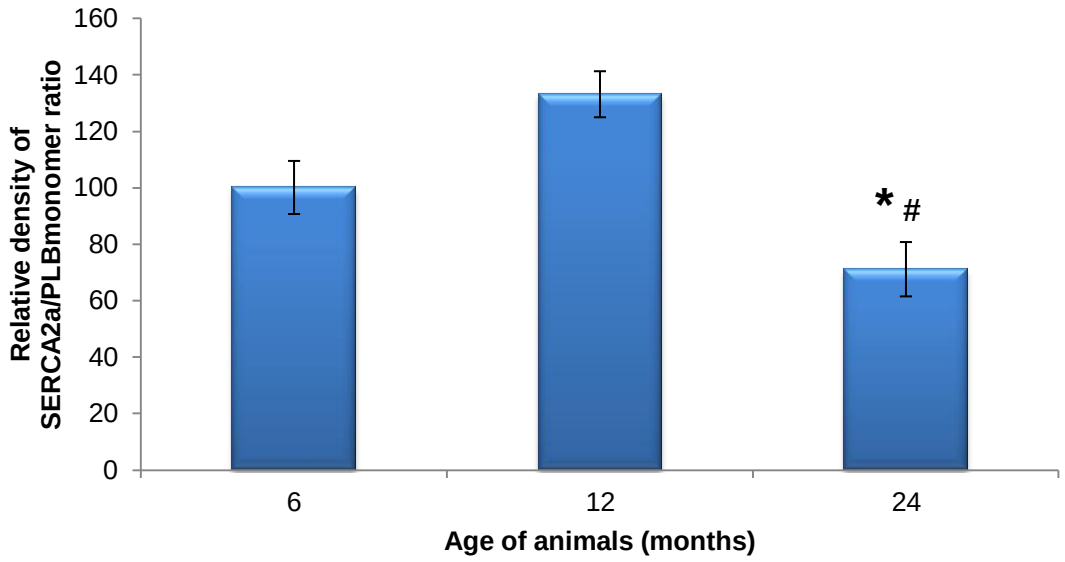

Figure 3.17 SERCA2a activity in the SA node with increasing age.

Raw PLB monomer expression data was normalised to SERCA2a protein expression which indicated the functional capacity of the Ca^{2+} pump SERCA2a. Data presented are means ± SEM. Statistical differences were determined by one way ANOVA with Holm-Sidak comparisons; * denotes $p<0.05$ vs. 6 months SA node, # denotes $p<0.05$ vs. 12 months SA node. n=5 per age group.

SERCA2a activity increased from 100±9.4% at 6 months to 133±8.1% in the 12 months age group (Figure 3.17). However, with increasing age there was a decline in SERCA2a activity to 71±8.5% below both the 6 and 12 months age groups. This decline in activity can at least be partially explained by the reduced expression of SERCA2a protein, but not a proportional decrease in PLB.

3.3.7 Age-associated changes in sensitivity and expression of proteins involved in CICR - Cav1.2 and RYR2

3.3.7.1 Effect of ageing on the sensitivity of the SA node to nifedipine

Sensitivity to nifedipine significantly changed with age. Hill curve coefficient of SA node preparations from 6 and 24 months of age were analysed (Figure 3.18). At 6 months of age there was a near linear response corresponding to the Hill slope coefficient (Table 3.6). A maximum dose of 30µM nifedipine was required for the SA node to cease pacing. Conversely at 24 months a tenth of the maximum dose (3µM) was required to cease pacing in the SA node preparations. Figure 3.18 shows the changes in these slopes between the two age groups; the 24 months old age group had a delayed response at 0.1µM and 0.3µM nifedipine compared with the 6 months of age rats. However, after 1µM nifedipine there was a steep decrease in intrinsic heart rate. This dramatic response to nifedipine occurred at dosages prescribed to patients highlighting this response occurs at pharmacologically relevant concentrations of nifedipine. This steep relationship between age and nifedipine sensitivity is not evidence via EC50 data, which was not significantly different between the two age groups (Table 3.6). Nevertheless there was a three-fold change in the Hill slope coefficient in the 24 months age group compared with the 6 months.

Table 3.6 EC50 and Hill slope coefficient data of nifedipine with increased age.

Parameter	6 months	24 months
EC50	1.360	1.265
Hill slope coefficient	-1.101	-3.152

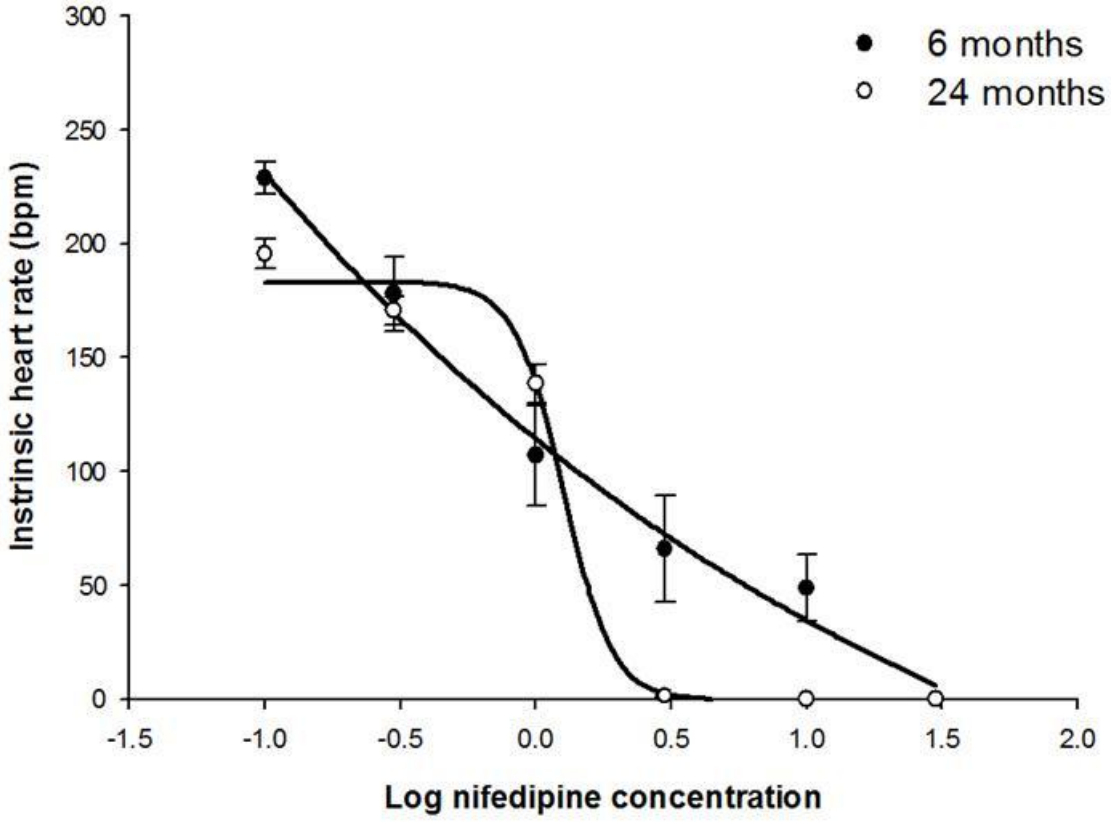

Figure 3.18 Nifedipine dose response curves for rats aged at 6 and 24 months.

All data compared with the average control 6 months of age data. Hill slope coefficient and EC50 was calculated. Data presented are means ± SEM. n=5 per age group.

3.3.7.2 Age-associated changes to RYR2 protein expression

At 12 months of age there was a significant rise in RYR2 protein (100±10.2%) compared with the 6 months age group (135±6.2%) (Figure 3.19C). Conversely the 24 months showed a decrease in expression (68±15.3%). RYR2 protein was occasionally observed in a minimal striated pattern at 6 months of age, as shown by the white arrows in Figure 3.19E, but the majority located in dense clumps throughout the nodal cells. With age there was a decrease in RYR2 density from 100±6.4% to 76±3.2% in the 24 months age group. Furthermore there were fewer dense clumps and instead RYR2 was localised at irregular lines in a small number of nodal cells.

3.3.7.3 Variations in $Ca_v1.2$ protein expression in the SA node with increasing age.

At 12 months of age there was a small but not significant (p=0.079) increase from 100±10.9% in the 6 months age group to 125±13.2% (Figure 3.20). In the 24 months age group there was a marked reduction in $Ca_v1.2$ protein to 59±13.9%. $Ca_v1.2$ protein was located throughout nodal cells in dense patches and also occasional lined patterns as shown by the white arrows (Figure 3.20E). Conversely the decrease in density with age from 100±9.5% at 6 months of age to 55±2.2% at 24 months of age, resulted in few dense patches and instead a streaked pattern was observed in only a few of the nodal cells (Figure 3.20D).

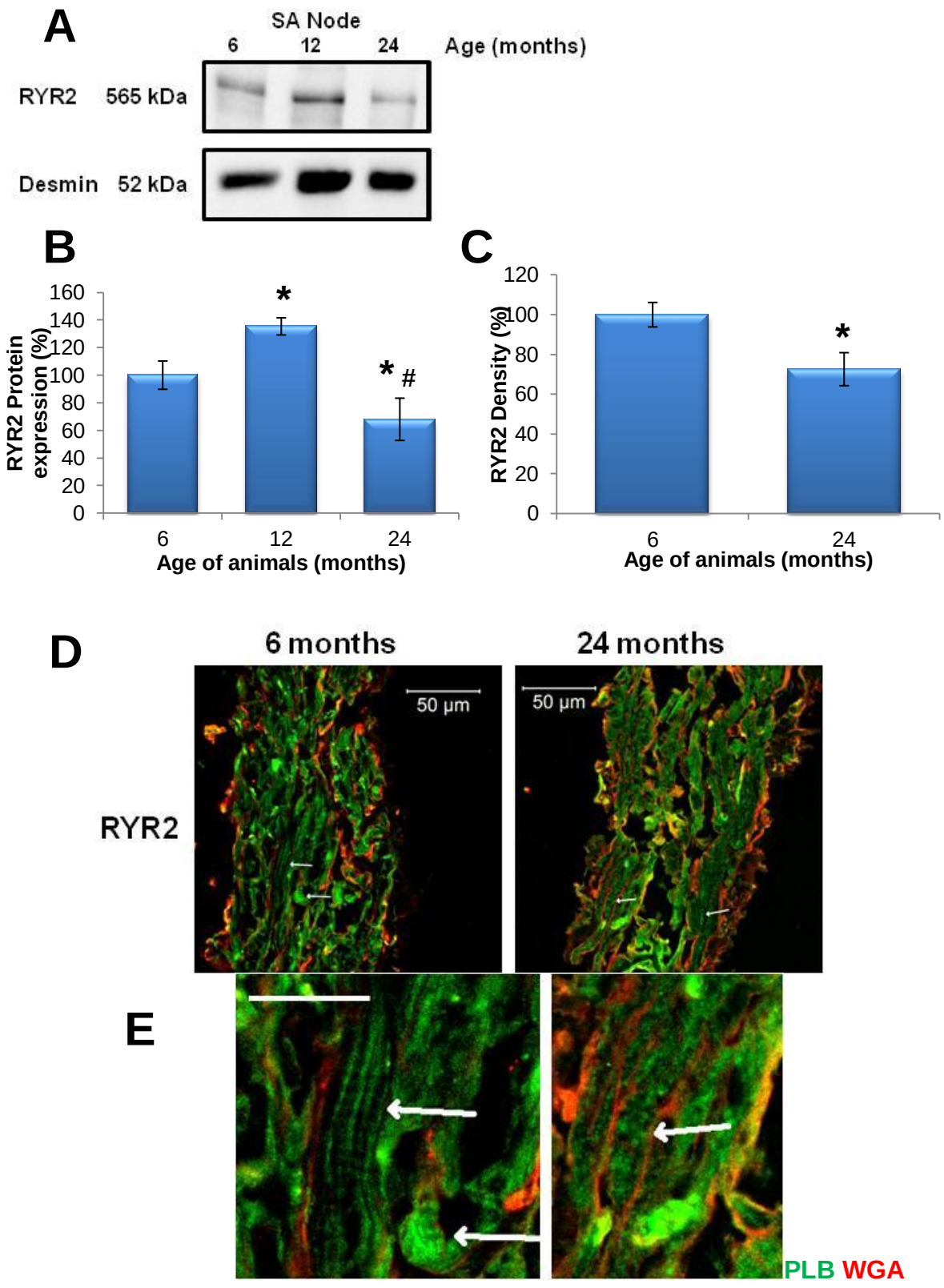

Figure 3.19 RYR2 protein expression in the SA node with increasing age

A) illustrative blot of RYR2 protein and desmin; B) RYR2 protein expression normalised to desmin; C) density of RYR2 label for SA node; D) illustrative images of the SA node sections; E) high resolution image with 15µm scale bar. * denotes $p<0.05$ vs. respective 6 months data; # denotes $p<0.05$ vs. respective 12 months data. (n=5)

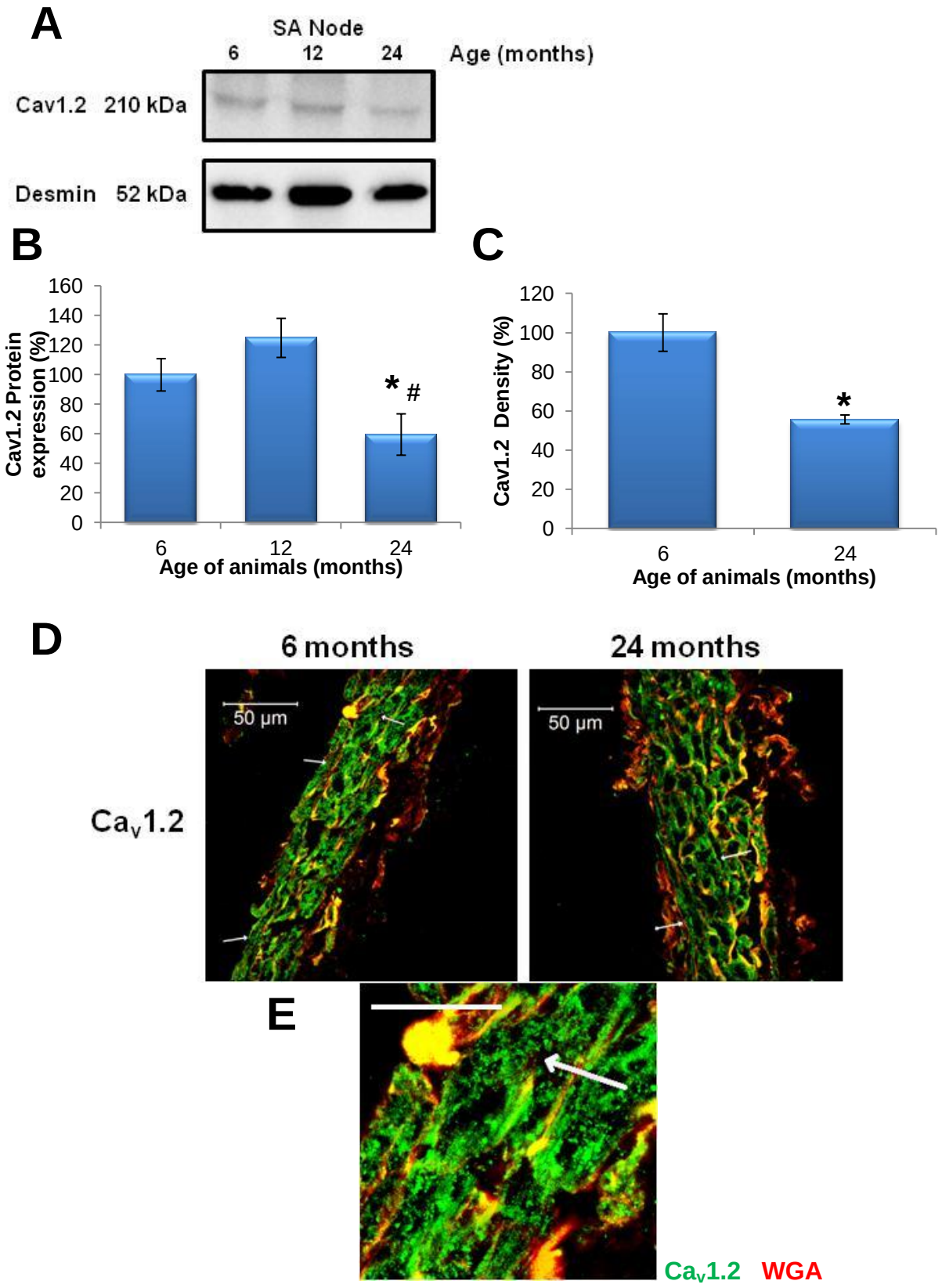

Figure 3.20 $Ca_v1.2$ protein expression in the SA node with increasing age

A) illustrative blot of $Ca_v1.2$ protein and desmin; B) $Ca_v1.2$ protein expression normalised to desmin; C) density of $Ca_v1.2$ label for SA node; D). illustrative images of the SA node sections; E) high resolution image with 15µm scale bar. * denotes $p<0.05$ vs. respective 6 months data; # denotes $p<0.05$ vs. respective 12 months data. (n=5)

3.3.8 Age-associated changes in sarcolemma membrane associated proteins within the SA node.

Extrusion of Ca^{2+} from the cell is not only conducted by SERCA2a, but also NCX1 and PMCA4a both located on the sarcolemma membrane. NCX1 showed no significant difference between 6 and 12 months of age, but by 24 months of age a significant increase to 172±13.6% (Figure 3.21B). At 6 months NCX1 was located along the periphery of nodal cells with sporadic higher density patches as shown by the white arrows (Figure 3.21D). With age there was a significant rise in NCX1 density (142±4.9%) and an increase in the labelling throughout the cell and at the sarcolemma membrane.

To determine the importance of sodium channels with age, $Na_v1.5$ was investigated within the SA node with increasing age (Figure 3.22). At 6 and 12 months of age there was no significant difference in $Na_v1.5$ protein expression. However, with advanced age there was enhanced protein expression (134±3.9%) to levels greater than those at 6 or 12 months of age. Whether these channels were closely located to NCX1 was not determined.

PMCA4a protein expression at 12 months of age had slightly elevated levels (111±7.0%) compared with the 6 months age group (100±5.7%) (Figure 3.23). Nevertheless with age there was a decline in PMCA4a expression to 78±1.7%. PMCA4a density was observed to concentrate at the sarcolemma membrane of nodal cells and showed possible co-localised binding with WGA (Figure 3.23E). However, with age there was a significant decrease in the density of PMCA4a from 100±4.9% to 76±9.5%. At 24 months of age though PMCA4a was still located at the sarcolemma membrane the labelling was significantly reduced and barely visible in many nodal cells.

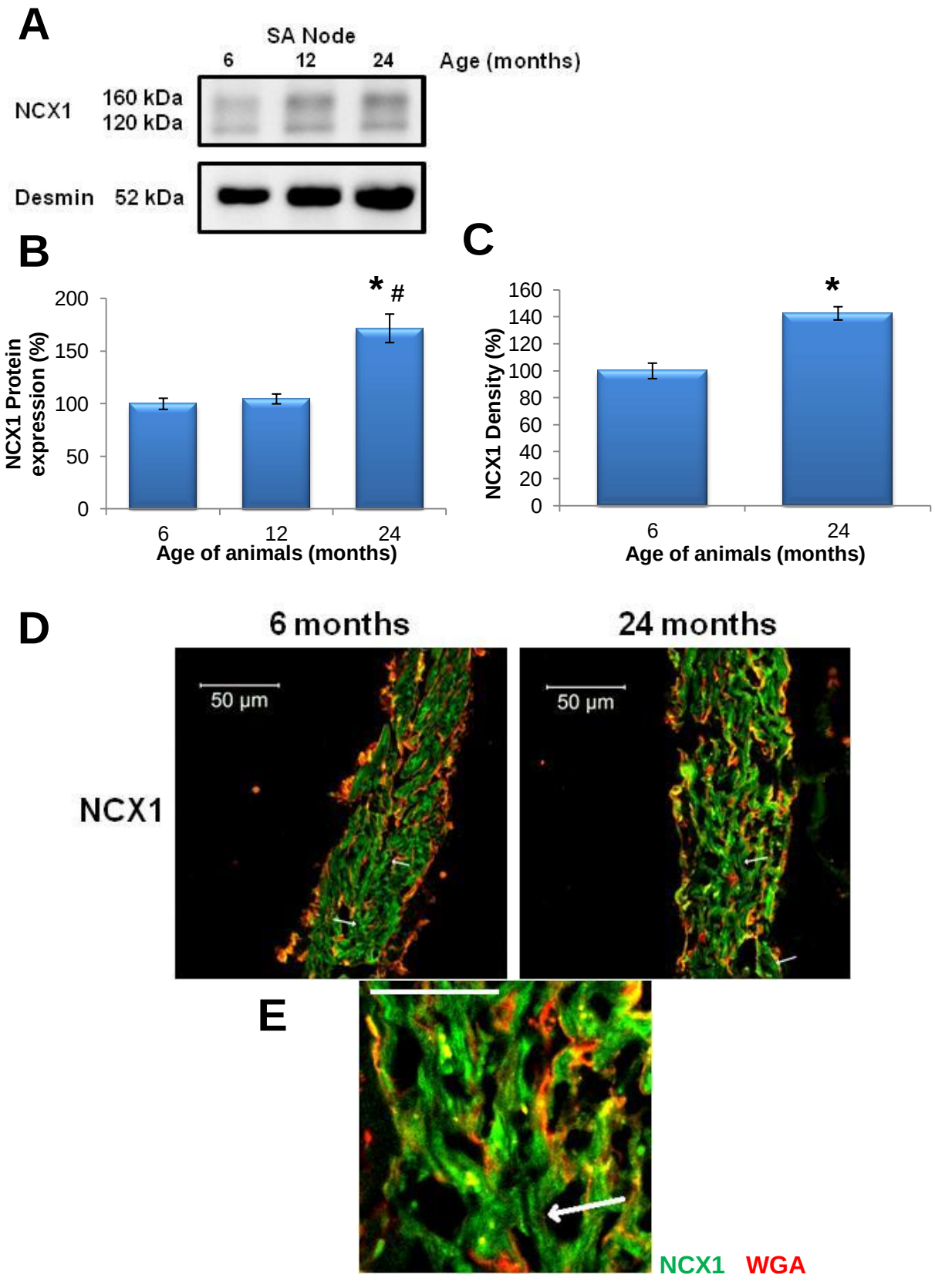

Figure 3.21 NCX1 protein expression in the SA node with increasing age

A) illustrative blot of NCX1 protein and desmin; B) NCX1 protein expression normalised to desmin; C) density of NCX1 label for SA node; D) illustrative images of the SA sections; E) high resolution image with 15µm scale bar. * denotes $p<0.05$ vs. respective 6 months data; # denotes $p<0.05$ vs. respective 12 months data. (n=5)

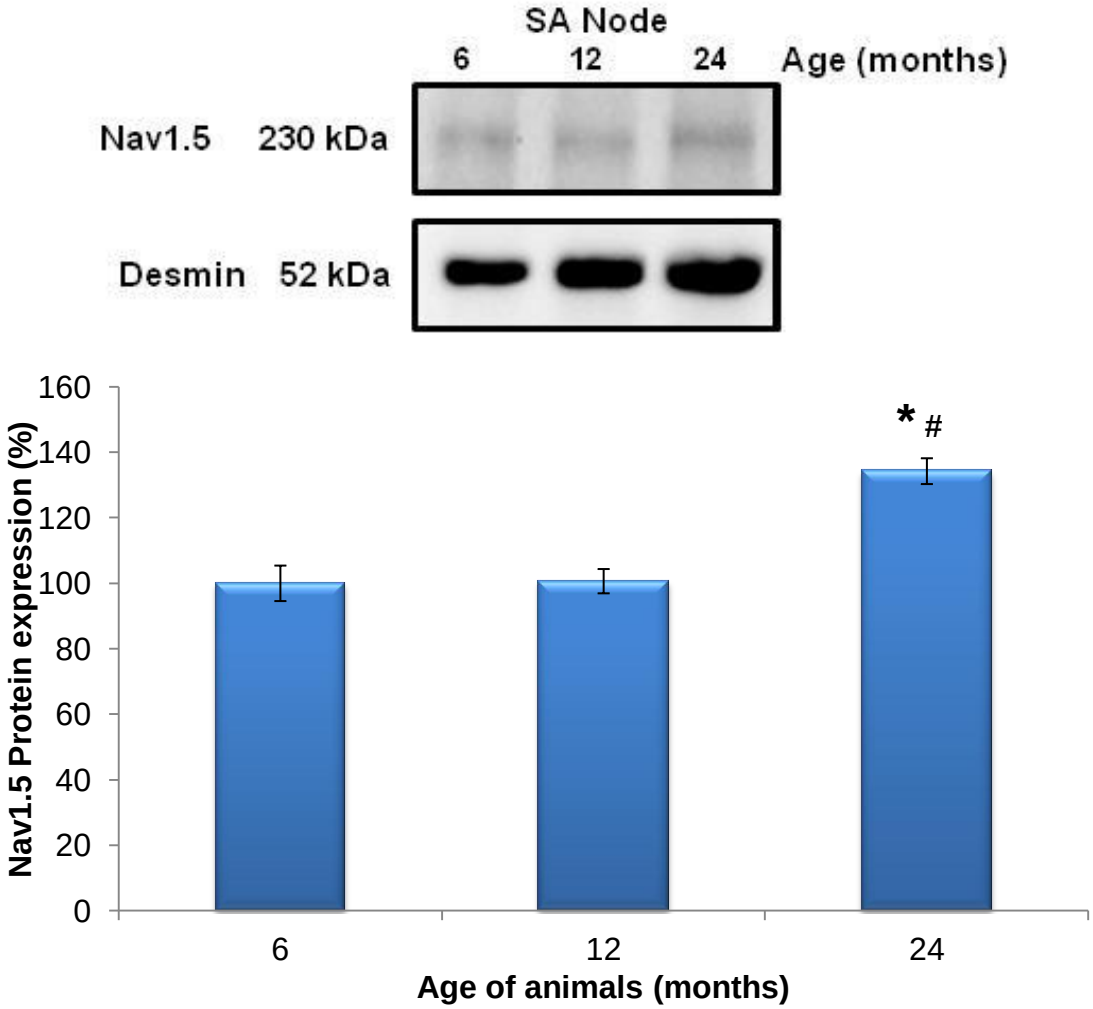

Figure 3.22 $Na_v1.5$ protein expression in the SA node with increasing age

A) illustrative blot of $Na_v1.5$ protein and desmin; B) $Na_v1.5$ protein expression normalised to desmin. * denotes $p<0.05$ vs. respective 6 months data, # denotes $p<0.05$ vs. respective 12 months data. n=5 per age group.

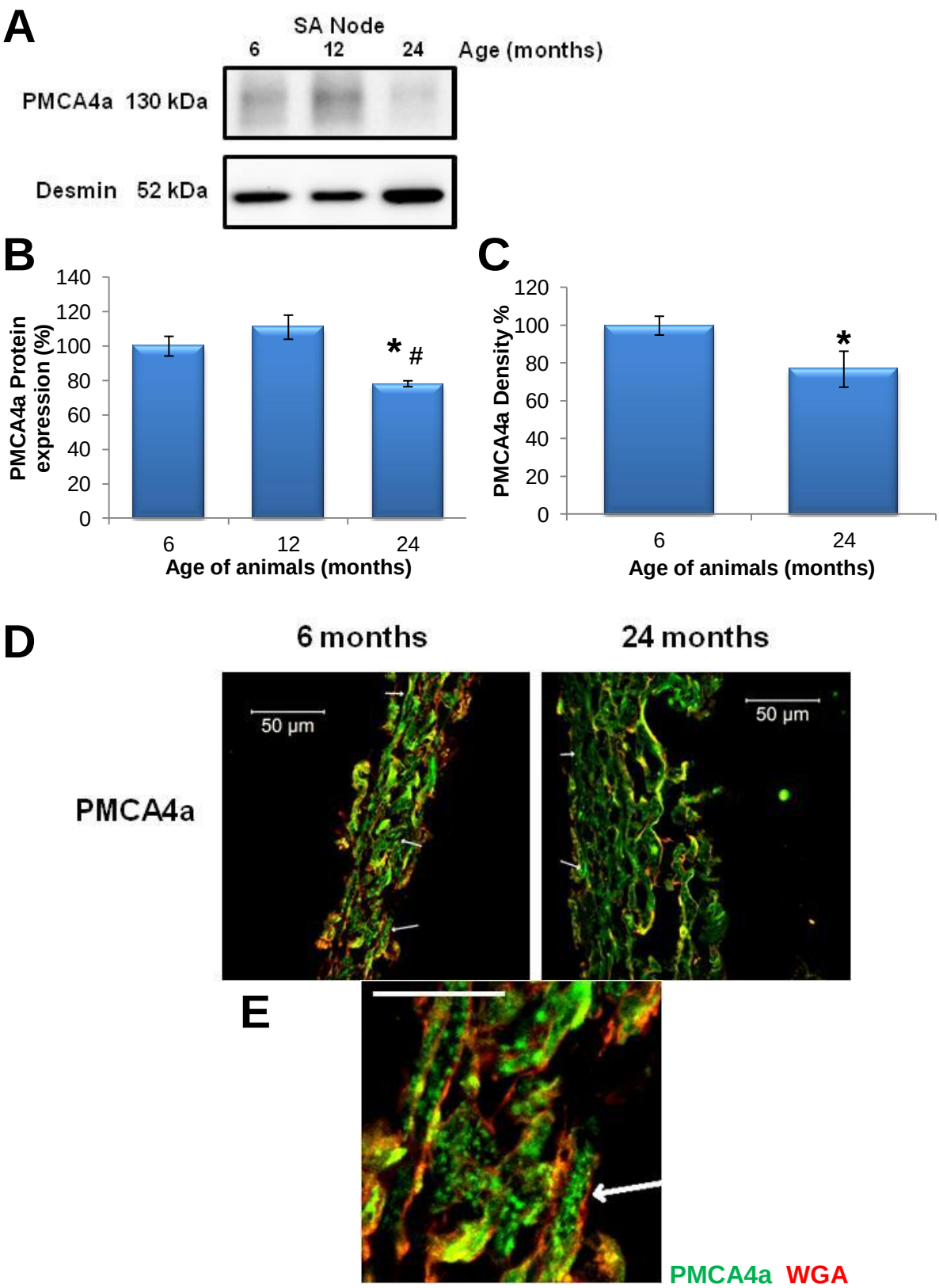

Figure 3.23 PMCA4a protein expression in the SA node with increasing age

A) illustrative blot of PMCA4a protein and desmin; B) PMCA4a protein expression normalised to desmin; C) density of NCX1 label for SA node; D) illustrative images of the SA node are shown from rat hearts at 6 and 24 months of age; E) high resolution image with 15µm scale bar. * denotes $p<0.05$ vs. respective 6 months data; # denotes $p<0.05$ vs. respective 12 months data. n=5 per age group.

3.4 Discussion

3.4.1 Summary of Chapter 3

At 24 months there was a significant increase in body weight and heart weight, but heart to body weight ratio decreased. Intrinsic heart rate decreased significantly and β-adrenergic response was diminished. Conduction velocity from the LPS across the CT showed a significant decrease at 24 months of age even in the presence of isoprenaline. Conduction maps showed competitive LPS sites in the elderly rat contrary to younger animals.

To determine the mechanisms underpinning the decline in β-adrenergic response SR associated proteins were investigated, at 24 months of age SERCA2a, PLB and RYR2 were significantly decreased in expression. SERCA2a activity was significantly decreased at 24 months of age, suggesting that this was responsible for diminished β-adrenergic response. Sensitivity to nifedipine was observed to increase with age, there was a 3 fold change in the Hill slope coefficient which could be linked to the decreased expression of $Ca_v1.2$ channels. In contrast NCX1 protein drastically increased by 72% at 24 months of age.

3.4.2 Age-associated physiological differences

Ageing was associated with a decline in intrinsic pacemaker activity without any evidence of structural remodelling, highlighting the importance of changes to cellular properties within the SA node (Alings et al., 1995). To determine whether hearts exhibited cardiac hypertrophy a common method used is normalisation of body weight to tibia length ratio which has previously been conducted in the ageing rat model (Yin et al., 1982). This study further used cardiac myocyte size to report an overall 15% hypertrophy of the LV in 28 months old rats compared with 5 months of age. However, in this chapter heart to body weight ratios were calculated and reported that elderly rats had 14% larger hearts suggesting hypertrophy, but rats were also heavier which resulted in a decrease in heart to body weight ratio. This provides somewhat conflicting data with the previous findings by Yin *et al.* , nevertheless a more recent ageing rat model study used heart to body weight ratio and reported similar results - 25 months of age rats had larger hearts but heart to body weight ratio declined (Tellez et al., 2011).

3.4.3 β-adrenergic response

3.4.3.1 Effect of ageing on sensitivity to isoprenaline

The response to isoprenaline was diminished with age. It has been previously established that the age-associated decline in β-adrenergic response is due to the decreased activity of β receptors and adenyl cylase (Scarpace et al., 1988). Reduced activity has been associated with the specific deficit in β adrenergic response signal transduction (Xiao et al., 1994), though inhibitory G proteins and receptor kinases changes were ruled out (Xiao et al., 1998), and decreased cAMP production associated with decreased adenyl cyclase activity (Farrell and Howlett, 2008). Inconsistent with these findings is the response to 1μM isoprenaline which at 24 months of age was no different to that of the younger age groups. This suggests that higher concentrations were required to gain a response from the older animals. This correlates to studies which suggests the beta stimulators norepinephrine and epinephrine are produced at increasingly higher concentrations with age due to inefficient reuptake (Esler et al., 1995). Age-associated increase in circulating neuro-transmitter indicates greater receptor occupancy leading to receptor desensitisation (Sakai et al., 1992). Evidence suggests that this may be the reason for the declined efficiency of post-synaptic β-adrenergic signalling (Lakatta, 1993). Consequently higher doses would be required to stimulate the same ligands at 24 months compared with younger adult which have yet to build a resistance. This may partially explain why older animals showed a lower sensitivity to isoprenaline but at the maximum dose a response similar to that at 6 and 12 months of age was observed.

3.4.3.2 Role of SERCA in β-adrenergic response

Within the SA node, isoprenaline stimulates the β receptors resulting in the activation of adenylyl cyclase-cAMP-PKA signalling cascade which is modulated by phosphodiesterase (PDE) activity (Vinogradova et al., 2006). Increased PKA has been shown to clearly affect SR Ca^{2+} cycling in particular phosphorylation of PLB which heightens SR Ca^{2+} pumping rate (Liu et al., 2011). These studies directly explain the data in this chapter; younger age groups were reported to have increased heart rates in the application of isoprenaline. In agreement SERCA2a activity has been reported vital in pacemaker activity and function (Vinogradova et al., 2010), thus increased pumping rate would clearly affect intrinsic heart rate (Frank et al., 2003).

In contrast the higher concentrations of isoprenaline required in the elderly animals suggests that SR Ca^{2+} pumping rate has a diminished role with age. In evidence of this, SERCA2a protein expression was decreased by 33%, thus the importance of SERCA2a in pacemaker activity may decline purely for the fact of decreased expression. SERCA2a activity is regulated by PLB, which declined but not to a similar extent, resulting in a fall of SERCA2a activity in the elderly heart. Usually SERCA2a activity has been investigated in ventricular tissue as an indication of myocardium dysfunction (Periasamy et al., 2008), in the atria during AF (Greiser et al., 2009) and in the healthy adult SA node (Vinogradova et al., 2010) but investigation in the SA node with increasing age is novel. The importance of SERCA2a activity in response to β-adrenergic stimulation is clear (Liu et al., 2011), hence the reported decline in activity directly explains the diminished response to isoprenaline at lower concentrations.

To abolish SERCA2a from the β-adrenergic response CPA was used; CPA binds to SERCA2a reducing its affinity for ATP resulting in diminished efficiency at pumping Ca^{2+} back into the SR (Plenge-Tellechea et al., 1997). At 6 and 12 months of age, CPA reduced basal intrinsic heart rate in conditions without isoprenaline, highlighting the importance of the SR Ca^{2+} pump in spontaneous activity. In the presence of isoprenaline, CPA significantly reduced the effects at all but the maximum dose, further confirming the role of SERCA2a in β-adrenergic response. CPA alone did not alter basal intrinsic heart rate in the elderly animals highlighting the already diminished role of SERCA2a in pacemaker activity. Even in the presence of isoprenaline, the 24 months group showed no significant difference on addition of 3μM CPA at lower concentrations, supporting the notion that the SR, with age, has a reduced role and perhaps other mechanisms are instrumental in pacemaker activity (Bogdanov et al., 2001) (see section 3.4.3.4).

Interestingly the hypothesised negative trend between increased age and decreased β-adrenergic response was linear across the age groups; at 12 months of age there was a significantly enhanced response compared with 6 months age group. Nevertheless this can be easily explained by the 50% rise in SERCA2a protein expression, consequently accounting for the 33% increase in SERCA2a activity. Conversely PLB monomer protein also increased by 40% which as an inhibitory regulator of the SR Ca^{2+} pump during β-adrenergic response (Liu et al., 2011) contradicts the previous statement. As an explanation β-adrenergic stimulation affects a multitude of Ca^{2+} proteins, thus at 12 months of age these additional proteins (Ullrich et al., 2012) would clarify the robust response observed.

Overall these data demonstrate a relationship between β-adrenergic response and the SR in line with other studies (Liu et al., 2011, Vinogradova et al., 2010) emphasising the significance of SERCA2a activity and its effect on pacemaker response. More importantly, the data reported in this chapter highlight that the function of the SR in β-adrenergic response is diminished with age.

3.4.3.3 Effect of ageing on conduction velocity in the SA node

The drive of propagation of an AP between nodal cells of the SA node would be partially due to the presence of connexins (Opthof, 1994). With advanced age there was a significant decrease in conduction velocity, similar to previous findings in the rabbit, cat and noted in humans (Alings and Bouman, 1993). Age-associated studies focusing on the expression of connexins, particularly connexin 43, have shown that there is a decrease in expression (Jones et al., 2004, Allah et al., 2011). Particularly in the study by Jones *et al.* the area of SA node lacking connexin 43 progressively increased with age. If this also occurred in the rat species studied in this chapter it would explain the decreased conduction velocity and its altered propagation in elderly rats. These studies provide sufficient evidence for clear species differences; to solve this discrepancy, a further study of connexin protein expression in the rat SA node would be of value. Ageing model studies of conduction velocity across the RA are few, but AF can be used as a moderate marker of increased age; consequently a recent study in humans reported slowing of atrial conduction before the onset of AF suggests that slowing of conduction could be a prequisite to the onset of an arrhythmia (Lalani et al., 2012). As a consequence age-associated decline in conduction velocity may contribute to reduced intrinsic heart rate, diminished β-adrenergic response and possibly AF or SA node dysfunction.

Other factors could include the method of measuring the conduction velocity which was achieved by measuring distance from the LPS to the reference point straight across the CT. It has been previously shown that the conduction velocity within the intercaval region can vary depending on the location of the measurement (Bleeker et al., 1980). In addition conduction velocity measured at the LPS parallel to the CT versus perpendicular to the CT was also different (Yamamoto et al., 1998). The outcome of this results in the AP arriving at the CT in a broad wavefront to which this tissue may act as a physiological block to protect the SA node from reentry and invasion from AP outside of the intercaval region (Bleeker et al., 1982, Boyett et al., 2000). Consequently conduction velocity measurements made in this study though informative may be biased due to the method of recording.

In the younger age groups on the addition of isoprenaline, conduction velocity increased fractionally but this small change resulted in significant elevations in heart rate; similar findings were reported in the elderly age group. The large change in heart rate suggests that a dynamic response is possible with low variations in conduction velocity. With age this ability to produce increased AP firing highlights the link between low conduction velocity and an onset of an arrhythmia/AF (Lalani et al., 2012).

In contrast 1µM isoprenaline caused near double conduction velocity in 6 and 12 months even compared with 100nM isoprenaline. However, at lower concentrations, this difference in conduction velocity was not reflected in the intrinsic heart rate recordings. Interestingly CPA, although having no effect on any previous conduction velocity recording, completely removed this sharp rise at 1µm isoprenaline highlighting SR Ca^{2+} load as a factor. However, studies on conduction velocity during β-adrenergic stimulation in the SA node or RA tissue are minimal. Through the knowledge of the known effects of β-adrenergic stimulation on SR activity, the increased SR content and consequently high Ca^{2+} levels could influence level conduction velocity (Jia et al., 2012). In addition Ca^{2+} tolerance threshold has been shown to be reduced with age (Hano et al., 1995); thus during period of stress or exercise in the elderly heart this reduced tolerance to Ca^{2+} could affect propagation via conduction velocity.

3.4.3.4 Effect of isoprenaline on other protein targets further explains the age-associated decline in β-adrenergic response

CPA highlighted the importance of SR Ca^{2+} pumping rate in β-adrenergic response in the younger age groups. At 6 and 12 months of age in the presence of 1µM isoprenaline and 3µM CPA, heart rate still increased compared with the control conditions. This provided support for the involvement of other proteins in β-adrenergic response within the SA node that include RYR2, $Ca_v1.2$, I_f and NCX1 (Ullrich et al., 2012, Liu et al., 2011, Vinogradova et al., 2010, Ke et al., 2007).

β-adrenergic stimulation has been shown to affect RYR2 via PKA or calmodulin dependent kinase (CaMKII) (Takasago et al., 1991) though the site of phosphorylation remains controversial (Ullrich et al., 2012). Firstly PKA-dependent phosphorylation of RYR2 enhances channel sensitivity Ca^{2+} hence increasing the open probability and the onset of CICR (Vinogradova et al., 2006). A mechanism for increased Ca^{2+} release is the PKA phosphorylation of the accessory regulator calstabin-2, which was reported to lead to subconductance states of RYR2 (Marx et al., 2000).

Secondly RYR2 sensitivity and thus Ca^{2+} wave propagation is regulated by luminal Ca^{2+} (Szentesi et al., 2004). Following increased SERCA2a activity, SR Ca^{2+} load is substantially higher affecting RYR2 sensitivity and probability of opening. This heightened sensitivity may explain the robust response observed in the 12 months compared with the 6 months; there was a 35% and 25% augmented RYR2 and $Ca_v1.2$ protein levels respectively at 12 months of age. With RYR2 being instrumental in spontaneous activity and $Ca_v1.2$ channels for the upstroke of the AP, combined changes cause altered CICR gain.

Lastly disabling phosphorylation of one out of three sites in the RYR2 channels-S2808A demonstrated impaired synchronisation of SR Ca^{2+} release during β-adrenergic stimulation (Ullrich et al., 2012). It can then be surmised that PKA aids in synchronising local Ca^{2+} release to result in a cumulative event. Within pacemaker nodal cells as RYR2 release is responsible for spontaneous activity this LCR process could be directly affected due to the age-associated decrease in adenylyl cyclase-cAMP activity observed in ventricular cardiomyocytes (Farrell and Howlett, 2008). Furthermore in contrast to the increased protein expression at 12 months of age, in the elderly age group RYR2 and $Ca_v1.2$ was markedly reduced which affects basal heart rate and the response to β-adrenergic stimulation. On the other hand at the maximal dose of isoprenaline with CPA heart rate significantly increased in the elderly age group highlighting the reduced role of SERCA2a, and the additional mechanisms involved in β-adrenergic response.

To explain these findings the role of NCX1 has yet to be considered. Certainly the majority of Ca^{2+} released into the cytosol is transported back into the SR via SERCA2a, approximately 70% in the rabbit SA nodal cells (Vinogradova et al., 2010), but the remainder is extruded via NCX1 (and to a much lesser extent by PMCA4a). The purported decrease of SERCA2a, RYR2 and $Ca_v1.2$ obviously explains the overall diminished β-adrenergic response but the resilient increase at 1μM isoprenaline is linked to the 72% rise in NCX1 protein reported in the elderly SA node. This rise in NCX1 levels has a dual effect: the molecular partnership between RYR2 and NCX1 (Bogdanov et al., 2001) causes increased inward NCX1 current during diastolic depolarisation, and the augmented availability of exchangers signifies faster removal of Ca^{2+} from the cytosol especially during periods of high demand. In summation this supports the previous statement that NCX1 is fundamentally important in pacemaker activity (Sanders et al., 2006), but moreover it also plays a vital role in β-adrenergic response in the elderly SA node.

Isoprenaline is also known to affect I_f via elevated cAMP (Brown et al., 1979), however, HCN4 knockout mice exhibited a normal response to β-adrenergic stimulation (Herrmann et al., 2007). This may not be fully conclusive as a recent study has reported HCN1 mRNA present in rat SA node tissue (Tellez et al., 2011). Unfortunately in this chapter HCN of either isoform was not investigated, but another cardiac Na^+ channel, $Na_v1.5$ was reported to increase by 34% in the elderly SA node.

3.4.3.5 Effect of isoprenaline and CPA on pacemaker shift

The origin of the AP in the SA node, known as the leading pacemaker site (LPS) is dynamic and changing according to surrounding conditions (Schuessler et al., 1996). Shift of the pacemaker site was reported to be induced by nerve stimulation of the atria or pharmacological intervention alongside changes in deflections of diastolic depolarisation in different locations; pacemaker shift affects excitability and AP propagation (Yamamoto et al., 1998). In combination with the conduction and manually drawn maps isoprenaline and CPA affected the location of the LPS. Unfortunately no previous studies were found that investigated pacemaker shift in the presence of isoprenaline and/or CPA in an ageing model but consequences of age related pacemaker shift response can be speculated.

With age the response of pacemaker shift to isoprenaline in the presence of CPA differed from the younger age group, with LPS location consistently shifted upwards. This may be explained by a combination of firstly, the age-associated reduced role of SERCA2a in β-adrenergic response, thus CPA had a lesser effect on LPS location, and secondly the reliance on alternative Ca^{2+} handling mechanisms which is important but not as instrumental in the younger age groups. The relationship between pacemaker shift and age as a response to isoprenaline could further elucidate the diminished β-adrenergic response. As previously reported different locations of the rabbit SA node showed slower AP deflections (Yamamoto et al., 1998), instigating varied diastolic depolarisation that would affect spontaneous activity. Accordingly the location of the LPS would have a direct effect on β-adrenergic response.

In addition removal of the surrounding tissue was shown to affect the location of the LPS, which shifted from periphery to the centre, and spontaneous rate depending if the atrial muscle was attached (Kodama and Boyett, 1985). In this chapter the SA node preparation (see Figure 3.1) was left attached to the RA muscle therefore this could have affected pacemaker shift in younger animals but also influenced the elderly.

Isoprenaline caused positive pacemaker shift at all age groups suggesting a relationship between LPS location and β-adrenergic response. This could be correlated to the effect LPS location has on AP propagation; a different position of the LPS shapes the exit of an AP altering atrial muscle activation (Boineau et al., 1988) and affects heart rate in the dog (Boineau et al., 1983). Further studies have noted that there is a superior shift in the LPS of the SA node on the application of isoprenaline (Schuessler et al., 1996). Increased cytosolic Ca^{2+} or SR Ca^{2+} load during β-adrenergic stimulation could also shift the LPS. Pacemaker shift in relation to extracellular Ca^{2+} has been previously noted to relocate in combination with temperature (Mackaay et al., 1980) but no studies have investigated whether changes to age-associated changes in intracellular Ca^{2+} content in associated with pacemaker shift.

Interestingly in the 24 months SA node preparation (Figure 3.13) two main LPS were observed with an additional anomalous point located close to the CT tissue the latter of which has been implicated as a cause for AF (Kalman et al., 1998) (see Chapter 4). β-adrenergic stimulation had a clear affect on the LPS location and though this did not change with age, the removal of SERCA2a resulted in altered pacemaker shift in the young but not in the elderly, demonstrating an age-associated change in pacemaker movement.

3.4.4 Effect of ageing on the sensitivity to nifedipine

3.4.4.1 Age-associated affect on the influx of Ca^{2+} via $Ca_v1.2$

There was an age-associated increase in sensitivity to nifedipine. This correlates with previously documented clinical findings (Maxwell et al., 2000). $Ca_v1.2$ channels are directly blocked by nifedipine without other calcium channels being affected (Verheijck et al., 1999). In this chapter sensitivity of the SA node to nifedipine was reported to significantly differ in the elderly rats compared with the younger age group. However, studies on a rat animal model, specifically on the separated SA node is novel and therefore the explanation behind such heightened sensitivity is speculative.

$Ca_v1.2$ channel knock out mouse model demonstrates $Ca_v1.2$ channels are crucial in pacemaker activity and overall muscle contraction (Seisenberger et al., 2000). Nifedipine directly affects the α-subunit of $Ca_v1.2$ protein blocking the channel; incrementing concentrations of nifedipine sequentially reduces spontaneous activity of the SA node until cessation occurs. The age-associated increased sensitivity to nifedipine is partially attributed to the decreased $Ca_v1.2$ protein expression observed in

the elderly SA node. At lower concentrations of nifedipine (0.1 and 0.3µM) reduced intrinsic heart rate was observed but 1µM was near lethal in the 24 months age group. The drug molecular concentration to binding site ratio is significantly higher in these elderly rats. In contrast the younger age group required considerably higher concentrations of nifedipine to exhibit the same response, with 30µM required for cessation; this data correlates to healthy levels of $Ca_v1.2$ protein expression in the SA node observed in the 6 months of age tissue.

Similar effects of nifedipine sensitivity has previously been reported alongside an age-associated decline in $Ca_v1.2$ within the guinea pig SA node (Jones et al., 2007a). In this study amplitude of extracellular potentials was also observed to decline and was correlated to cases of human AF, in which shortened AP duration, reduced Ca^{2+} current amplitude and decline in $Ca_v1.2$ density has also been documented (Bosch et al., 1999, Van Wagoner et al., 1999).

Alternatively cessation of pacemaker activity may be related to the combination of age-associated deterioration of proteins SERCA2a, $Ca_v1.2$ and RYR2 noted in this chapter. The reduced $Ca_v1.2$ channels and closely located RYR2 sites impedes CICR and Ca^{2+} influx, which would explain the diminished amplitude of Ca^{2+} transients in the elderly. In addition, decreased SERCA2a activity causes lower SR Ca^{2+} content, creating a negative feedback loop to reduce RYR2 sensitivity to Ca^{2+} (Szentesi et al., 2004). Therefore nifedipine would have a profound effect on already dysfunctional Ca^{2+} cycling in the elderly SA node. Interestingly, in the 24 months age group at 0.1µM and 0.3µM nifedipine a minimal response compared with the 6 months age group was reported, suggesting an alternative mechanism in aiding pacemaker activity. Research into increased NCX1 protein levels provides an explanation for the low concentration discrepancy. NCX1 increased by 72% in the elderly SA node compensating for the lost of documented Ca^{2+} handling proteins; NCX1 in the healthy, young SA node is vital in pacemaker activity (Sanders et al., 2006), perhaps in the elderly its up-regulation acts as a compensatory mechanism. Conversely extrusion of cytosolic Ca^{2+} via NCX1 competes with SERCA2a (Vinogradova et al., 2010), normally there is an efficient balance between the two to maintain SR Ca^{+} content; however, with up-regulation of NCX1 and down-regulation of SERCA2a, extrusion of cytosolic Ca^{2+} by more exchangers would reduce intracellular Ca^{2+} to be taken up by SERCA2a further diminishing SR Ca^{2+} load. In summation the increased sensitivity to nifedipine in the elderly SA node and the more lethal response at higher concentrations, may be a result of ever decreasing SR Ca^{2+} load, via a combination of reduced influx by $Ca_v1.2$, lower RYR2 and SERCA2a levels and finally elevated NCX1 protein.

3.4.5 Age-associated changes in calcium handling proteins and their effect on SA node function/activity.

There has been continuous debate on the dominating factor in SA node pacemaker activity (Lakatta and Difrancesco, 2009). SR pumping kinetics have been shown to regulate LCR and spontaneous beating in the rabbit SA node (Vinogradova et al., 2010). The cycle length per spontaneous beat is defined by the rate of SR replenishment; this would occur based on SERCA2a activity and the cytosolic Ca^{2+} available due to $Ca_v1.2$ influx and RYR2 release flux (Vinogradova et al., 2010). Even though the role of the SR in instigating an AP is debatable there are clear changes in SR associated proteins with age. SERCA2a mRNA levels have previously been shown to decrease (Lompre et al., 1991a). In addition to reduced SERCA2a protein/activity, diminished SR Ca^{2+} content directly affects RYR2 sensitivity (Szentesi et al., 2004) and is linked to LCR frequency, duration and period (Vinogradova et al., 2010); overall a combination of which translates to reduced AP firing within the SA node. Evidently this explains the reported lower intrinsic heart rate in elderly animals.

Previous studies have confirmed that the up-regulation of RYR2 is instrumental in arrhythmia generation and sudden cardiac death suggesting SR Ca^{2+} leakage as the consequential culprit (Chelu et al., 2009, Cerrone et al., 2005). But in this chapter RYR2 protein was documented to decrease in the elderly SA node which would theoretically have the opposite effect and act as protective remodelling. Unfortunately this may not be the case; a more recent study by Bround *et al.* investigated RYR2 knock-out mice with 50% removal of RYR2 protein. In this study the decreased protein level was sufficient in causing bradycardia and arrhythmia (Bround et al., 2012); highlighting that loss of RYR2 function is firstly, important to SA node AP firing rate but secondly can lead to fatal arrhythmias previously observed in gain-of-function mutations.

In contrast to all other protein levels, NCX1 significantly increased at 24 months by approximately double that found in the young age groups. NCX1, as previously mentioned, is an important mechanism in Ca^{2+} extrusion and is vital for pacemaker activity (Sanders et al., 2006) and closely linked to RYR's LCRs (Bogdanov et al., 2001); but unfortunately NCX1 is considered a leaky protein (Philipson et al., 2002). NCX1 over expression, at least within the ventricles, is associated with heart failure (Flesch et al., 1996) and with the purported leaky property the 72% rise in NCX1

protein in the SA node provides evidence for the age-associated increased risk of generating an arrhythmia.

Increased RYR2 activity primarily affects AP firing rate through the augmented NCX1 current (Liu et al., 2011) therefore due to the decreased expression of RYR2 protein, along with the reduced role of SERCA2a with age, NCX1 increased protein levels would amplify NCX1 current (Bogdanov et al., 2006) and protect SA node activity. In addition $Na_v1.5$ was observed to increase in protein expression at 24 months, this provided extra Na^+ for the shuttling of Ca^{2+} aiding both Ca^{2+} influx and efflux during diastolic depolarisation and repolarisation respectively. Furthermore heterozygous SCN5A, gene coding for $Na_v1.5$, knock-out mice showed depressed heart rates and SA node block (Lei et al., 2005), supporting that $Na_v1.5$ is both important in SA node pacemaker activity but also AP propagation.

3.4.6 Limitations

Conduction velocity was only calculated by using the LPS site and the reference site, thus the distance and time between AP were measured. The propagation was measured across the CT and into the RA muscle, but no consideration was made for how the CT would affect propagation. The conduction maps clearly show that near/at the CT region there is a change in the conduction velocity, this could be purely due to the CT or connective tissue observed in the SA node from other species (Coppen et al., 1999).

Although protein changes were investigated and functionality tested through the use of CPA and isoprenaline, pumps and exchangers such as NCX1 and PMCA4a or channels such as RYR2 were not effectively tested; decreases in protein levels are apparent, but their function is not. Therefore this is a limitation that can be removed by electrophysiological recordings of each current and using selective blockers to assess the changes in current with age such as Li+ exchange or ryanodine (Bogdanov et al., 2001). Furthermore though decreases in these proteins were observed, no investigation was made into the cause, qPCR would have determined whether mRNA levels were decreased comparatively. Nevertheless this is partially flawed as mRNA does not always correlate to protein data as previously demonstrated (Tellez et al., 2011).

In regards to SERCA2a activity, only PLB was investigated; sarcolipin (SLN), previously thought to only affect SERCA1, was shown to interact with SERCA2a affecting Ca^{2+} affinity, just like PLB (Vangheluwe et al., 2005). Furthermore in humans SLN mRNA was found in the heart, and could thus have an effect on SERCA2a

(Vangheluwe et al., 2006). Consequently as SLN was not investigated, the decrease in SERCA2a activity may not be highly accurate if solely calculated using PLB monomer levels.

Lastly SR Ca^{2+} load has been a underlying theme with proteins directly involved such as RYR2 and SERCA2a being discussed. However, no consideration has been made for another Ca^{2+} store within the SA node, the mitochondria. In a very recent study Yaniv *et al.* reported crosstalk between mitochondrial and SR Ca^{2+} cycling, with the former having direct effects on SR Ca^{2+} load and LCR frequency, duration, amplitude and period. Therefore a change in mitochondrial Ca^{2+} flux may translate into altered firing rate of the SA node (Yaniv et al., 2012b).

3.4.7 Conclusions

In conclusion SR Ca^{2+} cycling is crucial for pacemaker activity and with age there were evident changes in Ca^{2+} handling within the SA node. β-adrenergic response was significantly diminished in the elderly age group. The removal of SERCA2a activity via application of 3μM CPA profoundly affected the response to isoprenaline in the younger age groups but had no effect in the elderly elucidating the age-associated reduced role of SR Ca^{2+} pumping rate in the response to β-adrenergic stimulation. The reduced protein expression of SERCA2a, RYR2 and $Ca_v1.2$ provides sufficient evidence for dysfunctional spontaneous activity in the elderly SA node and impaired response to increased demand. In addition the age related increase in sensitivity to nifedipine highlights not only the importance of $Ca_v1.2$ channels in pacemaker activity but also the purported compensatory NCX1 up-regulation, though initially useful, this has been argued as deleterious remodelling and a predisposition for SA node dysfunction.

Chapter 4 Age-associated changes in Ca^{2+} handling proteins within atrial tissue

4.1 Introduction

4.1.1 RA heterogeneity

4.1.1.1 Structure of the RA

As discussed in Chapter 3, the SA node is located on the endocardial wall of the RA. Between the SA node and RA muscle is the crista terminalis (CT), possessing morphological and physiologically different properties to that of surrounding tissue (Boyett et al., 2000). Chapter 3 showed Ca^{2+} handling proteins changed their expression with advanced age within the SA node, however, whether similar alterations occur in the surrounding tissue is unknown. Often RA muscle has been used as a protein and mRNA comparison with the SA node (Allah et al., 2011), but a comprehensive investigation into calcium handling proteins and their changes with age, in particular the CT tissue, has not been conducted.

4.1.1.2 Crista terminalis

The CT is a strip of tissue on the interior wall of the RA; the structure provides a barrier between the SA node and RA muscle that alters the electrical activity from the SA node propagating to the RA muscle producing non-radial spread of the action potential (Bleeker et al., 1980). Studies have shown that the CT mimics RA muscle (D'Amato et al., 2009), but also some have suggested a connection between the CT and the generation of arrhythmias (Akcay et al., 2007). Consequently the CT has recently become a target for interventional therapy for atrial arrhythmias (Li-jun et al., 2012).

One study comparing cells of the CT with RA pectinate muscle observed a comparatively longer AP duration in CT cells and changes in conduction velocity depending on whether AP was measured transversely or longitudinally (Li-jun et al., 2012). Li-jun et al. also showed CT cells possessed some level of spontaneous activity; under control conditions a rate of 42-71 beats/min was observed. This finding suggests that the CT may have the ability to create ectopic excitation which coincides with local auricular tachycardias reported to originate from and/or along the CT (Kalman et al., 1998). Furthermore reentrant atrial AP arising from the right atrium were also observed to distribute at the CT and root of the superior vena cava (Xianda et al., 2003). Consequently it has been reported that improper nodal activity manifesting as

tachycardia and leading to AF can be terminated by ablation at the CT (Man et al., 2000).

4.1.1.3 Ageing and CT tissue

These investigations suggest that the CT can be regarded as a separate type of tissue to be compared with the SA node and RA muscle; however, studies focusing on the age-associated changes within the CT are novel. Most studies of the CT focus on the increased association between age and AF, with the CT as a culprit but rarely the underlying causes pre-AF (Matsuyama et al., 2004). Age-associated changes to Ca^{2+} handling proteins such as $Ca_v1.2$ within the SA node, have been previously associated with increased SA node dysfunction (Jones et al., 2007a). Consequently age-associated changes in the regulation of Ca^{2+} within the CT may be responsible for the dysfunction of the CT tissue and increased cause of reentrant and ectopic tachycardias.

4.1.2 Right and left atria

4.1.2.1 Role of the atria in the heart

The AP propagates from the SA node to both atria causing them to contract simultaneously and push blood into the ventricles. Although the force of atrial contraction is smaller than that in the ventricles, the atria can enhance the amount of blood pushed into the ventricles before systole (Bootman et al., 2011). The majority of ventricular refilling occurs due to venous return and ventricular relaxation; during periods of exercise or stress, when increased heart rate is required, atrial contraction can account for approximately 20-30% of the volume of blood entering the ventricles (Lo et al., 1999).

4.1.2.2 Cardiac arrhythmias originating outside of the SA node

As discussed in Chapter 1, one of the most common cardiac arrhythmias is AF (Kannel et al., 1982); electrical impulses occur spontaneously at high frequency from sites around the atria and notably from the CT (Li-jun et al., 2012). The contribution of atrial contraction during exercise, also termed 'atrial kick', is lost during AF, which results in the blood pumping capacity of the heart to be reduced by a third (Alpert et al., 1988).

Though AF is not immediately life threatening, stagnation of blood flow arising from AF severely increases the risk of thrombosis which can lead to a stroke (Wolf et al., 1991, Quinn and Fang, 2012). There is an extensive number of studies which indicate dysregulation of Ca^{2+} signalling is an important factor in the genesis and maintenance of AF (Greiser et al., 2011).

4.1.2.3 Effect of ageing on calcium regulation within the atria

Chapter 1 introduced the concept of 'normal' Ca^{2+} handling in atrial myocytes which includes minimal t-tubule organisation and CICR (see section 1.4). With age RYR2 and SERCA2a protein have been previously shown to be unchanged, although SERCA2a activity decreased (Kaplan et al., 2007). Many studies focusing on the factors of AF and to a lesser extent on ageing, have shown multiple alterations in atrial Ca^{2+} handling. In humans suffering from AF, SERCA2a and $Ca_v1.2$ mRNA declined (Lai et al., 1999), Greiser *et al*. also showed a decrease in SERCA2a and PLB protein (Greiser et al., 2009). Conversely other human studies have shown increased SERCA2a function (El-Armouche et al., 2006). RYR2 was observed to increase in canine atrial myocytes exhibiting AF, consistent with the theory of Ca^{2+} 'leak' from the SR (Vest et al., 2005). SR and $Ca_v1.2$ channel activities are instrumental in cardiac beat-beat stability (Llach et al., 2011). Consequently age-associated changes in Ca^{2+} handling proteins could evoke similar dysregulation of Ca^{2+} as observed in AF.

This chapter investigated changes in the RA wall encompassing the SA node, CT and RA muscle using an ageing rat model. Chapter 3 demonstrated age-associated changes in Ca^{2+} handling proteins within the SA node. Therefore a further investigation of whether these changes occur in surrounding tissues is warranted. The increasing correlation between ageing and development of atrial arrhythmias justified a comparison of age-associated changes in Ca^{2+} handling proteins within left and right atria.

4.1.3 Objectives

The aims of the current study were:

i. To determine age-associated changes in the protein expression of the Ca^{2+} transporters - SERCA2a, PLB, RYR2, Cav1.2, NCX1, PMCA4a within the RA wall inclusive of the SA node, CT and RA muscle.

ii. To elucidate similarities and differences between LA and RA protein expression of the Ca^{2+} handling channels, pumps and exchangers with advancing age.

iii. To determine whether the protein changes within the LA and RA are accompanied by decreased/increased levels of corresponding mRNA.

4.1.4 Hypothesis

1. The CT and RA muscle exhibit different levels of Ca^{2+} handling proteins compared with the SA node. Age-associated changes to these proteins particularly in the CT region may explain the increased risk of arrhythmia generation in the elderly.

2. Differences in Ca^{2+} handling protein expression occurs across the left and right atria. Ageing will cause Ca^{2+} remodelling which will varying depending on the region. These changes will result in increased frequency of SR Ca^{2+} 'leakage' responsible for ecotopic beats.

4.2 Methods

4.2.1 Further dissection of the RA

The RA was removed from the whole heart and dissected into separate regions as shown in figure 4.1. Regions were crushed, proteins extracted and analysed by electrophoresis (see section 2.2). Methods were further optimised for the use of particular antibodies (see section 3.3).

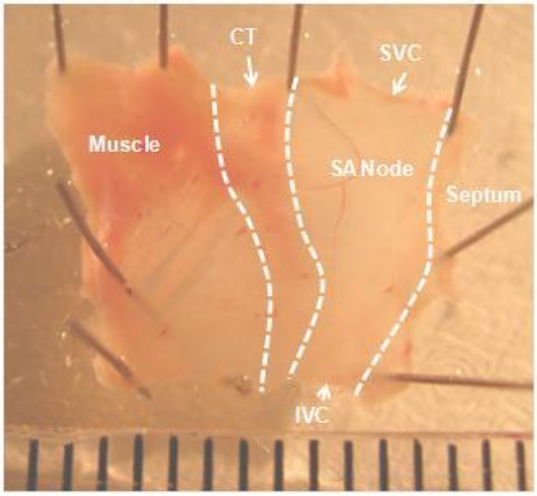

Figure 4.1 Right atrium.

The right atrium encompassing the SA node is shown with a ruler indicating 1mm intervals. Structures are labelled: crista terminalis (CT), sinoatrial (SA) node, superior vena cava (SVC), inferior vena cava (IVC)

4.2.2 RA tissue sections for immunocytochemistry

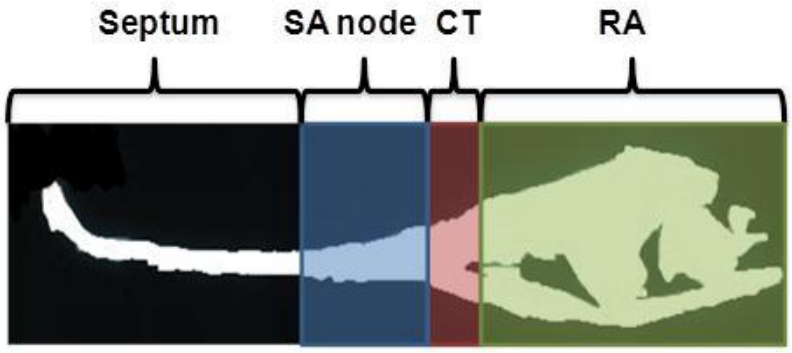

Figure 4.2

RA cross section.

Colours indicate the regions for each tissue type which change in size with age.

Immunocytochemistry was conducted as described in section 2.3 and an appropriate dilution used to visualise the specific protein (see Table 2.2); images were subsequently recorded from the appropriate region via confocal imaging (figure 4.2).

4.2.3 Statistical analysis

In Chapter 4 statistical differences were determined by two way ANOVA with Holm-Sidak comparisons. For each age group 6, 12 and 24 months, n=5. Data are presented as means ± SEM.

4.3 Results

4.3.1 Characterisation of qPCR technique

4.3.1.1 Test for positive and negative reverse transcriptase controls using actin primer

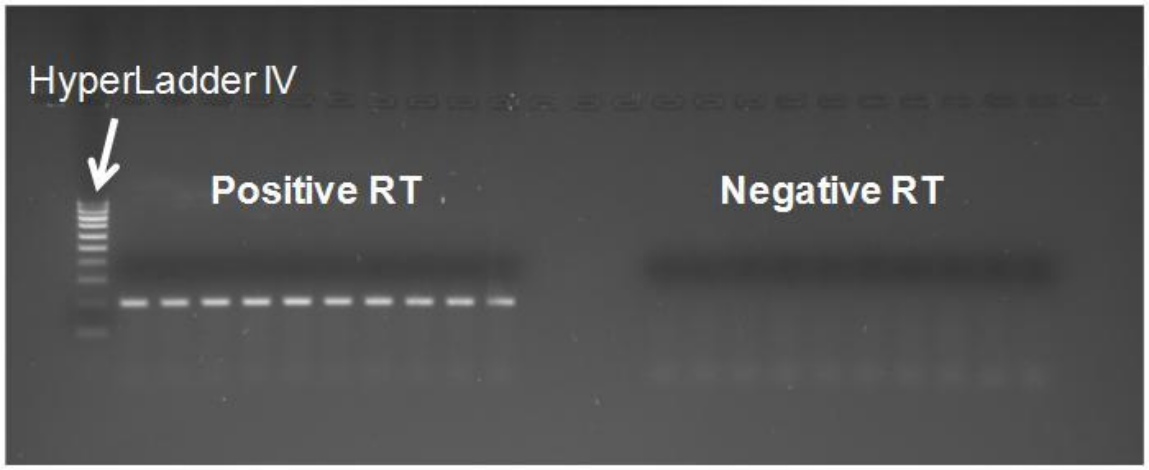

Figure 4.3 Actin transcript test amplification gel.

6 months and 12 months (n=5) samples from the left atria (LA). Negative RT samples replaced superscript III with RNAse/DNAse free H_2O.

For each sample 2µg of cDNA was loaded, analysed on a 2.5% agarose gel and imaged (see section 2.6.5). Fluorescence shown as white bands (Figure 4.3) indicates the amplification of actin, while the lack (negative RT) indicates successful negative controls. Consequently this shows that samples without superscript III was not able to replicate the actin transport and thus did not have any detectable cDNA/fluorescence.

4.3.1.2 Selection of endogenous control

Table 4.1 C_T values for atrial tissue with desmin as an endogenous control

Desmin	6 months	12 months	24 months
LA C_T	23.2	23.9	23.1
RA C_T	23.7	24.2	23.9
Max C_T	0.5	0.3	0.8

The cycle threshold (C_T) was detected and recorded; the C_T is defined as the number of cycles required for the fluorescent signal to exceed the threshold. CT is inversely proportional to the target nucleic acid present in the sample. High C_T variation indicates different abundant levels of nucleic acid in the sample.

Table 4.2 C_T values for atrial tissue with GADPH as an endogenous control

GAPDH	6 months	12 months	24 months
LA C_T	20.3	20.4	19.8
RA C_T	21.6	22.0	20.9
Max C_T	1.3	1.6	1.1

Highlighted boxes show a maximum C_T difference of 2.2 for GAPDH (table 4.2), indicating that GAPDH was expressed at different levels with age, which is unacceptable for an endogenous control. The maximum C_T for desmin across the age groups was 1.1 (table 4.1). Therefore, although GAPDH within the age groups did not differ significantly, comparison across age groups marked GAPDH mRNA expression to significantly change; and consequently GADPH could not be used as an endogenous control. This further emphasises the importance of a good endogenous control in qPCR, as high variation in C_T values in the endogenous control could result in false positive results. Subsequent qPCR was conducted using desmin as the endogenous control.

4.3.2 Calcium handling in the RA differs with age

Age-associated differences in SR associated proteins SERCA2a, PLB and RYR2, were investigated in the RA comprised of the SA node, CT and RA muscle. SERCA2a protein was detected at 110 kDa. PLB was detected at 30 kDa and 6 kDa, which correlates to the PLB pentameric and monomeric isoforms respectively. RYR2 protein was detected at 565 kDa. Age-associated differences in calcium flux protein $Ca_v1.2$ and Ca^{2+} extrusion proteins NCX1 and PMCA4a were also investigated. Immuno-labelling of $Ca_v1.2$ protein was exclusively detected at 210 kDa. NCX1 specific immuno-labelling was detected at 160 kDa and a second band at 120 kDa. For PMCA4a a single band was detected at 130 kDa.

4.3.2.1 Age-associated differences in SERCA2a activity and expression across the RA

The protein expression of SERCA2a and PLB monomer protein were used to calculate a ratio that indicates SERCA2a activity. At 6 months of age there was no significant difference in SERCA2a protein expression within the RA (Figure 4.4). But in the 12 months age group, expression in the SA node significantly increased by 50±9.2% whereas the CT and RA muscle unchanged. At 24 months of age SERCA2a protein expression decreased significantly in the SA node, CT and RA muscle; furthermore expression levels were equivalent across all areas.

The CT was observed to have occasional striated patterns with SERCA2a located along the periphery and radiating inwards, however, at 24 months of age the fluorescence was significantly reduced by 28±6.2% and striated patterns were no longer visible. RA muscle was examined to have had significantly higher density of SERCA2a protein at both 6 and 24 months of age compared with both the SA node and CT. Similar to the CT, a dense t-tubule pattern of SERCA2a was observed in the RA muscle that remained at the periphery of the myocyte. With age the level of SERCA2a protein significantly declined in the RA muscle from 126±5.9% to 96±9.6% the latter was equivalent to protein levels observed in the SA node and CT at 6 months of age (Figure 4.5).

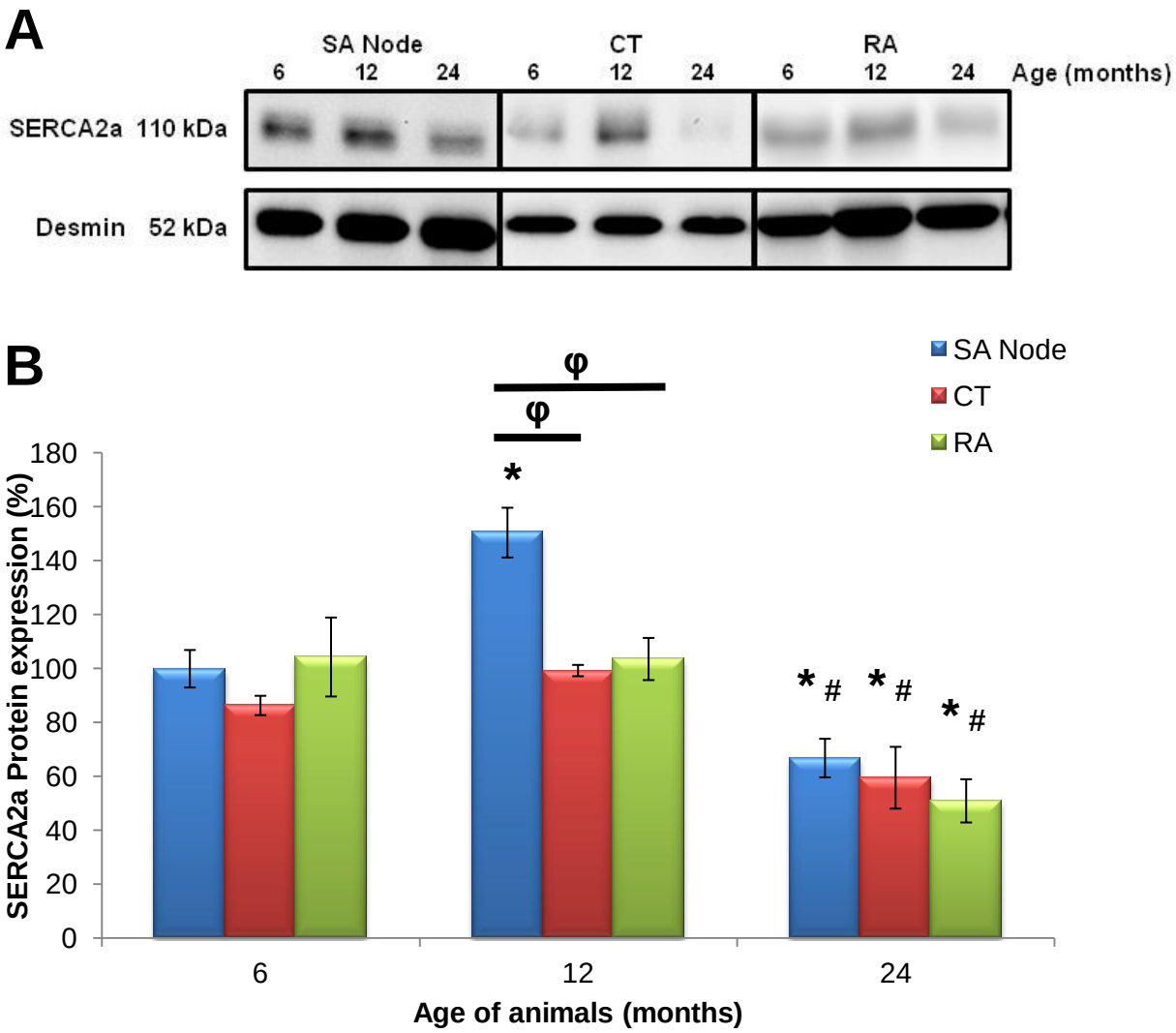

Figure 4.4 Profile of SERCA2a protein expression across the RA with increasing age

A) illustrative blot of SERCA2a protein and desmin; B) SERCA2a protein expression normalised to desmin. * denotes $p<0.05$ vs. respective 6 months data, # denotes $p<0.05$ vs. respective 12 months data, φ $p<0.05$ vs. within age group. n=5 per age group.

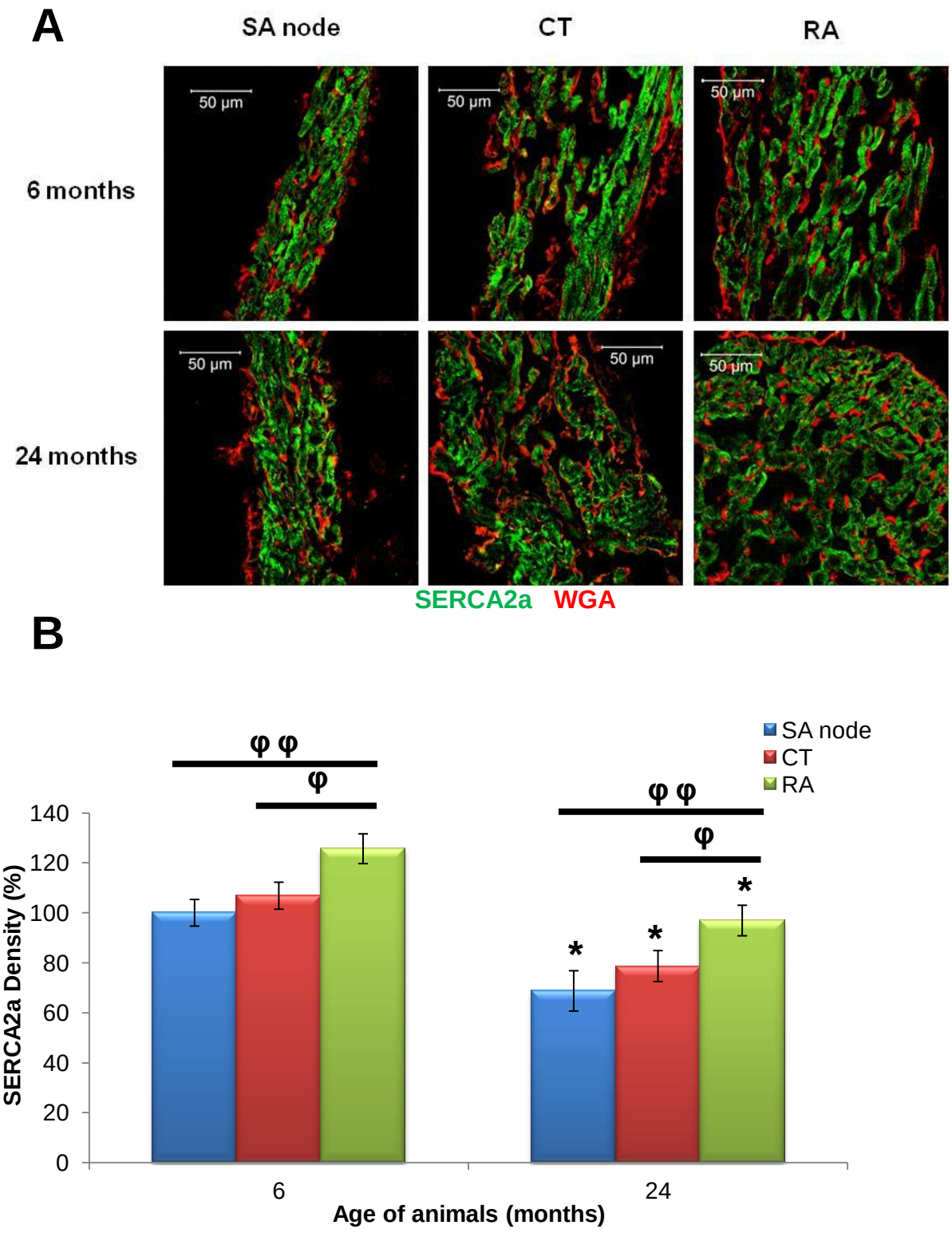

Figure 4.5 Localisation of SERCA2a protein expression within regions of the RA

A) illustrative images across the RA are shown from rat hearts at 6 and 24 months of age; B) density of SERCA2a label for SA node, CT and RA muscle. * denotes $p<0.05$ vs. respective 6 months data, φ $p<0.05$ vs. within age group. n=5 per age group.

Within the 6 months age group, RA muscle demonstrated an 18±8.1% increase in PLB total protein expression compared with the SA node (100±7.2%)(Figure 4.6), whereas expression in the CT was significantly lower (57±13.8%) compared with the SA node and RA muscle tissue. In figure 4.6C different isoforms of PLB were shown; the greater expression at 6 months of age within the RA muscle can be explained by the significantly higher level of PLB pentamer compared with the SA node, even though the PLB monomer levels are equivalent between both.

At 12 months of age PLB total expression increased by 21±9.2% in within the CT, although this was not significant it resulted in equivalent levels across the SA node and RA muscle (Figure 4.6B); this rise is due to the significant increase in PLB pentamer within the CT (Figure 4.6C). There was no age-associated difference in PLB total protein expression within the SA node or RA muscle. Conversely at 24 months of age the CT showed a significant rise 36±14.5% in PLB total, which was significantly higher than the SA node or RA muscle. The rise of PLB total was a combination of approximately two-fold increases in PLB pentamer and PLB monomer protein when compared to the 6 months age group (Figure 4.6C).

There was no significant difference between the SA node and CT, the latter showing PLB located at the periphery of the myocytes with occasional striated patterns (Figure 4.7). Conversely the RA muscle had a significantly higher level of PLB protein (139±12.5%) which was observed to be densely packed throughout the myocytes. With age in the SA node and RA muscle PLB protein density decreased significantly. The SA node was observed to have no dense clumps and reduced PLB protein within the myocytes. Similarly the RA muscle had an elevated level of fluorescence at the periphery of cardiac myocytes (Figure 4.7). At 24 months of age the CT significantly increased in PLB protein from 102±14.7% to 130±6.8%; dense clumps were observed throughout the myocytes, with t-tubule patterns occasionally visible. Both CT and RA muscle showed significantly higher densities of PLB protein at 24 months of age when compared with the SA node (Figure 4.7).

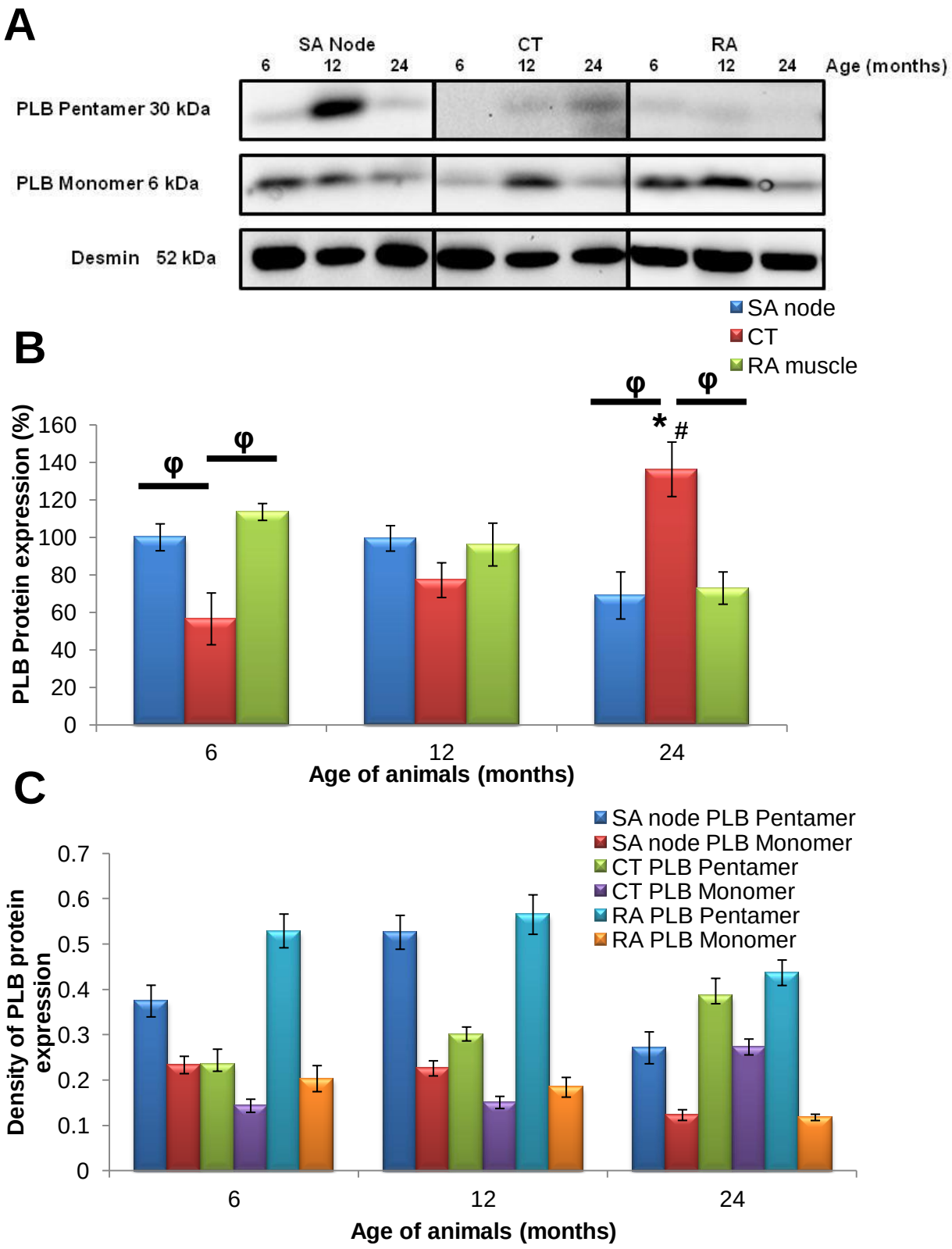

Figure 4.6 Profile of PLB protein expression across the RA with increasing age.

A) illustrative blots of PLB monomer and pentamer B) PLB total protein expression normalised to desmin C) PLB pentamer and monomer protein expression. * denotes $p<0.05$ vs. 6 months age group; # denotes $p<0.05$ vs. 12 months age group, φ $p<0.05$ vs. within age group. n=5 per age group.

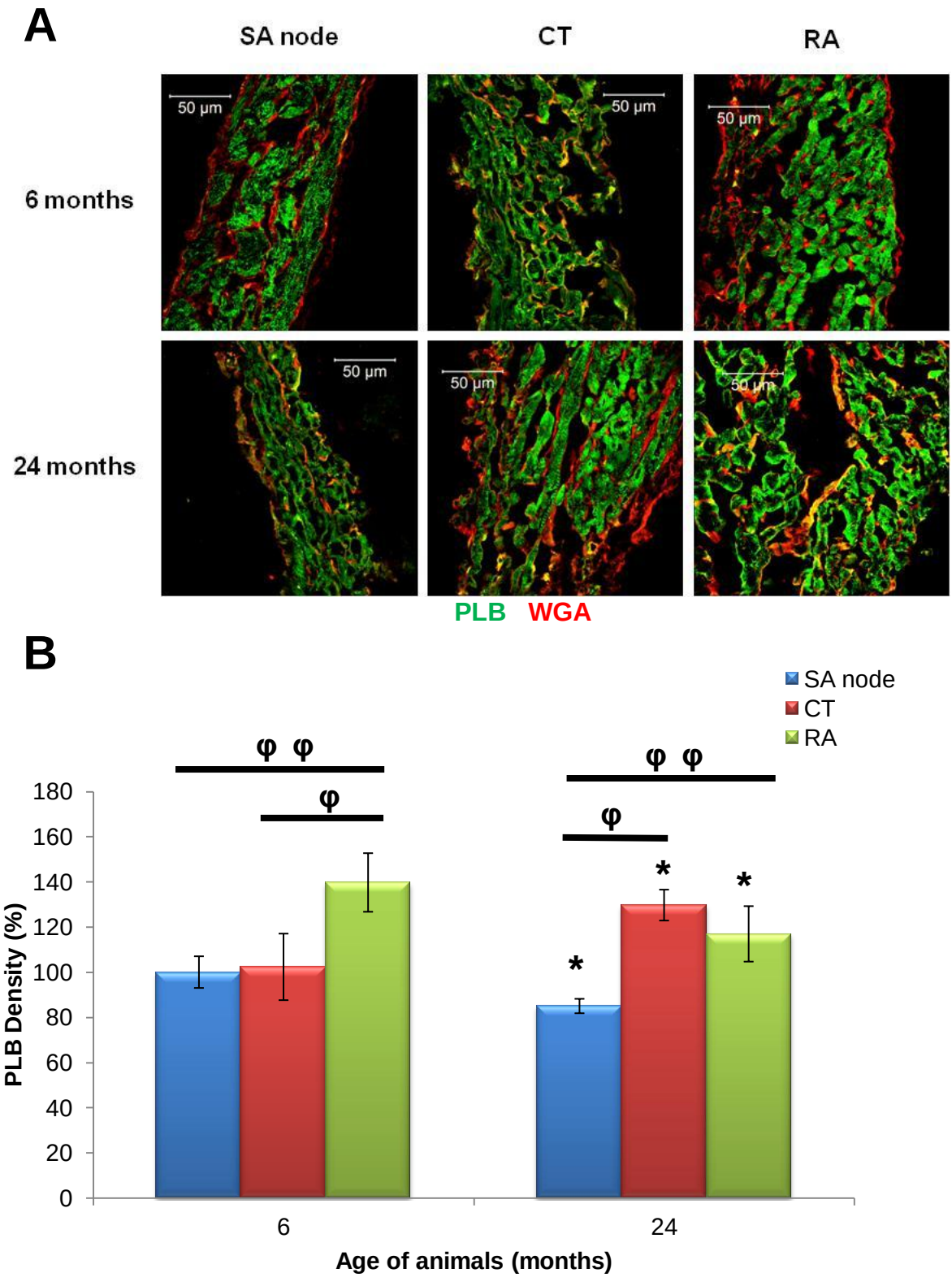

Figure 4.7 Localisation of PLB protein expression within regions of the RA

A) illustrative images across the RA are shown from rat hearts at 6 and 24 months of age; B) density of PLB label for SA node, CT and RA muscle. * denotes $p<0.05$ vs. respective 6 months data, φ $p<0.05$ vs. within age group. n=5 per age group.

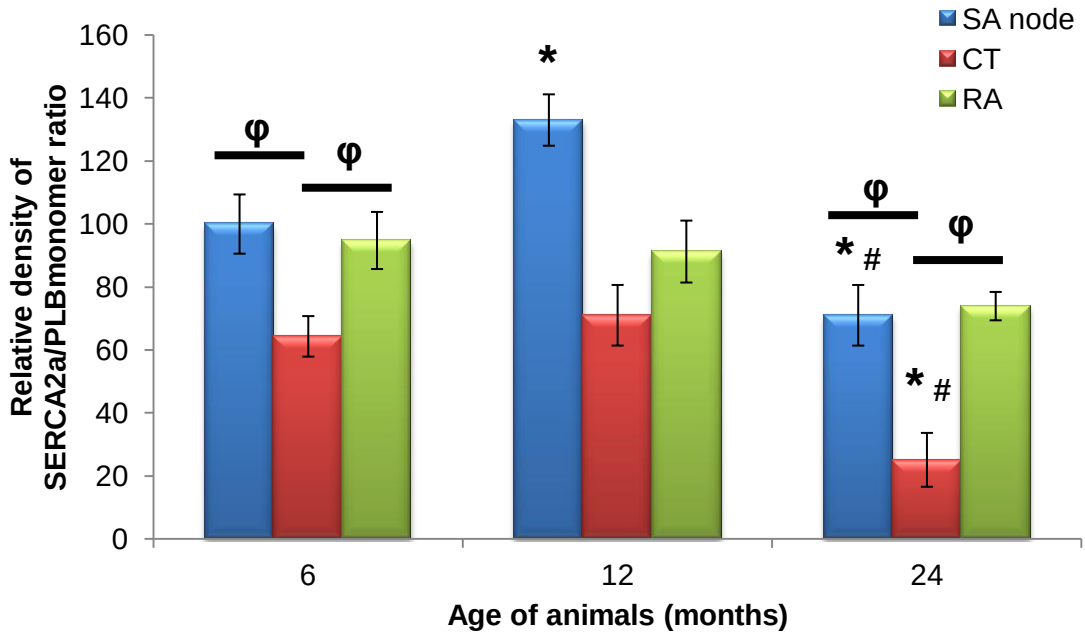

Figure 4.8 SERCA2a activity in the RA with advancing age.

SERCA2a protein expression normalised to PLB monomer expression indicates the functional capacity of the calcium pump SERCA2a. * denotes $p<0.05$ vs. respective 6 months age group, # denotes $p<0.05$ vs. respective 12 months age group, φ $p<0.05$ vs. within age group. n=5 per age group.

There was no significant difference in SERCA2a activity in the 6 months age group between the SA node (100±9.4%) and RA muscle (95±9.0%), however, the CT was comparatively lower (64±6.4%)(Figure 4.8). As shown in Chapter 3, the SA node showed a 33±8.1% increase in SERCA2a activity at 12 months of age but in the 24 months age group, activity dropped to levels below that observed in the younger age groups. The CT increased by 7% at 12 months, though not significant, this rise resulted in equivalent levels of SERCA2a activity between the RA muscle and CT. Nevertheless in the 24 months age group CT SERCA2a activity was dramatically reduced to 25±8.5%. This decline in SERCA2a activity within the CT was significantly lower than the bordering SA node or RA muscle, both of which showed similar levels of activity within the 24 months age group and were also equivalent to levels observed at 6 months of age.

4.3.2.2 Effect of ageing on the protein expression of RYR2

Within the 6 months age group there was a significantly higher level of RYR2 protein in the RA muscle (137±4.2%) compared with the SA node (100±10.2%) or CT (79±4.7%) (Figure 4.9). At 12 months of age both the SA node and RA muscle significantly increased in RYR2 protein to 135±6.2% and 168±7.3% respectively, however, the RA muscle was still markedly higher than surrounding tissue types. With age there was a significant increase in the expression of RYR2 protein in the CT (121±6.1%) even though at 6 and 12 months of age, levels were significantly lower than bordering tissue. At 24 months of age there was a drastic decline in RYR2 protein within the SA node (68±15.3%) and RA muscle (101±11.1%)(Figure 4.9).

At 6 months of age, the CT had sparsely localised RYR2 protein with irregular t-tubule striations but higher levels of density in the CT compared with the SA node, 141±7.1% and 100±6.4% respectively (Figure 4.10). The RA muscle had an extremely high density of RYR2 (224±7.4%), located at the periphery and throughout the cardiac myocytes, t-tubule striations though sporadic were visible at the cell membrane. With age RYR2 protein within the CT showed no change in expression, however, the majority of RYR2 protein was now located at the periphery of the cardiac myocytes (Figure 4.10). In the SA node and RA muscle there was a significant decline in RYR2 protein, although within the 24 months age group the RA muscle maintained an elevated level of RYR2 protein (169±7.8%) compared with the CT (121±6.7%). This was also significantly higher than in the SA node (77±3.4%). Ageing had a similar effect on the RA muscle as in the CT; RYR2 protein was concentrated at the periphery of myocytes rather than throughout the cells and t-tubule striations were no longer as visible (Figure 4.10).

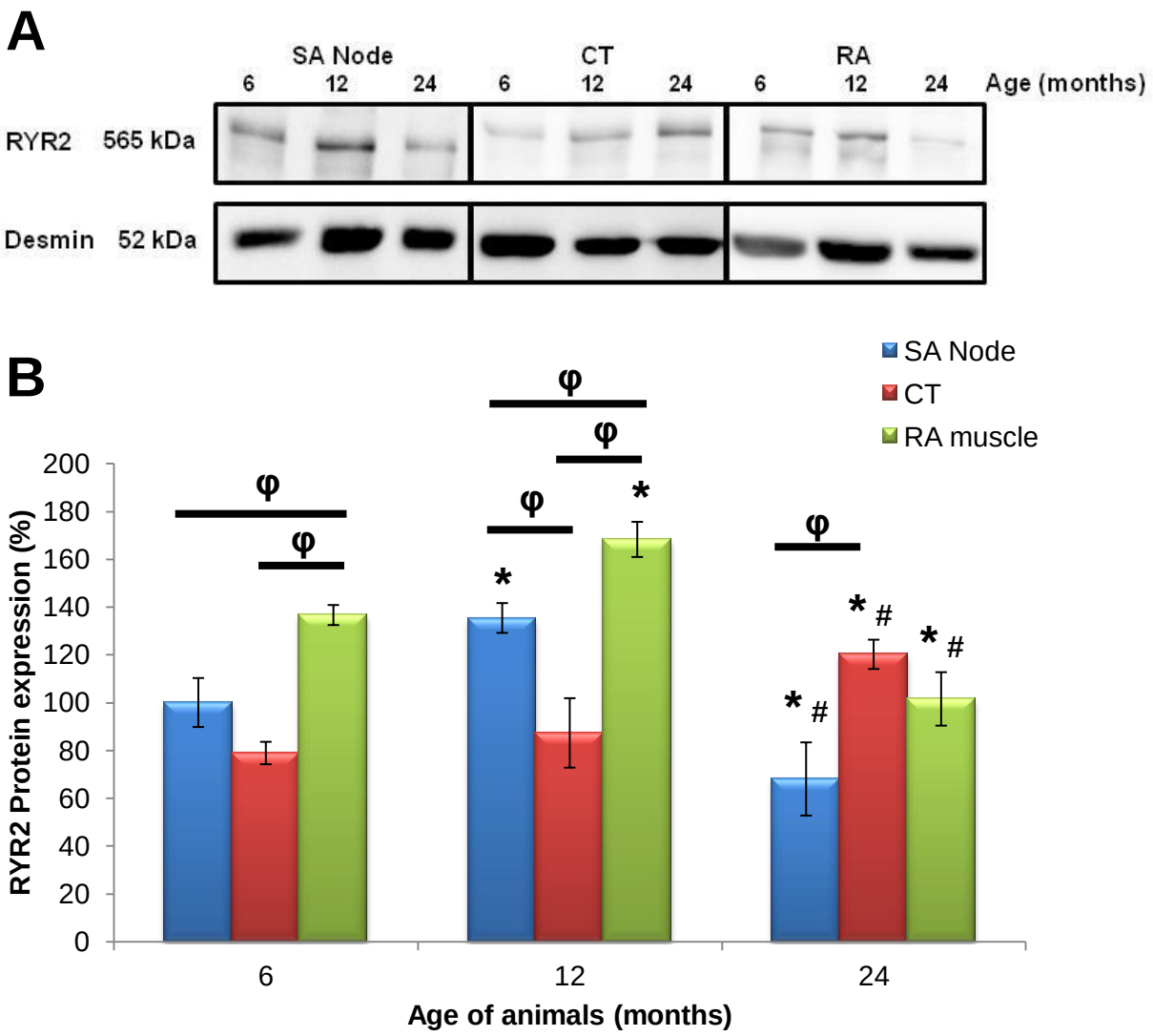

Figure 4.9 Profile of RYR2 protein expression across the RA with increasing age

A) illustrative blot of RYR2 protein and desmin; B) RYR2 protein expression normalised to desmin. * denotes $p<0.05$ vs. respective 6 months data, # denotes $p<0.05$ vs. respective 12 months data; φ $p<0.05$ vs. within age group. n=5 per age group.

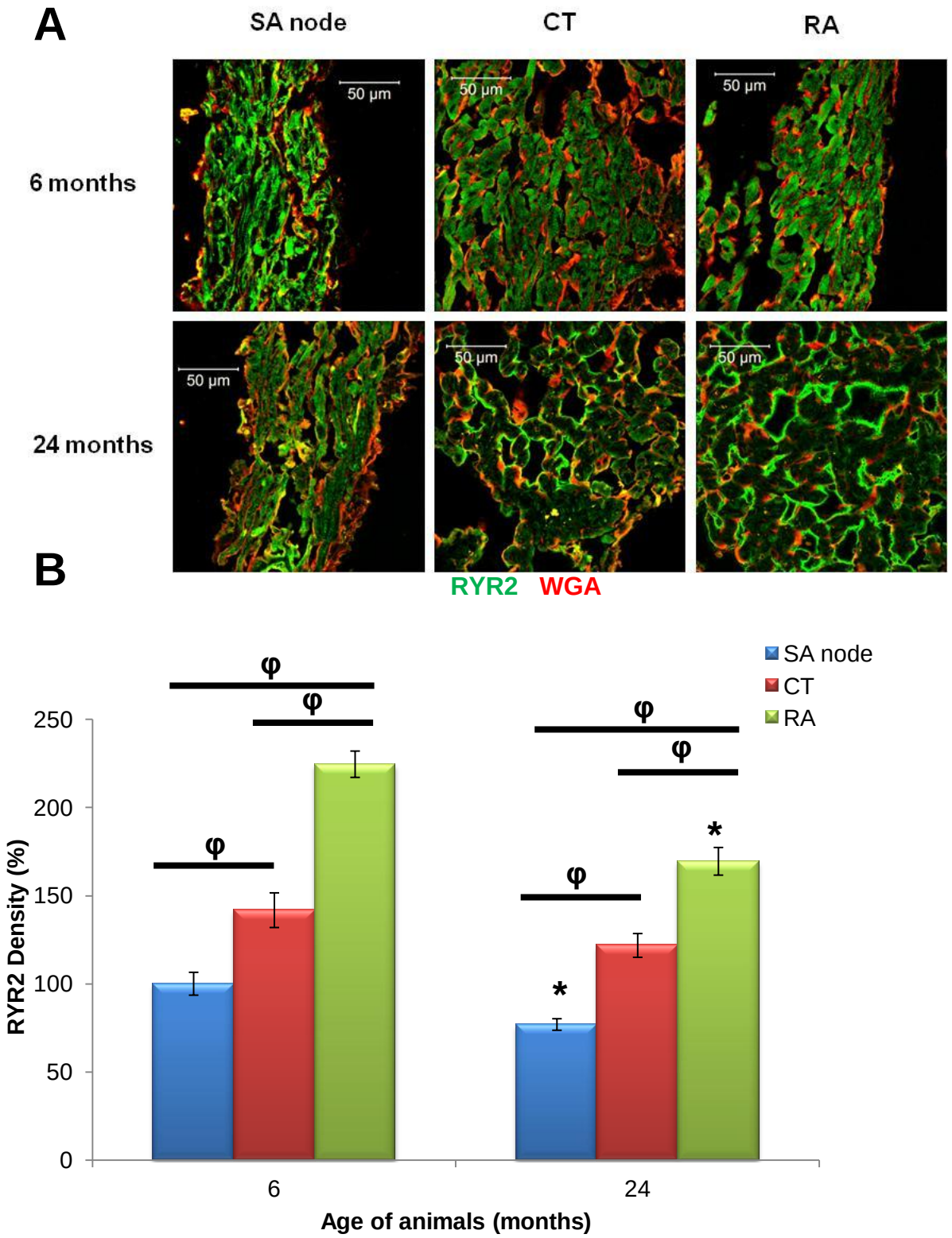

Figure 4.10 Localisation of RYR2 protein expression within regions of the RA

A) illustrative images across the RA are shown from rat hearts at 6 and 24 months of age; B) density of RYR2 label for SA node, CT and RA muscle. * denotes $p<0.05$ vs. respective 6 months data, φ $p<0.05$ vs. within age group. n=5 per age group.

4.3.2.3 Expression of $Ca_v1.2$ channels within RA regions changes with increasing age.

At 6 months of age no significant difference in $Ca_v1.2$ protein expression across the RA was observed, whilst at 12 months of age there was an increase within the SA node, from 100±10.9% to 125±13.2% (Figure 4.11). RA muscle and CT remained at similar levels of $Ca_v1.2$ protein expression to that observed at 6 months of age. Within the 24 months age group there was a significant decline in expression in the SA node and RA muscle, resulting in similar levels of $Ca_v1.2$ protein (Figure 4.11). Conversely within the CT $Ca_v1.2$ protein increased sharply at 24 months of age from 71±17.9% at 6 months of age to 116±8.5% at 24 months of age. Consequently with advanced age, the CT showed extreme variation in $Ca_v1.2$ protein expression when compared with bordering SA node and RA muscle.

At 6 months of age, $Ca_v1.2$ protein was densely packed throughout the SA nodal cells, but within the CT $Ca_v1.2$ was concentrated in the periphery of the cardiac myocytes with occasional t-tubules visualised as shown in Figure 4.12. RA muscle had a significantly higher density of $Ca_v1.2$ (118±7.4%) compared with the SA node (100±3.4%) and CT (92±7.8%); the protein was located through the RA muscle cardiac myocytes with t-tubules visualised at the periphery of cells and radiated inwards by a short distance. With age the density of $Ca_v1.2$ decreased significantly in the SA node (77±1.7%) and RA muscle (103±6.6%) but the RA muscle remained significantly higher. Furthermore there was a change in localisation, with $Ca_v1.2$ protein concentrated on the periphery of RA muscle cardiac myocytes rather than densely packed throughout, occasionally t-tubules on the outskirts of cells were still visible. Conversely the CT had markedly increased $Ca_v1.2$ protein density (119±3.4%), with myocytes becoming highly packed though t-tubules were still occasionally visible these were sporadic with irregular densities of $Ca_v1.2$.

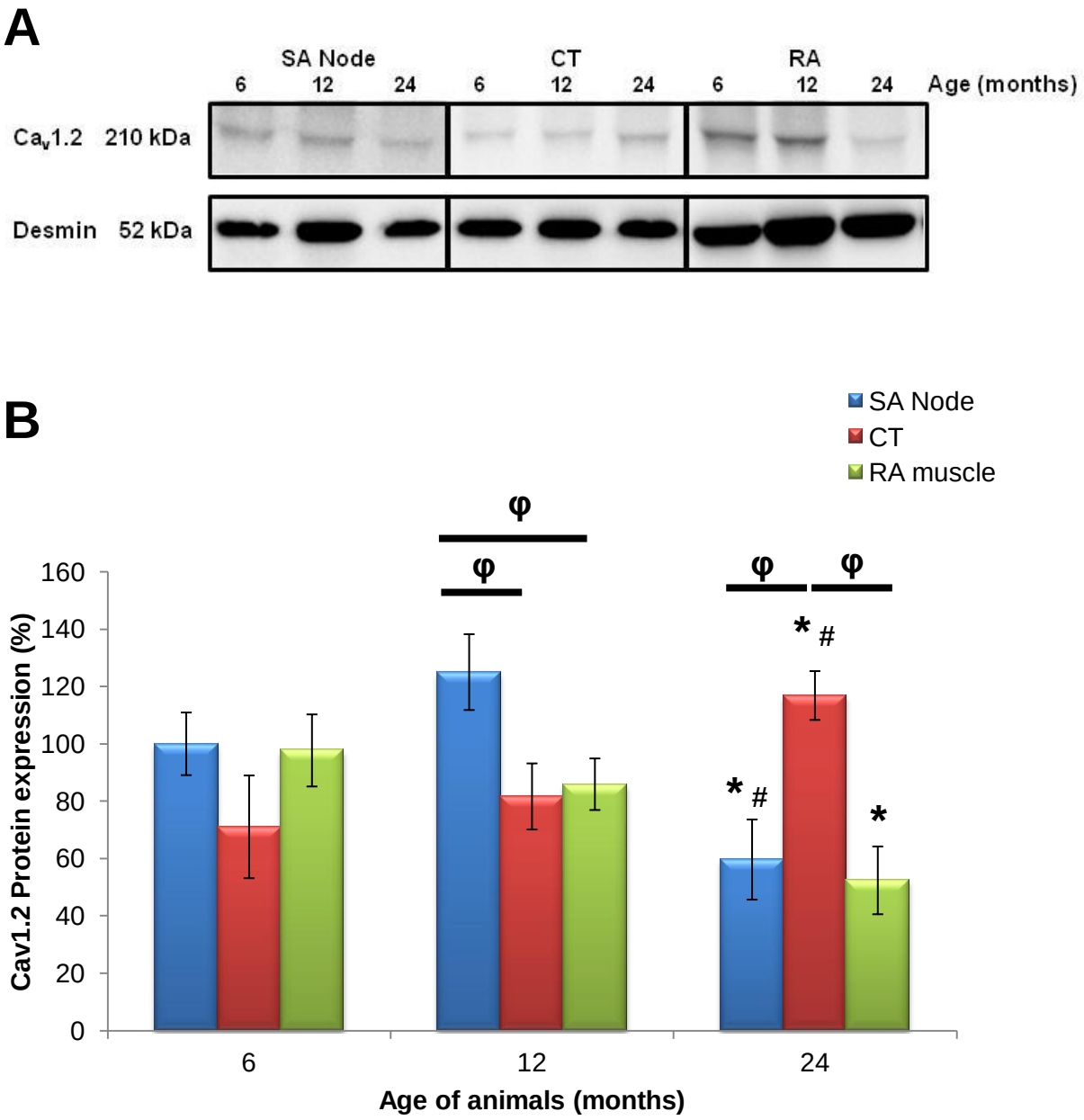

Figure 4.11 Profile of Ca$_v$1.2 protein expression across the RA with increasing age

A) illustrative blot of RYR2 protein and desmin; B) Ca$_v$1.2 protein expression normalised to desmin. * denotes $p<0.05$ vs. respective 6 months data, # denotes $p<0.05$ vs. respective 12 months data; φ $p<0.05$ vs. within age group. n=5 per age group.

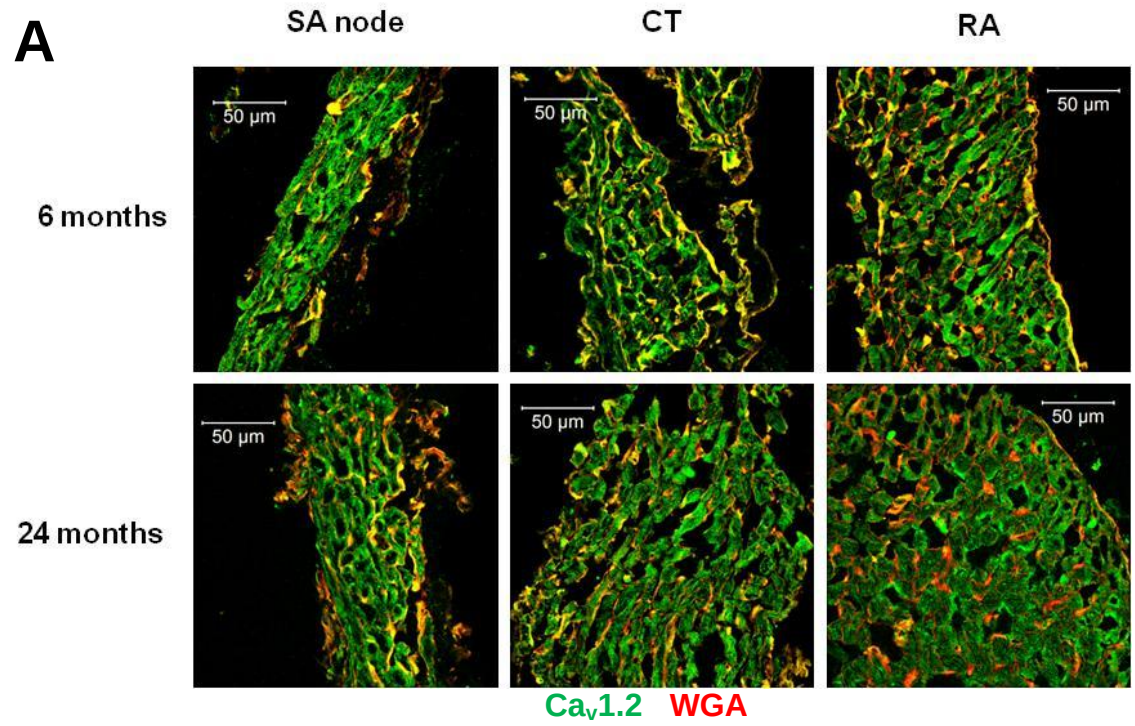

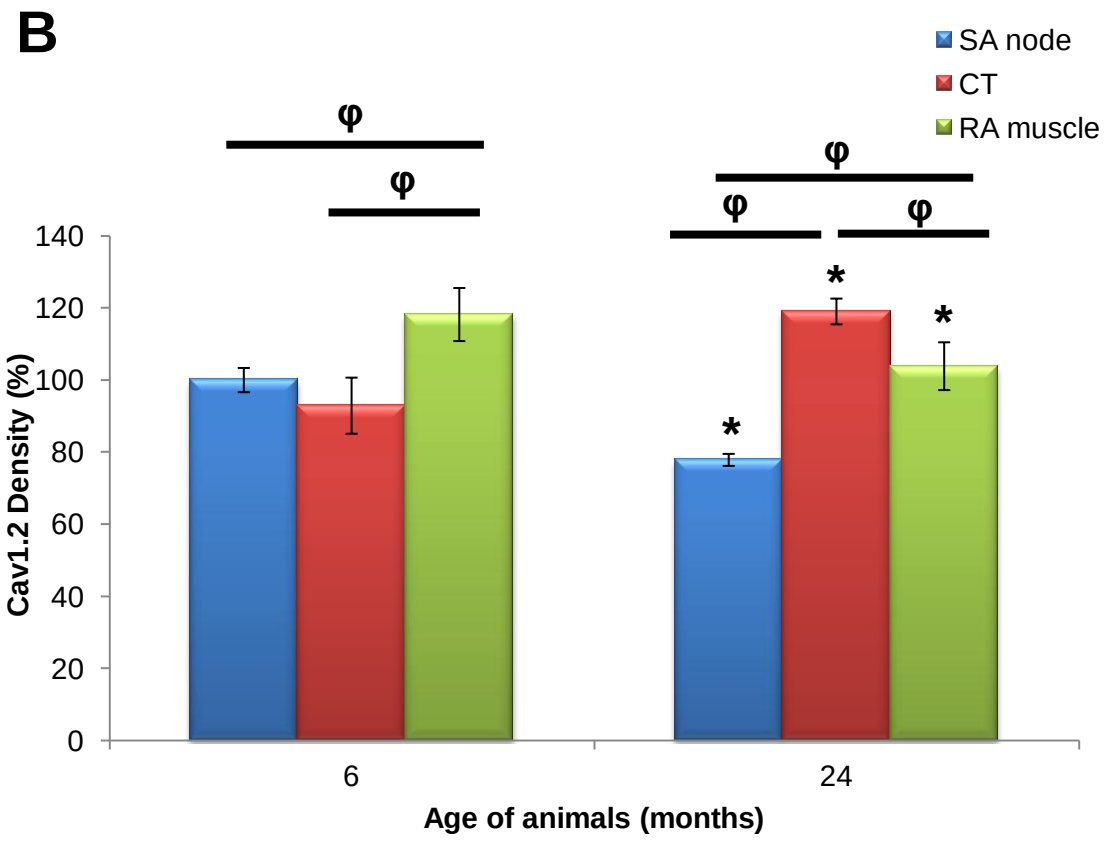

Figure 4.12 Localisation of $Ca_v1.2$ protein expression within regions of the RA

A) illustrative images across the RA are shown from rat hearts at 6 and 24 months of age; B) density of $Ca_v1.2$ label for SA node, CT and RA muscle. * denotes $p<0.05$ vs. respective 6 months data, φ $p<0.05$ within age group; φ $p<0.05$ vs. within age group. n=5 per age group.

4.3.2.4 Age-associated changes in cell membrane calcium handling proteins across the RA

In the 6 months group NCX1 protein expression was significantly higher in RA muscle (141±15.4%) compared with the SA node (100±5.3%) and CT (88±14.7%) as illustrated in Figure 4.13. At 12 months the SA node and CT increased slightly to 104±4.6% and 101±7.8% respectively. Overall this increase resulted in no change in NCX1 protein levels across the RA, even though the RA muscle was still observed to have elevated levels (138±14.9%). At 24 months of age there was a significant divergence in NCX1 protein levels; the SA node dramatically increased in protein expression (171±13.5%) whilst the RA muscle declined (72±7.9%). Within the 24 months age group, the 72% increase in the SA node NCX1 expression resulted in similar levels to that observed in the RA muscle at 6 and 12 months of age. Conversely the CT showed no significant difference in NCX1 protein expression with age (Figure 4.13).

NCX1 protein was sparsely localised in the SA node at 6 months of age, with the majority located at the sarcolemma membrane (Figure 4.14). Similarly within the CT NCX1 protein was located at the periphery of the cells and was significantly higher (142±5.5%) compared with the SA node (100±8.1%). As with the quantitative protein data, RA muscle was observed to have significantly higher densities of NCX1 protein (169±13.3%) compared with the SA node but not with the CT. With age there was a dramatic increase in NCX1 protein within the SA node (174±6.3%); the protein was located throughout the nodal cells in dense clumps and at the sarcolemma membrane. At 24 months of age contrary to western blotting data, the RA muscle remained unchanged in expression levels (174±8.4%), but the density of NCX1 was observed to be highly concentrated at the periphery of myocytes. There was no age-associated difference in NCX1 protein expression within the CT (130±4.5%), but within the 24 months age group the SA node and RA muscle were significantly higher (Figure 4.14).

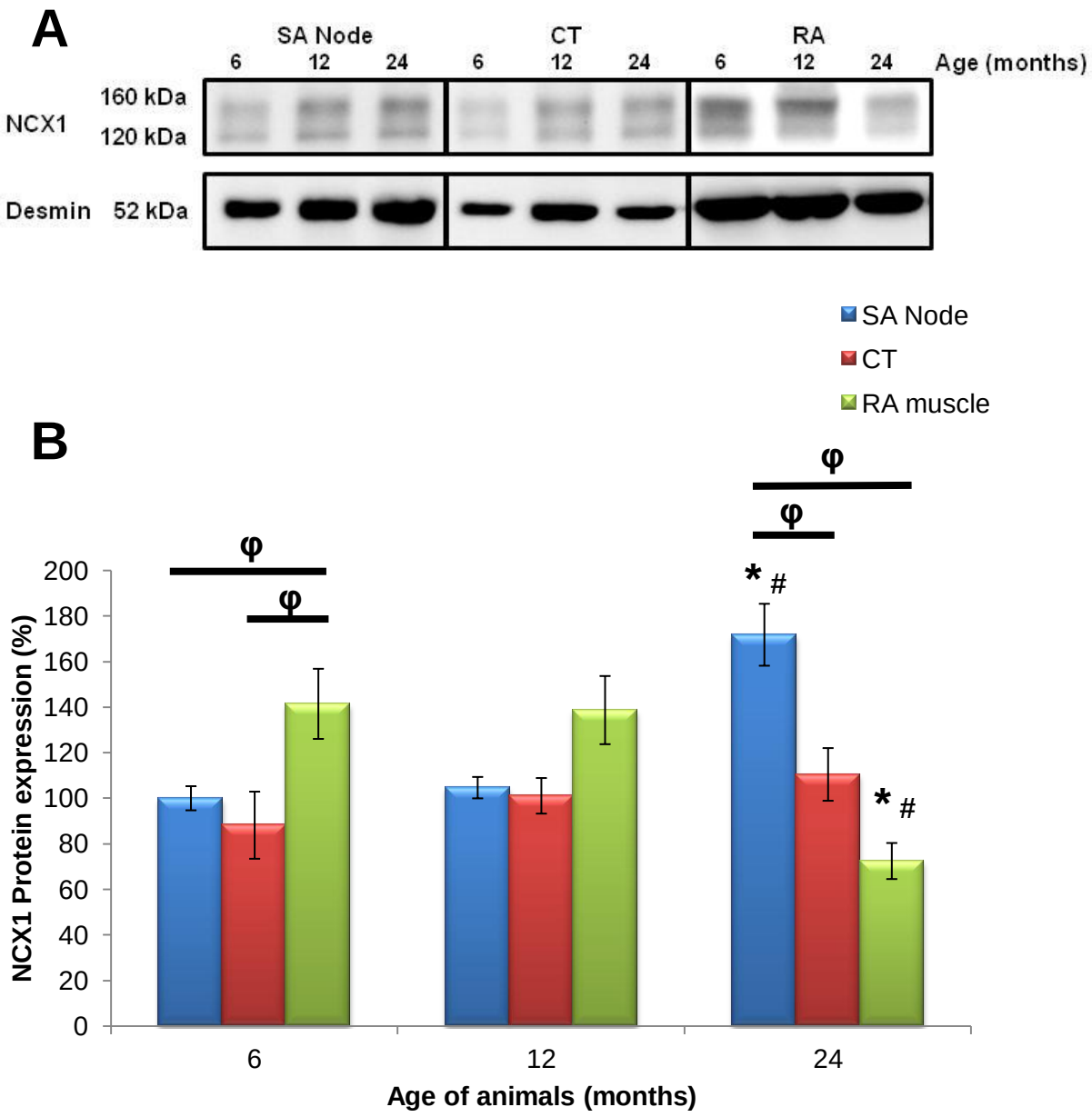

Figure 4.13 Profile of NCX1 protein expression across the RA with increasing age

A) illustrative blot of NCX1 protein and desmin; B) NCX1 protein expression normalised to desmin. * denotes $p<0.05$ vs. respective 6 months data, # denotes $p<0.05$ vs. respective 12 months data; φ $p<0.05$ vs. within age group. n=5 per age group.

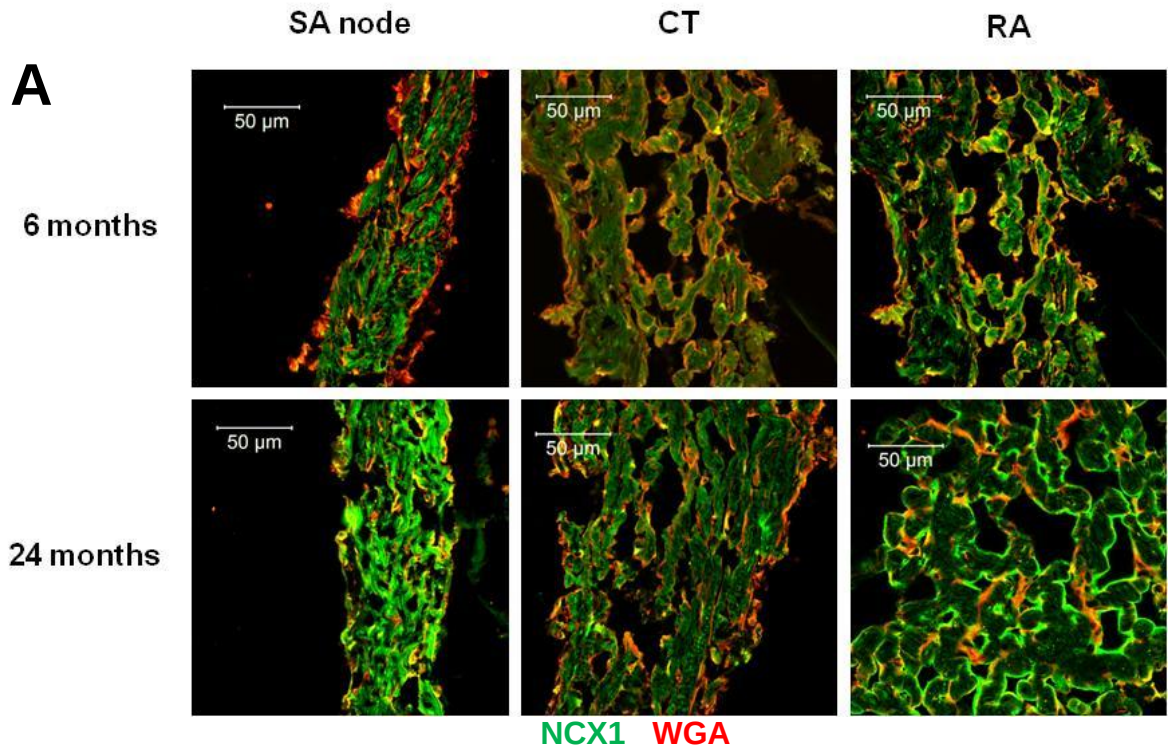

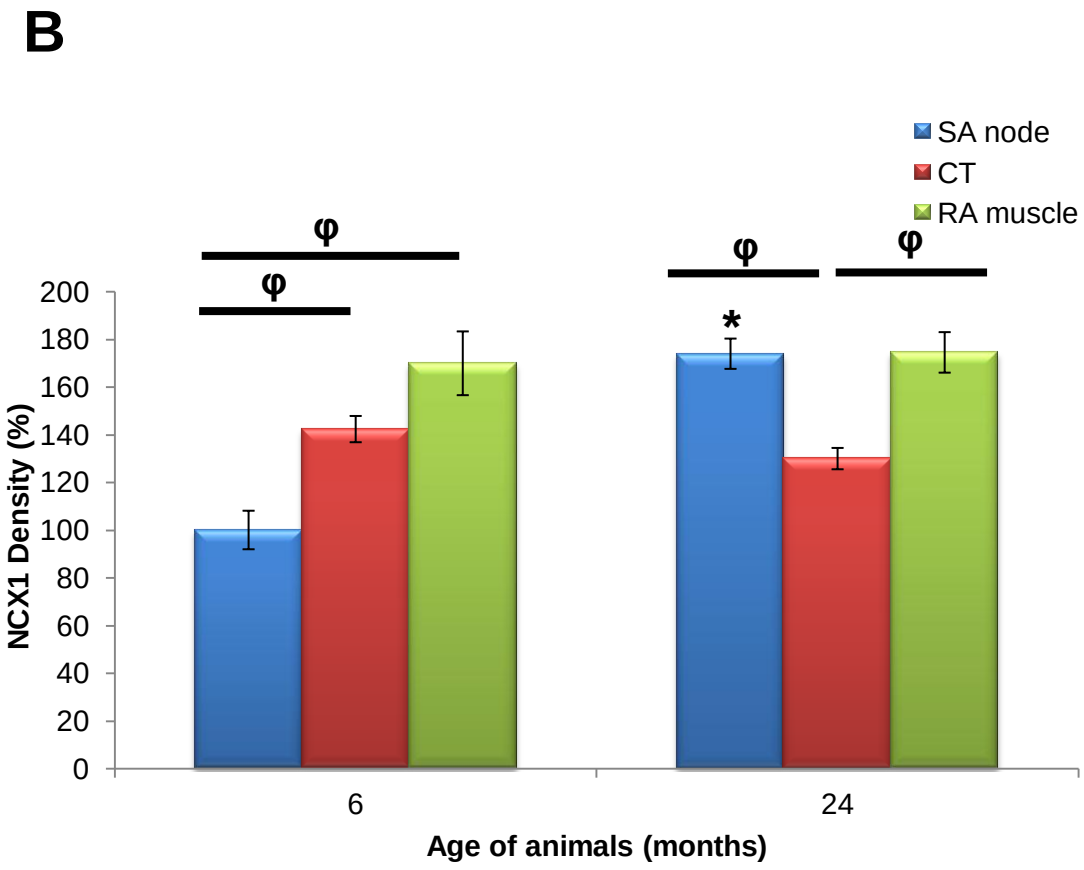

Figure 4.14 Localisation of NCX1 protein expression within regions of the RA

A) illustrative images across the RA are shown from rat hearts at 6 and 24 months of age; B) density of NCX1 label for SA node, CT and RA muscle. * denotes $p<0.05$ vs. respective 6 months data, φ $p<0.05$ within age group. n=5 per age group.

As shown in Figure 4.15 no significant difference in PMCA4a protein expression was observed between the SA node (100±5.7%) and the CT (76±14.9%) within the 6 months age group. However, RA muscle had markedly higher levels of PMCA4a protein at 6 months (137±4.8%), but by 12 months of age this declined by 27±3.2%. Consequently within this age group there were similar PMCA4a protein levels across all the RA regions. At 24 months of age there was a significant decrease in the SA node (78±1.8%) though this remained similar to levels of PMCA4a protein observed in the CT (87±10%) and RA muscle (103±10.4%).

At 6 months of age the SA node showed similar densities (100±7.4%) of PMCA4a protein to the CT (83±12 %); dense clumps were observed in the nodal and CT cells, with the majority concentrated in the sarcolemma membrane (Figure 4.16). As with the quantitative data, the RA muscle showed extremely high levels (151±3.8%) of PMCA4a protein compared with other regions; these were located in dense clumps with the majority at the periphery of myocytes but occasionally shown in an unusual transverse striated pattern throughout some myocytes. With age PMCA4a protein expression decreased significantly expression within the SA node (66±10.7%), although the location of protein remained at the sarcolemma membrane but density was sparse. The RA muscle had declined in PMCA4a density (129±4.8%) but remained significantly higher compared to the SA node and CT (95±6.1%). With age there was no age-associated difference in the CT, though within the 24 months age group, PMCA4a protein levels were observed to be significantly higher than that in the SA node (Figure 4.16).

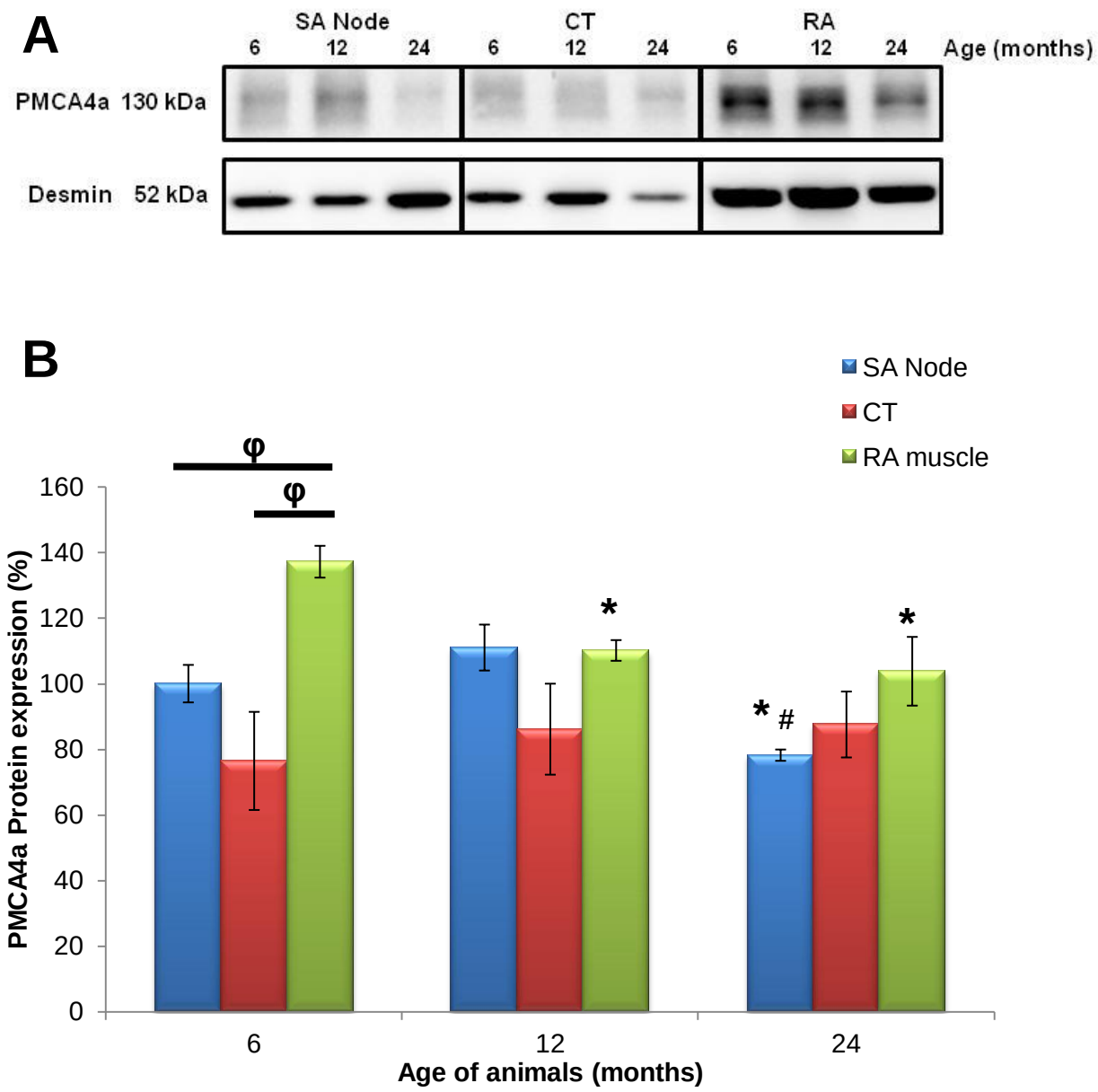

Figure 4.15 Profile of PMCA4a protein expression across the RA with increasing age

A) illustrative blot of PMCA4a protein and desmin; B) PMCA4a protein expression normalised to desmin. * denotes $p<0.05$ vs. respective 6 months data, # denotes $p<0.05$ vs. respective 12 months data; φ $p<0.05$ vs. within age group. n=5 per age group.

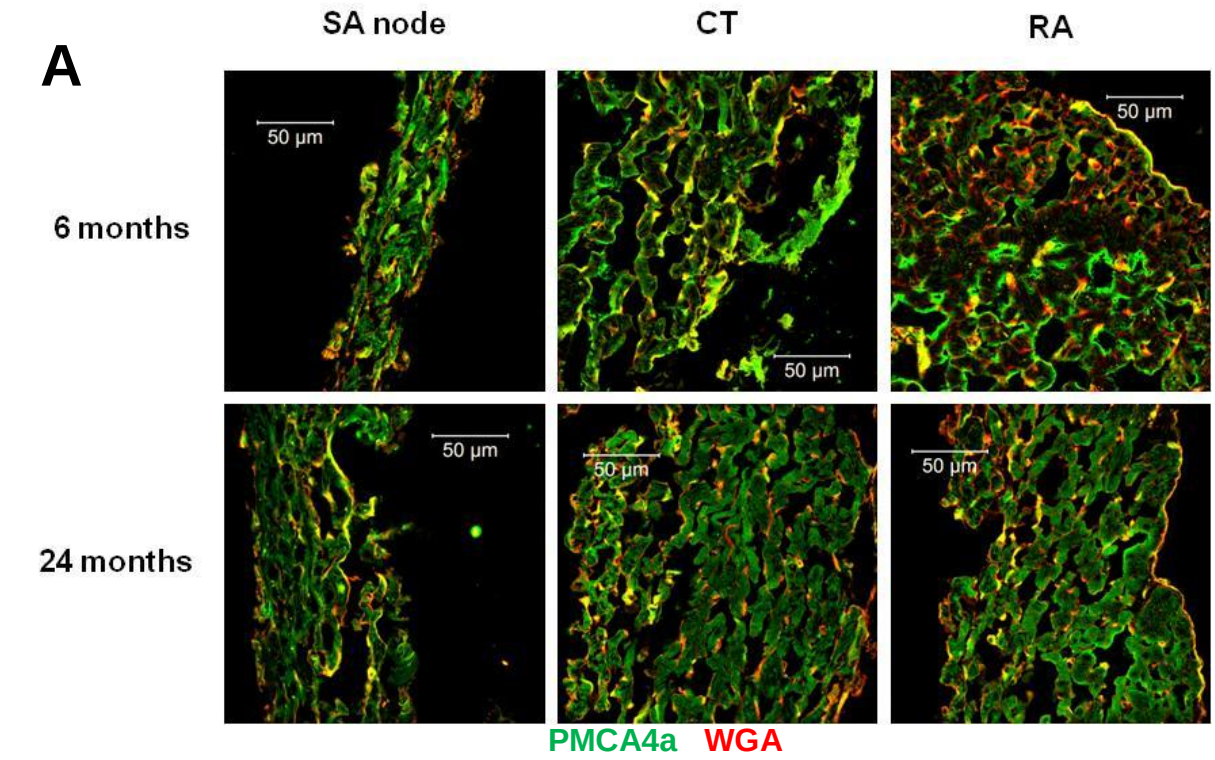

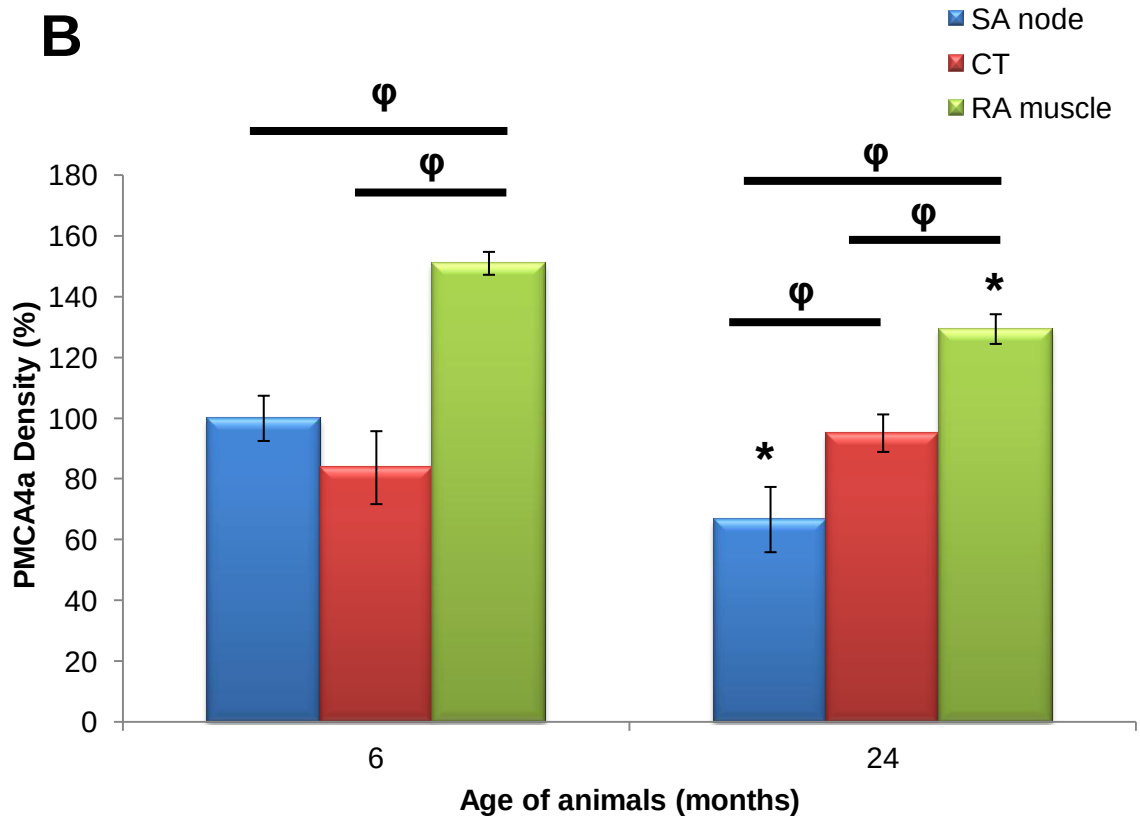

Figure 4.16 Localisation of PMCA4a protein expression within regions of the RA

A) illustrative images across the RA are shown from rat hearts at 6 and 24 months of age; B) density of PMCA4a label for SA node, CT and RA muscle. * denotes $p<0.05$ vs. respective 6 months data, φ $p<0.05$ within age group. n=5 per age group.

4.3.3 Age-associated comparison of alterations in calcium regulation in the left and right atria

Age-associated changes in calcium handling proteins may result in electrical remodelling that could increase the risk of an arrhythmia. Therefore changes in calcium handling proteins: SERCA2a, PLB, RYR2, Cav1.2 NCX1 and PMCA4a were investigated in the LA compared with the RA muscle. To determine the cause behind the expression and regional changes, qPCR was used to investigate mRNA levels.

4.3.3.1 Age-associated changes in SERCA2a activity across the left and right atria

SERCA2a protein expression was significantly higher within the LA (100±4.1%) compared with the RA (60±14.6%) at 6 months of age (Figure 4.17). Similar differences in mRNA expression were observed in the LA which was almost two-fold higher (100±7.7%) compared with the RA (54±4%). Comparable disparities in SERCA2a protein were observed within the 12 months age group, 122±9.5% in the LA compared with 59±7.8% in the RA. At 24 months of age SERCA2a protein significantly increased in the LA (142±17.2%) compared to the 6 months group; conversely the RA showed a significant decline (29±8%). Though qPCR results concur with protein data at 6 and 12 months of age, at 24 months of age, mRNA was observed to decrease in the LA and RA.

Density of SERCA2a was higher within the LA (100±6.2%) compared to the RA (77±4.8%) as indicated in Figure 4.18. In both LA and RA sections SERCA2a was occasionally localised at t-tubular sites throughout the cardiomyocytes; however, the t-tubules were more visible at the periphery of myocytes and radiated inwards a short distance. At 24 months there was a significant decline within the LA (76±6.4%), but no difference was observed in the RA (64±7.8%).

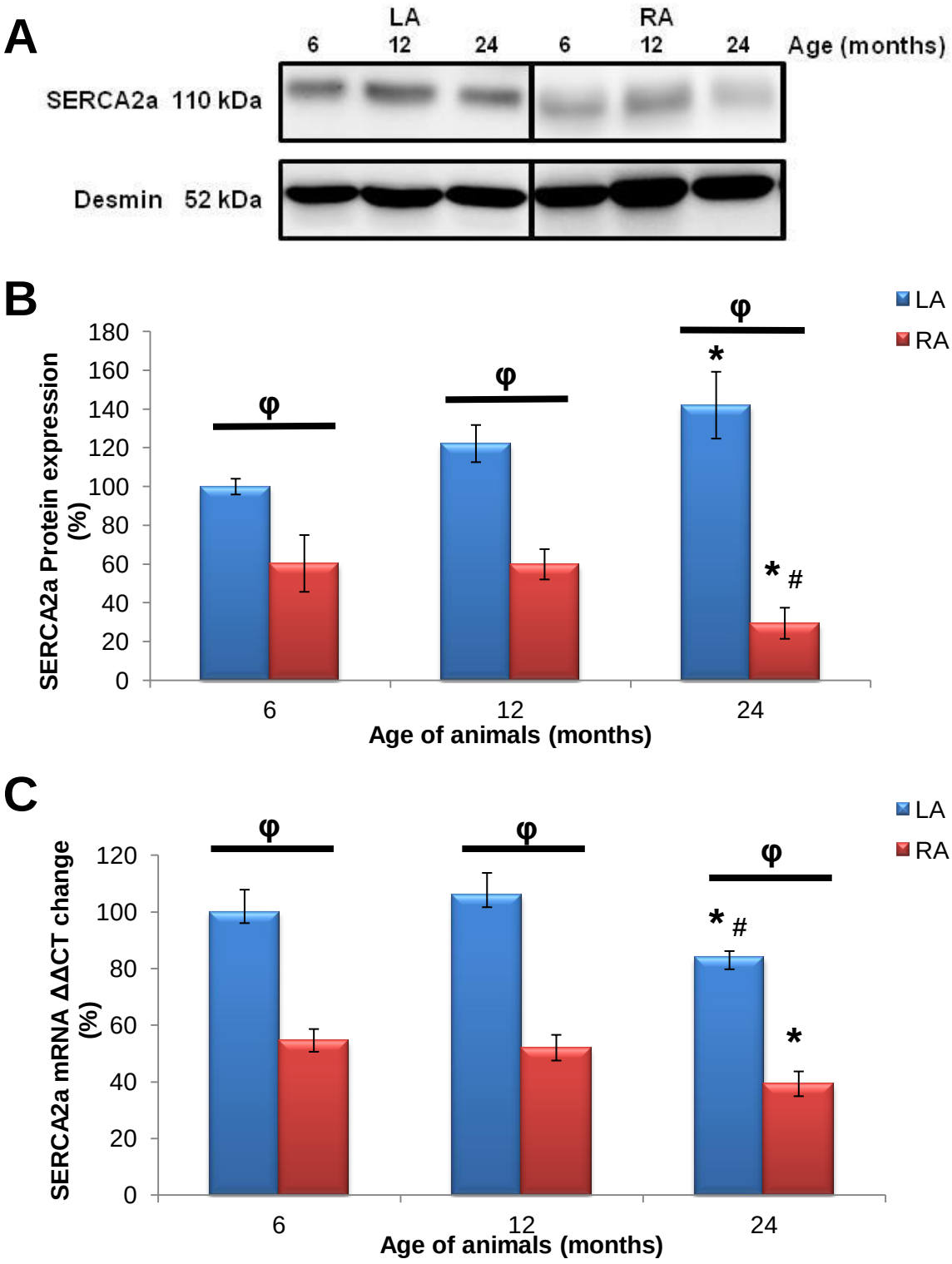

Figure 4.17 Profile of SERCA2a protein expression across the atria with increasing age

A) illustrative blot of SERCA2a protein and desmin; B) SERCA2a protein expression normalised to desmin; C) qPCR showing fold change of mRNA. * denotes $p<0.05$ vs. respective 6 months data, # denotes $p<0.05$ vs. respective 12 months data, φ $p<0.05$ within age group. n=5 per age group.

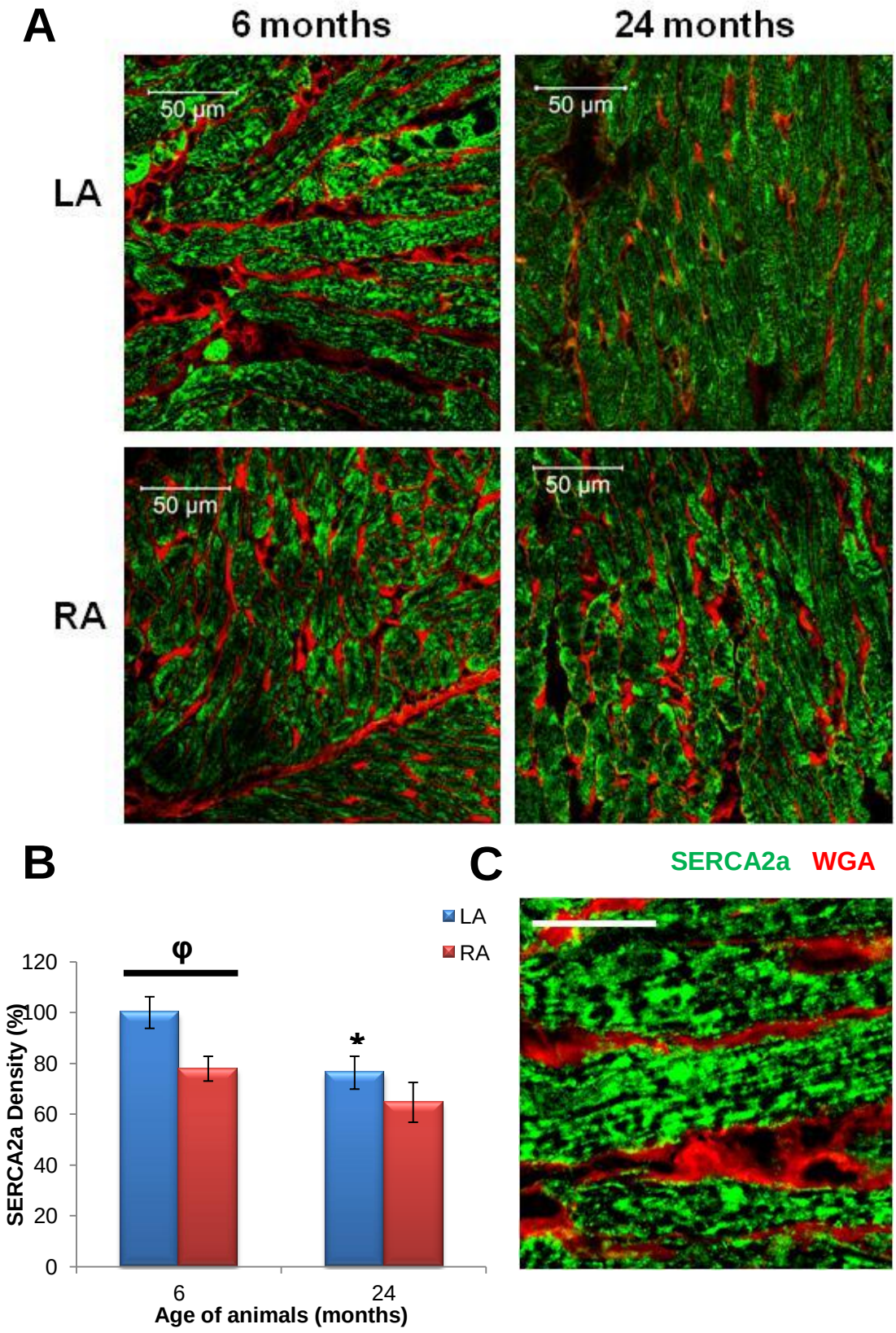

Figure 4.18 Localisation of SERCA2a protein expression across the atria

A) illustrative images across the atria are shown from rat hearts at 6 and 24 months of age; B) density of SERCA2a label for LA and RA; C) high resolution image with 25µm scale bar. * denotes $p<0.05$ vs. respective 6 months data, φ $p<0.05$ within age group.

There was no difference in PLB total protein expression between the LA or RA at 6 or 12 months of age (Figure 4.19B). The similarity in PLB total was also apparent in the separate isoforms, as no significant different in PLB pentamer or monomer were observed. At 24 months of age PLB protein significantly increased in the LA from 99±6.7% to 127±5.7%. The rise in LA PLB was primarily due to elevated levels of PLB pentamer (Figure 4.19C). Conversely the RA showed a decline (65±8.6%) compared with the 6 months age group (101±4.4%) (Figure 4.19B). Figure19C indicates both the pentamer and monomer protein levels decreased in the RA at 24 months of age.

Figure 4.20 showed PLB was localised in dense patches throughout the cardiomyocytes in the LA and RA. T-tubule striations were clearly visible at the sarcolemma of multiple myocytes, with a patterned distribution within the middle. There was no regional difference between the LA (100±10.8%) and RA (93±7.5%) at 6 months of age; though both declined slightly at 24 months of age, 94±8% within the LA compared with 75±7.7% in the RA, there was no age-associated difference.

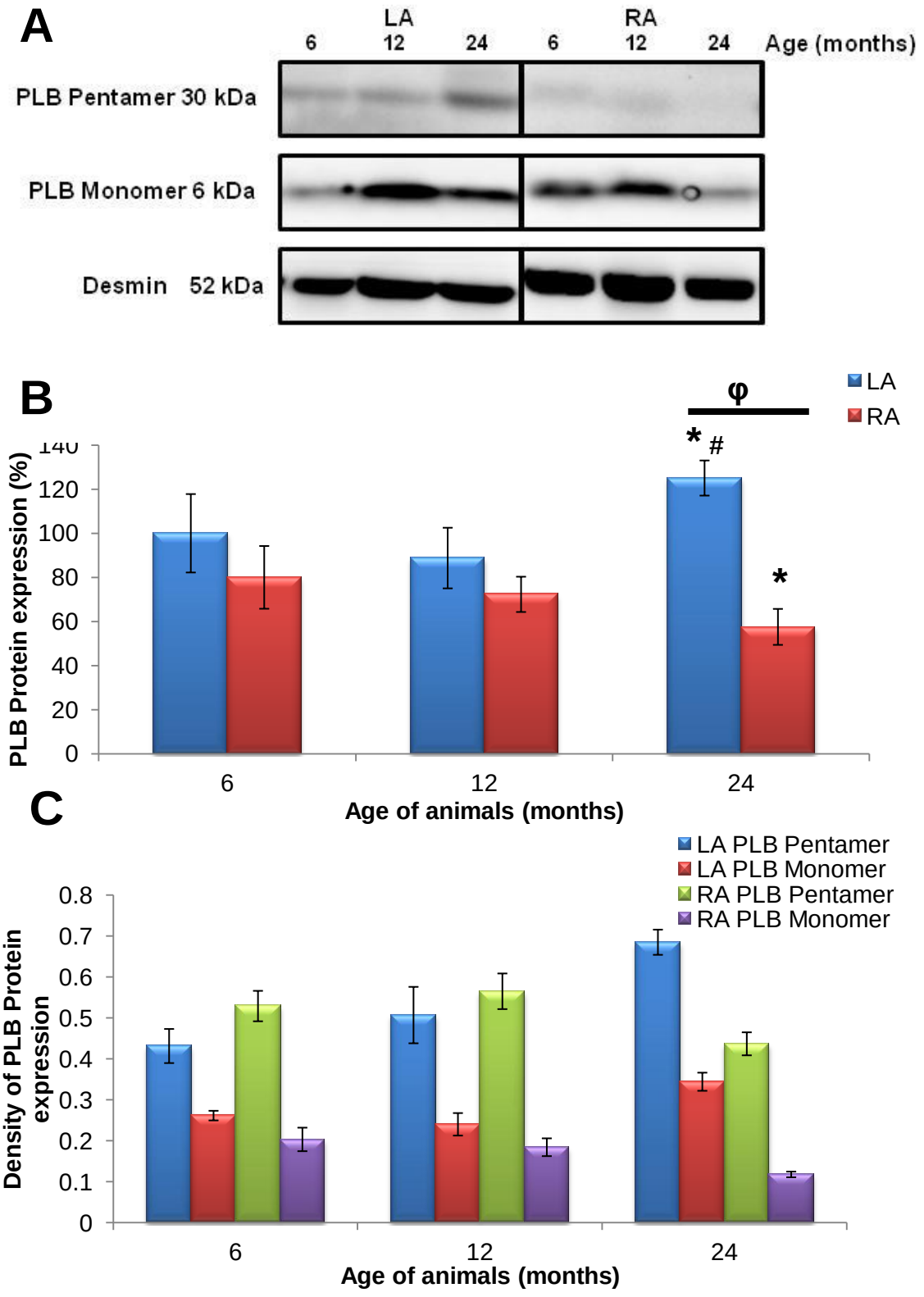

Figure 4.19 Profile of PLB expression in the LA and RA

A) representative western blots with ages shown in months; B) analysis of PLB protein expression normalised to desmin. Data presented as mean ± SEM; * $p<0.05$ vs. respective 6 months age group, # vs. respective 12 months age group ; φ $p<0.05$ vs. within age group. n=5 per age group.

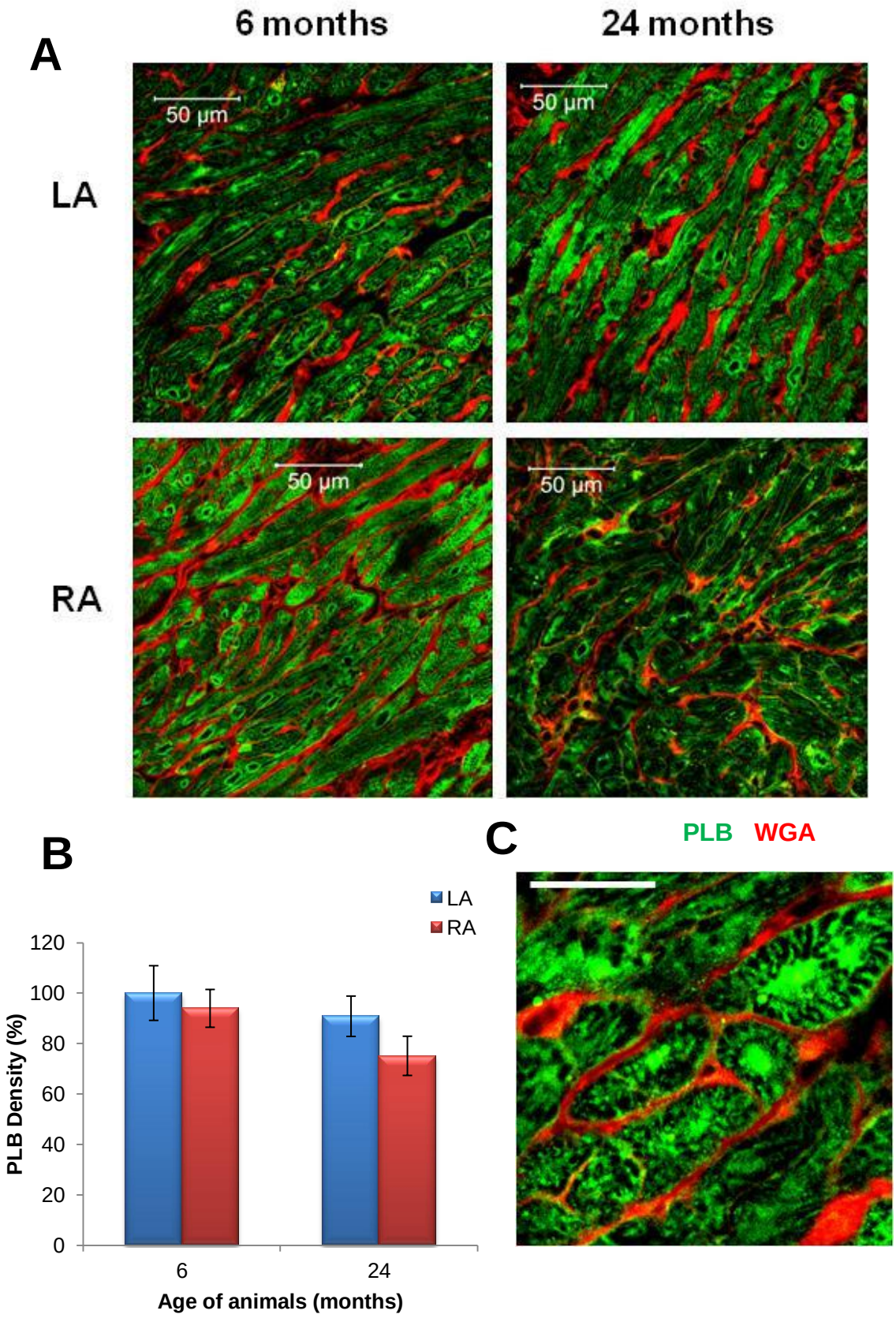

Figure 4.20 Localisation of PLB protein expression across the atria

A) illustrative images across the atria are shown from rat hearts at 6 and 24 months of age; B) density of PLB label for LA and RA; C) high resolution image with 25µm scale bar. n=5 per age group.

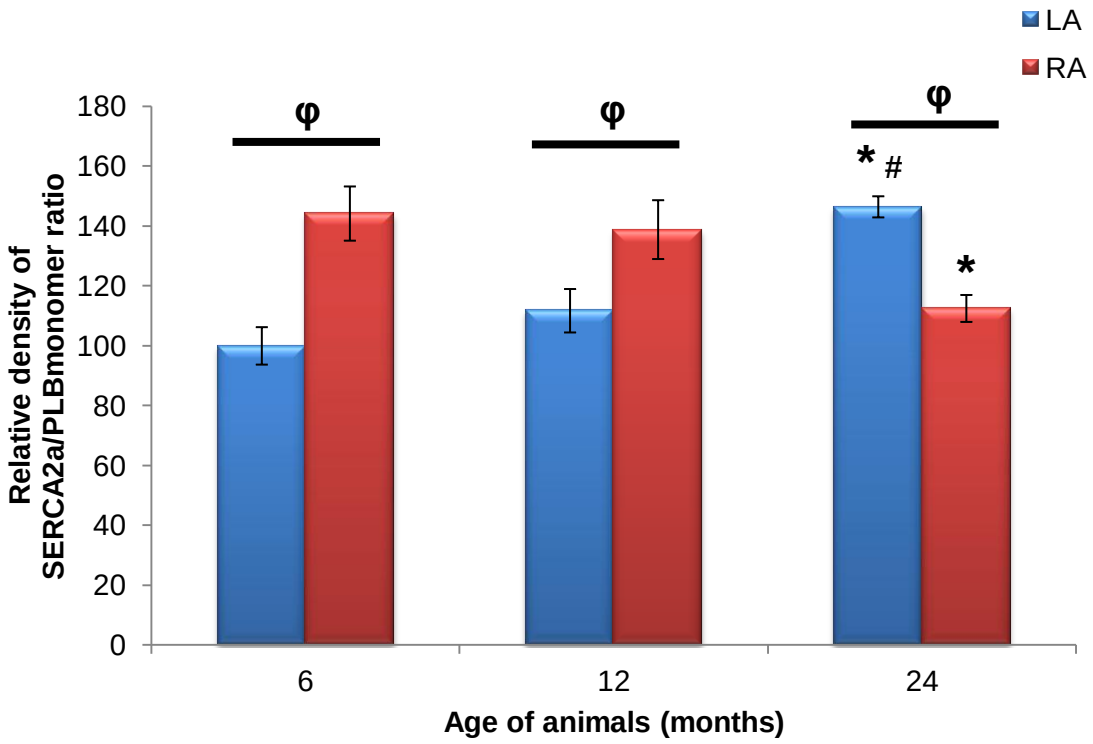

Figure 4.21 SERCA2a activity across the atria with advancing age.

SERCA2a protein expression normalised to PLB monomer expression indicates the functional capacity of the calcium pump SERCA2a. * denotes $p<0.05$ vs. respective 6 months age group, # denotes $p<0.05$ vs. respective 12 months age group, φ denotes $p<0.05$ within age group. n=5 per age group.

Within the 6 months age group, the RA muscle showed a significant 44% higher level of SERCA2a activity when compared with the LA (Figure 4.21). At 12 months of age there was a small rise (111±7.2%) and decline (138±9.8%) in activity in the LA and RA respectively; but SERCA2a activity within the RA was still significantly higher. With age the RA muscle significantly decreased in activity from 144±9.1% to 112±4.5%. Conversely SERCA2a activity within the LA was observed to significantly increase by 46±3.5%; this rise in activity positioned the LA at equivalent levels to that observed in the RA muscle at 6 and 12 months of age.

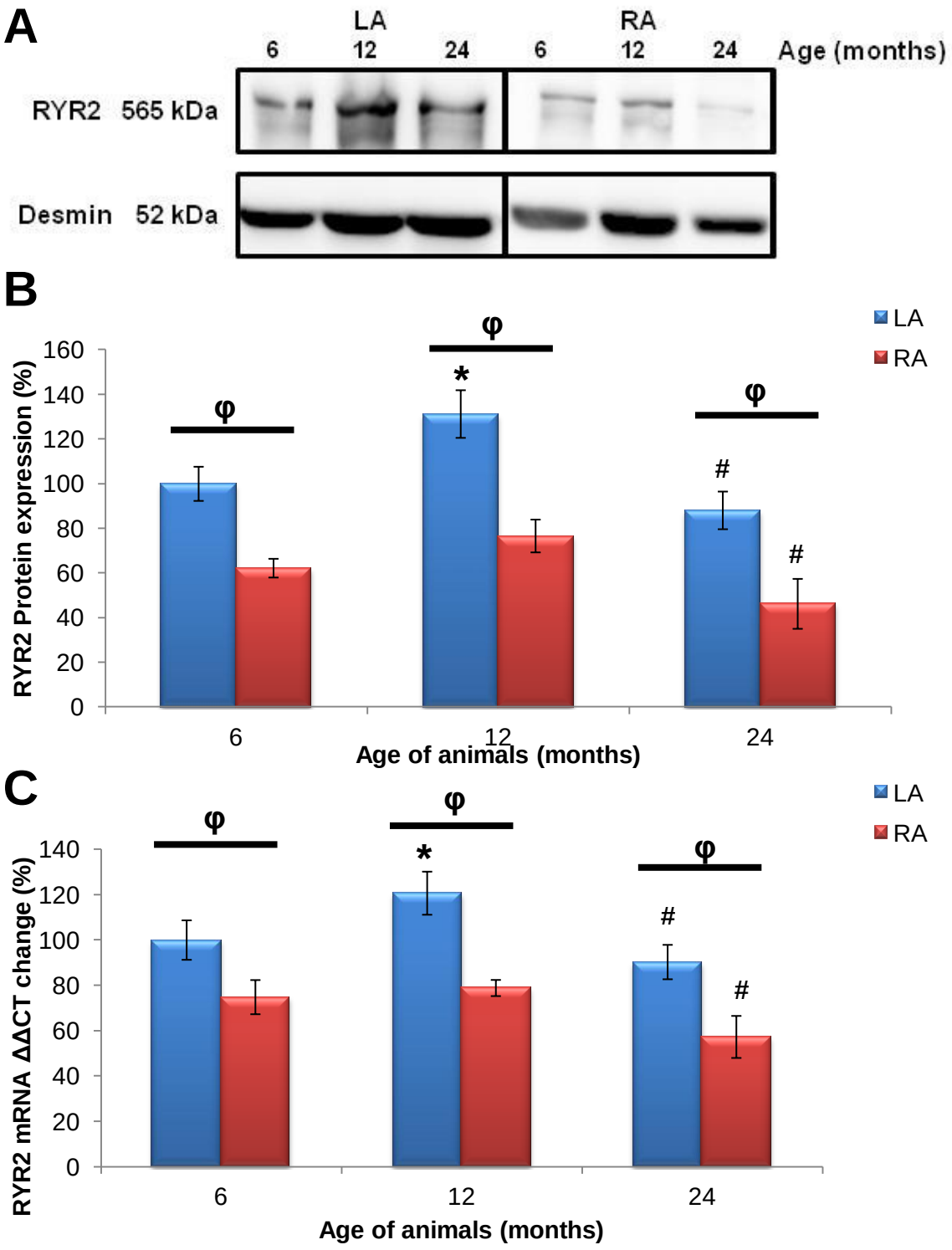

Figure 4.22 Profile of RYR2 protein expression across the atria with increasing age

A) illustrative blot of RYR2 protein and desmin; B) RYR2 protein expression normalised to desmin; C) qPCR showing fold change of mRNA. * denotes $p<0.05$ vs. respective 6 months data, # denotes $p<0.05$ vs. respective 12 months data, φ $p<0.05$ within age group. n=5 per age group.

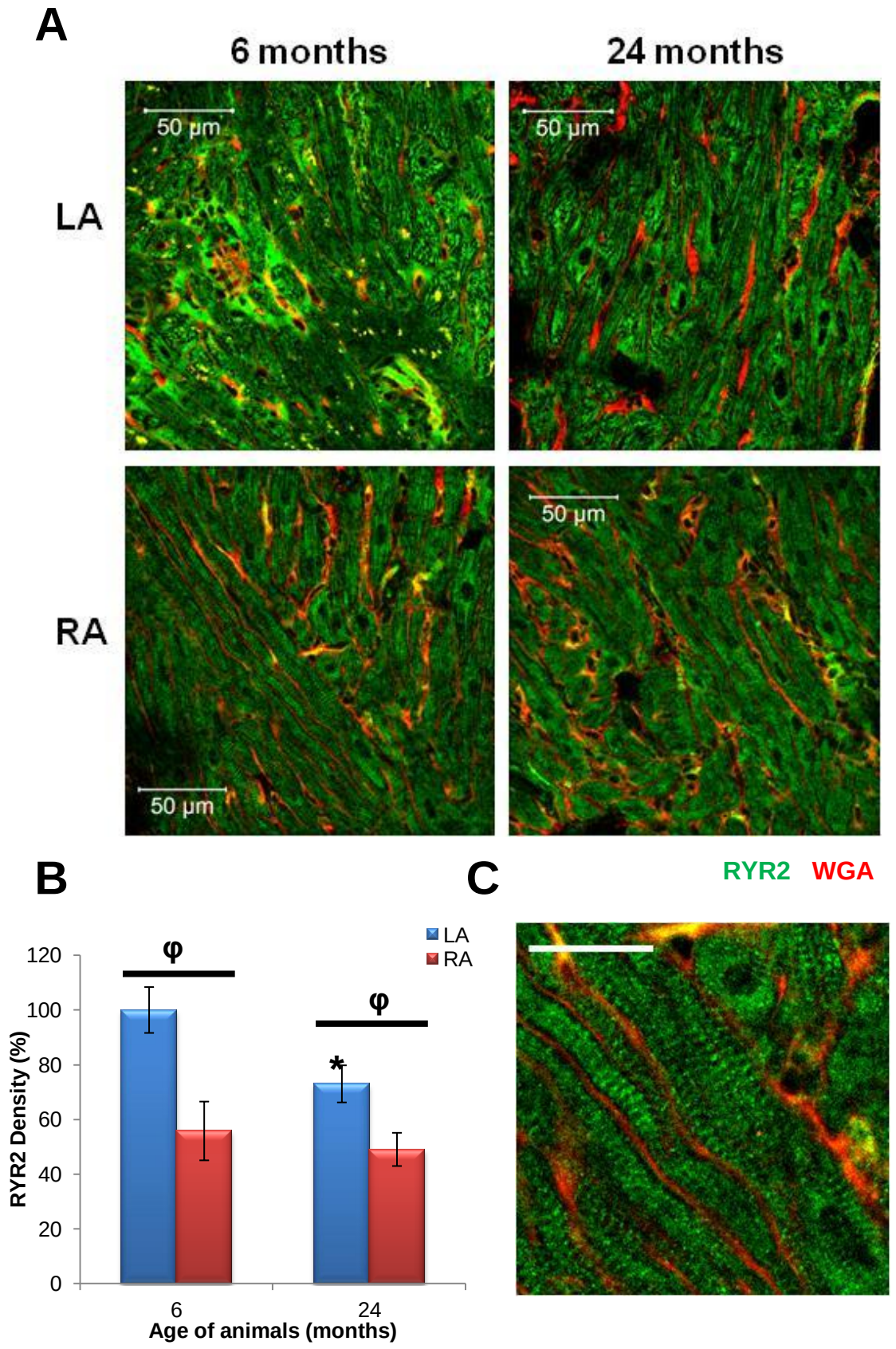

Figure 4.23 Localisation of RYR2 protein expression across the atria

A) illustrative images across the atria are shown from rat hearts at 6 and 24 months of age; B) density of RYR2 label for LA and RA; C) high resolution image with 25µm scale bar. * denotes $p<0.05$ vs. respective 6 months data, φ $p<0.05$ within age group. (n=5)

4.3.3.2 Age-associated changes in CICR release proteins, RYR2 and $Ca_v1.2$

At 6 months of age there was an elevated level of RYR2 protein expression within the LA (100±7.6%) compared with the RA (62±4.2%) (Figure 4.22B). This difference may be explained by the divergence in mRNA levels between the two atria, with 100±8.6% in the LA versus 74±7.5% in the RA (Figure 4.22C). Within the 12 months age group, the divergence was even clearer at both the protein and mRNA level, but compared to the 6 months age group, RYR2 protein significantly increased in the LA (131±10.6%). At 24 months of age there was a significant decline in RYR2 protein in both the LA (88±8.4%) and RA (46±11.1%) when compared to the 12 months group. Nevertheless there was still a higher amount of protein in the LA that correlated with mRNA levels (Figure 4.22C).

Within the LA, RYR2 protein was densely packed at the sarcolemma membrane with occasional t-tubule striations in the periphery of myocytes. Alongside the quantitative data, the LA had a substantially higher density of RYR2 protein (100±8.3%) compared with the RA (55±10.7%) in the 6 months age group (Figure 4.23). At 24 months of age RYR2 protein within the LA was no longer localised in dense patches, reduced striations visualised and fluorescence sparsely distributed across myocytes (Figure 4.23). RYR2 density in the LA decreased to 72±6.7% but was still markedly higher than in the RA which remained unchanged with age at 49±6.1%.

There was no regional difference in $Ca_v1.2$ protein expression at 6 and 12 months age groups (Figure 4.24B). This was contrary to qPCR data which showed elevated level of $Ca_v1.2$ mRNA in the LA compared with the RA at 6 and 12 months of age. At 24 months of age there was a significant divergence in $Ca_v1.2$ protein; LA increased to 152±11.1% compared with the RA which showed a 40±11.8% decline.

$Ca_v1.2$ protein was observed in dense clumps within cardiomyocytes in the LA, occasional t-tubules were noted at the sarcolemma membrane (Figure 4.25). Similar findings were observed in the RA, though the location of $Ca_v1.2$ was considerable more striated. There was no significant difference at 6 months of age between the LA (100±3.4%) and RA (97±7%), although at 24 months, there was a divergence in $Ca_v1.2$ protein expression. LA showed a small (113±5.2%) but significant increase in density, whereas density declined in the RA (65±5.4%); resulting in a dramatic divergence across the atria. Within the LA $Ca_v1.2$ was located at a higher number of t-tubular sites with reduced dense clumps but increased spread (Figure 4.25).

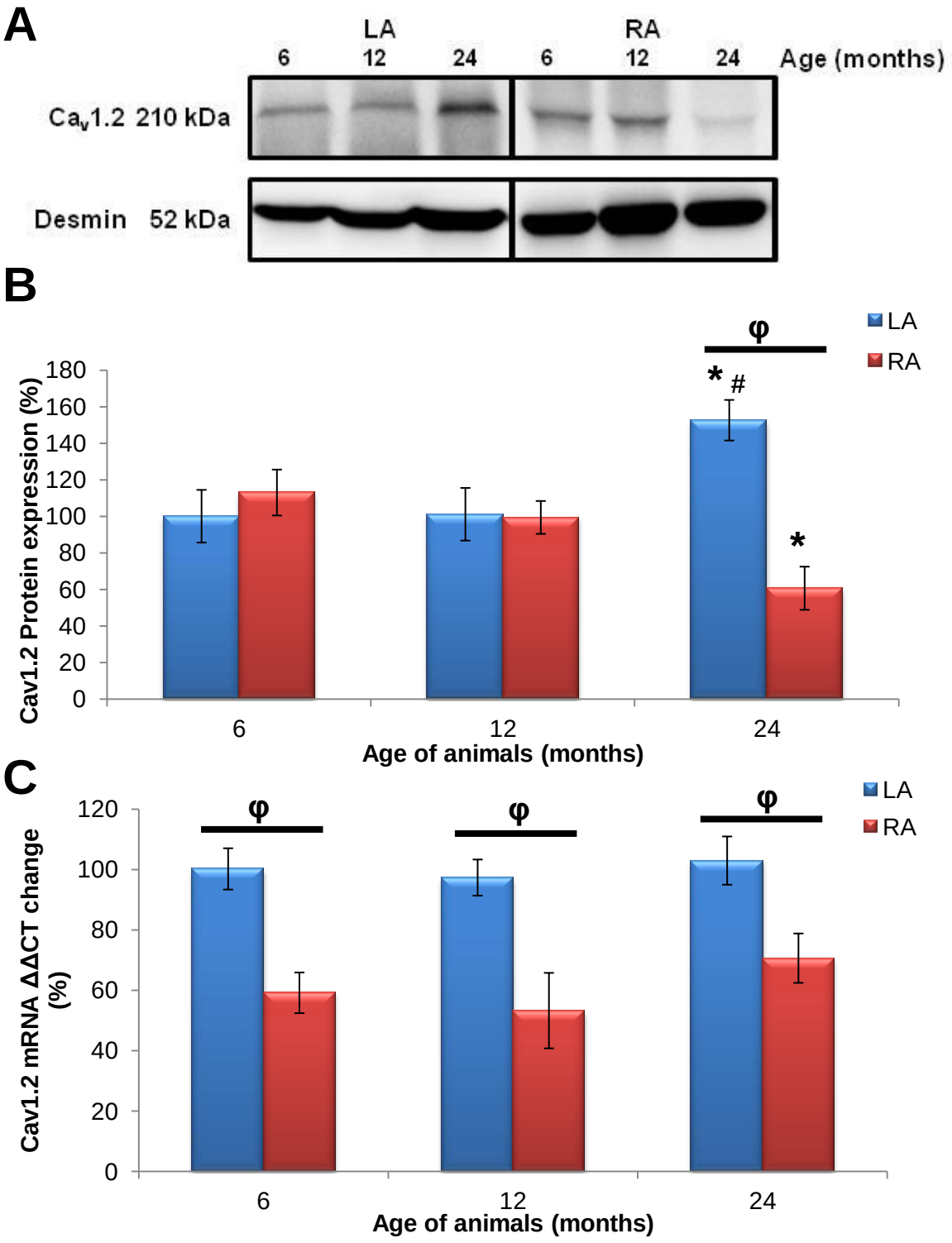

Figure 4.24 Profile of $Ca_v1.2$ protein expression across the atria with increasing age

A) illustrative blot of $Ca_v1.2$ protein and desmin; B) $Ca_v1.2$ protein expression normalised to desmin; C) qPCR showing fold change of mRNA. * denotes $p<0.05$ vs. respective 6 months data, # denotes $p<0.05$ vs. respective 12 months data, φ $p<0.05$ within age group. n=5 per age group.

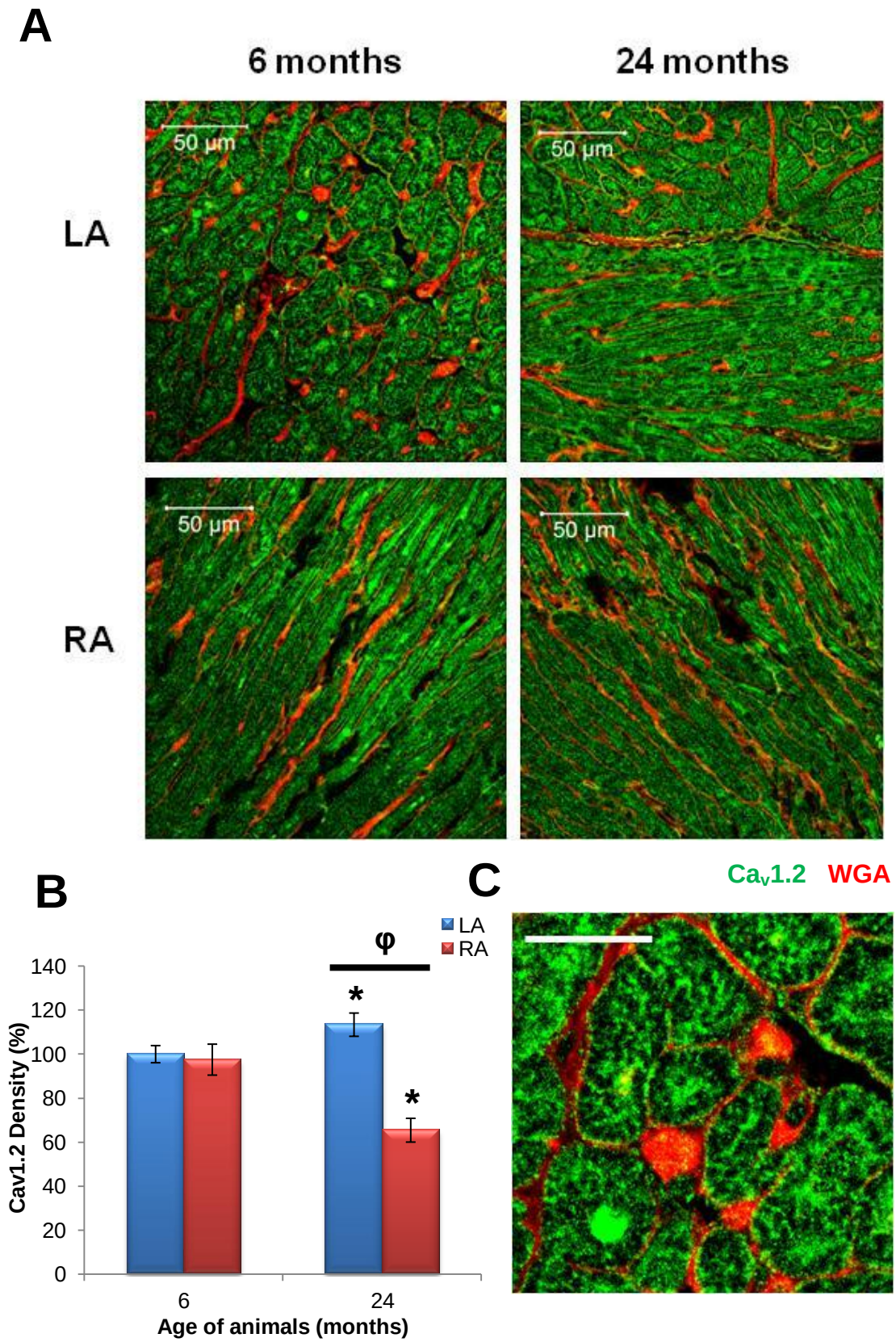

Figure 4.25 Localisation of $Ca_v1.2$ protein expression across the atria

A) illustrative images across the atria are shown from rat hearts at 6 and 24 months of age; B) density of $Ca_v1.2$ label for LA and RA; C) high resolution image with 25µm scale bar. * denotes $p<0.05$ vs. respective 6 months data, φ $p<0.05$ within age group. n=5 per age group.

4.3.3.3 Age associated changes in cell membrane calcium handling proteins NCX1 and PMCA4a

There was no significant difference in NCX1 protein expression at 6 or 12 months of age between the atria (Figure 4.26B). Nevertheless, mRNA provided contradictory data, with significant differences in the LA (100±8.3%) compared with the RA at 6 months of age (69±17.2%). A further divergence was observed in the 12 months age group, with a slight marked rise in the LA (113±6.8%) and decline in the RA (56±15.6%. Within the 24 months age group NCX1 protein expression increased significantly in the LA (127±9.8%); this rise in protein can be explained by the elevated levels of mRNA (133±2.3%) (Figure 4.26C). Conversely the RA had lower NCX1 protein levels at 24 months of age (49±7.9%) when compared with the younger age group, however, there was no age-associated difference in mRNA levels within the RA (Figure 4.26C)

NCX1 protein was localised at the sarcolemma of myocytes with slightly denser levels observed in the RA (114±6.8%) compared with the LA (100±4.4%) within the 6 months age group. With age there was a significant increase in the intensity of NCX1 in the LA (129±5.3%), but rather than concentrated in the periphery, the majority of fluorescence was observed in streaked patterns throughout myocytes (Figure 4.27). In contrast the RA showed decreased levels of NCX1 protein with age (94±4.3%).

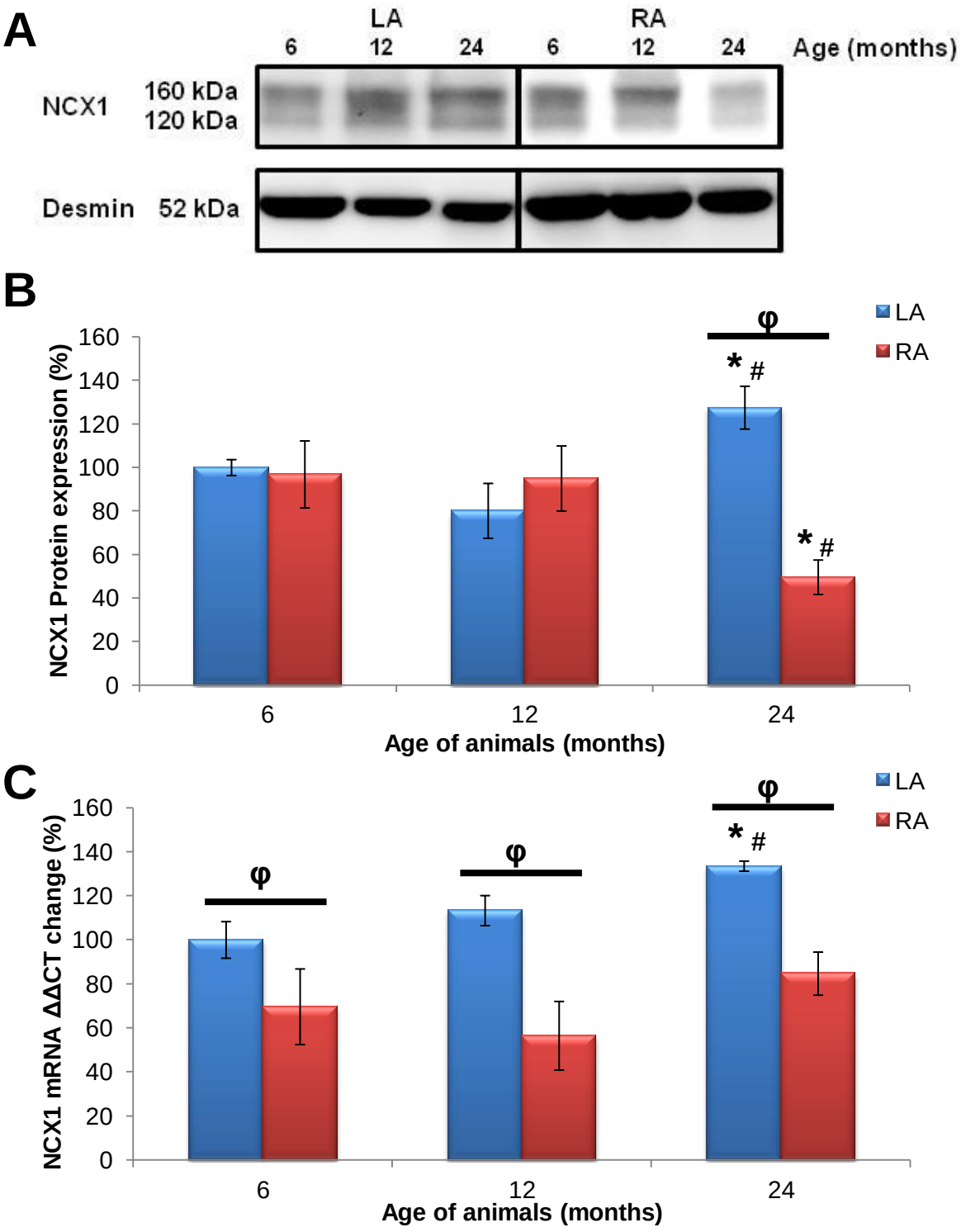

Figure 4.26 Profile of NCX1 protein expression across the atria with increasing age

A) illustrative blot of NCX1 protein and desmin; B) NCX1 protein expression normalised to desmin; C) qPCR showing fold change of mRNA. * denotes $p<0.05$ vs. respective 6 months data, # denotes $p<0.05$ vs. respective 12 months data, φ $p<0.05$ within age group. n=5 per age group.

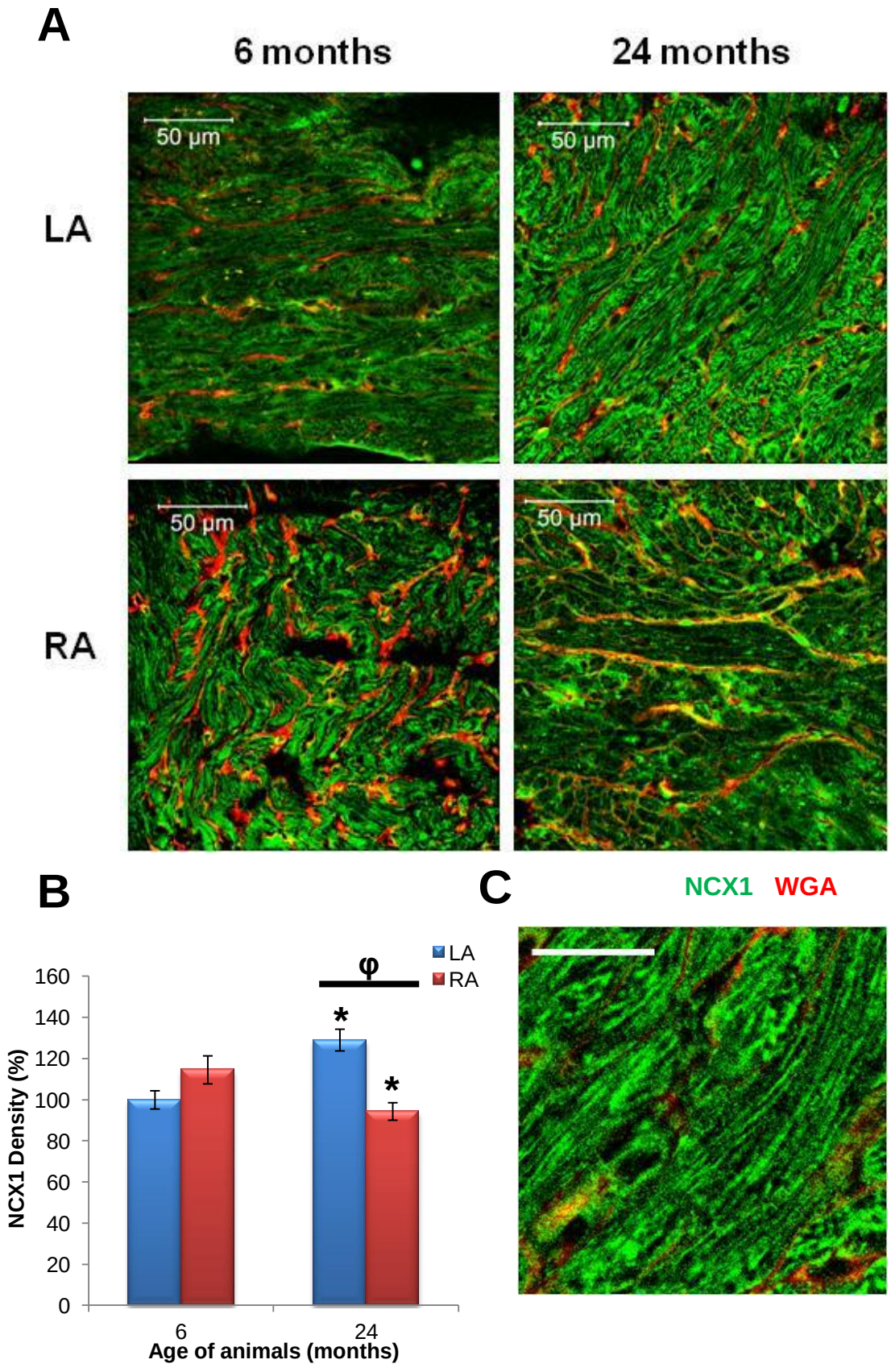

Figure 4.27 Localisation of NCX1 protein expression across the atria

A) illustrative images across the atria are shown from rat hearts at 6 and 24 months of age; B) density of NCX1 label for LA and RA; C) high resolution image with 25µm scale bar. * denotes p<0.05 vs. respective 6 months data, φ p<0.05 within age group. n=5

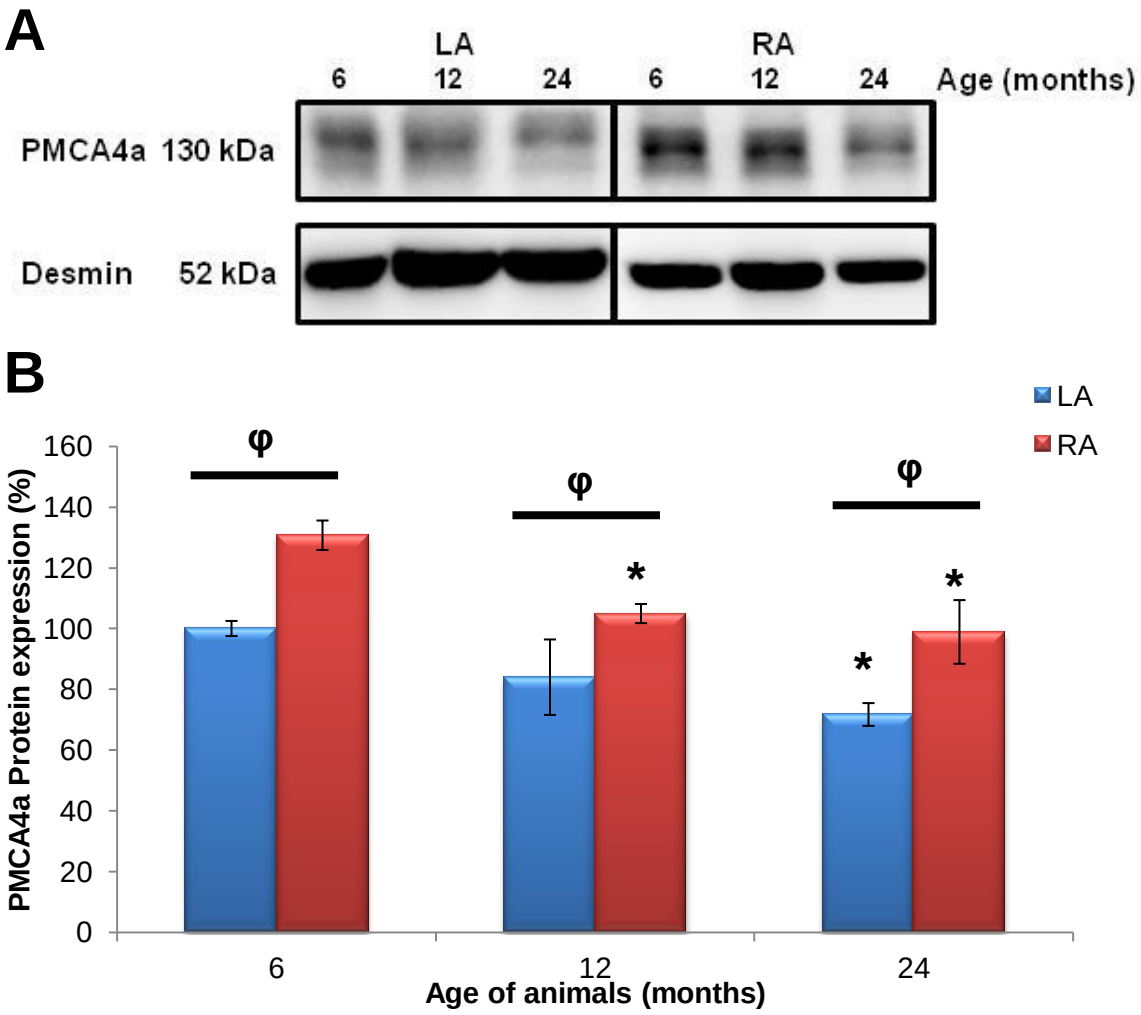

Figure 4.28 Profile of PMCA4a protein expression across the atria with increasing age

A) illustrative blot of SERCA2a protein and desmin; B) PMCA4a protein expression normalised to desmin. * denotes $p<0.05$ vs. respective 6 months data, # denotes $p<0.05$ vs. respective 12 months data and φ $p<0.05$ within age group. n=5 per age group.

As shown in Figure 4.28 PMCA4a protein was expressed at higher levels in the RA compared with the LA at all age groups. With age there was a significant decrease within the RA, from 130±4.8% at 6 months of age, to 104±3.1%, 98±10.4% at 12 and 24 months of age respectively. Although there was no change in the LA at 6 and 12 months of age, with advanced age a significant decline in PMCA4a protein expression (71±3.7%) was observed. PMCA4a was visualised at the periphery of cardiomyocytes within the RA, however, in the LA a streaked pattern was observed throughout some myocytes (Figure 4.29). Contrary to western blotting data the LA showed elevated levels of PMCA4a protein at both 6 and 24 months age groups.

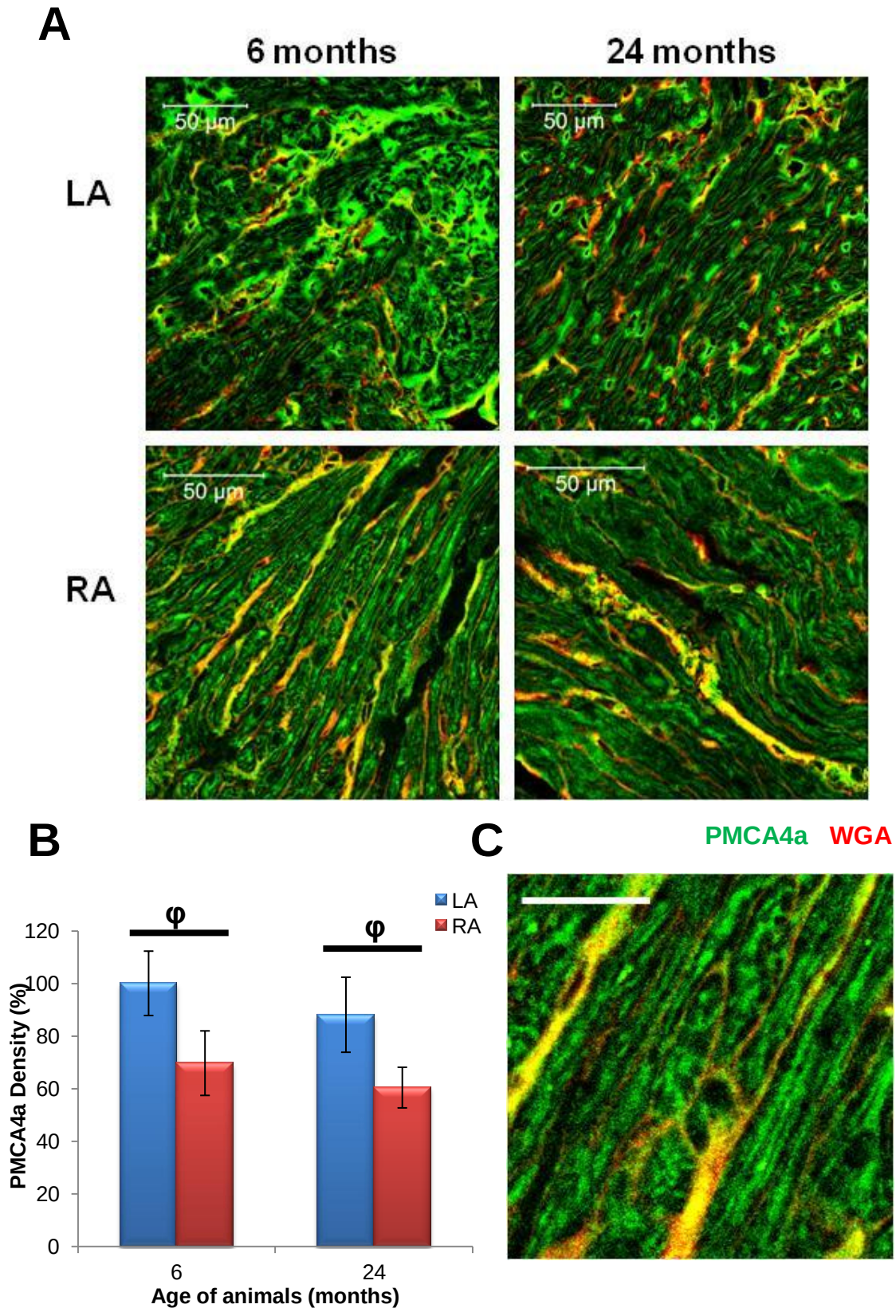

Figure 4.29 Localisation of PMCA4a protein expression across the atria

A) illustrative images across the atria are shown from rat hearts at 6 and 24 months of age; B) density of PMCA4a label for LA and RA. C) high resolution image with 25µm scale bar.* denotes $p<0.05$ vs. respective 6 months data, φ $p<0.05$ within age group. n=5 per age group.

4.4 Discussion

4.4.1 Summary of Chapter 4

This study investigated age-associated and regional differences across the RA and across both atria. There was significant diversity in expression of calcium handling proteins in the SA node, CT and RA muscle (Table 4.3). The most significant findings included up regulation of PLB, RYR2 and Cav1.2 within the CT and down regulation in the RA muscle of all proteins apart from PLB. A clear profile was observed within the SA node, with the 12 months age group showing elevated levels of Cav1.2, RYR2 and SERCA2a, but all these proteins declined with advanced age.

Furthermore protein expression varied across the atria, partially explained by age-associated changes in mRNA expression (Table 4.4). Main findings included: down regulation of the Ca^{2+} handling proteins and mRNA in the RA muscle at 24 months of age, significantly elevated levels of proteins and mRNA in the LA compared with the RA muscle and clear differences in Ca^{2+} transporter proteins with age.

Table 4.3 Profile of expression of Ca^{2+} handling proteins across the right atria and impact of age.

Parameter	SA node			CT			RA muscle		
	6	12	24	6	12	24	6	12	24
SERCA2a	×	↑↑↑	↓↓	×	×	↓↓	×	×	↓↓
PLB Total	×	×	×	↓	×	↑↑↑	×	×	×
SERCA2a activity	×	↑↑↑	↓↓	↓	×	↓↓↓	×	×	↓
RYR2	×	↑	↓↓	×	×	↑	↑	↑↑↑	↓↓
$Ca_v1.2$	×	↑	↓↓	×	×	↑↑↑	×	×	↓↓
NCX1	×	×	↑↑↑	×	×	×	↑	×	↓↓
PMCA4a	×	×	↓↓	×	×	×	↑	↓↓	↓↓

Protein expression (P) and SERCA2a activity are summarised for the SA node, CT and RA muscle over the 6, 12 and 24 months age groups. Significant differences ($p<0.05$) were obtained from western blot and qPCR data; X denotes no significant difference, ↑ in red denotes higher levels within age group, ↓ in red denotes lower levels within age group, ↑↑ significant increase across the age groups, ↓ ↓ significant decrease across the age groups.

Table 4.4 Profile of expression of Ca^{2+} handling proteins and mRNA across the left and right atria and the impact of age.

Parameter		LA			RA		
		6	12	24	6	12	24
SERACA2a	M	↑	↑	↑↓↓	×	×	↓↓
	P	↑	↑	↑↑↑	×	×	↓↓
PLB total		×	×	↑↑↑	×	×	↓↓
SERCA2a activity		×	×	↑↑↑	↑	↑	↓↓
RYR2	M	↑	↑↑↑	↑↓↓	×	×	↓↓
	P	↑	↑↑↑	↑↓↓	×	×	↓↓
$Ca_v1.2$	M	↑	↑	↑	×	×	×
	P	×	×	↑↑↑	×	×	↓↓
NCX1	M	↑	↑	↑↑↑	×	×	×
	P	×	×	↑↑↑	×	×	↓↓
PMCA4a		×	×	↓↓	↑	↑↓↓	↑↓↓

Protein expression (P), mRNA levels (M) and SERCA2a activity are summarised for the LA and RA over 6, 12 and 24 months age groups. Significant differences ($p<0.05$) were obtained from western blot and qPCR data; X denotes no significant difference, ↑ in red denotes higher levels within age group, ↓ in red denotes lower levels within age group, ↑↑ significant increase across the age groups, ↓ ↓ significant decrease across the age groups.

4.4.2 Heterogeneity of the tissue surrounding the SA node

In Chapter 3 expression of Ca^{2+} handling proteins changed with age, which warranted study into the surrounding CT and RA muscle to determine if similar alterations occurred. Chapter 4 showed heterogeneity of Ca^{2+} transporters expression across all regions in the RA. This variation was exhibited in the young age groups and was altered with age. Overall the CT and RA muscle displayed a differed response to the ageing process compared with the SA node, consequently this may have implications on spontaneous activity, AP propagation and the generation of arrhythmogenic episodes.

4.4.2.1 Effect of age and region on SERCA2a activity; its role in the generation of arrhythmias

Reduced SERCA2a activity, measured by SERCA2a to PLB monomer protein ratios (Cain et al., 1998), is an indication of cardiac myocyte dysfunction (Chen et al., 2004b). Decreased SERCA2a protein but an increase in PLB will not only result in alterations in Ca^{2+} cycling but was shown to play a role in Ca^{2+}-induced arrhythmogenesis (Rubio et al., 2005). Consequently within the CT, SERCA2a protein decreased whilst PLB was markedly up-regulated; this resulted in a severe reduction in SERCA2a activity to a quarter of that compared with the young SA node. The alterations in Ca^{2+} handling may result in an inefficient reuptake of Ca^{2+} and could result in Ca^{2+} overload within the CT, possibly a cause for the known ecoptic and reentrant arrhythmias (Kalman et al., 1998).

4.4.2.2 Effect of ageing on the spontaneous activity of the CT: a cause for concern

The CT has previously shown to have spontaneous activity (Li-jun et al., 2012); thus explaining the connection made between the CT and the generation of arrhythmias (Akcay et al., 2007). Within the SA node, spontaneous activity is instigated by a few key proteins; RYR2, Cav1.2, I_f and NCX1 (see Chapter 3). As such spontaneous activity within the CT would use similar proteins (Li-jun et al., 2012). With age there was a significant increase in RYR2 protein levels. RYR2 protein is not only linked to spontaneous activity (Bogdanov et al., 2001), but spontaneous release is also connected to 'SR leakage' that results in an ecoptic beat (Vest et al., 2005). In

supporting these findings, blocked RYR2 protein was shown to prevent spontaneous calcium transients in atrial myocytes (Yeh et al., 2008).

Reduced SERCA2a activity and increased 'SR leakage' would result in diminished SR Ca^{2+} load, another factor in arrhythmia generation (Venetucci et al., 2007). Atrial ectopic pacemakers were found to be located at the lower base of the CT and commented to be dependent on the ‘membrane clock’ for its automaticity rather than the 'SR clock' (Shinohara et al., 2010). As such, to compensate for the loss of SR Ca^{2+} load, $Ca_v1.2$ channel expression was increased within the CT. Therefore the increased RYR2 protein levels and leakage at close proximity to the $Ca_v1.2$ channels could result in an ectopic beat. Furthermore there is reduced threshold for myocardial cell calcium with age (Hano et al., 1995).The increase in $Ca_v1.2$ is not mimicked by an increase in any Ca^{2+} extrusion mechanisms such as NCX1, SERCA2a or PMCA4a, thus the sudden increase in $Ca_v1.2$ would result in higher influx with reduced efflux suggesting Ca^{2+} overload.

4.4.2.3 Age-associated changes in protein expression: comparing the RA muscle and CT

CT tissue structure mimics RA muscle (D'Amato et al., 2009) but is electrophysiologically different in its AP profile along the whole zone (Boyett et al., 1999). In addition there are variations in the molecular profile of the CT, warranting the CT as separate tissue from the RA muscle or the SA node (Boyett et al., 2000). Compared with the CT, at 6 months of age, the RA muscle had significantly higher levels of RYR2, NCX1 and PMCA4a protein with elevated SERCA2a activity. By 24 months, expression of SERCA2a protein decreased alongside PLB, thus SERCA2a activity was affected minimally. In contrast SERCA2a activity was dramatically reduced in the CT; this highlighted that the ageing process impacted the CT and RA muscle to different degrees.

4.4.3 Overall comparison of atria

4.4.3.1 Age-associated changes across the atria

The ageing process normally results in cardiac myocytes dysfunction including altered Ca^{2+} regulation. This study showed decreased expression in all Ca^{2+} handling proteins

investigated (SERCA2a, PLB, RYR2, $Ca_v1.2$, NCX1, PMCA4a), furthermore mRNA data correlated with all results apart from NCX1 mRNA which showed no change with age. Alterations in SERCA2a and RYR2 protein expression in the RA muscle was previously shown not to change with age, but SERCA2a activity was significantly decreased, thus indicating contradictory results (Kaplan et al., 2007). In contrast a more recent paper showed decreases in SERCA2a, RYR2 and $Ca_v1.2$ mRNA levels (Tellez et al., 2011). Nonetheless studies focusing specifically on ageing are infrequent as many incorporate the aspect of AF and the role Ca^{2+} dysregulation on atrial cardiomyocytes (Bootman et al., 2011). In addition although few studies have compared Ca^{2+} handling protein expression from atria to ventricle (Luss et al., 1999), rarely is the RA compared with the LA.

There were clear regional variations in protein expression; significant up regulation of SERCA2a, PLB and NCX1 was observed in the LA compared with the RA muscle. Age-associated increases in NCX1 has been observed in ventricles (Mace et al., 2003) and is linked to early signs of heart failure (Flesch et al., 1996). Within the LA this rise could be linked to atrial remodelling (Sun et al., 1998) which may be indicative of atrial fibrillation (Schotten et al., 2002). NCX is not a tightly controlled protein, thus it is considered a leaky exchanger; this may cause an imbalance of Ca^{2+} ions into the cell of which tolerance is reduced with age (Hano et al., 1995). Furthermore Ca^{2+} overload may increase the risk of developing an ectopic beat resulting in an arrhythmia. The link between NCX1 and its role in pacemaker activity (Sanders et al., 2006), alongside the increased sensitivity of RYR2 due to SR Ca^{2+} overload (Ginsburg et al., 1998), may partially explain the development of a second pacemaker site.

PMCA4a protein was not significantly different between the left and right atria and decreases with age to equivalent levels. PMCA4a has been previously shown to be important in controlling Ca^{2+} dependent signalling effectors (Chen et al., 2004a, Caride et al., 2007) but it also acts as a structural molecular regulator of local cyclic nucleotides and hence cardiac β-adrenergic signalling (Strehler et al., 2007). Consequently the age-associated decrease in PMCA4a protein may play a role in the diminished β-adrenergic response, documented to occur with age (Xiao et al., 1998).

4.4.3.2 Changes in SERCA2a activity across the atria and its role in atrial fibrillation

SERCA2a, vital for SR calcium content and myocardium contractility, has been previously studied in the ventricles with age (Cain et al., 1998) and in atria exhibiting

AF (Greiser et al., 2009). Although there is a clear trend in patients with AF and advanced age, studies are only recently beginning to investigate changes to Ca^{2+} transporter proteins pre-AF (Greiser et al., 2011). Within the LA, SERCA2a protein increased in expression alongside PLB, which should have resulted in no overall change in SERCA2a activity; nevertheless only PLB pentamer showed a significant increase and not PLB monomer. Conversely in the RA SERCA2a activity decreased, clearly showing a divergence in Ca^{2+} regulation between the atria. Nonetheless this is similar to inconclusive findings on SERCA2a function in AF which has been shown to be unchanged (Schotten et al., 2002), reduced (Greiser et al., 2009) and increased (El-Armouche et al., 2006). Furthermore over expression of SERCA2a within the LA has been linked to increased generation of acute arrhythmias (Rubio et al., 2005).

Elevated SERCA2a protein and activity improves the removal of Ca^{2+} into the SR and thus increasing SR Ca^{2+} load. In association with causing increased RYR2 sensitivity (Ginsburg et al., 1998), SR Ca^{2+} overload is considered a major factor in an arrhythmogenic episode (Venetucci et al., 2007). Therefore the ageing process may increase LA contractility as an adaptation to elevate LV load and thus output, but as a consequence a deleterious factor crucial in the generation of an arrhythmia is produced.

SERCA2a activity is regulated by PLB, and thus is a crucial regulator of cardiac contractility (MacLennan and Kranias, 2003). However, atrial cells have been shown to ultilise a smaller proteolipid peptide known as sarcolipin (SLN) which has been shown to regulate SERCA2a activity in a similar fashion to PLB (Vangheluwe et al., 2006). Furthermore atrial myocytes have been studied to abundantly express sarcolipin (Minamisawa et al., 2003), but down regulation has been associated with atrial fibrillation (Uemura et al., 2004). This emphasises the importance of sarcolipin and that it may also play a role in SERCA2a activity across the atria.

4.4.3.3 Protein and mRNA data disparity: age-associated changes in mRNA translation

The underlying mechanisms behind age-associated protein changes were investigated via qPCR to study mRNA levels of corresponding proteins. Within the RA muscle mRNA correlated to protein data for SERCA2a, RYR2 and Cav1.2; but not NCX1, which showed a decrease in protein levels but no change in mRNA. In addition SERCA2a protein was up regulated in the LA, whilst mRNA levels decreased. Though some studies show correlated mRNA to protein data (Kaplan et al., 2007), others have

remarked differences between qPCR findings and western blot data (Tellez et al., 2011). Down-regulation of mRNA together with up-regulation of protein levels may occur if the protein half-life is increased or normal turnover interrupted and the protein becomes stabilised either through the former or via protein-protein interactions (Zaun et al., 2012).

4.4.4 Limitations

Protein data were analysed via western blotting and immunocytochemistry of which the latter also showed the location. Nevertheless both techniques did not consistently produce similar findings, although the same antibodies were used, SERCA2a protein was severely elevated in the LA versus the RA, but in the immunocytochemistry the difference was minimal resulting in no divergence across the atria. Similarly in PMCA4a contrary data was reported with elevated levels in the RA in western blotting, but the opposite was shown with immunocytochemistry. Western blotting provides a general profile from the whole dissected region, however, immunocytochemistry showed the localisation of proteins that may be heterogeneously expressed across the section.

4.4.5 Conclusion

These results indicate that the expression of key Ca^{2+} handling proteins varies across the SA node, CT and RA muscle. With age the heterogeneity of expression across this region was observed to alter. CT tissue showed increased $Ca_v1.2$ and RYR2, which are key components in generating arrhythmogenic episodes in the CT tissue with direct affect on the SA node. The LA was observed to contain higher expression levels of Ca^{2+} transport proteins when compared with the RA; with age these proteins were observed to further diverge in expression with the exception of PMCA4a. The combined increase of $Ca_v1.2$, RYR2 and SERCA2a activity greatly augments SR Ca^{2+} content and the probability of SR 'leakage' leading to an arrhythmia. In contrast the RA exhibited dramatic Ca^{2+} remodelling with decreased expression of all Ca^{2+} handling proteins. Overall major disparity exists across the atria and these age-associated alterations to Ca^{2+} regulation could indicate progressive AF.

Chapter 5 Effect of age on Ca^{2+} handing proteins in the ventricles

5.1 Introduction

5.1.1 Consequences of advancing age on the ventricles

Advancing age is associated with changes to the cardiovascular system that results in a diminished capacity for the heart to respond to increased ventricle loading (Schulman et al., 1992). The reduced capacity is due to a combination of arterial and cardiac stiffness that result in increased myocardium wall thickness, prolonged contraction and incomplete relaxation (Lakatta et al., 1987, Lakatta, 1987). In most species of rats the elderly heart experiences left ventricular hypertrophy compared with younger animals (Yin et al., 1980); in humans the left ventricle (LV) chamber dilates rather than increases wall thickness (Shreiner et al., 1969). Comparing ventricular myocytes from young-adults to elderly, the extent of cell shortening is lower in the aged mouse and re-lengthening is prolonged indicating slow removal of intracellular Ca^{2+} (Lim et al., 2000). However, few studies have compared the left and right ventricles, with the majority of studies have focused on the LV.

5.1.1.1 Calcium remodelling within the left and right ventricles

Reduced cardiac contractile function is reflected by diminished Ca^{2+} transients (Lim et al., 2000). In the young adult myocytes transient amplitude is high and duration is short at higher stimulated frequencies; whereas in the senescent ventricular myocytes peak Ca^{2+} transients were smaller and extended duration of AP (Isenberg et al., 2003). The age-associated discrepancy at higher stimulated frequencies is due to the decline in capacity to react to exercise and stress; this is reflected by the diminished ability to respond to β-adrenergic stimulation (Xiao et al., 1994). The young-adult Ca^{2+} transient is based on excitation-contraction (EC) coupling, which revolves around the influx of Ca^{2+} via $Ca_v1.2$, which triggers Ca^{2+} from the SR via RYR2 (Anderson et al., 1989). Consequently to understand mechanisms that suppress contractile function in the elderly heart numerous studies have investigated the effect of age on the expression of key E-C coupling proteins (Assayag et al., 1998, Nicholl and Howlett, 2006).

RYR2 protein expression was shown to decrease in the ageing heart (Nicholl and Howlett, 2006). Coupled with this is the reduced phosphorylation of RYR2 by Ca^{2+}/calmodulin (CaM) kinase (Xu and Narayanan, 1998) and the number of RYR2 binding sites is slightly reduced in cardiac SR within the aged hamster model (Ueyama et al., 1998). A decline in RYR2 protein expression, number of binding sites and a

decline in 'activity' of RYR2, would affect CICR and hence SR Ca^{2+} release; overall partially explaining the smaller peak Ca^{2+} transient noted in elderly ventricular myocytes.

On the other hand Ca^{2+} transients, though predominantly caused by SR Ca^{2+} release, are also contributed to by the $Ca_v1.2$ channels located at t-tubule sites in close proximity to RYR2 (Fabiato, 1983). With age, calcium current ($I_{Ca,L}$) is significantly increased in elderly rat hearts relative to young rats (Walker et al., 1993). This enhancement of I_{CaL} could partially be attributed to changes in the protein expression or properties of $Ca_v1.2$. With age a rise in $Ca_v1.2$ expression was observed in hypertrophied senescent myocytes and suggested to be an adaptive response (Bangalore and Triggle, 1995). Furthermore in 24 months of age rats $Ca_v1.2$ channels had altered gating properties with increased probability of being open, slower inactivation, and greater availability of single calcium currents (Josephson et al., 2002). The combined increase in density and activity of $Ca_v1.2$ would explain the increased calcium current with age.

5.1.1.2 Age-associated changes in the removal of Ca^{2+} from the cytosol

Prolonged AP duration occurs due to the remaining high levels of intracellular Ca^{2+}, thus the cell is prevented from repolarising and relaxation. Ca^{2+} is primarily removed via SERCA2a attached to the SR (Bers, 2002). Age-associated decrease in the activity or ability of SERCA2a to sequester Ca^{2+} would slow contraction and relaxation (Wei et al., 1984). Studies found reduced expression of SERCa2a mRNA in aged rat myocytes (Lompre et al., 1991a, Maciel et al., 1990) but no change in SERCA2a protein in the LV (Kaplan et al., 2007). Nevertheless Kaplan *et al.* observed an age-associated decrease in SERCA2a activity. PLB, a key regulator of SERCA2a activity, is phosphorylated by protein kinase A (PKA); with advanced age the phosphorylation process is decreased (Xu and Narayanan, 1998). Combined either with lower PKA phosphorylation or higher PLB protein, the decline in SERCA2a activity slows the reuptake of Ca^{2+} delaying relaxation and thus overall contraction time.

NCX has three isoforms (NCX1, NCX2 and NCX3) with NCX1 primarily present in the heart (Aceto et al., 1992); it is a multiple purpose protein functioning in Ca^{2+} uptake at the upstroke of an AP and in the removal of Ca^{2+} after an AP. Multiple studies have investigated NCX1 activity in the ageing heart with inconsistent findings of decreased (Lim et al., 1999) or unchanged activity (Abete et al., 1996). A more recent study by

Mace *et al.* showed that NCX activity increased with age in ventricular myocytes (Mace et al., 2003). Interestingly during heart failure expression of NCX1 was elevated alongside CaM kinase II (CaMKII) (Xu et al., 2012); the latter responds to β-adrenergic stimulation resulting in an up-regulation of NCX1 (Mani et al., 2010).

5.1.2 Comparison of the left and right ventricles

The majority of studies have focused on LV changes with age, disease and general dysfunction (Lakatta and Sollott, 2002) and little attention has been paid to the basic physiology of the RV. It has been generally assumed that changes associated with age and health in the LV was the same in the RV, however, the latter is significantly dissimilar structurally, mechanically and possibly molecularly (Haddad et al., 2008) and thus may be affected by age differently. The RV is geared towards the pulmonary system and thus has a thinner wall, undertakes lower ventricular pressure and has lower elasticity compared with the LV (Haddad et al., 2008).

Even in light of this, few studies have cross compared Ca^{2+} handling between the LV and RV; although studies have found dissimilarities in the affect of autonomic input on inflow/outflow and higher adrenergic and cholinergic receptor density in the RV (Bristow et al., 1992). A more recent study by Kondo *et al.* investigated contraction and Ca^{2+} handling in the adult LV and RV; the study demonstrated differences in peak Ca^{2+} values and sarcomere shortening (Kondo et al., 2006).

5.1.3 Variations in calcium handling protein expression across the LV myocardium wall

The LV wall can be split up into three main regions, the epicardium (EPI), endocardium (ENDO) and myocardium (Antzelevitch et al., 1991). Studies have shown that Ca^{2+} handling proteins such as SERCA2a are more abundant in the EPI than in the ENDO (Prestle et al., 1999). Similarly RYR2 and NCX1 in adult hearts showed decreased expression in the endocardium in rats exhibiting progressive heart failure (Currie et al., 2005, Xiong et al., 2005). Heart failure, which is used as detrimental focus in most left ventricular studies, was shown to affect the transmural gradient, with up-regulation of NCX1 protein occurring in the ENDO rather than in the EPI in contrast to the normal heart (Mani et al., 2010). Regardless of the focus on healthy or failing hearts heterogeneity in the expression of Ca^{2+} handling proteins is associated as a susceptibility to developing Ca^{2+} transient alternans (Prestle et al., 1999). Calcium

alternans is a result of different levels of intracellular Ca^{2+} concentration across myocytes that will cause force of contraction to be reached at alternative depolarisations (Clusin, 2008). The development of Ca^{2+} transient alternans is a crucial arrhythmogenic mechanism (Prestle et al., 1999) and a key component in sudden cardiac arrest (Weiss et al., 2006). In summation accentuated transmural gradient of Ca^{2+} handling proteins could provide the basis for the generation of ventricular arrhythmias (Antzelevitch et al., 1991).

The ageing process has not been as extensively studied across the LV myocardial wall. A recent paper by Abd Allah *et al.* investigated Ca^{2+} handling proteins across the ventricular myocardium in neonatal and adult rabbits. This study found a divergence in mRNA and density of key proteins in the EPI and ENDO but this also varied between the neonatal and adult tissue (Abd Allah et al., 2012). Although this study did not investigate an elderly model, their data indicates heterogeneity across the LV wall and sub-regions may respond differently to advancing age.

Consequently age-associated changes in Ca^{2+} handling proteins SERCA2a, PLB, RYR2, Cav1.2, NCX1 and PMCA4a were investigated in the ventricles across the lifespan of rats. To further study protein remodelling within the LV, transmural gradient, protein expression and mRNA analysis was performed across the LV wall; the latter was possible via the separate removal of the LV epicardium and endocardium.

5.1.4 Objectives

i. To investigate age-associated changes in the expression of calcium handling proteins and mRNA of SERCA2a, PLB, Cav1.2, NCX1, PMCA4a and RYR2 in the left ventricle (LV) and right ventricle (RV).

ii. To determine whether divergence exists in calcium handling proteins within the whole LV differs across the myocardium to include the epicardium (EPI) or endocardium (ENDO).

5.1.5 Hypothesis

1. Calcium handling proteins expressions of the LV and RV is significantly different depending on region and would explain the lower Ca^{2+} transients and contractile function reported in the RV.

2. Ageing induces significant alterations to the expression of Ca^{2+} transporters. The varied cardiac demand on the LV and RV results in differences in the extent of Ca^{2+} remodelling with age.

3. LV protein expression is not universal across the myocardium wall and with age and this gradient will vary between the EPI and ENDO affecting functionality and increased risk of arrhythmia generation.

5.2 Methods

5.2.1 Western blotting

Hearts were removed, dissected into separate regions, crushed, protein extracted and analysed by electrophoresis (see section 2.2). The epicardium (EPI) and endocardium (ENDO) were shaved off the LV as previously described in section 2.1.2. For the results obtained, further adapted methods were used for particular antibodies (see methods section 3.2).

5.2.2 qPCR actin and endogenous control

Negative and positive reverse transcriptase samples were analysed using actin transcripts (see section 4.2.2). Desmin was used as an endogenous control for all qPCR experiments (see section 4.2.3).The same primer transcripts were used as in previous chapters.

5.2.3 Immunocytochemistry

Immunocytochemistry was conducted as described in section 2.3 and antibodies diluted to appropriate concentrations (see Table 2.2). For the comparison of the ventricles to ensure unbiased data from the LV, scans from the epicardium, endocardium and central myocardium were recorded and averaged to produce an overall density of the LV.

5.2.3.1 Transmural gradient across the LV myocardium

Single tile scans were taken across the horizontal LV section which started at the epicardium (EPI) through the central myocardium and finishing at the endocardium (ENDO). Tile scans were made of composite pictures creating a transmural gradient across the LV wall. A profile was conducted with a line drawn across the section (Figure 5.1A) which recorded density of the fluorescent label at 0.208µm steps. Consequently a graph was drawn showing the intensity of label alongside the distance of the LV wall section (Figure 5.1B). A table was also generated with all the data which was be copied into Sigma Stat (version 12) software, a graph drawn, and a linear regression algorithm plotted.

A

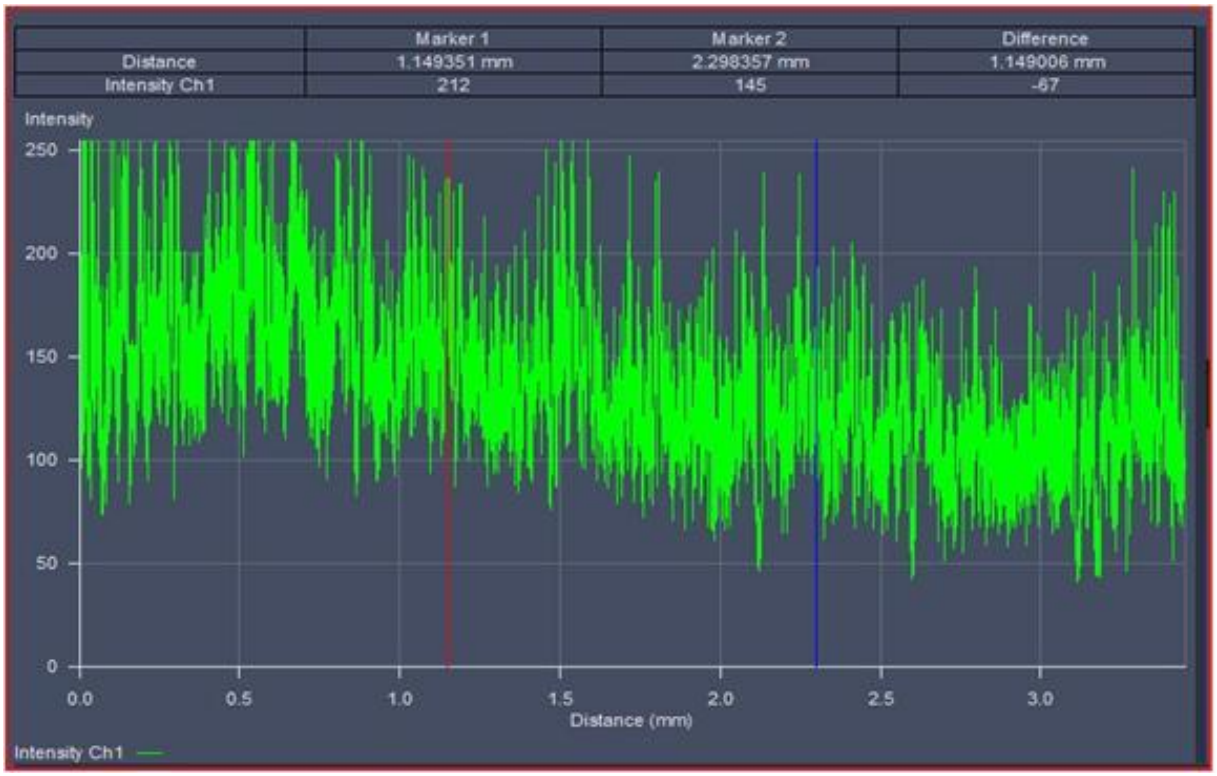

B

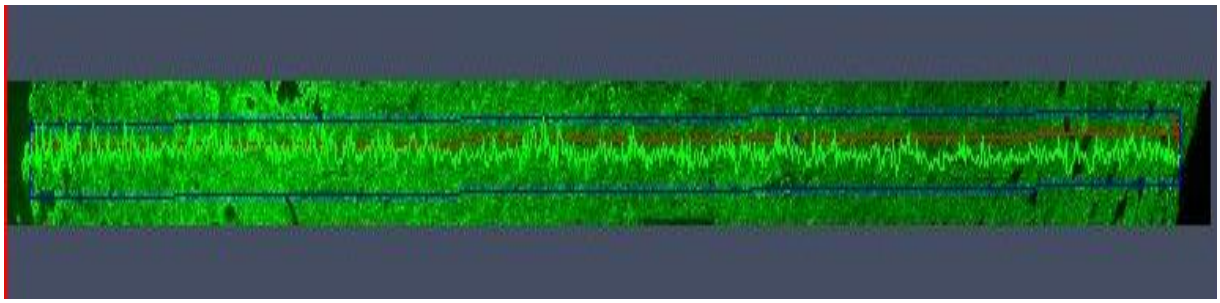

Figure 5.1 Example profile of a LV wall tile scan.

(A) Representative graph of SERCA2a density taken from (B) SERCA2a labelled LV wall image consisting of individual tile scans.

5.2.4 Statistical analysis

For all data, unless specified otherwise, statistical differences were determined by two way ANOVA with Holm-Sidak comparisons. For each age group 6, 12 and 24 months, n=5. Data are presented as means ± SEM. Data was normalised to the averaged 6 months LV data.

5.3 Results

5.3.1 Effect of ageing on left and right ventricular tissue

The LV and RV was investigated at 6 months (young-adult), 12 months (adult) and 24 months (elderly) of age animals. Age-associated changes in calcium handling proteins: SERCA2a, PLB, RYR2, Cav1.2 NCX1 and PMCA4a were studied, qPCR was used to determine mRNA alterations and immunocytochemistry used to analyse the location and density.

5.3.1.1 Age-associated changes in SERCA2a activity across the ventricles

Within the 6 months age group double SERCA2a protein was expressed in the LV (100±7.7%) compared with the RV (52±5.6%) (Figure 5.2B). This divergence in protein is due to higher expression of mRNA in the LV (100±5.2%) versus RV (51±5.2%) (Figure 5.2C). At 12 months, SERCA2a protein decreased in the LV to 89±11.9%, whilst increasing by 20±7.4% in the RV. With advanced age there was a significant decrease in SERCA2a protein within the LV (55±7.4%) and this was mimicked by decreases in mRNA (75±11.8%). The RV exhibited no changes in protein or mRNA expression across the age groups.

Within both ventricles SERCA2a was localised at the sarcolemma membrane and t-tubular network (Figure 5.3). At 6 months of age there was a significantly higher density of SERCA2a in the LV (100±3.1%) compared to the RV (65±6.7%). With advanced age, SERCA2a density decreased to 75±5.7%, which removed the discrepancy between the ventricles. Furthermore at 24 months SERCA2a protein was concentrated at the sarcolemma membrane of the left ventricular myocytes in dense clumps rather than in a t-tubule pattern. No change in SERCA2a density was observed in the RV, although localisation did vary compared to the younger sections.

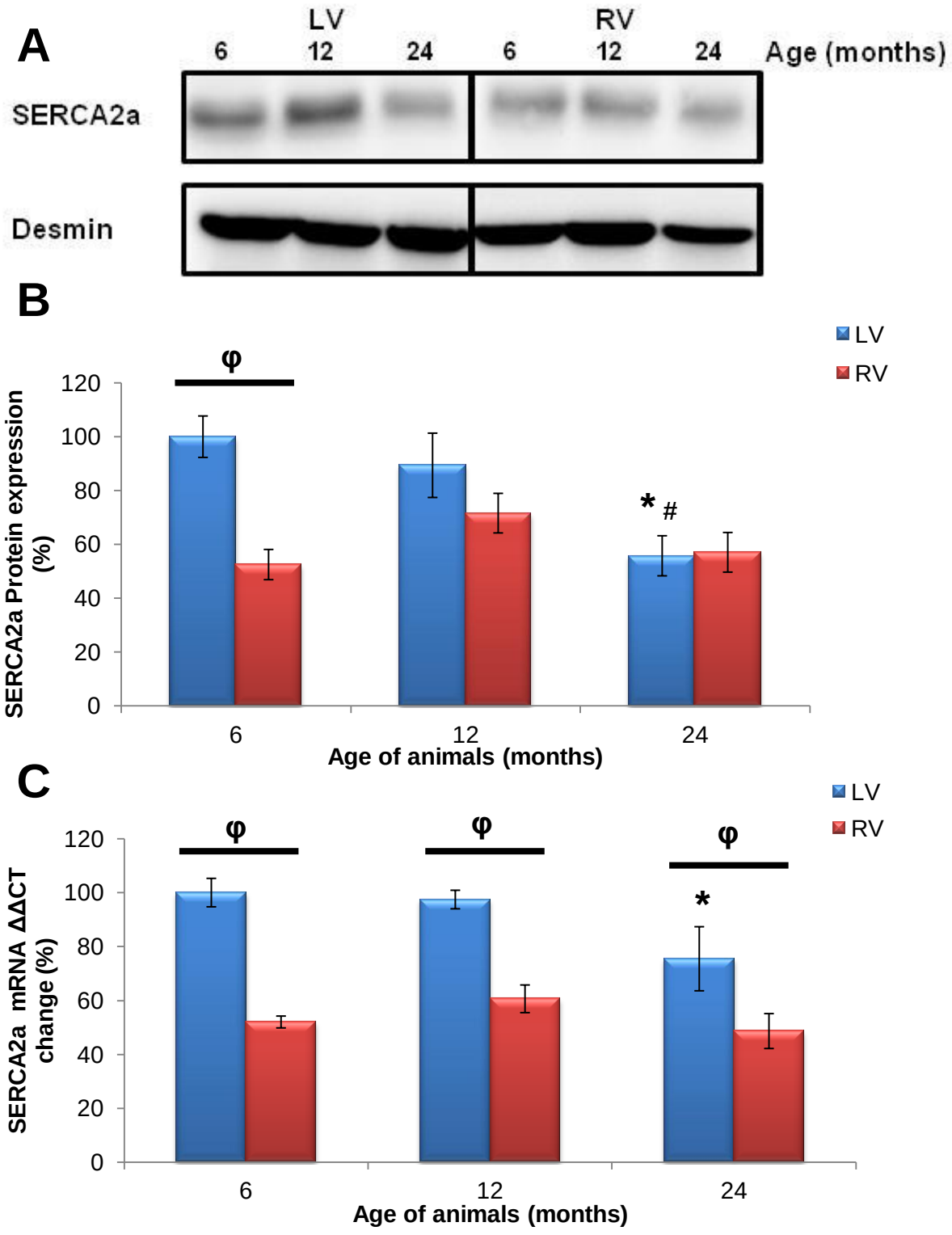

Figure 5.2 Profile of SERCA2a protein expression across the ventricles with increasing age

A) illustrative blot of SERCA2a protein and desmin; B) SERCA2a protein expression normalised to desmin; C) qPCR showing fold change of mRNA. * denotes $p<0.05$ vs. respective 6 months data, # denotes $p<0.05$ vs. respective 12 months data, φ $p<0.05$ within age group. n=5 per age group.

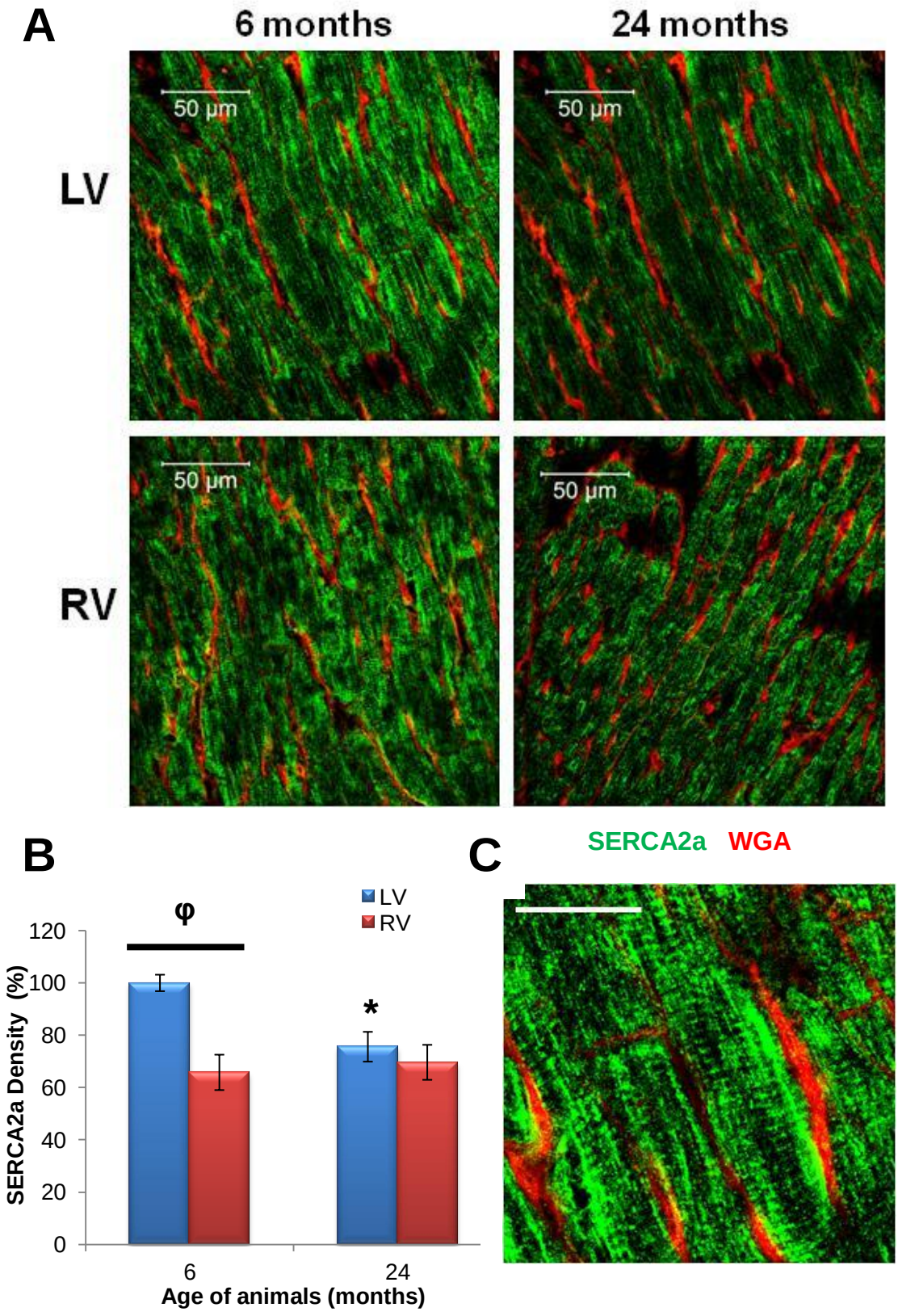

Figure 5.3 Localisation of SERCA2a protein expression across the ventricles

A) illustrative images across the ventricles are shown from rat hearts at 6 and 24 months of age; B) density of SERCA2a label for LV and RV; C) high resolution image with 25µm scale bar. * denotes $p<0.05$ vs. respective 6 months data, φ $p<0.05$ within age group. n=5 per age group.

PLB total expression at 6 months of age which was greater in the LV (100±5.9%) contrast to the RV (78±3.5%) (Figure 5.4B). Investigating the separate isoforms of PLB showed that this difference was due to the significantly higher levels of PLB monomer (Figure 5.4C). At 12 months of age PLB total expression decreased in the LV (87±10.8%) which reduced diversity between the ventricles and was reflected by lower PLB monomer expression. Nevertheless at 24 months of age, PLB total expression significantly decreased in the LV (72±5.1%) due to reduced PLB monomer levels, whilst PLB pentamer remained relatively unchanged across the age groups. Comparatively at 24 months old PLB total increased in the RV (97±4.7%) this was attributed to the PLB monomer.

As PLB is associated with SERCA2a, a similar pattern was observed with PLB total density being located at the sarcolemma membrane of ventricular myocytes and along the t-tubular network (Figure 5.5). PLB density was substantially greater in the 6 months LV (100±6.0%) compared with the RV (73±4.4%). However, at 24 months old there was a decrease in PLB density in the LV (84±3.3%) which reduced the divergence. With age there are clear changes in PLB location within the LV which showed a higher proportion of dense patches at the sarcolemma membrane and a reduced localisation at the t-tubules. In the RV similar to previous quantitative data, with age PLB expression increased slightly to 83±6.5% but this was not significantly higher (Figure 5.5).

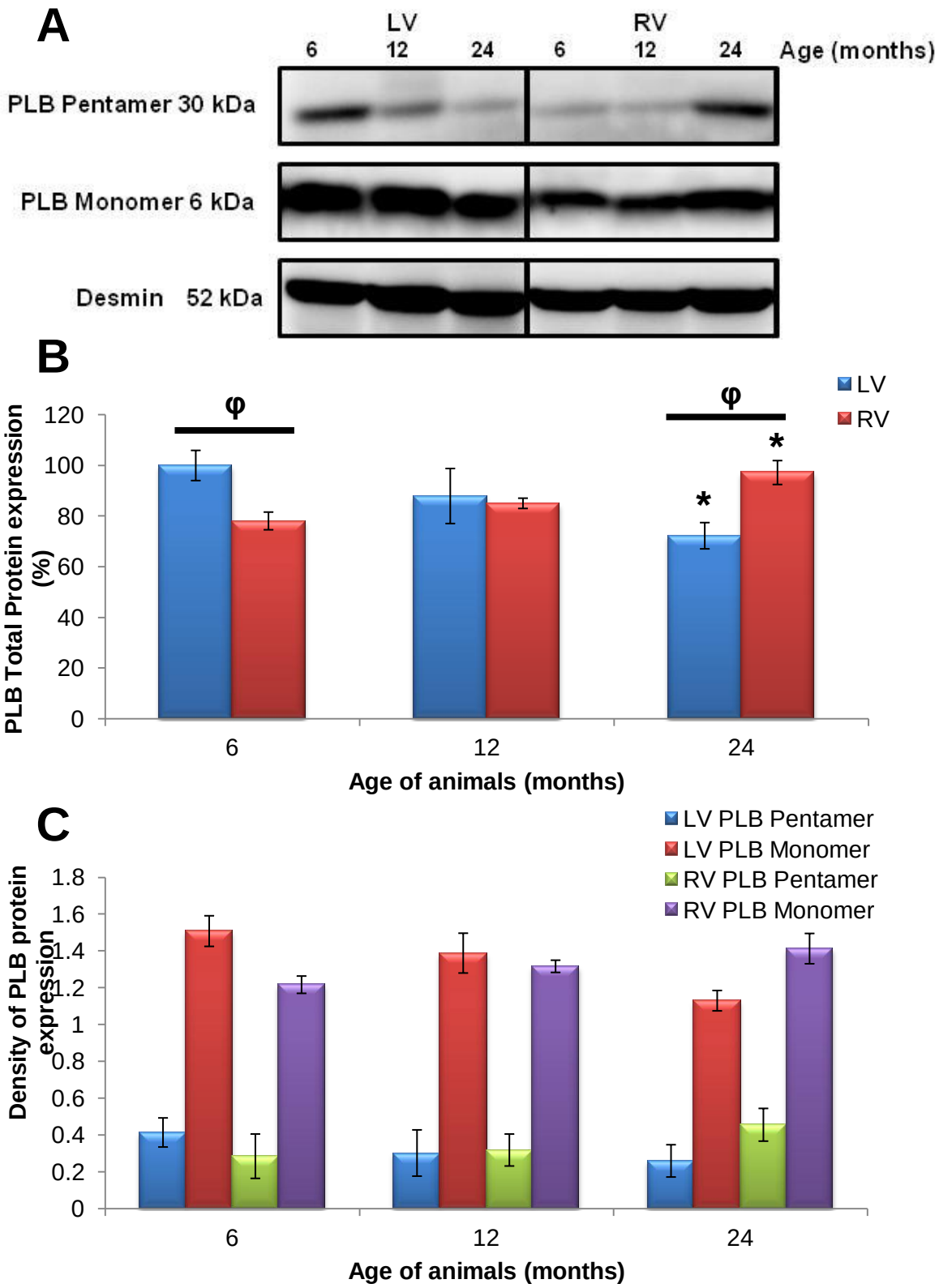

Figure 5.4 Profile of PLB protein expression across the ventricles with increasing age.

A) illustrative western blots of PLB monomer and pentamer B) PLB total protein expression normalised to desmin C) PLB pentamer and monomer protein expression. * denotes $p<0.05$ vs. 6 months age group; # denotes $p<0.05$ vs. 12 months age group, φ $p<0.05$ vs. within age group. (n=5 per age group)

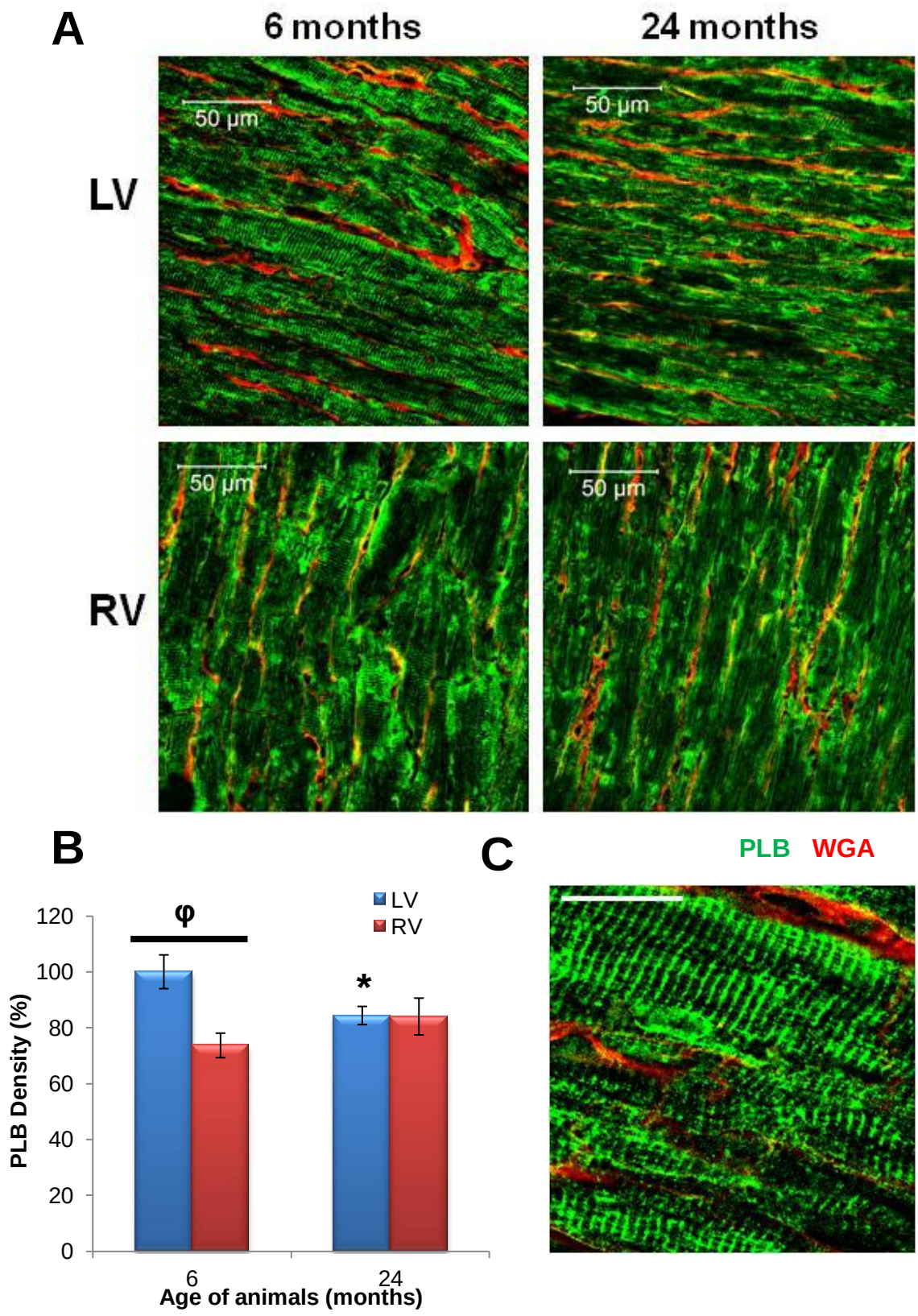

Figure 5.5 Localisation of PLB protein expression across the ventricles

A) illustrative images across the ventricles are shown from rat hearts at 6 and 24 months of age; B) density of PLB label for LV and RV; C) high resolution image with 25µm scale bar. * denotes $p<0.05$ vs. respective 6 months data, φ $p<0.05$ within age group. n=5 per age group.

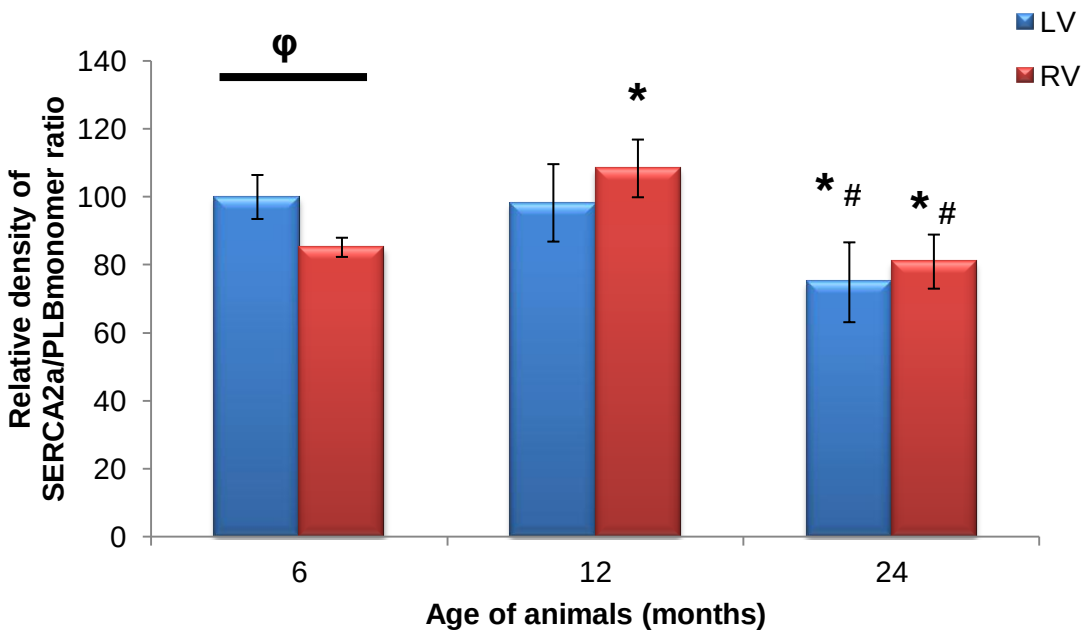

Figure 5.6 SERCA2a activity in the LV and RV with advancing age.

SERCA2a protein expression normalised to PLB monomer expression indicates the functional capacity of the calcium pump SERCA2a. * denotes $p<0.05$ vs. respective 6 months age group, # denotes $p<0.05$ vs. respective 12 months age group, φ $p<0.05$ vs. within age group. n=5 per age group.

SERCA2a activity was 15±2.8% lower in the RV at 6 months of age (Figure 5.6). The LV showed no change in activity between 6 and 12 months of age, however, in the RV SERCA2a activity significantly increased by 23±8.4% causing equivalent activity across the ventricles by the adult stage. With advanced age both showed a decline in SERCA2a activity by 26±11.7% in the LV and 28±7.9% in the RV when compared to the 6 months age group.

5.3.1.2 Age associated changes to proteins involved in CICR within the ventricles

Within 6 and 12 month age groups RYR2 protein expression was not significantly different between the LV (100±10.5%) and RV (83±6.2%), however, LV tissue was slightly elevated levels (Figure 5.7). This was contrary to mRNA results which showed significantly higher levels of RYR2 mRNA in the RV (125±5.8%) compared with the LV (100±3.8%). Conversely mRNA expression decreased significantly in the RV at 12 months of age (97±3.7%) which removed divergence of mRNA between the ventricles. With advanced age RYR2 protein expression declined in the LV (66±9.1%) and the RV (55±3.3%). This reduced protein expression is reflected by significantly decreased mRNA expression (Figure 5.7C).

RYR2 density label showed increased background fluorescence in ventricular sections with higher levels of green label throughout myocytes (Figure 5.8). At 6 months of age especially within the RV section RYR2 density was localised along the t-tubules. Within the LV density was visualised at the periphery of myocytes with occasional transverse striated/streaked patterns. Corresponding to the mRNA data, but not protein data, RYR2 density was significantly higher in the RV (161±13.6%) compared with the LV (100±9.3%) at 6 months. With age there was no change within the LV but a slight decrease in the RV (150±14.8%); leaving the divergence unchanged (Figure 5.8).

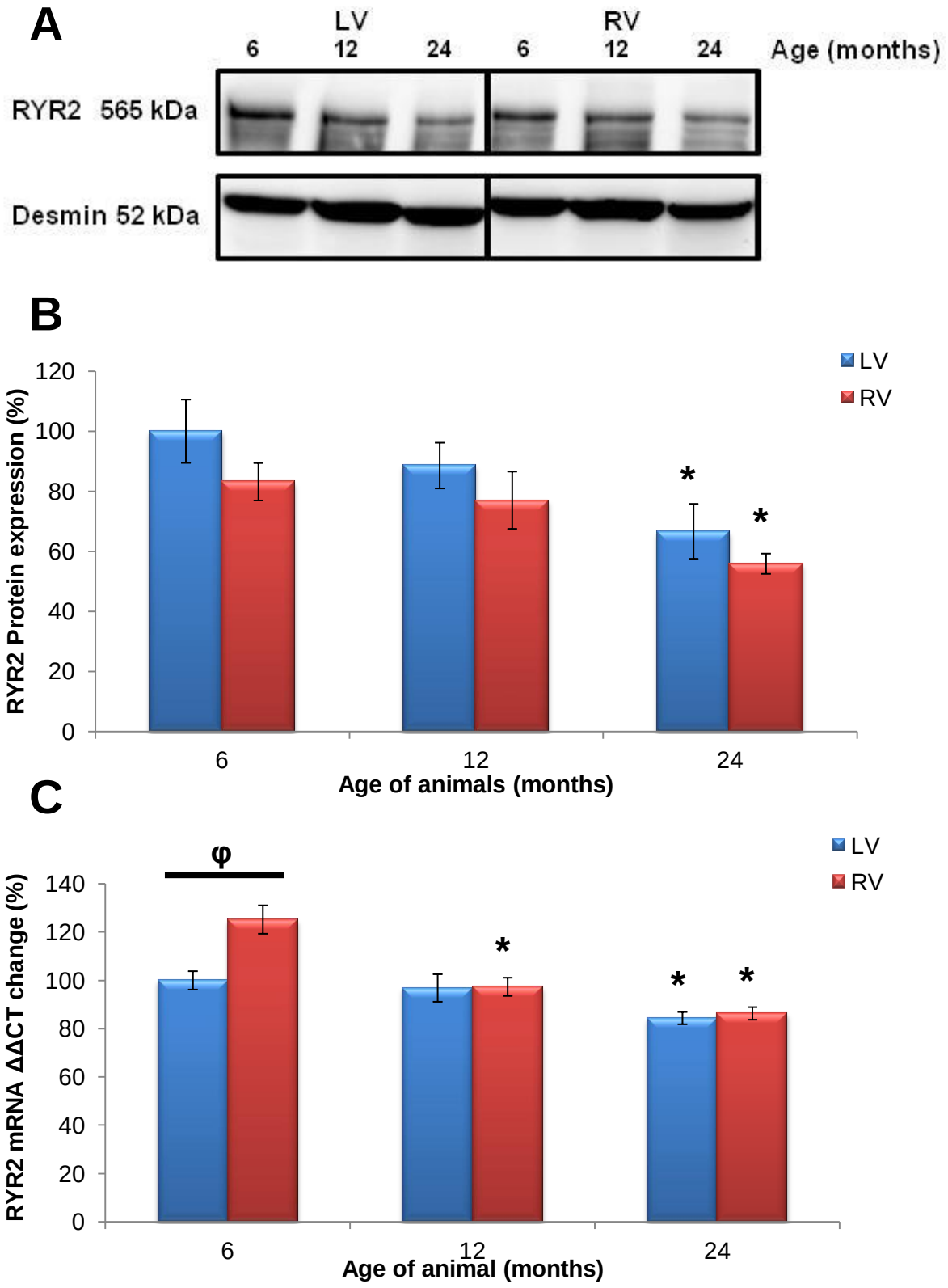

Figure 5.7 Profile of RYR2 protein expression across the ventricles with increasing age

A) illustrative blot of RYR2 protein and desmin; B) RYR2 protein expression normalised to desmin; C) qPCR showing fold change of mRNA. * denotes $p<0.05$ vs. respective 6 months data, # denotes $p<0.05$ vs. respective 12 months data, φ $p<0.05$ within age group. n=5 per age group.

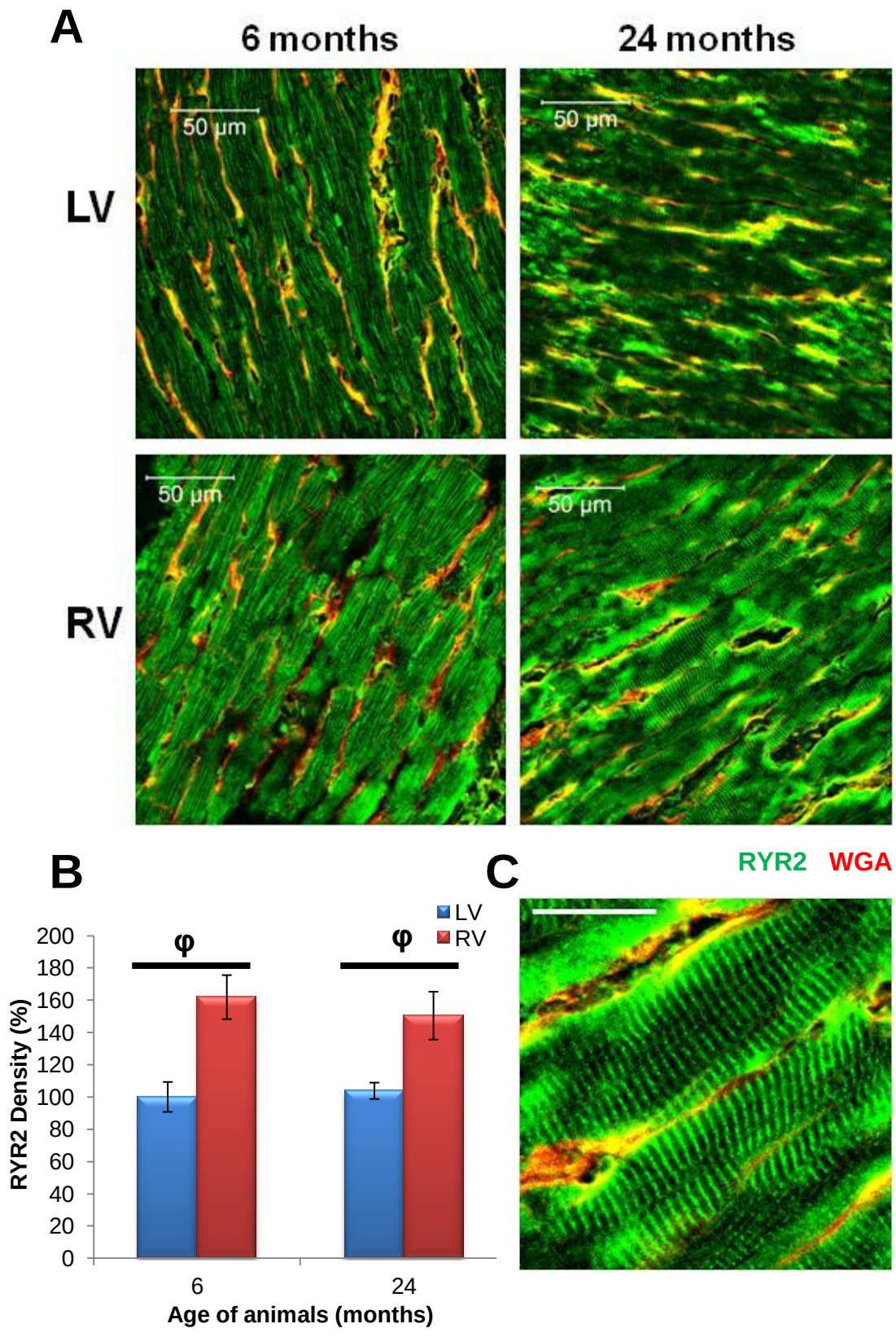

Figure 5.8 Localisation of RYR2 protein expression across the ventricles

A) illustrative images across the ventricles are shown from rat hearts at 6 and 24 months of age; B) density of RYR2 label for LV and RV; C) high resolution image with 25µm scale bar. * denotes $p<0.05$ vs. respective 6 months data, φ $p<0.05$ within age group. n=5 per age group.

As shown in Figure 5.9, $Ca_v1.2$ protein expression did not differ between the ventricles at 6 and 12 months of age, this was mimicked by the mRNA data. Both ventricles also showed decreased protein expression, though not significant, at 12 months of age, which is reflected by reductions in mRNA. In the 24 months age group, $Ca_v1.2$ protein expression within the LV increased by 37±7.4%. RV protein levels remained unchanged resulting in a divergence between the ventricles; also reflected in the mRNA data which showed 34% elevated levels at 24 months of age in the LV (Figure 5.9C).

As with the RYR2 density, $Ca_v1.2$ label within the LV was observed to have a streaked pattern and a greater network of t-tubules visualised. Within the RV clear t-tubular network was observed throughout most myocytes and no streaked patterns. Contradictory data at 6 months in the RV showed a significantly greater Cav1.2 density of 37±5.4% greater compared with the LV; which was the opposite of the western blotting data. With age there was a sharp 29±9.4% rise within the LV but no overall change in the RV. At 24 months of age, $Ca_v1.2$ visualised in LV sections was concentrated at the sarcolemma membrane and junctions between myocytes, with no striations and sporadic t-tubules. The RV exhibited no change in $Ca_v1.2$ localisation, although the visualisation of t-tubules was diminished.

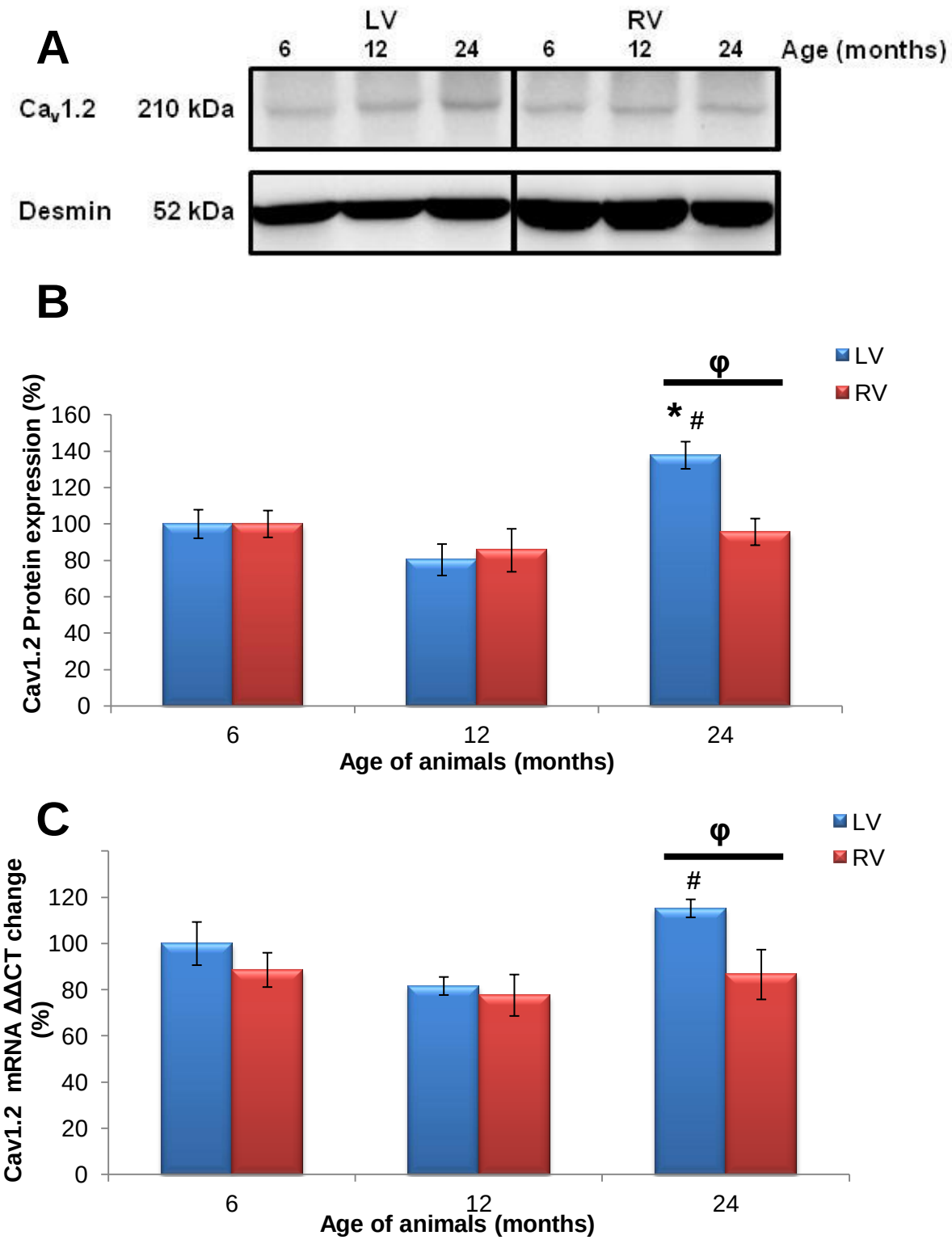

Figure 5.9 Profile of Ca$_v$1.2 protein expression across the ventricles with increasing age

A) illustrative blot of Ca$_v$1.2 protein and desmin; B) Ca$_v$1.2 protein expression normalised to desmin; C) qPCR showing fold change of mRNA. * denotes $p<0.05$ vs. respective 6 months data, # denotes $p<0.05$ vs. respective 12 months data, φ $p<0.05$ within age group. n=5 per age group.

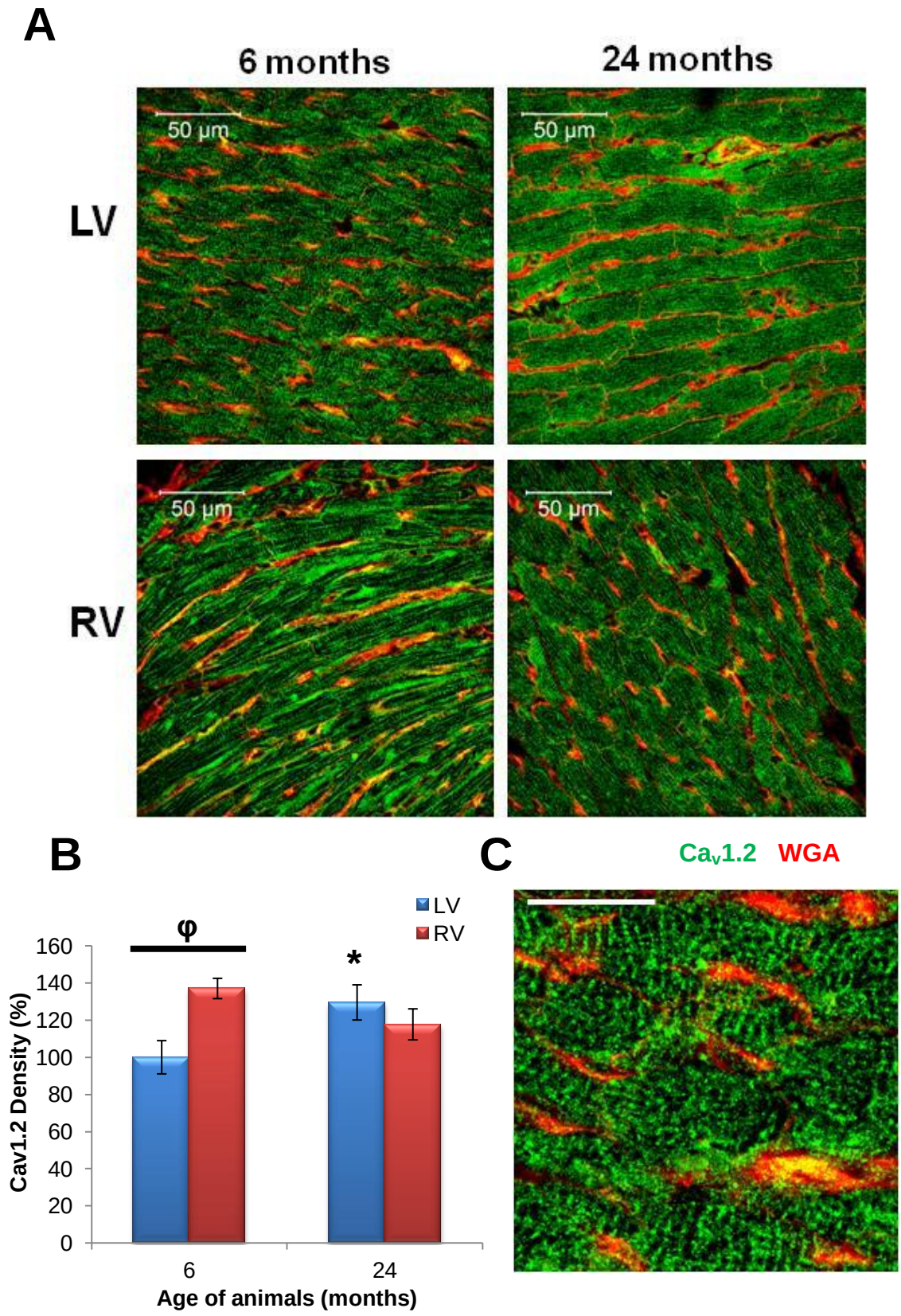

Figure 5.10 Localisation of $Ca_v1.2$ protein expression across the ventricles

A) illustrative images across the ventricles are shown from rat hearts at 6 and 24 months of age; B) density of $Ca_v1.2$ label for LV and RV; C) high resolution image with 25µm scale bar. * denotes $p<0.05$ vs. respective 6 months data, φ $p<0.05$ within age group. n=5 per age group.

5.3.1.3 Effect of ageing on calcium extrusion within the ventricles

In the 6 months age group, NCX1 protein expression was not significantly different but the RV showed slightly lower levels of protein, 92±9.5% compared with 100±5.5% in the LV (Figure 5.11). This slight difference between the ventricles is reflected in the mRNA data (Figure 5.11C). In the 12 months age group NCX1 protein expression was 24±3.6% higher in the RV, this rise in protein is due to the 10±2.1% increased translation of the extra mRNA present. With advanced age, NCX1 protein levels remained raised (127±3.9%) compared with the 6 months age group and this was also mimicked in the mRNA results. On the other hand within the LV, protein and mRNA levels remained constant between 6 and 12 months but at 24 months a dramatic increase in both NCX1 protein (134±3.6%) and mRNA levels (119±4.1%) was observed.

NCX1 protein was predominately localised at the sarcolemma of myocytes with reduced amounts in the centre. Denser levels was observed in the RV (150±3.9%) compared with the LV (100±2.7%) within the 6 months age group, contrary to western blotting data. With age there was a significant increase in the density of NCX1 in the LV (141±3.9%), but rather than concentrated on the periphery, the majority of fluorescence was observed in streaked patterns throughout myocytes and at cellular junctions (Figure 5.12). In contrast, at 24 months, the RV exhibited 35±10.8% decreased NCX1 protein expression resulting in a divergence between the ventricles.

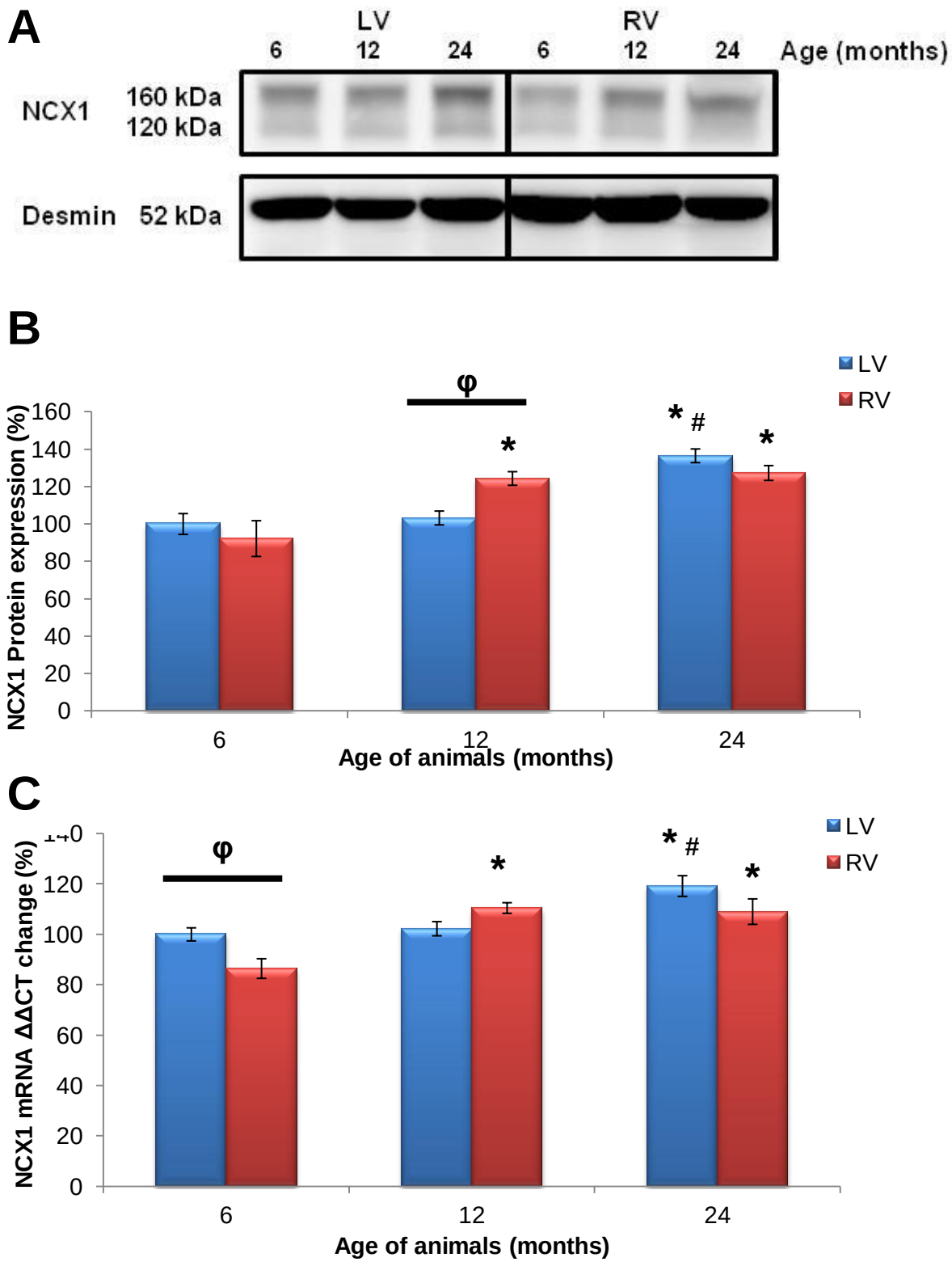

Figure 5.11 Profile of NCX1 protein expression across the ventricles with increasing age

A) illustrative blot of NCX1 protein and desmin; B) NCX1 protein expression normalised to desmin; C) qPCR showing fold change of mRNA. * denotes $p<0.05$ vs. respective 6 months data, # denotes $p<0.05$ vs. respective 12 months data, φ $p<0.05$ within age group. n=5 per age group.

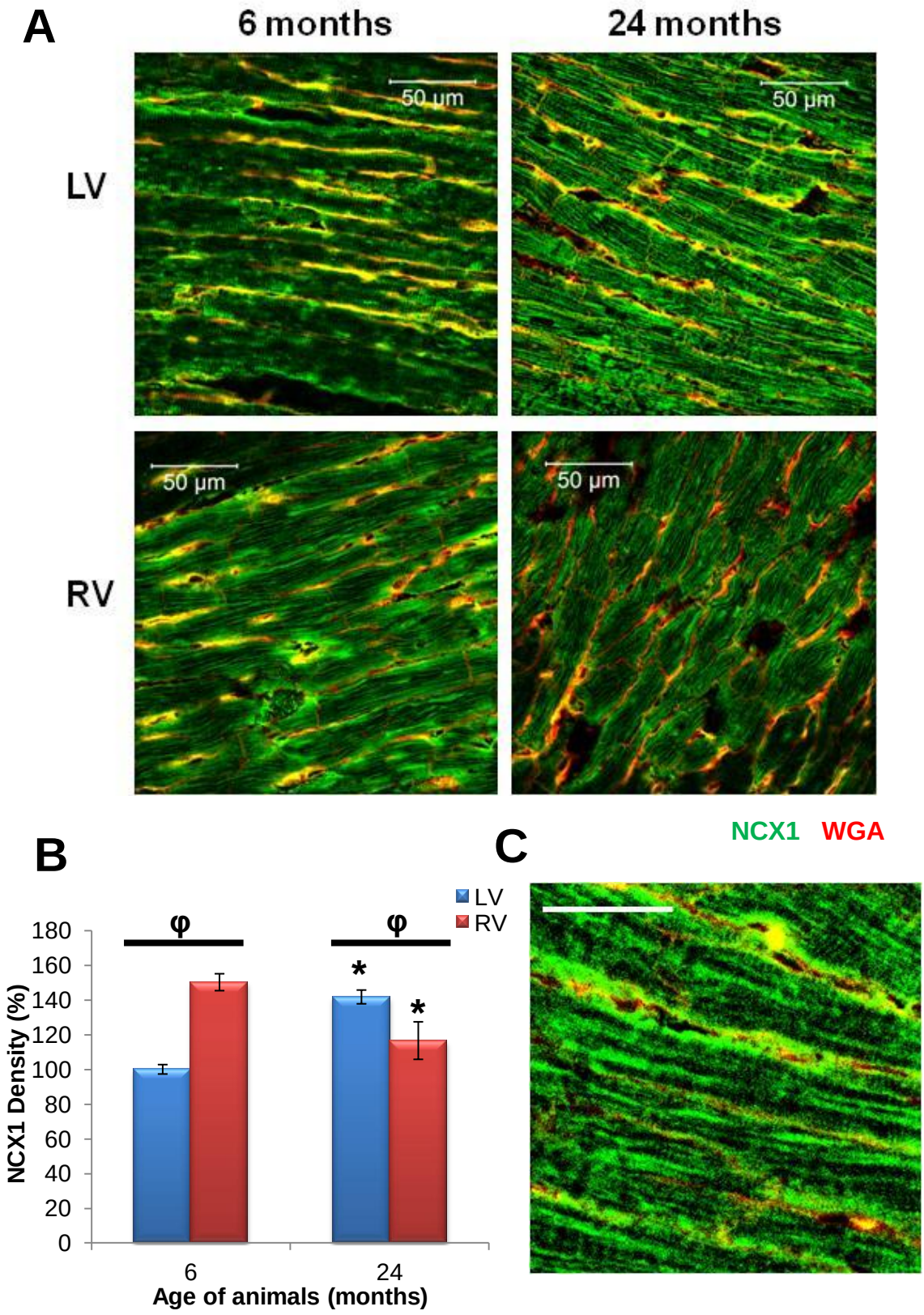

Figure 5.12 Localisation of NCX1 protein expression across the ventricles

A) illustrative images across the ventricles are shown from rat hearts at 6 and 24 months of age; B) density of NCX1 label for LV and RV; C) high resolution image with 25µm scale bar. * denotes $p<0.05$ vs. respective 6 months data, φ $p<0.05$ within age group. n=5 per age group.

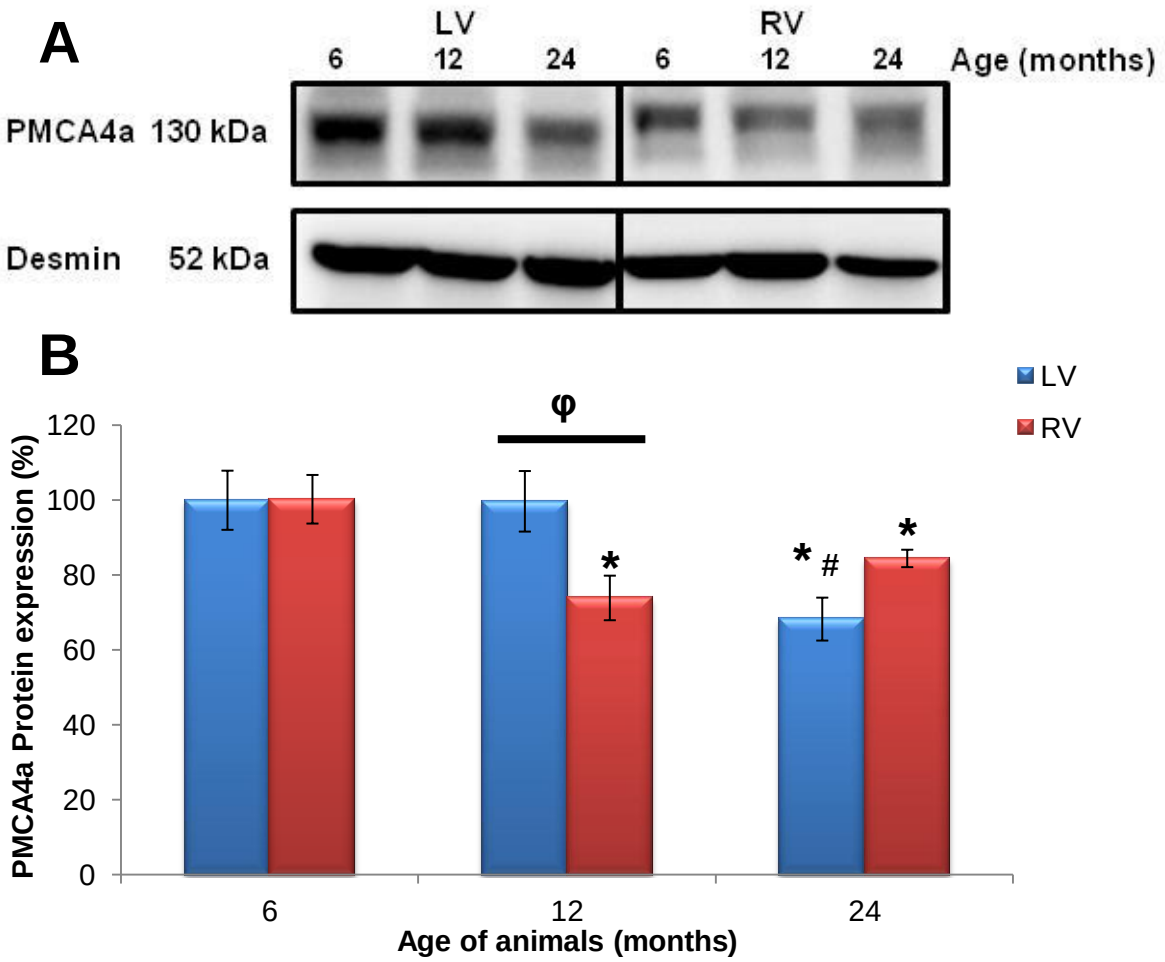

Figure 5.13 PMCA4a protein expression across the ventricles with increasing age

A) illustrative blot of SERCA2a protein and desmin; B) PMCA4a protein expression normalised to desmin. * denotes $p<0.05$ vs. respective 6 months data, # denotes $p<0.05$ vs. respective 12 months data. n=5 per age group.

As shown in Figure 5.13 PMCA4a protein was expressed at equal levels in the LV (100±7.8%) and RV (100±6.4%) at 6 months. With age there was a reduction in protein expression within the RV to 73±5.9% which resulted in significant variation between the ventricles; conversely at 24 months of age there was an increase to 84±2.3%. Within the LV there was no change in PMCA4a protein expression at 6 or 12 months of age, but declined in the 24 months old animals (68±5.7%). PMCA4a was observed in the periphery of myocytes within the RV and LV, however, in the LV a transverse streaked pattern was identified throughout some myocytes (Figure 5.13). Contrary to western blotting data the RV showed elevated levels of PMCA4a protein at 6 months of age (121±7.3%) compared with the LV (100±2.4%). Both ventricles showed an age-associated decline in density of PMCA4a, with 78±2.5% in the LV and 105±7.3% in the RV, although the divergence in protein expression remained across the ventricles.

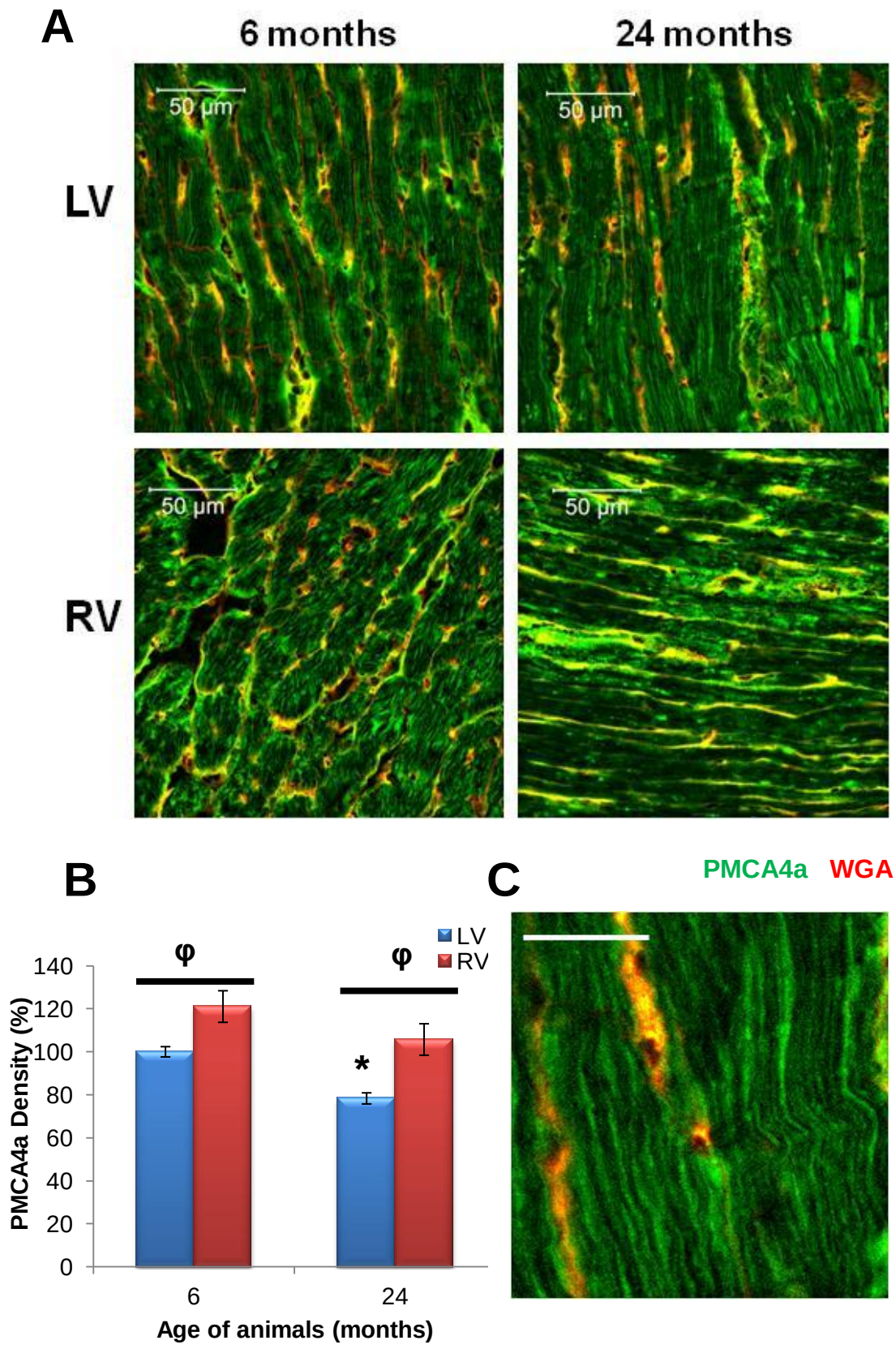

Figure 5.14 Localisation of PMCA4a protein expression across the ventricles

A) illustrative images across the atria are shown from rat hearts at 6 and 24 months; B) density of PMCA4a label for LV and RV; C) high resolution image with 25µm scale bar. * denotes p<0.05 vs. respective 6 months data, φ p<0.05 within age group. n=5

5.3.2 Effect of ageing on transmural changes across the left ventricular wall

Expression of Ca^{2+} handling proteins varied with increasing age in the LV. The LV was spilt into the epicardium (EPI) and endocardium (ENDO) to determine which regions were responsible for the altered protein levels. Therefore changes in Ca^{2+} handling proteins: SERCA2a, PLB, RYR2, Cav1.2 NCX1 and PMCA4a were investigated in the EPI compared with the ENDO. Furthermore qPCR was used to determine mRNA alterations and immunocytochemistry used to analyse the transmural gradient of corresponding protein density.

5.3.2.1 Age-associated changes to SERCA2a activity between the epicardium and endocardium of the LV wall

SERCA2a content in the LV was elevated in the EPI at both 6 and 12 months of age in contrast to the ENDO (Figure 5.14B). The variation in protein expression was reflected in mRNA levels, which at 6 months was 100±5.4% in the EPI and 61±4.9% in the ENDO (Figure 5.14C). Protein expression, at 12 months within the ENDO, was significantly increased from 54±5.3% at 6 months to 78±5.6%; although this increase was not mimicked by the mRNA data. In the 24 months old age group SERCA2a protein dramatically decreased in the EPI from 100±8.6% at 6 months of age to 44±11.1% at 24 months old; this was reflected by a decline in mRNA from 100±5.4% to 50±4.9%. Parallel age-associated reduction in SERCA2a mRNA was noted in the ENDO which decreased to 40±4.7%, as a result protein expression decreased to 33±2.6%. Due to the decreased protein expression, unlike at the younger age groups, with advanced age there was no longer a difference in SERCA2a protein or mRNA levels across the LV wall.

Illustrated in Figure 5.16 is a transmural gradient across the LV wall with labelled SERCA2a; in the 6 months old age group there was a clear negative correlation. This emphasised the increased density of SERCA2a at the EPI rather than the ENDO highlighting the divergence across the myocardium. With age the transmural gradient difference is removed, reducing the variation between the EPI and ENDO.

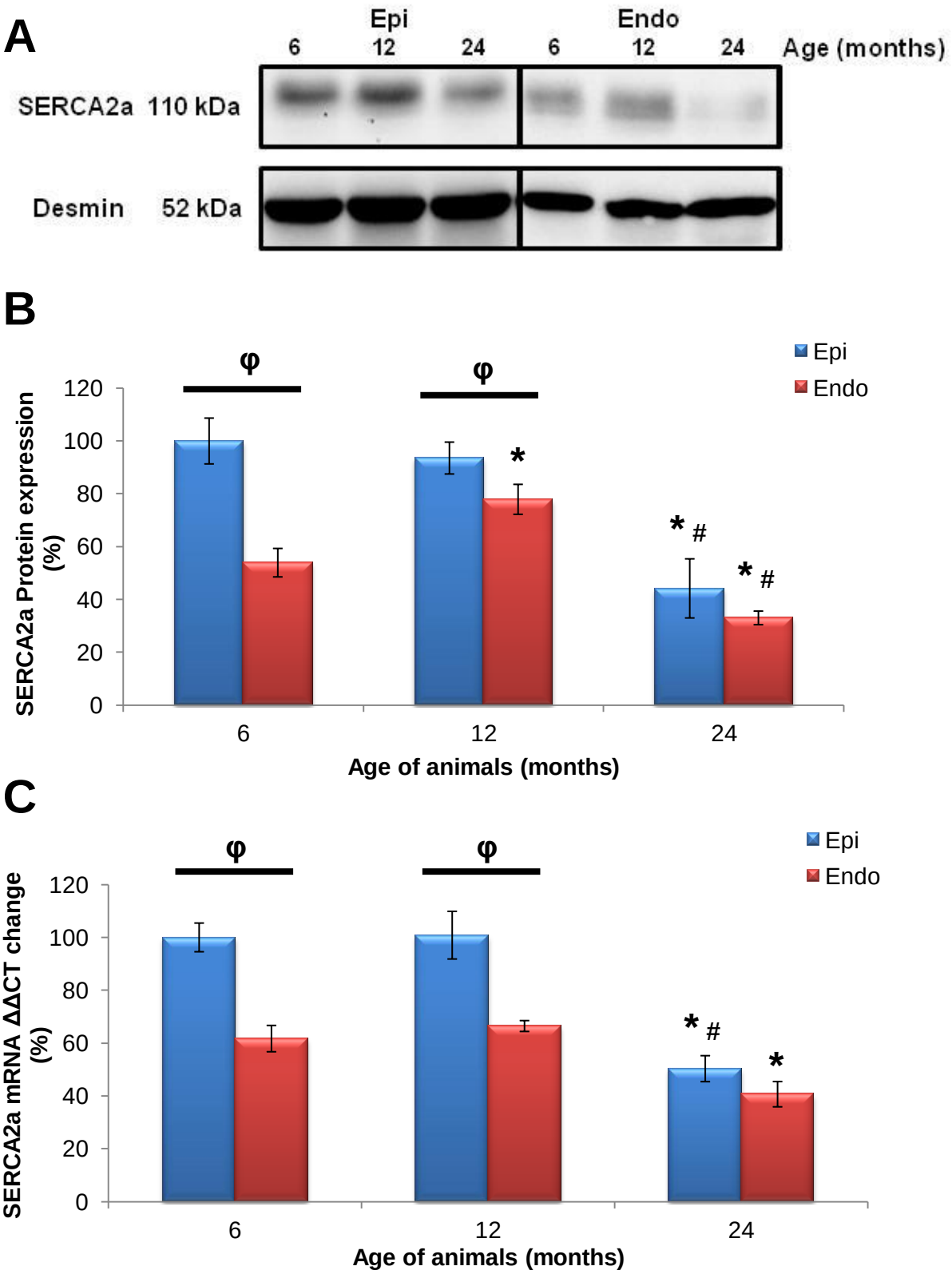

Figure 5.15 SERCA2a protein expression across the LV wall with increasing age

A) illustrative blot of SERCA2a protein and desmin; B) SERCA2a protein expression normalised to desmin; C) qPCR showing fold change of mRNA. * denotes $p<0.05$ vs. respective 6 months data, # denotes $p<0.05$ vs. respective 12 months data, φ $p<0.05$ within age group. n=5 per age group.

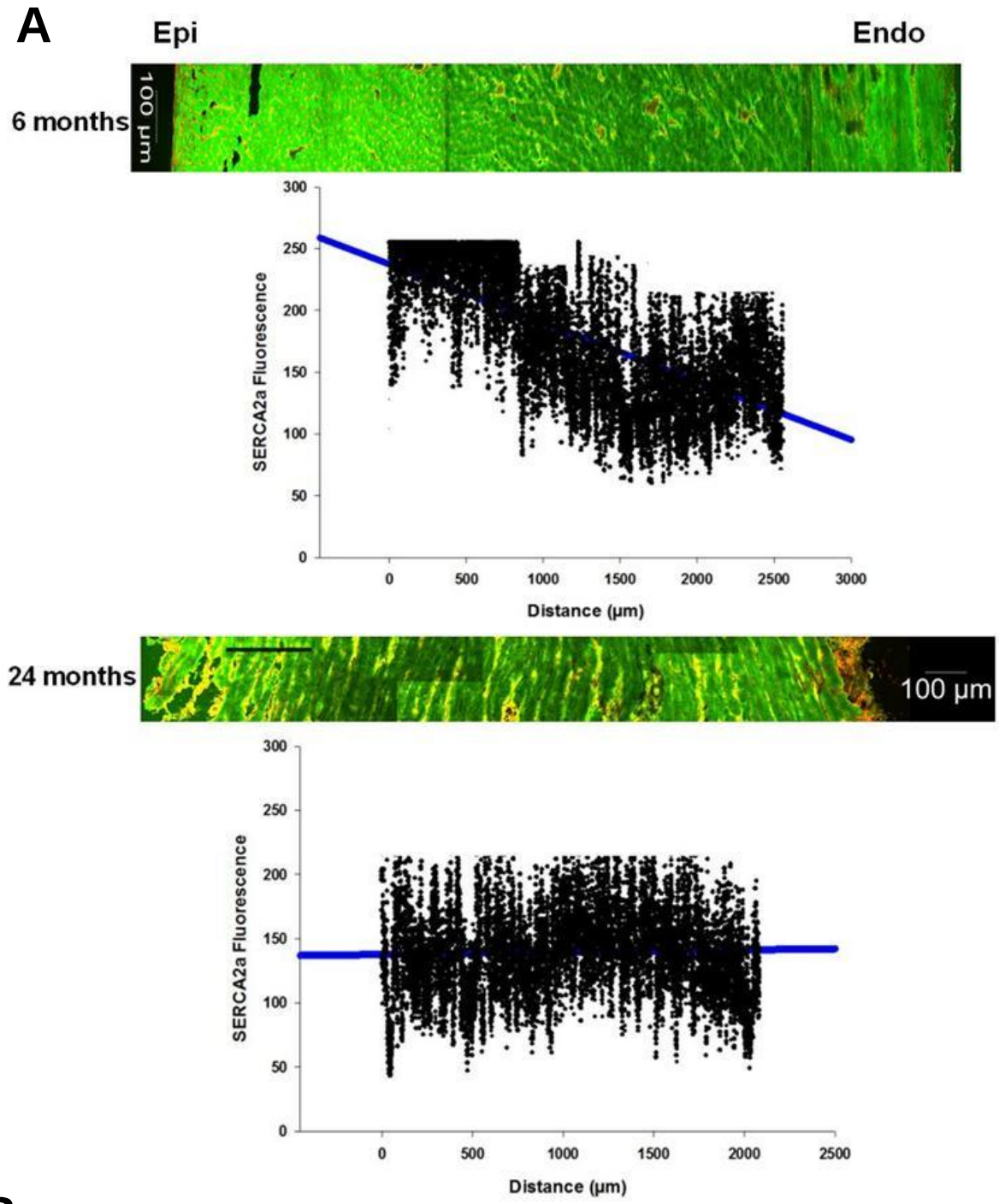

B

SERCA2a WGA

SERCA2a	6 months	24 months
Gradient	-0.0278±0.0057	-0.0070±0.0067*

Figure 5.16 Localisation of SERCA2a protein expression across the LV wall

A) illustrative images of the LV wall are shown from rat hearts at 6 and 24 months of age and transmural gradient graphs of SERCA2a density with plotted regression; B) table of gradients. Data are means ± S.E.M. Statistical analysis was conducted via one way ANOVA and comparison made using Holm-Sidak test. * denotes $p<0.05$ vs. 6 months data. n=5 per age group.

PLB total protein levels were equivalent across the LV wall at both 6 and 12 months (Figure 5.17). With age PLB total remained unchanged at 96±7.6% in the EPI; but within the ENDO, expression declined from 100±9.4% to 76±5.5% in the 6 and 24 months respectively. This reduction is due to decreased PLB monomer expression from 1.5±0.06 to 1.15±0.05 at 6 and 24 months of age respectively (Figure 5.17C). Due to this decline in the ENDO but not EPI, a divergence in the LV wall appears with age.

Transmural gradient indicates no change in PLB density in the LV wall at 6 months of age, with a slight positive correlation with gradient value of $3.5x10^{-3}$±0.0063 (Figure 5.18) which correlated with the protein data. In the 24 months there was a decline in PLB density within the EPI, but not in the ENDO; thus, a negative correlation was exhibited with a significantly decreased gradient.

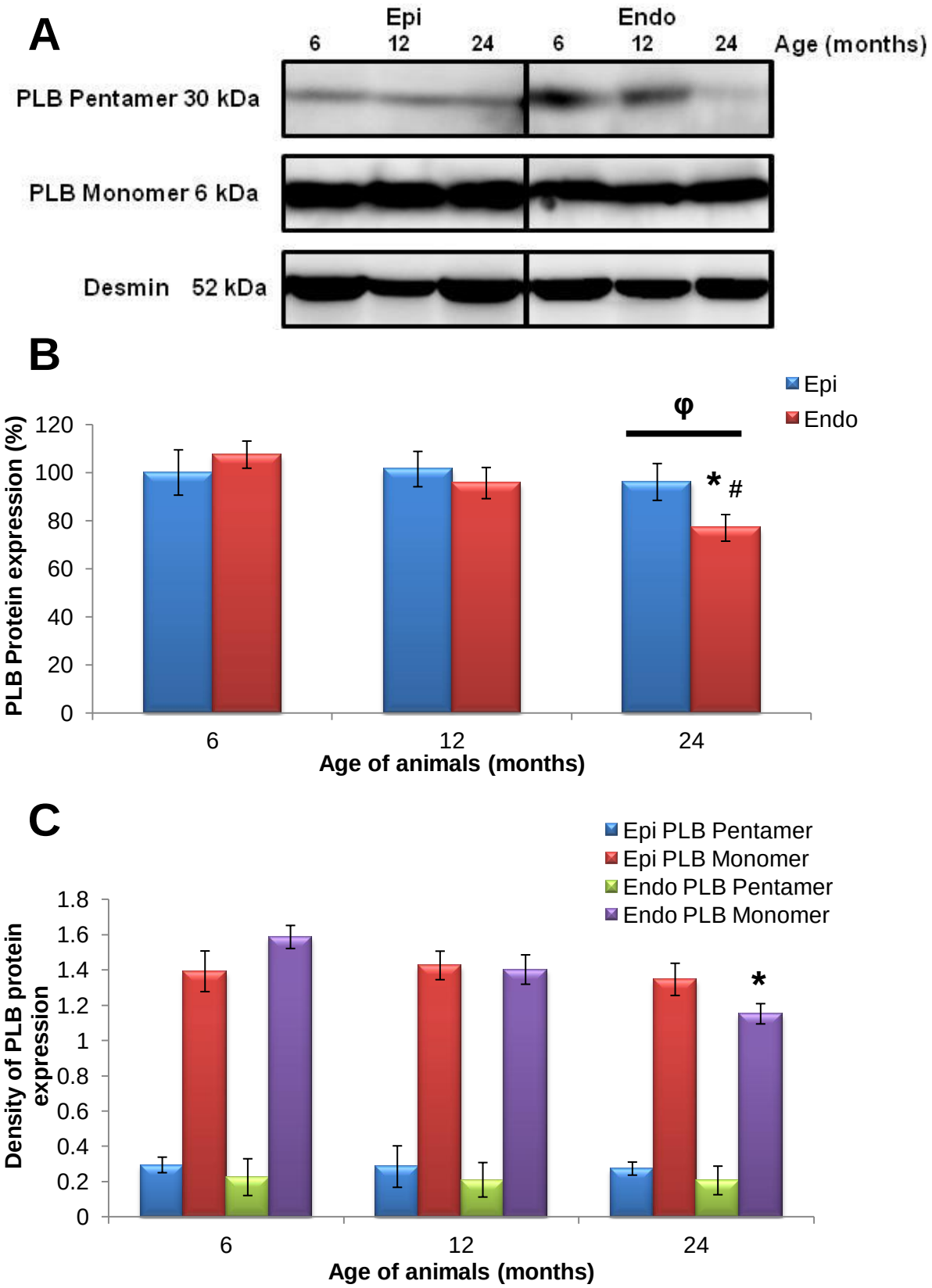

Figure 5.17 PLB protein expression across the LV wall with increasing age.

A) illustrative blots B) PLB total protein expression normalised to desmin C) PLB pentamer and monomer protein expression. * denotes p<0.05 vs. 6 months age group; # denotes p<0.05 vs. 12 months age group, φ p<0.05 vs. within age group. (n=5)

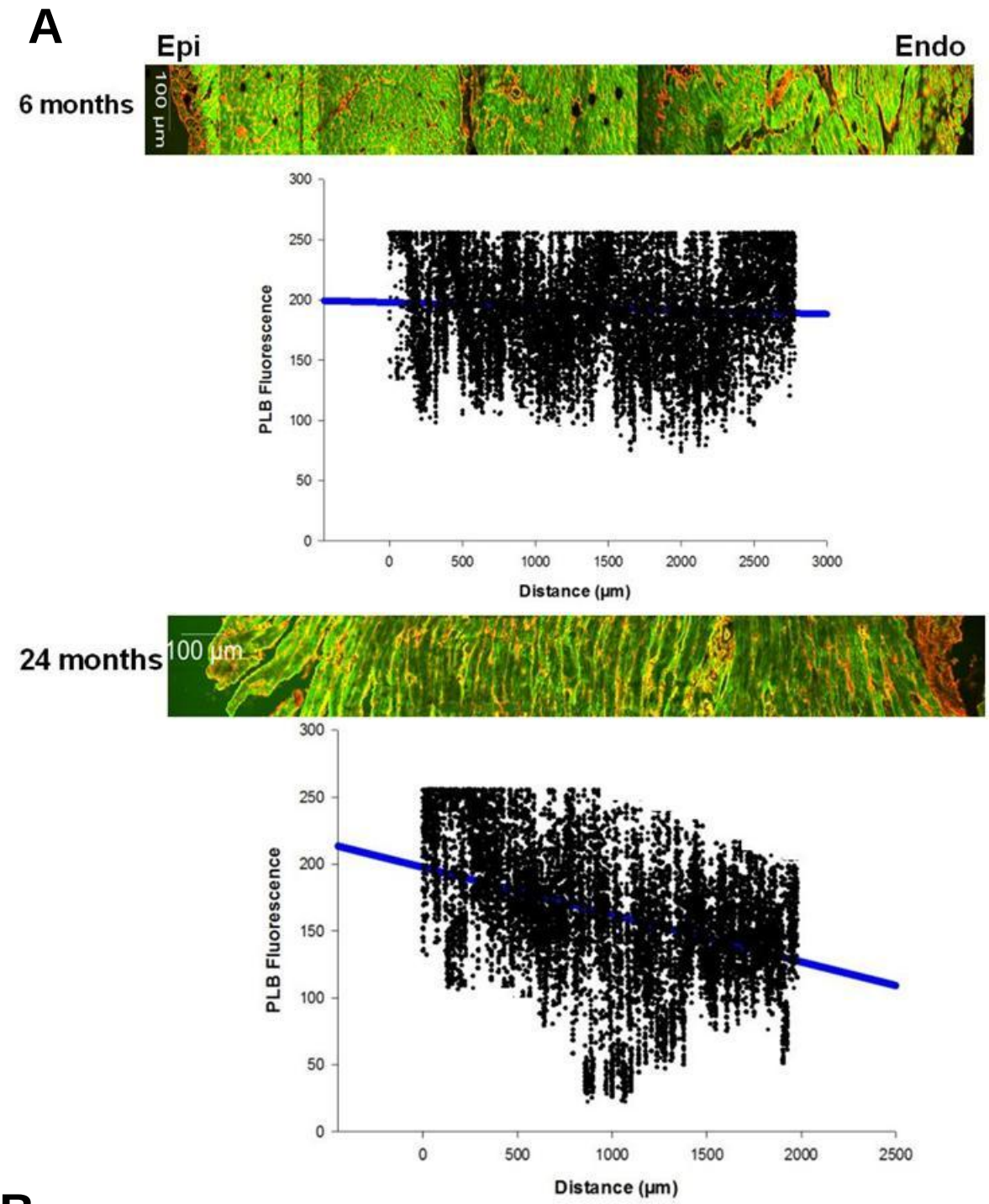

PLB	6 months	24 months
Gradient	$3.5x10^{-3}$±0.0063	$-2.1x10^{-2}$±0.0041*

Figure 5.18 Location of PLB protein expression across the LV wall

A) illustrative images of the LV wall are shown from rat hearts at 6 and 24 months of age and density of PLB label with plotted regression; B) table of gradients. Data are means ± SEM. Statistical analysis was conducted via one way ANOVA and comparison made using Holm-Sidak. * denotes $p<0.05$ vs. 6 months data. (n=5)

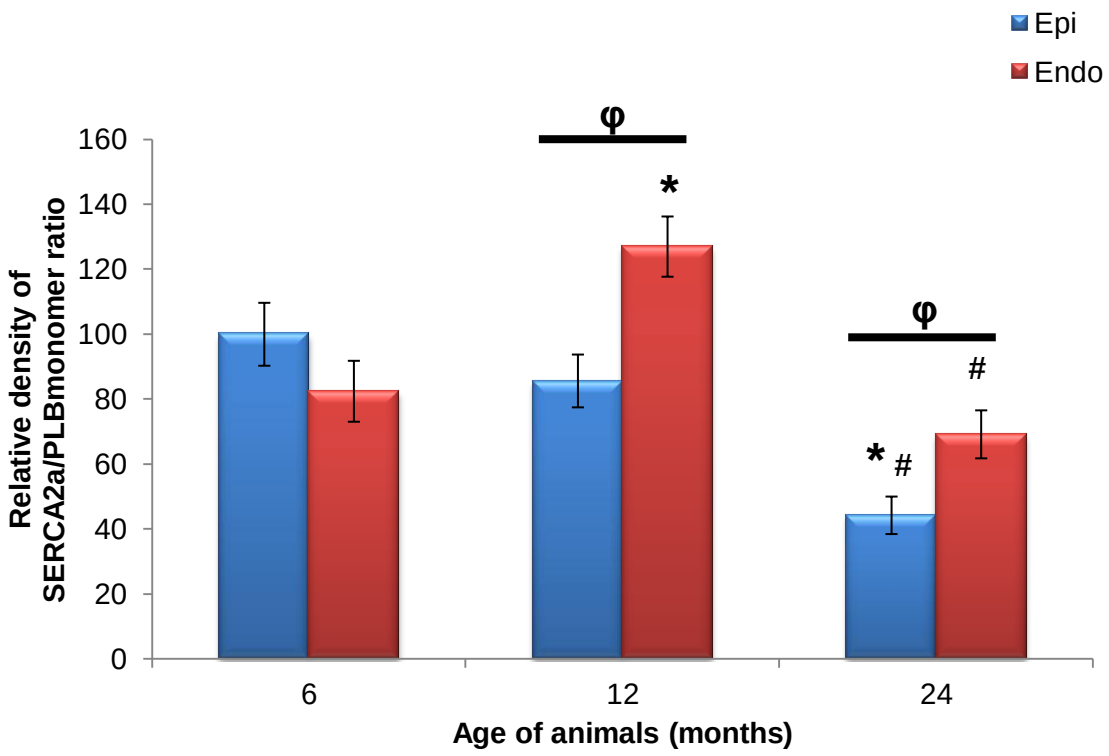

Figure 5.19 SERCA2a activity in the LV wall with advancing age.

SERCA2a protein expression normalised to PLB monomer expression indicates the functional capacity of the calcium pump SERCA2a. * denotes $p<0.05$ vs. respective 6 months age group, # denotes $p<0.05$ vs. respective 12 months age group, φ $p<0.05$ vs. within age group. n=5 per age group.

SERCA2a activity was compared across the LV wall and found to not differ between the ENDO (100±9.6%) and EPI (82±9.3%) at 6 months (Figure 5.19). However, by 12 months activity increased significantly to 127±9.2% in the EPI and declined to 85±8.1%in the ENDO, thus creating a divergence in SERCA2a activity across the myocardium. With advanced age activity in the ENDO decreased to 69±7.3% which was significantly lower than compared with 12 months but not 6 months. Comparatively EPI SERCA2a activity was dramatically reduced in the 24 months of age to 44±5.7%. Although both regions exhibited an age-associated decrease in SERCA2a activity, this was non-parallel with severely greater decreased activity observed in the EPI; hence an age-associated deviation in SERCA2a activity formed across the LV wall.

5.3.2.2 Analysis of ageing on the effect of CICR associated proteins across the LV

RYR2 protein was severely higher in the ENDO compared with the EPI across all age groups with up to 78±6.1% elevated levels at 6 months (Figure 5.20). More dramatic variation was observed in mRNA results which showed up to 4 times higher levels in the ENDO. This highlighted that extreme levels of mRNA were required for small changes in protein expression. Within the EPI there was no age-associated change in mRNA but RYR2 protein significantly decreased by 22±7.0% in the elderly age group.

Conversely in the ENDO, RYR2 protein decreased by 11±6.1% from 6 to 12 months of age. This change is underlined by a 60±3.1% decline in mRNA levels. At 24 months of age RYR2 protein expression was reduced significantly by 45±3.6% which correlated to a 93±1.9% decrease in mRNA compared to the 6 months age group (Figure 5.20C).

Figure 5.21 demonstrated the density of RYR2 with increased age; background noise from RYR2 label was greater than compared with other antibodies. At 6 and 12 months of age there was a clear positive correlation in increased RYR2 density and location within the ENDO, however the level of fluorescence and positive correlation was not as marked as the qualitative data obtained from western blotting and qPCR.

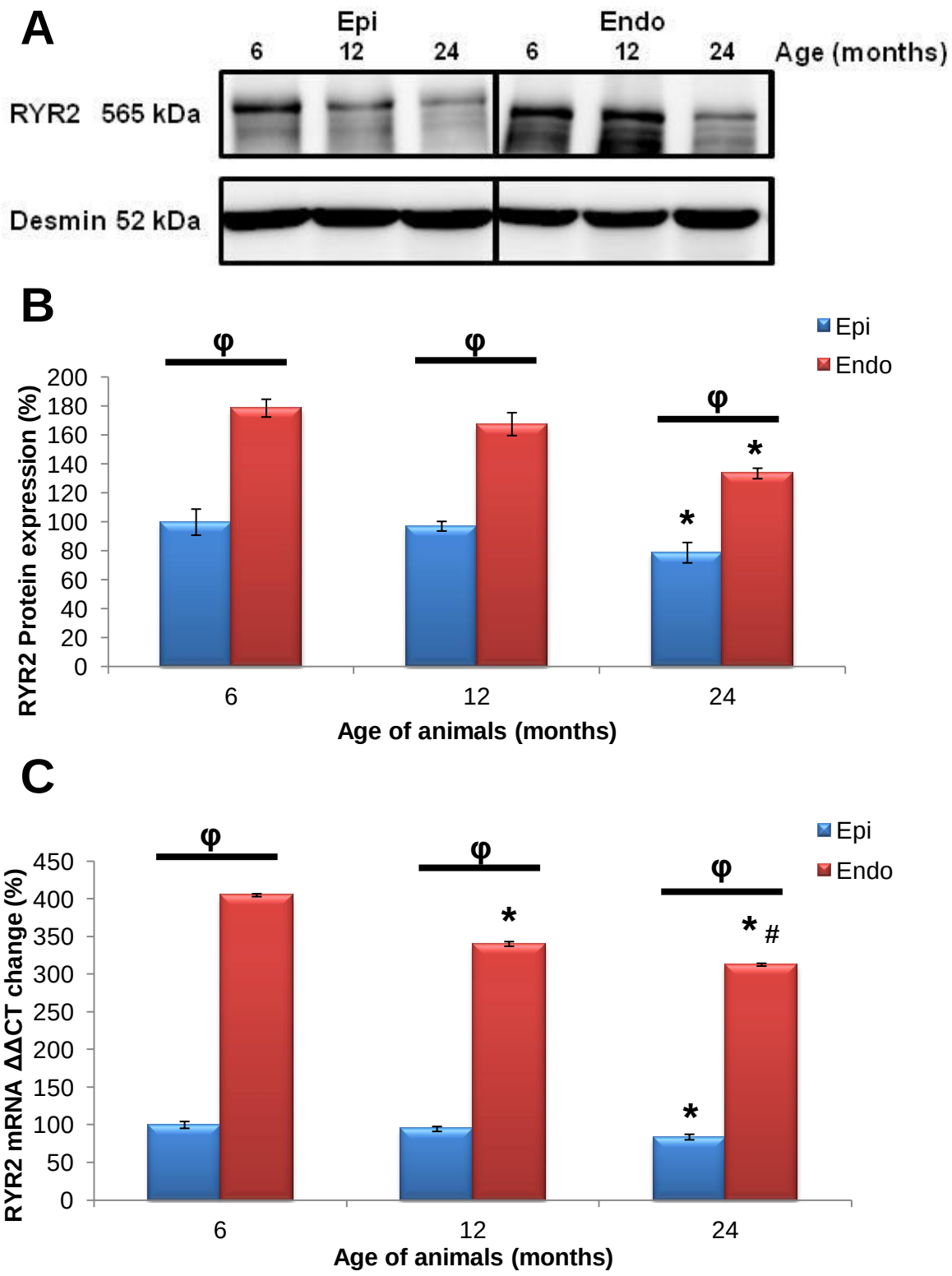

Figure 5.20 RYR2 protein expression across the LV wall with increasing age

A) illustrative blot of RYR2 protein and desmin; B) RYR2 protein expression normalised to desmin; C) qPCR showing fold change of mRNA. * denotes $p<0.05$ vs. respective 6 months data, # denotes $p<0.05$ vs. respective 12 months data, φ $p<0.05$ within age group. n=5 per age group.

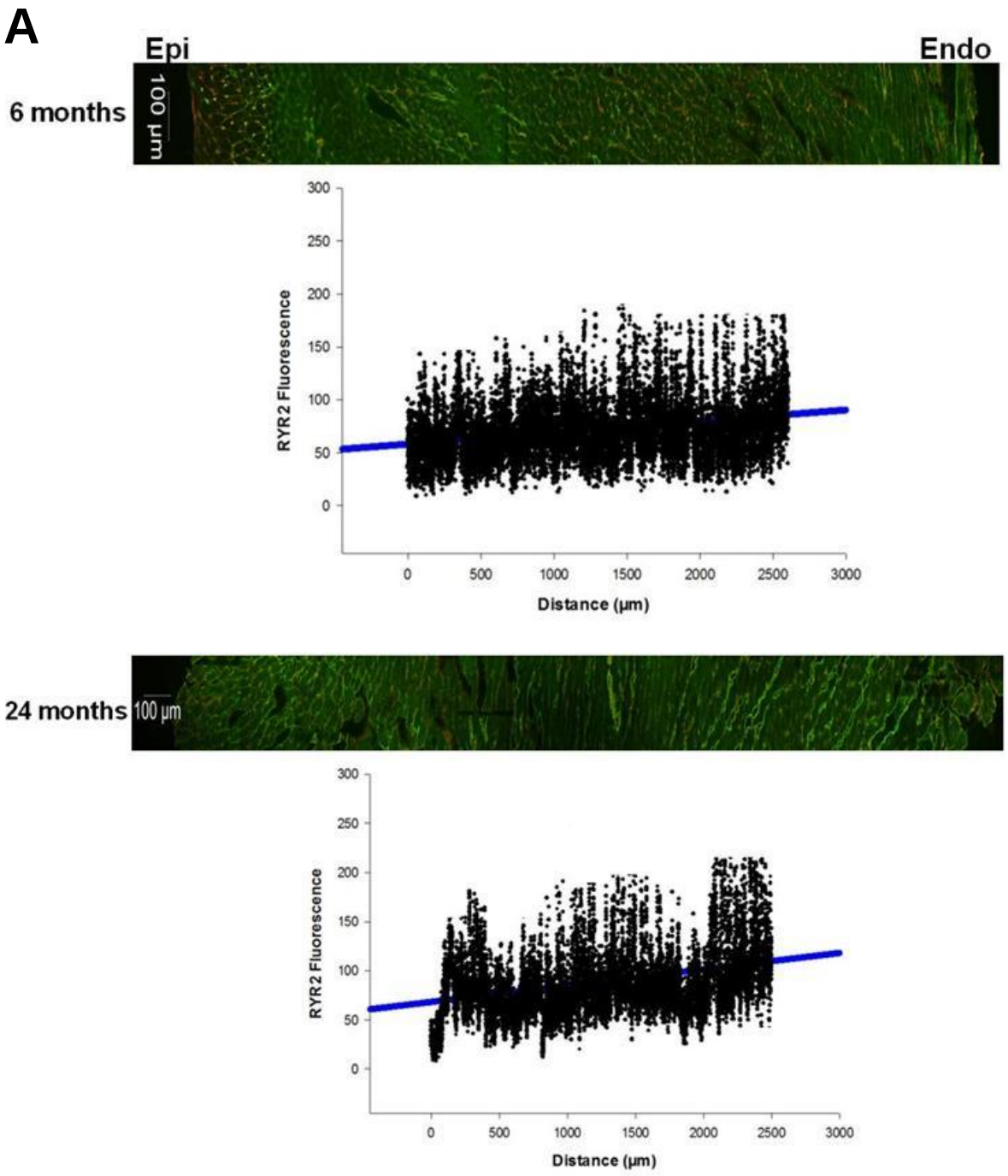

B

RYR2 WGA

RYR2	6 months	24 months
Gradient	0.0183±0.0058	0.0162±0.0017

Figure 5.21 Location of RYR2 protein expression across the LV wall

A) illustrative images of the LV wall are shown from rat hearts at 6 and 24 months of age and density of RYR2 label with plotted regression; B) table of gradients. Data are means ± SEM. Statistical analysis was conducted via one way ANOVA and comparison made using Holm-Sidak. n=5 per age group.

$Ca_v1.2$ channels was significantly higher in the ENDO (126±5.6%) compared with the EPI (100±8.3%) at 6 months of age (Figure 5.21). This correlated with mRNA expression which in the ENDO was 12±3.2% higher. At 12 months $Ca_v1.2$ protein expression decreased by 15±2.3% within the ENDO, which removed the divergence across the LV wall.

As documented, $Ca_v1.2$ protein increased significantly in the LV with age. This rise was due to the EPI which had increased expression by 31±5.1% while the ENDO remained unchanged across the ages. This increase in protein was duplicated in the mRNA data which showed a 28±6.4% rise (Figure 5.21).

There was a positive correlation in density of $Ca_v1.2$ from EPI to ENDO within the 6 months age group. With age localisation of $Ca_v1.2$ at the EPI was significantly increased, balancing the expression across the LV myocardial wall and reduced the gradient to $1.6x10^{-4}$±0.006. Consequently the divergence between the EPI and ENDO was removed with age.

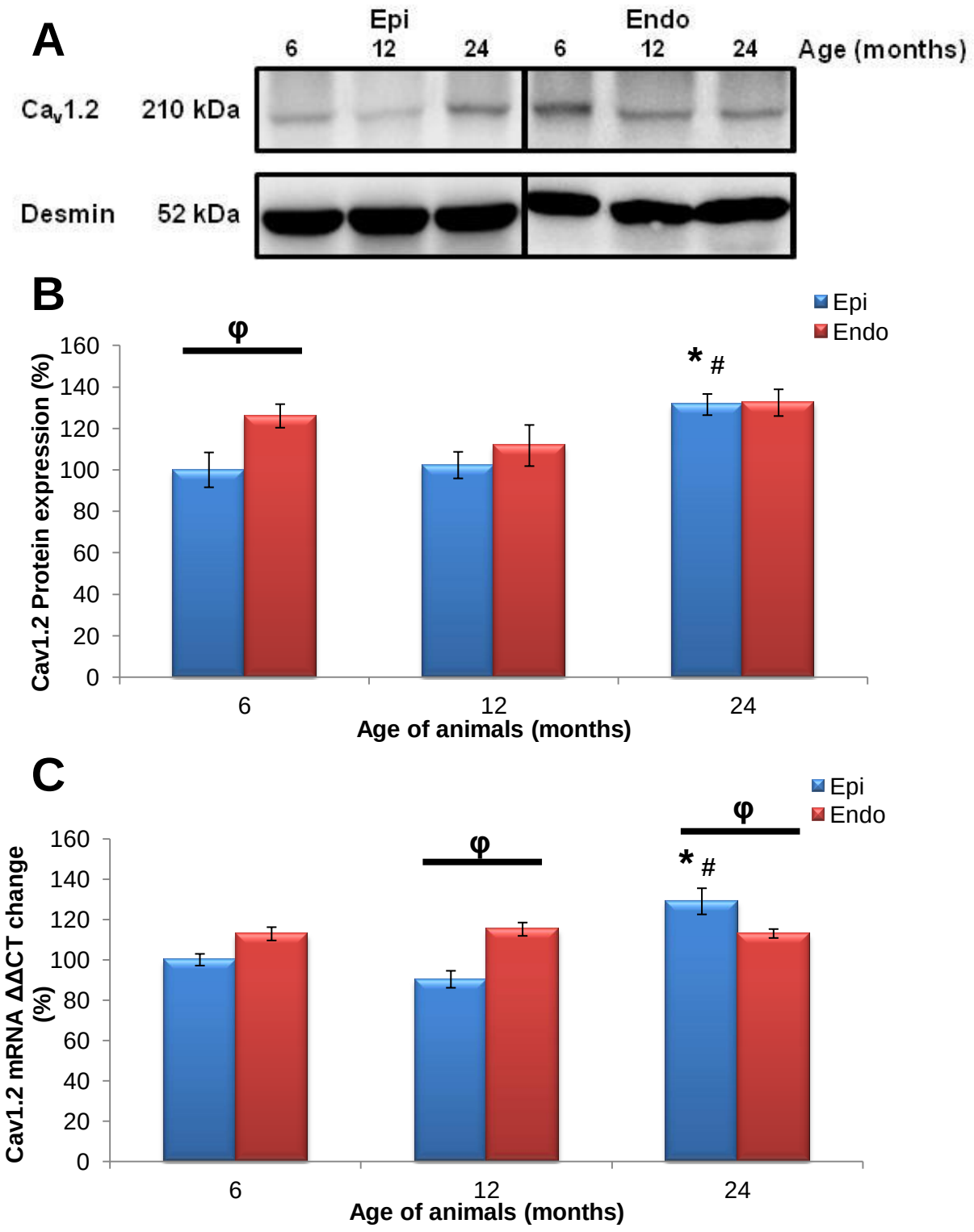

Figure 5.22 $Ca_v1.2$ protein expression across the LV wall with increasing age

A) illustrative blot of $Ca_v1.2$ protein and desmin; B) $Ca_v1.2$ protein expression normalised to desmin; C) qPCR showing fold change of mRNA. * denotes $p<0.05$ vs. respective 6 months data, # denotes $p<0.05$ vs. respective 12 months data, φ $p<0.05$ within age group. n=5 per age group.

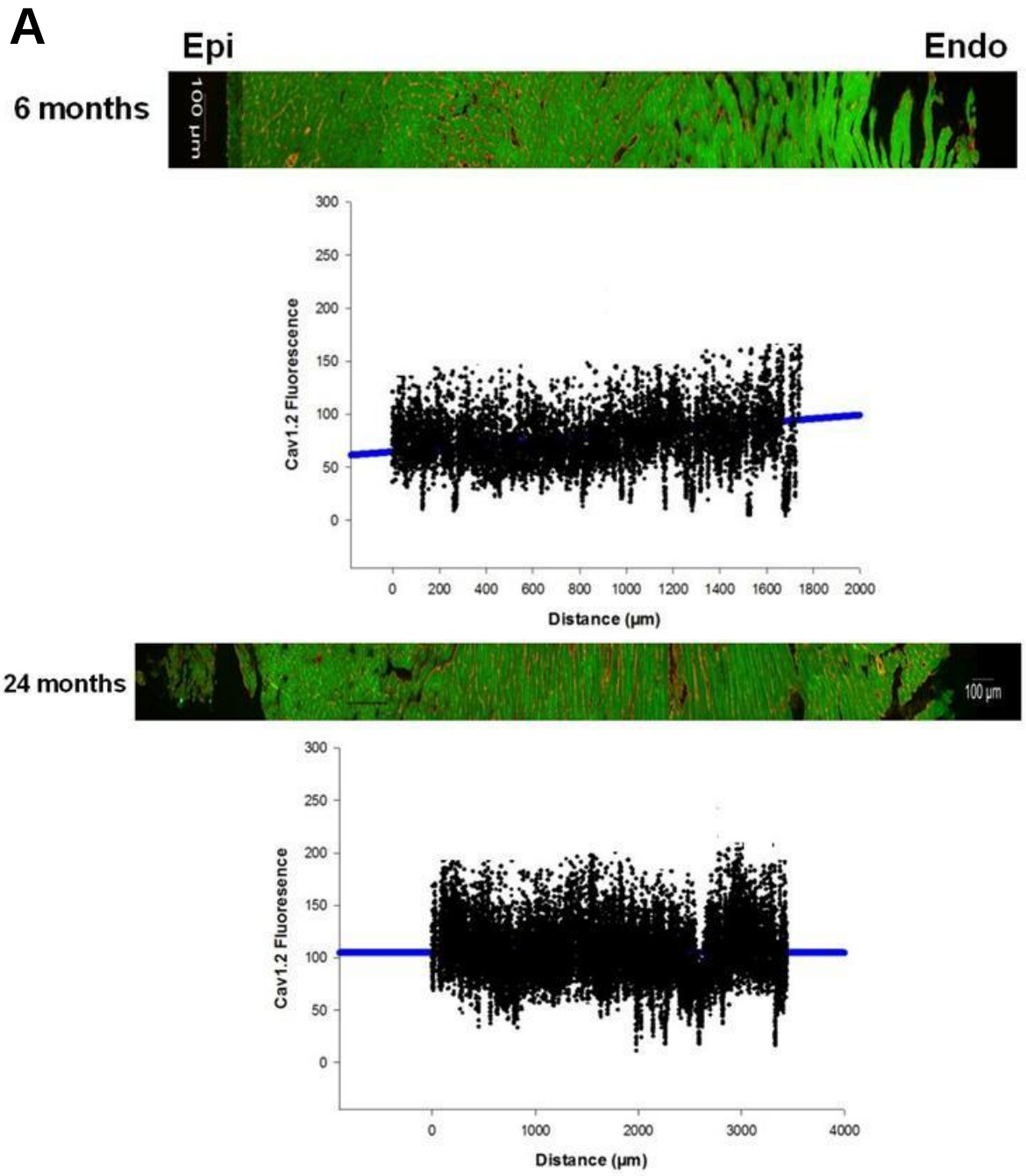

B

$Ca_V1.2$ WGA

$Ca_V1.2$	6 months	24 months
Gradient	0.00508±0.0019	-0.0001±0.0006

Figure 5.23 Location of $Ca_V1.2$ protein expression across the LV wall

A) illustrative images of the LV wall are shown from rat hearts at 6 and 24 months of age and density of $Ca_V1.2$ label with plotted regression; B) table of gradients. Data are means ± SEM. Statistical analysis was conducted via one way ANOVA and comparison made using Holm-Sidak. * denotes $p<0.05$ vs. 6 months data. (n=5)

5.3.2.3 Investigation into the effect of ageing on NCX1 and PMCA4a across the LV myocardium

NCX1 protein and mRNA expression were considerably higher in the ENDO at both 6 and 12 months of age (Figure 5.24). Over increasing age the ENDO exhibited increased protein expression by 19±3.4% from 6 to 24 months age groups. This was surprisingly similar to mRNA which increased by 13±6.3% at 24 months of age. Nevertheless the increased protein expression in the ENDO was not significant and would not account for the large rise observed in the whole LV. Instead elevated NCX1 protein expression at 24 months was due to the EPI which remained unchanged from 6 to 12 months of age, but with advanced age increased by 40±6.3%. In correlation to the protein data, qPCR showed a 33±7.4% rise in NCX1 mRNA at 24 months of age in the EPI compared to the 6 months age group (Figure 5.24).

Transmural gradient showed overall localisation across the LV myocardium with higher densities in the ENDO at 6 months of age, which resulted in a positive correlation (Figure 5.25). Conversely at 24 months localisation of NCX1 protein was concentrated at the EPI which produced a negative correlation across the myocardium into the ENDO. Therefore ageing caused a divergence in visualised NCX1 protein, but this was not mimicked by the western blotting data.

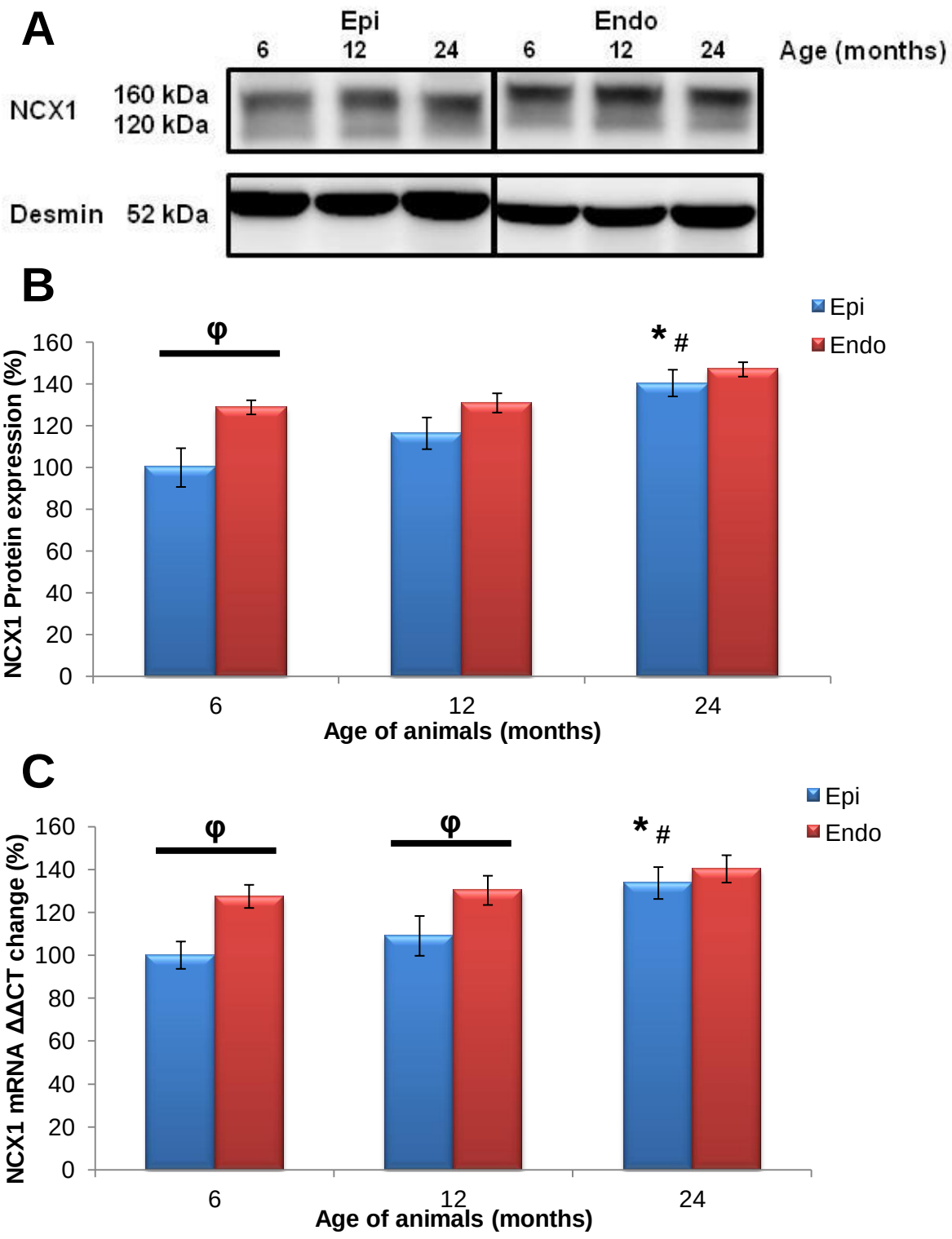

Figure 5.24 NCX1 protein expression across the LV wall with increasing age

A) illustrative blot of NCX1 protein and desmin; B) NCX1 protein expression normalised to desmin; C) qPCR showing fold change of mRNA. * denotes $p<0.05$ vs. respective 6 months data, # denotes $p<0.05$ vs. respective 12 months data, φ $p<0.05$ within age group. n=5 per age group.

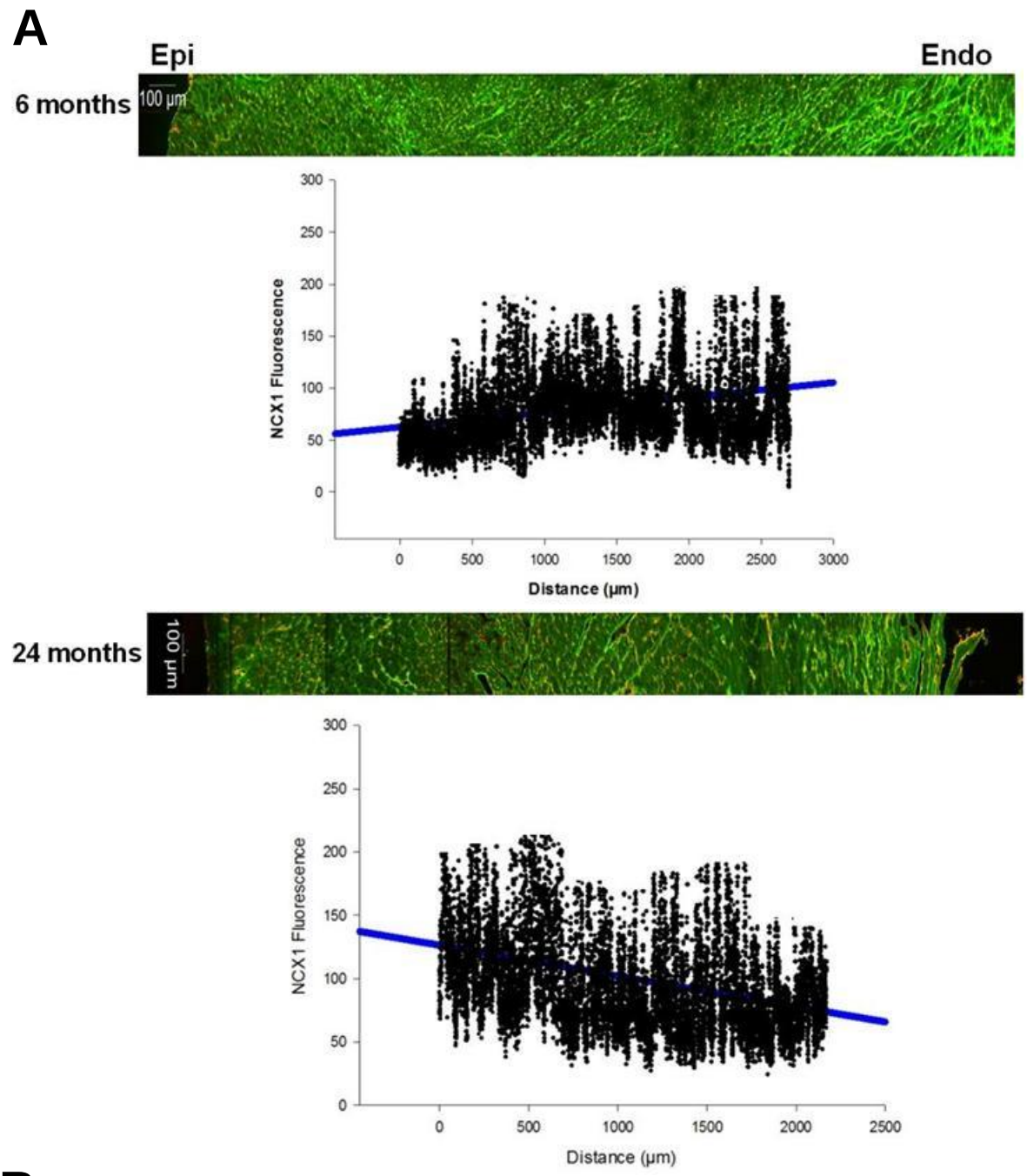

NCX1	6 months	24 months
Gradient	0.0146±0.0009	-0.01422±0.0095*

Figure 5.25 Location of NCX1 protein expression across the LV wall

A) illustrative images of the LV wall are shown from rat hearts at 6 and 24 months of age and density of NCX1 label with plotted regression; B) table of gradients. Data are means ± SEM. Statistical analysis was conducted via one way ANOVA and comparison made using Holm-Sidak. * denotes $p<0.05$ vs. 6 months data. (n=5)

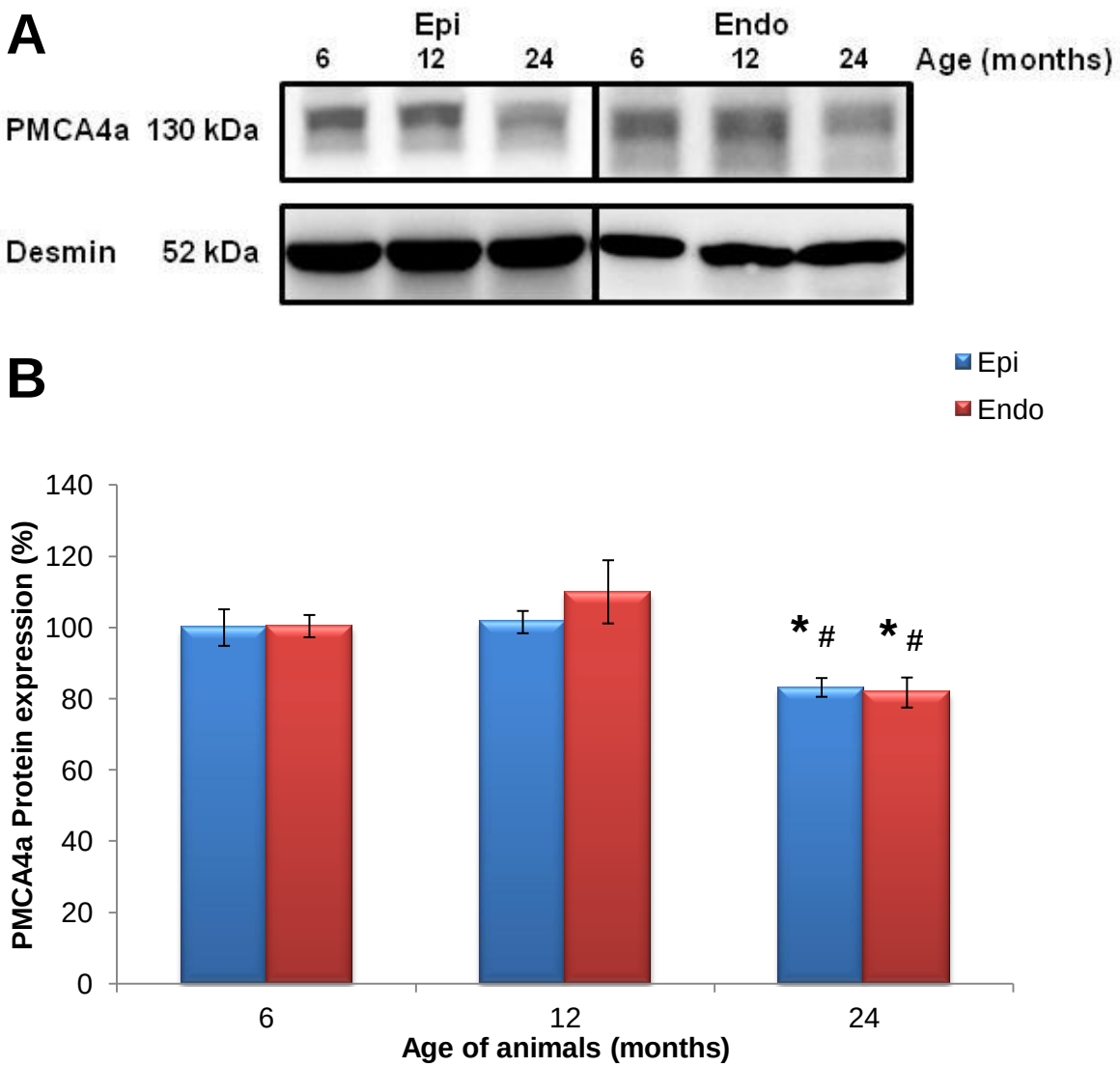

Figure 5.26 PMCA4a protein expression across the LV wall with increasing age

A) illustrative blot of PMCA4a protein and desmin; B) PMCA4a protein expression normalised to desmin. * denotes $p<0.05$ vs. respective 6 months data, # denotes $p<0.05$ vs. respective 12 months data. n=5 per age group.

There was no overall differences in PMCA4a protein levels between the ENDO and EPI indicating universal expression across the LV myocardium. With age PMCA4a protein decreased significantly in the ENDO and EPI from 100±5.1% and 100±3.1% at 6 months of age to 83±2.6% and 81±4.2% at 24 months of age respectively. This was consistent with the transmural scan data which at 6 months exhibited equivalent PMCA4a density across the LV wall. However, at 24 months the transmural gradient decreased to $1.4x10^{-2}$±0.0095 which was a small but significantly negative correlation in density across the LV wall section.

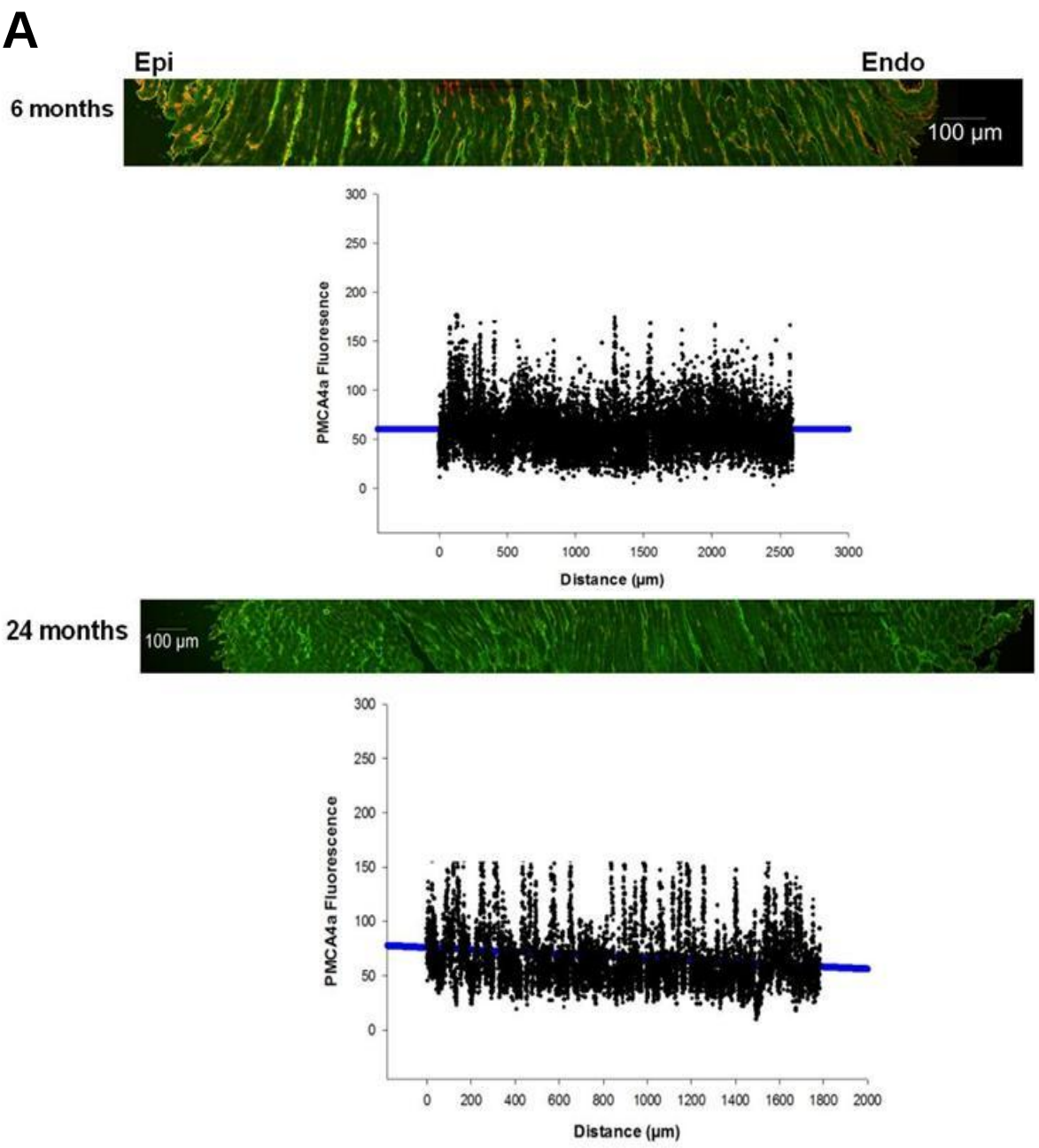

B

PMCA4a WGA

PMCA4a	6 months	24 months
Gradient	0.0051±0.0023	-0.0083±0.0059*

Figure 5.27 Location of PMCA4a protein expression across the LV wall

A) illustrative images of the LV wall are shown from rat hearts at 6 and 24 months of age and density of PMCA4a label with plotted regression; C) table of gradients. Data are means ± SEM. Statistical analysis was conducted via one way ANOVA and comparison made using Holm-Sidak. * denotes $p<0.05$ vs. 6 months data. n=5 per age group.

5.4 Discussion

5.4.1 Summary of Chapter 5

This study investigated age-associated and regional differences across the ventricles. There was significant diversity in expression of Ca^{2+} handling proteins in LV and RV (Table 5.1). The most significant findings included up regulation of PLB which resulted in reduced SERCA2a activity within the RV and upregulation of $Ca_v1.2$ channels in the LV.

To investigate variations across the LV myocardium, protein and mRNA expression of the EPI and ENDO were studied (Table 5.2). Main findings included: upregulation of $Ca_v1.2$ and NCX1 proteins and mRNA in the EPI muscle at 24 months old but not in the ENDO, significantly elevated levels of RYR2 proteins and mRNA in the ENDO compared with the EPI and clear differences in SERCA2a activity and its contributing proteins across the ventricular myocardium.

Table 5.1 Profile of expression of Ca^{2+} handling proteins and mRNA across the left and right ventricle and the impact of age.

Parameter		LV			RV		
		6m	12m	24m	6	12m	24m
SERACA2a	M	×	×	↓↓	↓	↓	↓
	P	×	×	↓↓	↓	×	×
PLB total		×	×	↓↓	↓	×	↑↑
SERCA2a activity		×	×	↓↓	×	↑↑	↓↓
RYR2	M	×	×	↓↓	↑	×	↓↓
	P	×	×	↓↓		×	↓↓
$Ca_v1.2$	M	×	×	↑↑	×	×	×
	P	×	×	↑↑	×	×	×
NCX1	M	×	×	↑↑	↓	↑↑	↑↑
	P	×	×	↑↑	×	↑↑↑	↑↑
PMCA4a		×	×	↓↓	×	↓	↓↓

Protein expression (P), mRNA levels (M) and SERCA2a activity are summarised for the LV and RV including over 6, 12 and 24 months age groups. Significant differences ($p<0.05$) were obtained from western blot and qPCR data; X denotes no significant difference, ↑ in red denotes higher levels within age group, ↓ in red denotes lower levels within age group, ↑↑ significant increase across the age groups, ↓↓ significant decrease across the age groups.

Table 5.2 Profile of expression of Ca^{2+} handling proteins and mRNA across the LV myocardial wall and the impact of age.

Parameter		EPI			ENDO		
		6m	12m	24m	6m	12m	24m
SERACA2a	M	×	×	↓↓	↓	↓	↓↓
	P	×	×	↓↓	↓	↓	↓↓
PLB total		×	×	×	×	×	↓↓↓
SERCA2a activity		×	×	↓↓	×	↑↑↑	↓↓↓
RYR2	M	×	×	↓	↑	↑↓↓	↑↓↓
	P	×	×	↓↓	↑	↑	↑↓↓
$Ca_v1.2$	M	×	×	↑↑	×	↑	↓
	P	×	×	↑↑	↑	×	×
NCX1	M	×	×	↑↑	↑	↑	×
	P	×	×	↑↑	×	×	×
PMCA4a		×	×	↓↓	×	×	↓↓

Protein expression (P), mRNA levels (M) and SERCA2a activity are summarised for the epicardium (EPI) and endocardium (ENDO) over 6, 12 and 24 months age groups. Significant differences ($p<0.05$) were obtained from western blot and qPCR data; X denotes no significant difference, ↑ in red denotes higher levels within age group, ↓ in red denotes lower levels within age group, ↑↑ significant increase across the age groups, ↓↓ significant decrease across the age groups.

5.4.2 Implications of ageing on calcium regulation within the LV

5.4.2.1 Effect of age on SERCA2a activity in the left ventricle

During ageing the rate of Ca^{2+} uptake was shown to decline by up to 30% (Taffet and Tate, 1993) which is similar to the 26% decrease noted in this chapter. The affinity for either Ca^{2+} or ATP of the SERCA2a pump is unaltered with age (Taffet and Tate, 1993), but protein levels are debatable with some noting a decrease in elderly hearts (Lompre et al., 1991a) or unchanged levels (Kaplan et al., 2007). This chapter showed a decline in SERCA2a protein by approximately 45% in the elderly heart whilst PLB protein expression declined by 28%; the divergence in down-regulation of these proteins resulted in a calculated ratio reduction of 26% in SERCA2a pump activity within the LV. Therefore with slower SR Ca^{2+} uptake delayed relaxation would occur in the elderly heart compared with the young-adult or adult heart. This can be further proven by studies investigating exercise-trained elderly rats which showed accelerated Ca^{2+} transient decay (Gwathmey et al., 1990) that was coupled with up-regulation of SERCA2a mRNA and protein levels as compared with non-trained elderly rats (Tate et al., 1996). Subsequently, age-related prolongation of the Ca^{2+} transient within the LV is partially a result of diminished SR Ca^{2+} pump function.

Debatable reports on age-associated changes in PLB protein expression have been noted with there being both no difference in rats (Xu and Narayanan, 1998) and an increase in mice (Lim et al., 1999). In this chapter a 28% decrease in PLB protein expression was observed which is contrary to both studies, however, in the study by Xu and Narayanan in 1998, ventricular myocardium was studied but did not specify whether this was left or right ventricle or a combination of both. If the latter was the case then this would correspond with this chapter's findings which reported a 19% increase within the RV offsetting any decrease when both ventricles were combined. Regardless of PLB protein expression, a consistent finding across all studies is a decrease in the rate of phosphorylation by PKA coupled with CaMKII (Jiang et al., 1993, Xu and Narayanan, 1998, Lim et al., 1999). As discussed in section 3.3 the age-associated diminished β-adrenergic receptor mediated PLB phosphorylation may be primarily caused by decreased β-adrenergic receptor density (Roth et al., 1998). In summation whether protein or phosphorylation was decreased in the senescent LV, both of these factors provided further evidence into why SERCA2a activity was reduced in the elderly heart.

5.4.2.2 SERCA2a activity across the left ventricular wall and its response to ageing

Heterogeneity in SERCA2a protein across the LV wall (Prestle et al., 1999) and SR Ca^{2+} pump activity within the whole LV has been previously documented (Xu and Narayanan, 1998), but an investigation into SERCA2a activity across the EPI and ENDO of the LV remains a novel approach. In the 6 months of age animals SERCA2a activity was 18% higher in the EPI which correlates to a previous study using a cat model, which reported variations in the prolongation of the AP in the ENDO (Furukawa et al., 1990) and is consistent with reduced activity of the SR Ca^{2+} pump. In the 24 months old animals the EPI exhibited a 56% decline in SERCA2a activity and a 30% decrease in the ENDO, creating an age-associated divergence across the LV wall. However, at 24 months the ENDO had 24% higher levels of SERCA2a activity than the EPI; consequently, although overall SERCA2a protein expression was reduced in the elderly LV, PLB monomer also declined in the ENDO. This resulted in lower but not dramatically hindered pump activity. The diminished levels of PLB would result in moderate regulation of SERCA2a Ca^{2+} affinity due to reduced levels of PKA-dependent phosphorylation being required to remove PLB from SERCA, thus SR Ca^{2+} pump function is relatively unhindered (Vangheluwe et al., 2006).

Furthermore this also explained the boosted activity in the 12 months ENDO which increased by 45% due to a 24% rise in SERCA2a protein expression, but no overall change in PLB protein levels. This divergence in the LV wall was not apparent when investigating the whole LV as there was a 15% decline in activity in the EPI. Therefore the averaged activity across the LV wall remained unchanged compared to the 6 months. Overall there are clear difference in the dynamicity of the LV wall in response to Ca^{2+} handling with age, the diminished SERCA2a activity in the EPI but not the ENDO is reverse to what was reported in the 6 months age group and to a previous study using AP duration (Furukawa et al., 1990). In addition the increased SERCA2a protein expression, which was reported in the 12 months age group, has been associated with acute arrhythmias and sudden death in rats (Chen et al., 2004b). Therefore this divergence in activity and protein levels within the adult LV could be a predisposition for Ca^{2+} remodelling and developing dysfunction in the elderly LV. In summation this correlates to a review of findings that variations in Ca^{2+} handling proteins across the myocardium were associated with increased risk of ventricular arrhythmias (Antzelevitch et al., 1991, Furukawa et al., 1990).

In addition the increased risk of ventricular arrhythmias can be further explained by the rise in probability of Ca^{2+} alternans episodes, as SERCA2a activity would have a direct

affect on SR Ca^{2+} load and concentration of Ca^{2+} in the cytosol (Diaz et al., 2004). Therefore in the 12 months age group the increased SERCA2a activity in the ENDO would result in augmented SR Ca^{2+} load, thus higher probability of Ca^{2+} alternans, which are associated with electrical instability (Smith et al., 1988a). However, a decrease in SR Ca^{2+} pump activity, as in the EPI, may be an adaptive mechanism to reduce SR Ca^{2+} release flux during increased demand; thus attempting to preserve optimal Ca^{2+} loading in the elderly heart and the probability of Ca^{2+} alternans (Janczewski et al., 2002).

5.4.2.3 Effect of ageing on EC coupling with focus on proteins involved in CICR

The Ca^{2+} sparks mechanism associated with the RYR2 was shown to be a key cause of Ca^{2+} alternans even with unchanging SR Ca^{2+} content (Rovetti et al., 2010). Consequently the extremely high levels of RYR2 protein and mRNA within the ENDO could explain the greater susceptibility of the ENDO to arrhythmias (Laurita and Rosenbaum, 2008). This would further reflect the increased frequency of Ca^{2+} sparks, but not duration in ventricular myocytes (Howlett et al., 2006) if they were obtained from the LV ENDO .

In contrast Adb Allah *et al.* found that RYR2 protein and mRNA was higher in the EPI in an adult heart (Abd Allah et al., 2012), however, tissue acquiring methods and quantitative techniques were comparatively different. In their study a whole section of the LV was frozen, slices taken through the myocardium after discarding the upper sections and separated into the apparent regions after a certain distance was achieved. In this chapter the EPI and ENDO was removed from fresh, unfrozen LV by a shearing technique. Although both methods have chances of contamination, the former method discards the first sections which would remove key EPI and ENDO tissue. Furthermore the width of a LV wall and its subsections would vary across each animal heart and consequently slices taken of a certain distance would not be equal and thus cause increased contamination.

In this chapter the 24 months age group exhibited decreased RYR2 protein and mRNA expression in both the EPI and ENDO, but the latter remained at severely higher levels. This data correlated with other studies that showed age-associated reduced RYR2 levels (Assayag et al., 1998, Nicholl and Howlett, 2006). As a consequence reduced RYR2 protein and activity via CaM kinase (Xu and Narayanan, 1998) would hinder the release of Ca^{2+} from the SR. Controversially reduced RYR2 protein may be a

compensatory mechanism to counter age-associated increased Ca^{2+} spark frequency (Howlett et al., 2006) and to try and prevent complete diminishment of SR Ca^{2+} content.

With reduced SERCA2a activity, SR Ca^{2+} load would be diminished and would result in reduced force of contraction in the elderly heart as previously documented (Lim et al., 2000). Perhaps to compensate for loss of contractility, increased SR Ca^{2+} load could be bolstered via CICR gain; $Ca_v1.2$ protein increased by 37% in the elderly heart, alongside slow inactivation kinetics so more Ca^{2+} can enter through the channels (Josephson et al., 2002), SR Ca^{2+} content would be increased and be responsible for prolonged contraction. Unfortunately the divergent decrease in RYR2 protein may result in dysfunctional EC coupling and so CICR gain would not be able to compensate for lower SR Ca^{2+} pump rate. In old rat hearts ventricular myocytes stimulated at a frequency akin to young hearts was noted to have reduced CICR gain through a combination of diminished SR Ca^{2+} content and increase demand (Janczewski et al., 2002).

5.4.2.4 Heterogeneity in calcium handling proteins across the left ventricular myocardium

In the young adults NCX1 protein levels diverged across the LV wall, with 28% more exhibited in the ENDO, but this variation was removed in the adult heart which is similar to recent findings (Abd Allah et al., 2012). No significant difference in NCX1 protein or mRNA in the ENDO was observed, so the marked increase in the whole LV data originates from the 40% rise in the EPI; but in the elderly heart NCX1 protein and mRNA is equivalent across the ventricular myocardium. Therefore heterogeneity across the LV wall varies with age further indicating Ca^{2+} remodelling across the whole LV wall is dynamic and may be adaptive to other changes, similar to findings in the failing heart (Xu et al., 2012).

The combined increase of $Ca_v1.2$ channels and NCX1 within the EPI, but not the ENDO may be in response to the significantly lower levels of RYR2. NCX1 alongside Cav1.2 and RYR2 plays a vital role in EC coupling (Sher et al., 2008) and may contribute to SR Ca^{2+} content. Consequently to compensate for the exceedingly low RYR2 density, and thus reduced sites for CICR, Ca^{2+} influx from NCX1 would be increased and may act as the mechanism behind increased Ca^{2+} sparks. However, increased intracellular Ca^{2+} can also be deleterious due to the age-associated reduced tolerance, as Ca^{2+} overloaded hearts showed increased spontaneous Ca^{2+} oscillations associated in the genesis of arrhythmias (Hano et al., 1995).

5.4.3 Calcium handling protein expression across the left and right ventricles is affected by age and region

5.4.3.1 Variation in SERCA activity across the ventricles

Across the ventricles there was no difference in SERCA2a activity even with increasing age. In both the LV and RV there was a decline in SR Ca^{2+} pump rate. Within the RV there was no change in SERCA2a protein across the age groups, but in the elderly heart PLB protein increased by 19% with the majority being PLB monomer. Equivalent SERCA2a activity across the LV (endo) and RV has also been noted in the adult mouse model, though no study of an ageing model was conducted (Kondo et al., 2006). This further correlated to the heterogeneity in AP recordings in the mouse heart across the transmural membrane of both the LV and RV (Knollmann et al., 2001).

5.4.3.2 Variations in calcium handling proteins across the ventricles

The LV was observed to have consistently higher levels of calcium handling proteins in the young-adult heart, with 48% higher SERCA2a, 22% higher PLB, 17% higher RYR2 and 8% higher PMCA4a. The higher levels of all these proteins would contribute to the significantly greater maximal contraction in LV myocytes compared with the RV myocytes (Kondo et al., 2006). Furthermore there was a correlation between larger influx in total Ca^{2+} per AP waveform and increased maximal myocyte shortening (Bouchard et al., 1995); which will explain why, due to the age related decrease in SERCA2a, PLB, and RYR2, contractile force is diminished. Heterogeneity across the ventricles is still present in the elderly heart with higher levels of $Ca_v1.2$ protein and NCX1 density but significantly lower levels of PMCA4a in the LV compared with the RV. Unfortunately apart from the previously noted studies, heterogeneity across the ventricles based on molecular data is extremely limited.

5.4.4 Limitations

Calcium handling proteins and mRNA were investigated in the left and right ventricles; however, there were occasional discrepancies between mRNA and protein levels. Within the LV wall as a cross comparison between the EPI and ENDO, RYR2 mRNA was observed to be 4 times higher in the ENDO than the EPI. However, when studying

protein data there was a general trend of elevated levels in the ENDO but not to the extent expected; highlighting that extreme levels of mRNA were required to produce small changes in protein. Discrepancies have also occurred in previous studies that used mRNA as a quantification of age-associated protein changes in the SA node (Tellez et al., 2011) and also found variations in NCX1 protein data versus mRNA data in the LV myocardium (Abd Allah et al., 2012). Consequently the changes in protein levels may not be solely reflected by mRNA levels and could involve further mechanisms such as $Ca_v1.2$ channels which are autoregulated by the C terminus (Schroder et al., 2009).

In this chapter protein and mRNA levels were extensively studied but no investigations into functional properties of the ventricles were conducted. The increased density of a protein may not correlate to increased function and *vice versa*. With age $Ca_v1.2$ channel density was shown to increase but also rate of inactivation was slowed, highlighting that both the molecular and functional properties of the channels were altered with age (Josephson et al., 2002). Similarly, NCX1 protein expression increased in this chapter, whilst no study on activity was conducted, in a previous study NCX1 activity was noted to increase with age (Mace et al., 2003). Consequently this study is limited by unknown age-associated alterations to functional properties of Ca^{2+} handling proteins.

5.4.5 Conclusion

SERCA2a activity was significantly lower in the RV compared with the LV which accounted for reduced SR Ca^{2+} load explaining the lower Ca^{2+} transients and contractile function in the RV. Dynamicity across the ventricles changed with age, $Ca_v1.2$ and PLB divergence developed in the 24 months age group; both coupled with changes to CICR influx and SERCA2a activity, highlighting the combination of ageing and demand affected the extent of Ca^{2+} remodelling. The changes in the LV were further investigated across the myocardial wall and found RYR2, $Ca_v1.2$ and NCX1 PLB to be elevated in the young ENDO compared with the EPI. Heterogeneity varied with age; there was a divergence in SERCA2a activity and RYR2 but other protein variation across the myocardium was removed. This highlights the effect of age on differences across the LV myocardial wall and that the age-associated alterations may contribute to the generation of ventricular arrhythmias.

Chapter 6 Discussion

6.1 Overall summary of study

This study aimed to characterise age-associated changes to Ca^{2+} handling proteins using the rat model as a reference to human ageing. It was found that the ageing process caused significant Ca^{2+} remodelling across the whole heart. In addition the SA node was shown to undergo changes to Ca^{2+} handling protein expression and age-associated altered sensitivity to β-adrenergic stimulation and nifedipine. Age-related variation in protein expression across the RA which included the SA node, CT and RA muscle, implicated the CT as a site of arrhythmogenic activity. Age induced modified regulation of $[Ca^{2+}]_i$ in the atria, with severe divergence between the left and right atria. Investigation of the ventricles, across the lifespan, reported significant changes to proteins that impact CICR; in addition the heterogeneity across the LV myocardial wall varied from young to old.

Ageing caused decreased sensitivity to β-adrenergic stimulation in the SA node, primarily due to the reduction in SERCA2a activity. Conduction velocity from the LPS across the CT was observed to decrease with age, impacting AP propagation and the ability to increase intrinsic heart rate. RYR2 and $Ca_v1.2$ channel proteins, both involved in LCR, were observed to decrease in the elderly heart, thus reducing LCR frequency and amplitude. However, NCX1 protein expression was dramatically increased, which was implicated as a compensatory Ca^{2+} influx mechanism and a deleterious arrhythmogenic substrate. In addition sensitivity to nifedipine was increased in the 24 months age group, either due to the decreased $Ca_v1.2$ channel density or altered $Ca_v1.2$ channel properties; stressing the importance of tapered nifedipine dosage to elderly patients.

In other regions of the heart ageing induced decreased SERCA2a activity in the ventricles and RA, but increased SR Ca^{2+} uptake in the LA, resulting in enhanced susceptibility to arrhythmogenic episodes in the atria. Heterogeneity across the LV was already present in the younger age groups, with further alterations to protein expression reported in the elderly. The LV endocardium was shown to express dramatically higher levels of RYR2 protein, theorised to be responsible for increased Ca^{2+} sparks and thus greater susceptibility to arrhythmias. It was also shown in the ventricles and LA that NCX1 protein expression, often used as an indication of HF, increased in the 24 months old age group; contributing to the theory that 'ageing' is a dominating risk factor to cardiac dysfunction.

6.2 Ca^{2+} handling in the atria versus ventricles

In Chapter 4 and 5 age-related alterations in Ca^{2+} regulation in the ventricles and atria were compared as right versus left, however, a comparison of ventricle to atria was not conducted. There have been previous studies that have looked at variations in Ca^{2+} regulation between the atria and ventricles, but none have used an ageing model.

6.2.1 Cardio myocytes structural differences with consequences on Ca^{2+} handling

Arial myocytes are relatively smaller than ventricular myocytes both in length and width; immunocytochemistry also highlighted the spindle shape of atrial myocytes versus the typical brick shaped cells of the LV or RV. This is consistent with previous findings that reported reduced length and width and dramatic 7 fold decreased volume (Walden et al., 2009). Another structural difference consistently mentioned in chapter 4 was the sporadic t-tubular network that were only located at the periphery of cells, in contrast to the ventricular myocytes which contained an atypical t-tubular pattern throughout. This correlates to previous studies that have noted the absence of t-tubules in atrial myocytes and linked to spatiotemporal differences in Ca^{2+} transient (Huser et al., 1996, Tanaami et al., 2005).

The absence of t-tubules in atrial myocytes is also species specific with no network reported in the guinea pig (Forbes and van Neil, 1988), but poorly developed t-tubules are present in rat atrial myocytes (Ayettey and Navaratnam, 1978), which correlates to those observed in the RA and LA in chapter 4. Removal of a t-tubular network would have a direct affect on CICR and may explain species differences in Ca^{2+} transients (Mackenzie et al., 2001, Huser et al., 1996). Apart from species, age was observed to have a deleterious effect on t-tubule patterns, as in the case of Figure 5.3, in the 24 months age group, t-tubules were infrequent and unorganised; suggesting that the elderly ventricles were showing attributes similar to that of atrial myocytes.

T-tubule structures are vital in the role of E-C; they are the source for the majority of $Ca_v1.2$ channels and the SR with attached RYRs are in close proximity to promote CICR. Removal of these invaginations affects CICR or 'local release' within the atrial myocytes; this is clearly seen by the Ca^{2+} wave which starts at the periphery and spreads towards the centre of the cell (Mackenzie et al., 2001). In contrast, chapter 5,

showed the LV and RV had organised t-tubules in the young-adult animals, effective in CICR and provides a uniform rise in $[Ca^{2+}]_i$ across the whole myocyte (Tanaami et al., 2005). The reduction in atrial myocyte width compared with ventricular myocytes is one of the first adaptive mechanisms in trying to facilitate propagation of Ca^{2+} from the cell surface membrane to the interior (Walden et al., 2009).

In this study ageing had a dual affect on normal CICR pathways; both the structure of the t-tubular network and protein expression of RYR2 and $Ca_v1.2$ channels were altered. In chapters 4 and 5 there were clear similarities and differences in protein expression variation with age in the atria versus the ventricles (see section 6.1.3); combined with the already dysfunctional 'local release', these changes will further alter Ca^{2+} influx. The decrease in $Ca_v1.2$ and RYR2 protein in the RA would further drive a reduced Ca^{2+} transient, however, RYR2 was seemingly expressed throughout the cell as with $Ca_v1.2$, of which the former has previously been reported (Hatem et al., 1997). This highlights that CICR at the sarcolemma or t-tubule invaginations may not be as critical for Ca^{2+} transient in the atrial myocytes, perhaps propagation from the surface to the centre is facilitated by these interior bound RYR2. Consequently age-associated reduction in RYR2 protein expression may not have a direct affect on CICR at the cell surface but would dramatically reduce propagation through the cell. Though there are no age-associated studies investigating both protein expression and t-tubule structures, in the sheep atrial myocytes suffering from HF, depletion of t-tubules was observed to drastically hinder Ca^{2+} release from the centre of the cells (Dibb et al., 2009); this study can be combined with a study which reported decreased RYR2 protein in HF (Vatner et al., 1994). In addition, as shown in figure 4.24, $Ca_v1.2$ protein decreased by 40% in the 24 months of age rats, further hindering a rise in $[Ca^{2+}]_i$. This would have a dual effect - Ca^{2+} influx is reduced and without t-tubule structures coupling is minimal with already dwindled ryanodine receptors (Gomez et al., 1997); overall this would reduce the Ca^{2+} transient and delay propagation to the centre of the myocytes.

In contrast to the RA, with age, $Ca_v1.2$ channels were observed to increase within the LA ; furthermore there was an organised pattern with fewer dense clumps and more t-tubule structures located at the cell surface. Coupled with only a 12% decline in RYR2 protein, the contractile function based on CICR seems to be preserved in the elderly LA. Unfortunately this is also coupled with a significant increase in NCX1 protein and SERCA2a activity, both of which will increase SR Ca^{2+} content becoming a high risk factor in the generation of arrhythmias (Venetucci et al., 2007, Mackenzie et al., 2002) (see section 6.1.4).

Young-adult ventricular myocytes on the other hand have extensive t-tubular structures which allow 'local release' throughout the myocyte via coupling of $Ca_v1.2$ channels and RYRs, generating Ca^{2+} sparks that in summation produce the Ca^{2+} transient observed in an AP (Fowler et al., 2004). Even with the extensive sarcolemma invaginations, the large volume of ventricular myocytes results in a low surface area to volume ratio (Walden et al., 2009), thus the coupling of Cav1.2 to RYR2 is vital in synchronous rise of $[Ca^{2+}]_i$. This is the major difference between the atrial and ventricular myocytes; both show similar CICR (in the young-adults) at the periphery, but only in the ventricular myocytes is peak $[Ca^{2+}]_i$ in the centre close to that of the periphery (Tanaami et al., 2005). Thus it can be concluded that the t-tubule structure is essential in the normal function of ventricular myocytes; however, in chapter 5 immunocytochemistry of LV and RV sections showed that advanced age declined the number and organisation of t-tubule structures, as seen in figure 5.5. The effect of ageing may be akin to detubulated ventricular myocytes which have been displayed to evoke highly variable Ca^{2+} response and synchronisation of the Ca^{2+} transient was not possible in any of the detubulated cells (Smyrnias et al., 2010).

Apart from age-associated structural changes, in correlation to the RA, the RV exhibited decreased RYR2 protein levels in the 24 months age group, though $Ca_v1.2$ levels remained unchanged. Vital for SR Ca^{2+} release is the activation of RYR2 channels, decreased coupling to $Ca_v1.2$ channels would result in decreased Ca^{2+} release (Gomez et al., 1997); thus, dysfunctional or decreased RYR2 protein may be an age-related predisposition for heart failure (Marx et al., 2000). Interestingly the LV exhibited protein changes akin to the LA at 24 months of age, with decreased RYR2 levels but elevated $Ca_v1.2$ protein. It can be argued that the increase in $Ca_v1.2$ protein would compensate for the reduced RYR2, however, linked to the fewer t-tubular structures CICR may still be hindered. Consequently the differences in protein expression between the atria and ventricles may have differing effects based on the presence of absence of t-tubule structures. Furthermore age related changes would provoke a varied response based on whether the cell was dependent on t-tubular-CICR for synchronised Ca^{2+} release.

6.2.1.1 Propagation of Ca^{2+} in atrial myocytes

Atrial myocytes are able to propagate Ca^{2+} from the periphery of the cell towards the centre without the aid of t-tubules. In chapter 4 RYR2 channels were observed to be present throughout the atrial sections, these are directly linked to the SR, which will activate to release Ca^{2+}. Thus, Ca^{2+} from the cell surface will spread inwards to the

next SR causing release and continuing the chain stimulation of RYR2 in the centre. This propagation is based on a few factors that highlights the difference of Ca^{2+} propagation between ventricles and atria. RYR2 sensitivity to Ca^{2+} can be directly elevated by increased luminal levels of Ca^{2+}, itself regulated by a combination of SR Ca^{2+} leak and uptake (Ginsburg et al., 1998). SR Ca^{2+} uptake is controlled by SERCA2a; combining the raw data from chapter 4 and 5, SERCA2a activity was observed to be 1.5 fold higher in the young-adult atria versus the ventricles and a further 2 fold higher in the elderly atria. A comparison of activity across the atria and ventricles reported SR Ca^{2+} uptake in adult rats was significantly higher in atrial versus ventricular myocytes (Freestone et al., 2000, Luss et al., 1999). Though increased SERCA2a activity would reduce Ca^{2+} diffusion in the cytosolic space, it would increase SR Ca^{2+} load thus increasing RYR2 sensitivity and probability of SR Ca^{2+} release in the centre of the cell. A further mechanism involved in buffering Ca^{2+} are mitochondria which are infrequent in atrial versus ventricular myocytes (Hirakow et al., 1980); the lower density could aid propagation of Ca^{2+} as less is being removed permanently via the mitochondrial Ca^{2+} uniporter (Seguchi et al., 2005).

6.2.2 Altered AP properties linked to variations in Ca^{2+} handing proteins and changes with age

Action potentials from ventricular myocytes versus atrial myocytes have already been shown to be drastically differ (see 1.2.5). The amplitude of systolic Ca^{2+} transient is significantly higher in ventricular myocytes with a prolonged period of decay. Although SR Ca^{2+} content was 3-fold higher in adult atrial myocytes compared with ventricular myocytes (Walden et al., 2009); the higher Ca^{2+} amplitude in ventricular tissue was due to the Ca^{2+} sinks available in the atrial myocytes. There are over 2-fold more SR structures in atrial myocytes compared with ventricular myocytes, coupled with the increased SERCA2a activity, short AP duration and smaller peak amplitude can be explained by the rapid removal of [Ca2+]i (Diaz et al., 2005). The increase in SR structures would also explain the occasional streaked pattern observed in some atrial sections immunolabelled with SR bound proteins. In addition to aid SR Ca^{2+} content, removal of Ca^{2+} via sarcolemma pathways is drastically lower in the atria. NCX protein levels and current was observed to be significantly lower in the atrial myocytes versus ventricular cells (Walden et al., 2009). This highlights the lower SR Ca^{2+} content in ventricular myocytes is not only due to diminished SERCA2a activity but also the increased importance of NCX during relaxation of the ventricles. Based on this concept data obtained in the 24 months age group, suggests the reduction in SERCA2a activity

caused a compensatory increase in NCX1 protein observed in both RV and LV (figure 5.11) to aid in I_{CaL} decay.

The SR has already been highlighted as the main mechanism for propagation through the atrial myocyte (Tanaami et al., 2005) but with age, the RA was reported to have lower levels of SERCA2a activity (Figure 4.21) which would directly affect SR Ca^{2+} content and the AP duration. In contrast the LA exhibited the most drastic age-related Ca^{2+} remodelling with increased NCX1, Cav1.2 protein levels and SERCA2a activity; AP duration would decrease but peak Ca^{2+} transient may increase, thus creating dysrhythmias across the atria.

6.2.3 Ca^{2+} handling protein differences and similarities across the heart

The atria and ventricles have vastly different roles during a typical heart beat and thus AP properties based on Ca^{2+} handling proteins will vary significantly. Initial data suggests age-related remodelling differs between the atria and ventricles, however, if the cardiovascular system was split into the pulmonary and systemic sections, similarities were noted.

$Ca_v1.2$ channels are already expressed at higher levels in the adult ventricles compared with atria (Hatano et al., 2006). With age Cav1.2 protein expression was reported to increase by 37% in the ventricles, figure 5.9, similarly levels were 52% elevated in the LA. This would affect Ca^{2+} influx, contributing to prolonged AP duration in the ventricles (Josephson et al., 2002) and combined with the lower SR Ca^{2+} uptake in the ventricles can cause Ca^{2+} overload (Hano et al., 1995). Whereas in the atria the extra CICR gain would further increase the SR Ca^{2+} content due to the contrasting higher SERCA2a activity. In contrast, though $Ca_v1.2$ is already expressed higher in the adult LV (Kondo et al., 2006), age had the opposite effect on the RV and RA, protein levels remained unchanged in the RV but decreased significantly in the RA.

A further similarity between the LA and LV is the decrease in RYR2 protein expression which would drastically effecting propagation in the former (Tanaami et al., 2005) and CICR in the latter (Diaz et al., 2005). In addition lower levels of RYR2 protein were also observed in the right side of the heart, suggesting that age appears to decrease RYR2 in all cardiac tissue, possibly as a predisposition to heart failure (Vatner et al., 1994). Linked as an indication of heart failure (Flesch et al., 1996) was the age-associated 34% increased expression of NCX1 in the LV and 33% rise in the LA. The rise in the LV is beneficial to aid relaxation, similarly a rise in the LA would mean more Ca^{2+} is

removed via the sarcolemma pathways, thus reducing SR Ca^{2+} load and the risk of spontaneous irregular SR Ca^{2+} release (Diaz et al., 1997). In contrast increased NCX1 density alongside SR 'leakage' from RYR2 could further drive atrial myocytes to produce a spontaneous beat via inward I_{NCX} (Mackenzie et al., 2002).

Another sarcolemma pathway that showed universal age-related diminished expression was PMCA4a, which decreased in the atria and ventricles. Nevertheless the use of PMCA4a would still affect $[Ca^{2+}]_i$ levels after Ca^{2+} transient, thus prolonging AP duration with age. Alternatively PMCA4a is important in nitric oxide signalling in the heart (Chang et al., 2008), with defects in the PMCA4 isoform causes dysfunctional cardiac repolarisation (Arking et al., 2006).

6.2.4 Culprits in the generation of arrhythmias in the atria and ventricles

The atria are the site of the commonest arrhythmia, AF (Kannel et al., 1998) which has gained intense clinical interest and studies into the role of Ca^{2+} as an arrhythmogenic substrate (Mackenzie et al., 2002, Venetucci et al., 2006). Age has long been considered the most prominent risk factor for developing AF (Lloyd-Jones et al., 2004). Consequently the age-associated changes in Ca^{2+} handling proteins reported in chapter 4, highlights remodelling that occurred in the atria and how this impacts risk of arrhythmia generation. In correlation, ventricular arrhythmias such as ventricle fibrillation (VF) also hold roots to dysfunctional Ca^{2+} homeostasis, though more fatal, ventricular arrhythmias are less common and are usually a predisposition to HF or occur at high frequency in HF patients (Lasisi et al., 2012).

Therefore the age-related increased likelihood of developing an arrhythmia may be due to the altered mechanisms behind spontaneous Ca^{2+} release. Many studies have linked high SR Ca^{2+} load to be directly responsible for spontaneous arrhythmogenic Ca^{2+} release in atria and ventricles (Venetucci et al., 2006, Venetucci et al., 2007, Jiang et al., 2004). Minimal studies investigate age combined with changes to Ca^{2+} regulation and its dual connection to arrhythmia generation. Nevertheless by combining data from this study with other studies that investigate the bases of an arrhythmia, speculations can be made.

In order for SR Ca^{2+} load to become elevated, the uptake of Ca^{2+} would have to be increased via SERCA2a. Thus, comparing ventricles to atria, the latter had a 1.5 fold increase in SERCA2a activity, similarly to previous findings (Diaz et al., 2005, Walden

et al., 2009). Consequently the adult atria would have higher SR Ca^{2+} content and therefore have an increased risk of a spontaneous arrhythmogenic Ca^{2+} release. Combining the effect of advanced age, chapter 4 reported a 46% rise in SERCA2a activity within the LA, this would drive the SR Ca^{2+} load to severe levels further increasing the frequency of an arrhythmogenic episode. In contrast the ventricles, which already have lower levels of SERCA2a activity (Walden et al., 2009), showed decreased SR Ca^{2+} uptake in the 24 months age groups (figure 5.6), thus SR Ca^{2+} content would be lowered. In addition the number of SR structures are near 3-fold greater in the atria than the ventricles (Walden et al., 2009), further increasing the probability of SR 'leakage' via the ryanodine receptors (Venetucci et al., 2006). Interestingly this provides an alternative theory to the universal age-associated reduction in RYR2 protein levels (figure 5.7 and 4.22); with reduced expression the risk of spontaneous Ca^{2+} release is minimised , thus protecting the heart; though not as effective as reduced SR Ca^{2+} content (Venetucci et al., 2007). In summation data from chapter 4 and 5 highlights why, with age, atrial arrhythmias are more common than ventricular arrhythmias, based purely on SR Ca^{2+} content (Venetucci et al., 2007, Jiang et al., 2004).

In summation though there are minimal age-associated regional comparison studies, there are a vast number based on arrhythmias as the main medical factor such as AF or VF as a predisposition to HF and sudden death. All of these studies seem to hold similarities akin to altered SR Ca^{2+} content which also occurs with age. Therefore this thesis was able to incorporate a regional study of Ca^{2+} homeostasis and its alterations with age, to fully understand why the elderly population are more susceptible to AF/VF.

6.3 Alternative mechanisms involved in Ca^{2+} influx

6.3.1 Alternative pathways for Ca^{2+} influx

In chapters 3, 4 and 5 not all mechanisms involved in the influx of Ca^{2+} were considered. As such further discussion is warranted of the other Ca^{2+} pathways and how they may influence pacemaker activity and the Ca^{2+} transient.

6.3.1.1 Stretch activated channels

In addition to normal voltage activated ionic channels, stretch activated channels are also presence in cardiac tissue primarily studied in the atria and ventricles (Kim and Fu,

1993). These channels can provide an additional increase to I_{CaL} and can cause diastolic depolarisation (Matsuda et al., 1996). An investigation into the response of axial stretch in the SA node indicated that a minor stretch of 7% produced a 5% increase in spontaneous beating (Cooper et al., 2000); though only a minor change, this study highlights that stretch-activated channels may play a role during a normal heartbeat. In addition electrophysiological data obtained in chapter 3 was from a pinned SA node; the tissue was not stretched but the influence of stretch-activated channels cannot be ruled out completely.

6.3.1.2 Store-operated calcium channels and depletion of SR Ca^{2+} content

Store operated calcium channels (SOCC), coded by the transient receptor potential canonical gene, were first identified in non-excitable cells which reported that on depletion of intracellular Ca^{2+} stores, a calcium current was activated (Hoth and Penner, 1992). The role of SOCC are unclear in cardiac tissue as NCX1 plus various Ca^{2+} channels would provide sufficient Ca^{2+} influx for SR Ca^{2+} content to be restored, nevertheless SOCC have been identified in ventricular myocytes and may play a minor role in E-C coupling (Seth et al., 2004, Nakayama et al., 2006). In particular due to the importance of SR Ca^{2+} stores in pacemaker activity (Vinogradova et al., 2010), depletion of these stores would cause activation of SOCC and provide a previously unaccounted influx of Ca^{2+}. A study of the mouse SA node reported the expression of the transient receptor potential canonical genes and positive labelling in the SA node region (Ju et al., 2007). In addition these SOCC were functionally active, with the aid of nifedipine, CPA and ryanodine, this study illustrated that an influx of Ca^{2+} was mediated by SOCC upon depletion of the SR.

Data on SOCC within the SA node remains relatively novel, thus no age-associated studies have yet been conducted. But in chapter 3 the activity of SERCA2a declined along with the expression of $Ca_v1.2$ channels and RYR2 protein; combined this would reduce CICR gain and thus SR Ca^{2+} content. Consequently the SOCC present would restore the SR Ca^{2+} load, but the level of contribution is unknown and whether this would also change with age. Unfortunately this may also provide an additional mechanism for an arrhythmogenic episode; due to age-related lower SR Ca^{2+} content, activated SOCC could cause dysfunctional influx of Ca^{2+}, which with the reduced SERCA2a activity, cannot be buffered. As such SOCC may not only play a role in dysfunctional pacemaker activity but also in arrhythmogenesis in the RA, depleted SERCA2a activity, plus reduced expression of all other Ca^{2+} handling proteins, would result in depleted SR Ca^{2+} content. Therefore, contrary to the typical literature findings

where SR Ca^{2+} overload is a component in arrhythmogenesis (Venetucci et al., 2007), perhaps the opposite is also true, such that overall dysfunction of SR Ca^{2+} homeostasis drives the heart into impulse mismanagement.

6.3.1.3 T type calcium channels in the SA node

An alternative to L-type calcium channels ($Ca_v1.2$) are the T-type calcium channels which stand for 'tiny transient' which has been difficult to distinguish from the class $Ca_v1.2$ channels as I_{CaT} and I_{CaL} are sensitive to the same compounds. T-type calcium channels or $Ca_v3.1$ is also expressed in the SA node but was not investigated in this thesis. Early studies reported Cav3.1 had minimal function in pacemaker activity (Doerr et al., 1989, Hagiwara et al., 1988), but use of mibefradil, one of the only compounds to solely target I_{CaT}, was able to significantly lower pacemaker activity after oral consumption (Madle et al., 2001). In addition mice lacking $Ca_v3.1$ displayed abnormal SA node pacemaker activity and also AV conduction; overall suggesting $Ca_v3.1$ is also an important factor to consider. Nevertheless having said this I_{CaT} seems to not be as significant in the actual SA node but in the automaticity in the transitional zone between the SA node and atrium, perhaps aiding in the propagation of the AP from the LPS.

Therefore $Ca_v3.1$ channels are important at the periphery of the SA node, thus removal would slow down rate of repolarisation at the LPS, however, I_{CaL} is still the main source for sarcolemma Ca^{2+} influx and predominantly aids the automaticity of the SA node. Consequently though $Ca_v3.1$ was not investigated within the SA node, this does not affect the speculation on spontaneous activity; instead it would have been interesting to investigate $Ca_v3.1$ in the CT tissue which provides the transition between the SA node and the RA muscle. In addition I_{CaT} has been shown to change over the lifespan of both young rabbits (Protas et al., 2001) and adult rats (Nair and Nair, 2001). Consequently as $Ca_v3.1$ is involved in automaticity and is known to be present in the transitional zone, the combination of increased $Ca_v1.2$ in the 24 months age group within the CT tissue (figure 4.11), plus possible increases to $Ca_v3.1$ in the same region, could additionally explain the link between arrhythmogenic episodes and proximity to the CT (Akcay et al., 2007).

6.4 Future work

Tracking of the LPS in the SA node was obtained using bi-polar electrodes which was moved after subsequent additions of chemicals and on the movement of the

pacemaker site. This provided results both on conduction velocity and AP propagation across the intercaval region, however, it did not provide continuous stream of data. Consequently as an alternative of bi-polar electrodes, the whole intercaval region can be recorded simultaneously using multiple electrodes attached at every 1mm of tissue. This technique would provide data on the current LPS but also show 'real time' competition between other LPSs. In addition this method would allow total AP propagation across the CT to be analysed, inclusive of locations parallel or perpendicular to the CT, removing the previously mentioned limitations of this study. Lastly simultaneous recordings would produce more accurate conduction velocity and pacemaker shift data; this would allow further research into the affect of SR Ca^{2+} load on both the sharp rise in conduction velocity in the younger age groups and the lack of pacemaker shift under the influence of CPA.

Data collected from the LA indicated increased SERCA2a activity and $Ca_v1.2$ protein levels which suggests elevated SR Ca^{2+} load, implicated in the age-associated higher frequency of arrhythmogenic episodes. In order to fully test SR Ca^{2+} load in left atrial myocytes caffeine would be used to measure SR Ca^{2+} content and whether it is higher in the elderly LA. Similarly with the decreased expression of all Ca^{2+} handling proteins in the RA, caffeine would empty the SR highlighting whether SR 'leakage' would be reduced in the RA. Lastly spontaneous activity in the SA node relies on LCR at the RYR2 sites which is also based upon SR Ca^{2+} content which our data indicates is reduced in the elderly SA node. Therefore if the SR has a reduced role in spontaneous activity, caffeine would have a reduced impact.

Protein expression data of Ca^{2+} transports in the left and right ventricle supports previous findings of the prolonged AP in the elderly and the enhanced Ca^{2+} amplitude; but to fully complement this thesis, functional recordings from whole ventricles and single cardiomyocytes should be obtained. Langendorff perfusions can be used to assess LV function across the three age groups; recordings will include: AP duration, Ca^{2+} amplitude, tolerance to extracellular Ca^{2+} and effect of increased demand via high frequency pacing and with the influence of a β-adrenergic stimulator. In addition the effect of ageing on the process of CICR can be investigated using a patch-clamp technique to measure altered NCX1 and $Ca_v1.2$ current in single left ventricular and atrial myocytes.

6.5 Clinical implications

This study has shown that treatment, such as nifedipine, had an increased response in the elderly at pharmacologically relevant concentrations. Consequently there is a risk in using nifedipine to treat hypertension or other pharmacological therapy for treating AF

and various arrhythmias, as similar drugs have been shown to be different according to gender and age (Maxwell et al., 2000, Hammerlein et al., 1998). Advances in treatment, although successful, are based on the universal concept that each patient has the same type of arrhythmia, response and similar symptoms. However, this study showed varied expression of Ca^{2+} handling proteins depending on region and age which would have diverse effects on cardiac function. Consequently, treatment given to a young adult may have a different effect than if given to an elderly patient.

In contrast to nifedipine, reduced β-adrenergic response partially due to diminished β-receptor density could affect the sensitivity to β-blocker drugs, also used to treat hypertension. However, clinical studies/reviews of age and response to β-blocker drugs are minimal but have shown that caution should be used with β-blocker drugs in the elderly not due to sensitivity but to them being renally eliminated (Piepho and Fendler, 1991). Therefore typically a multitude of drugs are prescribed which may interact, thus hospitalising the elderly patient (Gosney and Tallis, 1984).

6.6 Conclusion

The effect of ageing on cardiac tissue varies depending on the region and if the chamber is part of the systemic or pulmonary system. A major difference between the atria and ventricles is the presence of t-tubules, which is vital for Ca^{2+} propagation in the ventricles but not so much in the atria. Consequently altered expression of RYR2 and $Ca_v1.2$ protein would have a greater impact in the ventricles compared with the atria. Similarly NCX1 protein is involved both during CICR and Ca^{2+} extrusion and is of substantially greater importance in ventricular tissue; therefore elevated levels in the LV and RV would have a greater impact on the Ca^{2+} transient compared with decreased levels in the atria.

Using literature to compare the ventricles to atria, a factor that contributes greatly to dysfunctional Ca^{2+} release, is SR Ca^{2+} load, which is higher in the atria than in the ventricles; supporting the frequency of atrial versus ventricular arrhythmias. With age the LA had elevated SERCA2a activity, promoting SR Ca^{2+} overload, therefore acting as a substrate for arrhythmogenic episodes. Alternatively the severely depleted SR Ca^{2+} content in the RA, due to the down-regulation of all Ca^{2+} handling proteins, may cause the irregular activation of SOCCs which would provide a Ca^{2+} influx that could manifest into an irregular spontaneous event.

In conclusion there are clear age-associated variations in the expression of Ca^{2+} handling proteins. The type of cardiac tissue, whether from the systemic or pulmonary

system, ventricles or atria, affects the levels of Ca^{2+} transporter proteins. The consequences of age-related changes to Ca^{2+} handling proteins on the rise of $[Ca^{2+}]_i$ can be deleterious or beneficial based on type of protein and region.

Publications

Papers:

Hatch, F., Lancaster, M. K. & Jones, S. A. 2011. Aging is a primary risk factor for cardiac arrhythmias: disruption of intracellular Ca2+ regulation as a key suspect. Expert Rev Cardiovasc Ther, 9, 1059-67.

Published abstracts:

Hatch F, Lancaster MK & Jones SA. Does the crista terminalis possess a key role in the elevated risk of arrhythmogenic episodes in the elderly population?. Proc Physiol Soc 2013 IUPS

Hatch F, Lancaster MK & Jones SA. Ageing further increases the diversification between the atria in the expression of cellular calcium regulators: a substrate for increase arrhythmia risk?. Proc Physiol Soc 2013 IUPS

Hatch F, Lancaster MK & Jones SA. Age-associated alterations in intracellular calcium handling within the sinoatrial node. Proc Physiol Soc 2012:28;C04&PC04

Hatch F, Lancaster MK & Jones SA. Diminished SR function and adrenergic response co-associate in the ageing sinoatrial node. Proc Physiol Soc 2012:28;PC38

Hatch F, Lancaster MK & Jones SA. Age-associated changes in cardiac calcium handling. Northern Cardiac Research Group 201;OP9.

Hatch F, Lancaster MK & Jones SA. Changes in the role of the SR in SAN function across the lifespan may be responsible for changing pacemaker stability and response. Heart 2012;98(3);A17

References

ABD ALLAH, E. S., ASLANIDI, O. V., TELLEZ, J. O., YANNI, J., BILLETER, R., ZHANG, H., DOBRZYNSKI, H. & BOYETT, M. R. 2012. Postnatal development of transmural gradients in expression of ion channels and Ca(2)(+)-handling proteins in the ventricle. *J Mol Cell Cardiol,* 53**,** 145-55.

ABETE, P., FERRARA, N., CIOPPA, A., FERRARA, P., BIANCO, S., CALABRESE, C., NAPOLI, C. & RENGO, F. 1996. The role of aging on the control of contractile force by Na(+)-Ca2+ exchange in rat papillary muscle. *J Gerontol A Biol Sci Med Sci,* 51**,** M251-9.

ACETO, J. F., CONDRESCU, M., KROUPIS, C., NELSON, H., NELSON, N., NICOLL, D., PHILIPSON, K. D. & REEVES, J. P. 1992. Cloning and expression of the bovine cardiac sodium-calcium exchanger. *Arch Biochem Biophys,* 298**,** 553-60.

ADACHI-AKAHANE, S., CLEEMANN, L. & MORAD, M. 1996. Cross-signaling between L-type Ca2+ channels and ryanodine receptors in rat ventricular myocytes. *J Gen Physiol,* 108**,** 435-54.

AKCAY, M., BILEN, E. S., BILGE, M., DURMAZ, T. & KURT, M. 2007. Prominent crista terminalis: as an anatomic structure leading to atrial arrhythmias and mimicking right atrial mass. *J Am Soc Echocardiogr,* 20**,** 197 e9-10.

ALINGS, A. M., ABBAS, R. F. & BOUMAN, L. N. 1995. Age-related changes in structure and relative collagen content of the human and feline sinoatrial node. A comparative study. *Eur Heart J,* 16**,** 1655-67.

ALINGS, A. M. & BOUMAN, L. N. 1993. Electrophysiology of the ageing rabbit and cat sinoatrial node--a comparative study. *Eur Heart J,* 14**,** 1278-88.

ALLAH, E. A., TELLEZ, J. O., YANNI, J., NELSON, T., MONFREDI, O., BOYETT, M. R. & DOBRZYNSKI, H. 2011. Changes in the expression of ion channels, connexins and Ca2+-handling proteins in the sino-atrial node during postnatal development. *Exp Physiol,* 96**,** 426-38.

ALPERT, J. S., PETERSEN, P. & GODTFREDSEN, J. 1988. Atrial fibrillation: natural history, complications, and management. *Annu Rev Med,* 39**,** 41-52.

ANDERSON, K., LAI, F. A., LIU, Q. Y., ROUSSEAU, E., ERICKSON, H. P. & MEISSNER, G. 1989. Structural and functional characterization of the purified cardiac ryanodine receptor-Ca2+ release channel complex. *J Biol Chem,* 264**,** 1329-35.

ANTZELEVITCH, C., SICOURI, S., LITOVSKY, S. H., LUKAS, A., KRISHNAN, S. C., DI DIEGO, J. M., GINTANT, G. A. & LIU, D. W. 1991. Heterogeneity within the ventricular wall. Electrophysiology and pharmacology of epicardial, endocardial, and M cells. *Circ Res,* 69**,** 1427-49.

ARKING, D. E., PFEUFER, A., POST, W., KAO, W. H., NEWTON-CHEH, C., IKEDA, M., WEST, K., KASHUK, C., AKYOL, M., PERZ, S., JALILZADEH, S., ILLIG, T., GIEGER, C., GUO, C. Y., LARSON, M. G., WICHMANN, H. E., MARBAN, E., O'DONNELL, C. J., HIRSCHHORN, J. N., KAAB, S., SPOONER, P. M., MEITINGER, T. & CHAKRAVARTI, A. 2006. A common genetic variant in the NOS1 regulator NOS1AP modulates cardiac repolarization. *Nat Genet,* 38**,** 644-51.

ASSAYAG, P., D, C. H., MARTY, I., DE LEIRIS, J., LOMPRE, A. M., BOUCHER, F., VALERE, P. E., LORTET, S., SWYNGHEDAUW, B. & BESSE, S. 1998. Effects of sustained low-flow ischemia on myocardial function and calcium-regulating proteins in adult and senescent rat hearts. *Cardiovasc Res,* 38**,** 169-80.

AYETTEY, A. S. & NAVARATNAM, V. 1978. The T-tubule system in the specialized and general myocardium of the rat. *J Anat,* 127**,** 125-40.

BANGALORE, R. & TRIGGLE, D. J. 1995. Age-dependent changes in voltage-gated calcium channels and ATP-dependent potassium channels in Fischer 344 rats. *Gen Pharmacol,* 26**,** 1237-42.

BARUSCOTTI, M., BUCCHI, A. & DIFRANCESCO, D. 2005. Physiology and pharmacology of the cardiac pacemaker ("funny") current. *Pharmacol Ther,* 107**,** 59-79.

BASSANI, J. W., BASSANI, R. A. & BERS, D. M. 1994a. Relaxation in rabbit and rat cardiac cells: species-dependent differences in cellular mechanisms. *J Physiol,* 476**,** 279-93.

BASSANI, J. W., YUAN, W. & BERS, D. M. 1995a. Fractional SR Ca release is regulated by trigger Ca and SR Ca content in cardiac myocytes. *Am J Physiol,* 268**,** C1313-9.

BASSANI, R. A., BASSANI, J. W. & BERS, D. M. 1992. Mitochondrial and sarcolemmal Ca2+ transport reduce [Ca2+]i during caffeine contractures in rabbit cardiac myocytes. *J Physiol,* 453**,** 591-608.

BASSANI, R. A., BASSANI, J. W. & BERS, D. M. 1994b. Relaxation in ferret ventricular myocytes: unusual interplay among calcium transport systems. *J Physiol,* 476**,** 295-308.

BASSANI, R. A., BASSANI, J. W. & BERS, D. M. 1995b. Relaxation in ferret ventricular myocytes: role of the sarcolemmal Ca ATPase. *Pflugers Arch,* 430**,** 573-8.

BASSANI, R. A. & BERS, D. M. 1995. Rate of diastolic Ca release from the sarcoplasmic reticulum of intact rabbit and rat ventricular myocytes. *Biophys J,* 68**,** 2015-22.

BENNETT, P. B., VALENZUELA, C., CHEN, L. Q. & KALLEN, R. G. 1995. On the molecular nature of the lidocaine receptor of cardiac Na+ channels. Modification of block by alterations in the alpha-subunit III-IV interdomain. *Circ Res,* 77**,** 584-92.

BERS, D. M. 2002. Cardiac excitation-contraction coupling. *Nature,* 415**,** 198-205.

BERS, D. M. & BRIDGE, J. H. 1989. Relaxation of rabbit ventricular muscle by Na-Ca exchange and sarcoplasmic reticulum calcium pump. Ryanodine and voltage sensitivity. *Circ Res,* 65**,** 334-42.

BERS, D. M., CHRISTENSEN, D. M. & NGUYEN, T. X. 1988. Can Ca entry via Na-Ca exchange directly activate cardiac muscle contraction? *J Mol Cell Cardiol,* 20**,** 405-14.

BERS, D. M., PHILIPSON, K. D. & NISHIMOTO, A. Y. 1980. Sodium-calcium exchange and sidedness of isolated cardiac sarcolemmal vesicles. *Biochim Biophys Acta,* 601**,** 358-71.

BHAT, P. K., WATANABE, K., RAO, D. B. & LUISADA, A. A. 1974. Conduction defects in the aging heart. *J Am Geriatr Soc,* 22**,** 517-20.

BLACKWELL, B. N., BUCCI, T. J., HART, R. W. & TURTURRO, A. 1995. Longevity, body weight, and neoplasia in ad libitum-fed and diet-restricted C57BL6 mice fed NIH-31 open formula diet. *Toxicol Pathol,* 23**,** 570-82.

BLEEKER, W. K., MACKAAY, A. J., MASSON-PEVET, M., BOUMAN, L. N. & BECKER, A. E. 1980. Functional and morphological organization of the rabbit sinus node. *Circ Res,* 46**,** 11-22.

BLEEKER, W. K., MACKAAY, A. J., MASSON-PEVET, M., OP'T HOF, T., JONGSMA, H. J. & BOUMAN, L. N. 1982. Asymmetry of the sino-atrial conduction in the rabbit heart. *J Mol Cell Cardiol,* 14**,** 633-43.

BOGDANOV, K. Y., MALTSEV, V. A., VINOGRADOVA, T. M., LYASHKOV, A. E., SPURGEON, H. A., STERN, M. D. & LAKATTA, E. G. 2006. Membrane potential fluctuations resulting from submembrane Ca2+ releases in rabbit sinoatrial nodal cells impart an exponential phase to the late diastolic depolarization that controls their chronotropic state. *Circ Res,* 99**,** 979-87.

BOGDANOV, K. Y., VINOGRADOVA, T. M. & LAKATTA, E. G. 2001. Sinoatrial nodal cell ryanodine receptor and Na(+)-Ca(2+) exchanger: molecular partners in pacemaker regulation. *Circ Res,* 88**,** 1254-8.

BOINEAU, J. P., CANAVAN, T. E., SCHUESSLER, R. B., CAIN, M. E., CORR, P. B. & COX, J. L. 1988. Demonstration of a widely distributed atrial pacemaker complex in the human heart. *Circulation,* 77**,** 1221-37.

BOINEAU, J. P., SCHUESSLER, R. B., ROESKE, W. R., AUTRY, L. J., MILLER, C. B. & WYLDS, A. C. 1983. Quantitative relation between sites of atrial impulse origin and cycle length. *Am J Physiol,* 245**,** H781-9.

BOMHARD, E. M., KRINKE, G. J., ROSSBERG, W. M. & SKRIPSKY, T. 1997. Trimethylphosphate: a 30-month chronic toxicity/carcinogenicity study in Wistar rats with administration in drinking water. *Fundam Appl Toxicol,* 40**,** 75-89.

BOOTMAN, M. D., SMYRNIAS, I., THUL, R., COOMBES, S. & RODERICK, H. L. 2011. Atrial cardiomyocyte calcium signalling. *Biochim Biophys Acta,* 1813**,** 922-34.

BOSCH, R. F., ZENG, X., GRAMMER, J. B., POPOVIC, K., MEWIS, C. & KUHLKAMP, V. 1999. Ionic mechanisms of electrical remodeling in human atrial fibrillation. *Cardiovasc Res,* 44**,** 121-31.

BOUCHARD, R. A., CLARK, R. B. & GILES, W. R. 1995. Effects of action potential duration on excitation-contraction coupling in rat ventricular myocytes. Action potential voltage-clamp measurements. *Circ Res,* 76**,** 790-801.

BOYETT, M. R., HONJO, H. & KODAMA, I. 2000. The sinoatrial node, a heterogeneous pacemaker structure. *Cardiovasc Res,* 47**,** 658-87.

BOYETT, M. R., HONJO, H., YAMAMOTO, M., NIKMARAM, M. R., NIWA, R. & KODAMA, I. 1999. Downward gradient in action potential duration along conduction path in and around the sinoatrial node. *Am J Physiol,* 276**,** H686-98.

BRANDL, C. J., GREEN, N. M., KORCZAK, B. & MACLENNAN, D. H. 1986. Two Ca2+ ATPase genes: homologies and mechanistic implications of deduced amino acid sequences. *Cell,* 44**,** 597-607.

BRIGGS, F. N., LEE, K. F., WECHSLER, A. W. & JONES, L. R. 1992. Phospholamban expressed in slow-twitch and chronically stimulated fast-twitch muscles minimally affects calcium affinity of sarcoplasmic reticulum Ca(2+)-ATPase. *J Biol Chem,* 267**,** 26056-61.

BRILLA, C. G., JANICKI, J. S. & WEBER, K. T. 1991. Impaired diastolic function and coronary reserve in genetic hypertension. Role of interstitial fibrosis and medial thickening of intramyocardial coronary arteries. *Circ Res,* 69**,** 107-15.

BRISTOW, M. R., MINOBE, W., RASMUSSEN, R., LARRABEE, P., SKERL, L., KLEIN, J. W., ANDERSON, F. L., MURRAY, J., MESTRONI, L., KARWANDE, S. V. & ET AL. 1992. Beta-adrenergic neuroeffector abnormalities in the failing human heart are produced by local rather than systemic mechanisms. *J Clin Invest,* 89**,** 803-15.

BRITTSAN, A. G., CARR, A. N., SCHMIDT, A. G. & KRANIAS, E. G. 2000. Maximal inhibition of SERCA2 Ca(2+) affinity by phospholamban in transgenic hearts overexpressing a non-phosphorylatable form of phospholamban. *J Biol Chem,* 275**,** 12129-35.

BROUND, M. J., ASGHARI, P., WAMBOLT, R. B., BOHUNEK, L., SMITS, C., PHILIT, M., KIEFFER, T. J., LAKATTA, E. G., BOHELER, K. R., MOORE, E. D., ALLARD, M. F. & JOHNSON, J. D. 2012. Cardiac ryanodine receptors control heart rate and rhythmicity in adult mice. *Cardiovasc Res,* 96**,** 372-80.

BROWN, H. F. 1982. Electrophysiology of the sinoatrial node. *Physiol Rev,* 62**,** 505-30.

BROWN, H. F., DIFRANCESCO, D. & NOBLE, S. J. 1979. How does adrenaline accelerate the heart? *Nature,* 280**,** 235-6.

CAIN, B. S., MELDRUM, D. R., JOO, K. S., WANG, J. F., MENG, X., CLEVELAND, J. C., JR., BANERJEE, A. & HARKEN, A. H. 1998. Human SERCA2a levels correlate inversely with age in senescent human myocardium. *J Am Coll Cardiol,* 32**,** 458-67.

CAMPBELL, D. L., RASMUSSON, R. L. & STRAUSS, H. C. 1988. Theoretical study of the voltage and concentration dependence of the anomalous mole fraction effect in single calcium channels. New insights into the characterization of multi-ion channels. *Biophys J,* 54**,** 945-54.

CAPASSO, J. M., MALHOTRA, A., REMILY, R. M., SCHEUER, J. & SONNENBLICK, E. H. 1983. Effects of age on mechanical and electrical performance of rat myocardium. *Am J Physiol,* 245**,** H72-81.

CARAFOLI, E. & STAUFFER, T. 1994. The plasma membrane calcium pump: functional domains, regulation of the activity, and tissue specificity of isoform expression. *J Neurobiol,* 25**,** 312-24.

CARIDE, A. J., FILOTEO, A. G., PENNISTON, J. T. & STREHLER, E. E. 2007. The plasma membrane Ca2+ pump isoform 4a differs from isoform 4b in the mechanism of calmodulin binding and activation kinetics: implications for Ca2+ signaling. *J Biol Chem,* 282**,** 25640-8.

CARONI, P. & CARAFOLI, E. 1981. Regulation of Ca2+-pumping ATPase of heart sarcolemma by a phosphorylation-dephosphorylation Process. *J Biol Chem,* 256**,** 9371-3.

CARONI, P., REINLIB, L. & CARAFOLI, E. 1980. Charge movements during the Na+-Ca2+ exchange in heart sarcolemmal vesicles. *Proc Natl Acad Sci U S A,* 77**,** 6354-8.

CERRONE, M., COLOMBI, B., SANTORO, M., DI BARLETTA, M. R., SCELSI, M., VILLANI, L., NAPOLITANO, C. & PRIORI, S. G. 2005. Bidirectional ventricular tachycardia and fibrillation elicited in a knock-in mouse model carrier of a mutation in the cardiac ryanodine receptor. *Circ Res,* 96**,** e77-82.

CHAMORRO, A. 2010. Dual antiplatelet therapy is not optimal for stroke prevention in patients with atrial fibrillation. *Int J Stroke,* 5**,** 28-9.

CHANG, K. C., BARTH, A. S., SASANO, T., KIZANA, E., KASHIWAKURA, Y., ZHANG, Y., FOSTER, D. B. & MARBAN, E. 2008. CAPON modulates cardiac repolarization via neuronal nitric oxide synthase signaling in the heart. *Proc Natl Acad Sci U S A,* 105**,** 4477-82.

CHELU, M. G., SARMA, S., SOOD, S., WANG, S., VAN OORT, R. J., SKAPURA, D. G., LI, N., SANTONASTASI, M., MULLER, F. U., SCHMITZ, W., SCHOTTEN, U., ANDERSON, M. E., VALDERRABANO, M., DOBREV, D. & WEHRENS, X. H. 2009. Calmodulin kinase II-mediated sarcoplasmic reticulum Ca2+ leak promotes atrial fibrillation in mice. *J Clin Invest,* 119**,** 1940-51.

CHEN, J., MCLEAN, P. A., NEEL, B. G., OKUNADE, G., SHULL, G. E. & WORTIS, H. H. 2004a. CD22 attenuates calcium signaling by potentiating plasma membrane calcium-ATPase activity. *Nat Immunol,* 5**,** 651-7.

CHEN, Y., ESCOUBET, B., PRUNIER, F., AMOUR, J., SIMONIDES, W. S., VIVIEN, B., LENOIR, C., HEIMBURGER, M., CHOQUEUX, C., GELLEN, B., RIOU, B., MICHEL, J. B., FRANZ, W. M. & MERCADIER, J. J. 2004b. Constitutive cardiac overexpression of sarcoplasmic/endoplasmic reticulum Ca2+-ATPase delays myocardial failure after myocardial infarction in rats at a cost of increased acute arrhythmias. *Circulation,* 109**,** 1898-903.

CHENG, H., LEDERER, W. J. & CANNELL, M. B. 1993. Calcium sparks: elementary events underlying excitation-contraction coupling in heart muscle. *Science,* 262**,** 740-4.

CLUSIN, W. T. 2008. Mechanisms of calcium transient and action potential alternans in cardiac cells and tissues. *Am J Physiol Heart Circ Physiol,* 294**,** H1-H10.

COLYER, J. & WANG, J. H. 1991. Dependence of cardiac sarcoplasmic reticulum calcium pump activity on the phosphorylation status of phospholamban. *J Biol Chem,* 266**,** 17486-93.

COOPER, P. J., LEI, M., CHENG, L. X. & KOHL, P. 2000. Selected contribution: axial stretch increases spontaneous pacemaker activity in rabbit isolated sinoatrial node cells. *J Appl Physiol,* 89**,** 2099-104.

COPPEN, S. R., KODAMA, I., BOYETT, M. R., DOBRZYNSKI, H., TAKAGISHI, Y., HONJO, H., YEH, H. I. & SEVERS, N. J. 1999. Connexin45, a major connexin of the rabbit sinoatrial node, is co-expressed with connexin43 in a restricted zone at the nodal-crista terminalis border. *J Histochem Cytochem,* 47**,** 907-18.

CORDEIRO, J. M., SPITZER, K. W. & GILES, W. R. 1998. Repolarizing K+ currents in rabbit heart Purkinje cells. *J Physiol,* 508 (Pt 3)**,** 811-23.

CROWE, P. A. 2006. *Quotes on living a long life : mankind's wisdom on aging from diogenes to Dylan,* Arlington, VA, Richer Resources Publications.

CUKIERMAN, S. 1996. Regulation of voltage-dependent sodium channels. *J Membr Biol,* 151**,** 203-14.
CURRIE, S., QUINN, F. R., SAYEED, R. A., DUNCAN, A. M., KETTLEWELL, S. & SMITH, G. L. 2005. Selective down-regulation of sub-endocardial ryanodine receptor expression in a rabbit model of left ventricular dysfunction. *J Mol Cell Cardiol,* 39**,** 309-17.
D'AMATO, N., PIERFELICE, O. & D'AGOSTINO, C. 2009. Crista terminalis bridge: a rare variant mimicking right atrial mass. *Eur J Echocardiogr,* 10**,** 444-5.
DEAL, K. K., ENGLAND, S. K. & TAMKUN, M. M. 1996. Molecular physiology of cardiac potassium channels. *Physiol Rev,* 76**,** 49-67.
DELMAR, M. 2002. Connexin diversity: discriminating the message. *Circ Res,* 91**,** 85-6.
DIAZ, M. E., GRAHAM, H. K., O'NEILL S, C., TRAFFORD, A. W. & EISNER, D. A. 2005. The control of sarcoplasmic reticulum Ca content in cardiac muscle. *Cell Calcium,* 38**,** 391-6.
DIAZ, M. E., O'NEILL, S. C. & EISNER, D. A. 2004. Sarcoplasmic reticulum calcium content fluctuation is the key to cardiac alternans. *Circ Res,* 94**,** 650-6.
DIAZ, M. E., TRAFFORD, A. W., O'NEILL, S. C. & EISNER, D. A. 1997. A measurable reduction of s.r. Ca content follows spontaneous Ca release in rat ventricular myocytes. *Pflugers Arch,* 434**,** 852-4.
DIBB, K. M., CLARKE, J. D., HORN, M. A., RICHARDS, M. A., GRAHAM, H. K., EISNER, D. A. & TRAFFORD, A. W. 2009. Characterization of an extensive transverse tubular network in sheep atrial myocytes and its depletion in heart failure. *Circ Heart Fail,* 2**,** 482-9.
DIFRANCESCO, D., FERRONI, A., MAZZANTI, M. & TROMBA, C. 1986. Properties of the hyperpolarizing-activated current (if) in cells isolated from the rabbit sino-atrial node. *J Physiol,* 377**,** 61-88.
DOCHERTY, J. R. 1990. Cardiovascular responses in ageing: a review. *Pharmacol Rev,* 42**,** 103-25.
DOERR, T., DENGER, R. & TRAUTWEIN, W. 1989. Calcium currents in single SA nodal cells of the rabbit heart studied with action potential clamp. *Pflugers Arch,* 413**,** 599-603.
EL-ARMOUCHE, A., BOKNIK, P., ESCHENHAGEN, T., CARRIER, L., KNAUT, M., RAVENS, U. & DOBREV, D. 2006. Molecular determinants of altered Ca2+ handling in human chronic atrial fibrillation. *Circulation,* 114**,** 670-80.
ESLER, M. D., TURNER, A. G., KAYE, D. M., THOMPSON, J. M., KINGWELL, B. A., MORRIS, M., LAMBERT, G. W., JENNINGS, G. L., COX, H. S. & SEALS, D. R. 1995. Aging effects on human sympathetic neuronal function. *Am J Physiol,* 268**,** R278-85.
FABIATO, A. 1983. Calcium-induced release of calcium from the cardiac sarcoplasmic reticulum. *Am J Physiol,* 245**,** C1-14.
FARRELL, S. R. & HOWLETT, S. E. 2008. The age-related decrease in catecholamine sensitivity is mediated by beta(1)-adrenergic receptors linked to a decrease in adenylate cyclase activity in ventricular myocytes from male Fischer 344 rats. *Mech Ageing Dev,* 129**,** 735-44.
FLEG, J. L., MORRELL, C. H., BOS, A. G., BRANT, L. J., TALBOT, L. A., WRIGHT, J. G. & LAKATTA, E. G. 2005. Accelerated longitudinal decline of aerobic capacity in healthy older adults. *Circulation,* 112**,** 674-82.
FLESCH, M., SCHWINGER, R. H., SCHIFFER, F., FRANK, K., SUDKAMP, M., KUHN-REGNIER, F., ARNOLD, G. & BOHM, M. 1996. Evidence for functional relevance of an enhanced expression of the Na(+)-Ca2+ exchanger in failing human myocardium. *Circulation,* 94**,** 992-1002.
FORBES, M. S. & VAN NEIL, E. E. 1988. Membrane systems of guinea pig myocardium: ultrastructure and morphometric studies. *Anat Rec,* 222**,** 362-79.
FORNIERI, C., QUAGLINO, D., JR. & MORI, G. 1992. Role of the extracellular matrix in age-related modifications of the rat aorta. Ultrastructural, morphometric, and enzymatic evaluations. *Arterioscler Thromb,* 12**,** 1008-16.

FOWLER, M. R., DOBSON, R. S., ORCHARD, C. H. & HARRISON, S. M. 2004. Functional consequences of detubulation of isolated rat ventricular myocytes. *Cardiovasc Res,* 62**,** 529-37.

FRANK, K. F., BOLCK, B., ERDMANN, E. & SCHWINGER, R. H. 2003. Sarcoplasmic reticulum Ca2+-ATPase modulates cardiac contraction and relaxation. *Cardiovasc Res,* 57**,** 20-7.

FRATICELLI, A., JOSEPHSON, R., DANZIGER, R., LAKATTA, E. & SPURGEON, H. 1989. Morphological and contractile characteristics of rat cardiac myocytes from maturation to senescence. *Am J Physiol,* 257**,** H259-65.

FREESTONE, N. S., RIBARIC, S., SCHEUERMANN, M., MAUSER, U., PAUL, M. & VETTER, R. 2000. Differential lusitropic responsiveness to beta-adrenergic stimulation in rat atrial and ventricular cardiac myocytes. *Pflugers Arch,* 441**,** 78-87.

FRIES, J. F. 2002. Aging, natural death, and the compression of morbidity. 1980. *Bull World Health Organ,* 80**,** 245-50.

FROEHLICH, J. P., LAKATTA, E. G., BEARD, E., SPURGEON, H. A., WEISFELDT, M. L. & GERSTENBLITH, G. 1978. Studies of sarcoplasmic reticulum function and contraction duration in young adult and aged rat myocardium. *J Mol Cell Cardiol,* 10**,** 427-38.

FRY, C. H., POWELL, T., TWIST, V. W. & WARD, J. P. 1984. Net calcium exchange in adult rat ventricular myocytes: an assessment of mitochondrial calcium accumulating capacity. *Proc R Soc Lond B Biol Sci,* 223**,** 223-38.

FURUKAWA, T., MYERBURG, R. J., FURUKAWA, N., BASSETT, A. L. & KIMURA, S. 1990. Differences in transient outward currents of feline endocardial and epicardial myocytes. *Circ Res,* 67**,** 1287-91.

FUSTER, V., RYDEN, L. E., CANNOM, D. S., CRIJNS, H. J., CURTIS, A. B., ELLENBOGEN, K. A., HALPERIN, J. L., LE HEUZEY, J. Y., KAY, G. N., LOWE, J. E., OLSSON, S. B., PRYSTOWSKY, E. N., TAMARGO, J. L., WANN, S., SMITH, S. C., JR., JACOBS, A. K., ADAMS, C. D., ANDERSON, J. L., ANTMAN, E. M., HUNT, S. A., NISHIMURA, R., ORNATO, J. P., PAGE, R. L., RIEGEL, B., PRIORI, S. G., BLANC, J. J., BUDAJ, A., CAMM, A. J., DEAN, V., DECKERS, J. W., DESPRES, C., DICKSTEIN, K., LEKAKIS, J., MCGREGOR, K., METRA, M., MORAIS, J., OSTERSPEY, A. & ZAMORANO, J. L. 2006. ACC/AHA/ESC 2006 Guidelines for the Management of Patients with Atrial Fibrillation: a report of the American College of Cardiology/American Heart Association Task Force on Practice Guidelines and the European Society of Cardiology Committee for Practice Guidelines (Writing Committee to Revise the 2001 Guidelines for the Management of Patients With Atrial Fibrillation): developed in collaboration with the European Heart Rhythm Association and the Heart Rhythm Society. *Circulation,* 114**,** e257-354.

GELLENS, M. E., GEORGE, A. L., JR., CHEN, L. Q., CHAHINE, M., HORN, R., BARCHI, R. L. & KALLEN, R. G. 1992. Primary structure and functional expression of the human cardiac tetrodotoxin-insensitive voltage-dependent sodium channel. *Proc Natl Acad Sci U S A,* 89**,** 554-8.

GINSBURG, K. S., WEBER, C. R. & BERS, D. M. 1998. Control of maximum sarcoplasmic reticulum Ca load in intact ferret ventricular myocytes. Effects Of thapsigargin and isoproterenol. *J Gen Physiol,* 111**,** 491-504.

GOEGER, D. E., RILEY, R. T., DORNER, J. W. & COLE, R. J. 1988. Cyclopiazonic acid inhibition of the Ca2+-transport ATPase in rat skeletal muscle sarcoplasmic reticulum vesicles. *Biochem Pharmacol,* 37**,** 978-81.

GOMEZ, A. M., VALDIVIA, H. H., CHENG, H., LEDERER, M. R., SANTANA, L. F., CANNELL, M. B., MCCUNE, S. A., ALTSCHULD, R. A. & LEDERER, W. J. 1997. Defective excitation-contraction coupling in experimental cardiac hypertrophy and heart failure. *Science,* 276**,** 800-6.

GOONASEKARA, C. L., BALSE, E., HATEM, S., STEELE, D. F. & FEDIDA, D. 2010. Cholesterol and cardiac arrhythmias. *Expert Rev Cardiovasc Ther,* 8**,** 965-79.

GOSNEY, M. & TALLIS, R. 1984. Prescription of contraindicated and interacting drugs in elderly patients admitted to hospital. *Lancet,* 2**,** 564-7.
GREENBAUM, R. A., HO, S. Y., GIBSON, D. G., BECKER, A. E. & ANDERSON, R. H. 1981. Left ventricular fibre architecture in man. *Br Heart J,* 45**,** 248-63.
GREISER, M., LEDERER, W. J. & SCHOTTEN, U. 2011. Alterations of atrial Ca(2+) handling as cause and consequence of atrial fibrillation. *Cardiovasc Res,* 89**,** 722-33.
GREISER, M., NEUBERGER, H. R., HARKS, E., EL-ARMOUCHE, A., BOKNIK, P., DE HAAN, S., VERHEYEN, F., VERHEULE, S., SCHMITZ, W., RAVENS, U., NATTEL, S., ALLESSIE, M. A., DOBREV, D. & SCHOTTEN, U. 2009. Distinct contractile and molecular differences between two goat models of atrial dysfunction: AV block-induced atrial dilatation and atrial fibrillation. *J Mol Cell Cardiol,* 46**,** 385-94.
GWATHMEY, J. K., SLAWSKY, M. T., PERREAULT, C. L., BRIGGS, G. M., MORGAN, J. P. & WEI, J. Y. 1990. Effect of exercise conditioning on excitation-contraction coupling in aged rats. *J Appl Physiol,* 69**,** 1366-71.
GYORKE, S., STEVENS, S. C. & TERENTYEV, D. 2009. Cardiac calsequestrin: quest inside the SR. *J Physiol,* 587**,** 3091-4.
HADDAD, F., HUNT, S. A., ROSENTHAL, D. N. & MURPHY, D. J. 2008. Right ventricular function in cardiovascular disease, part I: Anatomy, physiology, aging, and functional assessment of the right ventricle. *Circulation,* 117**,** 1436-48.
HAGHIGHI, K., GREGORY, K. N. & KRANIAS, E. G. 2004. Sarcoplasmic reticulum Ca-ATPase-phospholamban interactions and dilated cardiomyopathy. *Biochem Biophys Res Commun,* 322**,** 1214-22.
HAGIWARA, N., IRISAWA, H. & KAMEYAMA, M. 1988. Contribution of two types of calcium currents to the pacemaker potentials of rabbit sino-atrial node cells. *J Physiol,* 395**,** 233-53.
HAKAMATA, Y., NAKAI, J., TAKESHIMA, H. & IMOTO, K. 1992. Primary structure and distribution of a novel ryanodine receptor/calcium release channel from rabbit brain. *FEBS Lett,* 312**,** 229-35.
HAMMERLEIN, A., DERENDORF, H. & LOWENTHAL, D. T. 1998. Pharmacokinetic and pharmacodynamic changes in the elderly. Clinical implications. *Clin Pharmacokinet,* 35**,** 49-64.
HAMMES, A., OBERDORF-MAASS, S., ROTHER, T., NETHING, K., GOLLNICK, F., LINZ, K. W., MEYER, R., HU, K., HAN, H., GAUDRON, P., ERTL, G., HOFFMANN, S., GANTEN, U., VETTER, R., SCHUH, K., BENKWITZ, C., ZIMMER, H. G. & NEYSES, L. 1998. Overexpression of the sarcolemmal calcium pump in the myocardium of transgenic rats. *Circ Res,* 83**,** 877-88.
HANO, O., BOGDANOV, K. Y., SAKAI, M., DANZIGER, R. G., SPURGEON, H. A. & LAKATTA, E. G. 1995. Reduced threshold for myocardial cell calcium intolerance in the rat heart with aging. *Am J Physiol,* 269**,** H1607-12.
HARFST, E., SEVERS, N. J. & GREEN, C. R. 1990. Cardiac myocyte gap junctions: evidence for a major connexon protein with an apparent relative molecular mass of 70,000. *J Cell Sci,* 96 (Pt 4)**,** 591-604.
HARTEL, G. & TALVENSAARI, T. 1975. Treatment of sinoatrial syndrome with permanent cardiac pacing in 90 patients. *Acta Med Scand,* 198**,** 341-7.
HATANO, S., YAMASHITA, T., SEKIGUCHI, A., IWASAKI, Y., NAKAZAWA, K., SAGARA, K., IINUMA, H., AIZAWA, T. & FU, L. T. 2006. Molecular and electrophysiological differences in the L-type Ca2+ channel of the atrium and ventricle of rat hearts. *Circ J,* 70**,** 610-4.
HATCH, F., LANCASTER, M. K. & JONES, S. A. 2011. Aging is a primary risk factor for cardiac arrhythmias: disruption of intracellular Ca2+ regulation as a key suspect. *Expert Rev Cardiovasc Ther,* 9**,** 1059-67.
HATEM, S. N., BENARDEAU, A., RUCKER-MARTIN, C., MARTY, I., DE CHAMISSO, P., VILLAZ, M. & MERCADIER, J. J. 1997. Different compartments of

sarcoplasmic reticulum participate in the excitation-contraction coupling process in human atrial myocytes. *Circ Res,* 80**,** 345-53.
HEINEKE, J. & MOLKENTIN, J. D. 2006. Regulation of cardiac hypertrophy by intracellular signalling pathways. *Nat Rev Mol Cell Biol,* 7**,** 589-600.
HERRMANN, S., STIEBER, J., STOCKL, G., HOFMANN, F. & LUDWIG, A. 2007. HCN4 provides a 'depolarization reserve' and is not required for heart rate acceleration in mice. *EMBO J,* 26**,** 4423-32.
HIRAKOW, R., GOTOH, T. & WATANABE, T. 1980. Quantitative studies on the ultrastructural differentiation and growth of mammalian cardiac muscle cells. I. The atria and ventricles of the rat. *Acta Anat (Basel),* 108**,** 144-52.
HIRANO, M., DAVIDSON, M. & DIMAURO, S. 2001. Mitochondria and the heart. *Curr Opin Cardiol,* 16**,** 201-10.
HOPPS, S. & MARCY, T. R. 2009. Warfarin versus aspirin: using CHADS2 to guide therapy for stroke prevention in nonvalvular atrial fibrillation. *Consult Pharm,* 24**,** 841-4.
HOTH, M. & PENNER, R. 1992. Depletion of intracellular calcium stores activates a calcium current in mast cells. *Nature,* 355**,** 353-6.
HOWLETT, S. E., GRANDY, S. A. & FERRIER, G. R. 2006. Calcium spark properties in ventricular myocytes are altered in aged mice. *Am J Physiol Heart Circ Physiol,* 290**,** H1566-74.
HUME, J. R. & UEHARA, A. 1985. Ionic basis of the different action potential configurations of single guinea-pig atrial and ventricular myocytes. *J Physiol,* 368**,** 525-44.
HUSER, J., LIPSIUS, S. L. & BLATTER, L. A. 1996. Calcium gradients during excitation-contraction coupling in cat atrial myocytes. *J Physiol,* 494 (Pt 3)**,** 641-51.
IMAGAWA, T., SMITH, J. S., CORONADO, R. & CAMPBELL, K. P. 1987. Purified ryanodine receptor from skeletal muscle sarcoplasmic reticulum is the Ca2+-permeable pore of the calcium release channel. *J Biol Chem,* 262**,** 16636-43.
IRISAWA, H., BROWN, H. F. & GILES, W. 1993. Cardiac pacemaking in the sinoatrial node. *Physiol Rev,* 73**,** 197-227.
ISENBERG, G., BORSCHKE, B. & RUECKSCHLOSS, U. 2003. Ca2+ transients of cardiomyocytes from senescent mice peak late and decay slowly. *Cell Calcium,* 34**,** 271-80.
JANCZEWSKI, A. M., SPURGEON, H. A. & LAKATTA, E. G. 2002. Action potential prolongation in cardiac myocytes of old rats is an adaptation to sustain youthful intracellular Ca2+ regulation. *J Mol Cell Cardiol,* 34**,** 641-8.
JIA, Z., BIEN, H., SHIFERAW, Y. & ENTCHEVA, E. 2012. Cardiac cellular coupling and the spread of early instabilities in intracellular Ca2+. *Biophys J,* 102**,** 1294-302.
JIANG, D., XIAO, B., YANG, D., WANG, R., CHOI, P., ZHANG, L., CHENG, H. & CHEN, S. R. 2004. RyR2 mutations linked to ventricular tachycardia and sudden death reduce the threshold for store-overload-induced Ca2+ release (SOICR). *Proc Natl Acad Sci U S A,* 101**,** 13062-7.
JIANG, M. T., MOFFAT, M. P. & NARAYANAN, N. 1993. Age-related alterations in the phosphorylation of sarcoplasmic reticulum and myofibrillar proteins and diminished contractile response to isoproterenol in intact rat ventricle. *Circ Res,* 72**,** 102-11.
JONES, L. R., SUZUKI, Y. J., WANG, W., KOBAYASHI, Y. M., RAMESH, V., FRANZINI-ARMSTRONG, C., CLEEMANN, L. & MORAD, M. 1998. Regulation of Ca2+ signaling in transgenic mouse cardiac myocytes overexpressing calsequestrin. *J Clin Invest,* 101**,** 1385-93.
JONES, S. A., BOYETT, M. R. & LANCASTER, M. K. 2007a. Declining into failure - The age-dependent loss of the L-type calcium channel within the sinoatrial node. *Circulation,* 115**,** 1183-1190.

JONES, S. A., BOYETT, M. R. & LANCASTER, M. K. 2007b. Declining into failure: the age-dependent loss of the L-type calcium channel within the sinoatrial node. *Circulation,* 115**,** 1183-90.

JONES, S. A., LANCASTER, M. K. & BOYETT, M. R. 2004. Ageing-related changes of connexins and conduction within the sinoatrial node. *J Physiol,* 560**,** 429-37.

JOSEPHSON, I. R., GUIA, A., STERN, M. D. & LAKATTA, E. G. 2002. Alterations in properties of L-type Ca channels in aging rat heart. *Journal of Molecular and Cellular Cardiology,* 34**,** 297-308.

JU, Y. K., CHU, Y., CHAULET, H., LAI, D., GERVASIO, O. L., GRAHAM, R. M., CANNELL, M. B. & ALLEN, D. G. 2007. Store-operated Ca2+ influx and expression of TRPC genes in mouse sinoatrial node. *Circ Res,* 100**,** 1605-14.

KALMAN, J. M., OLGIN, J. E., KARCH, M. R., HAMDAN, M., LEE, R. J. & LESH, M. D. 1998. "Cristal tachycardias": origin of right atrial tachycardias from the crista terminalis identified by intracardiac echocardiography. *J Am Coll Cardiol,* 31**,** 451-9.

KAMP, T. J. & HE, J. Q. 2002. L-type Ca2+ channels gaining respect in heart failure. *Circulation Research,* 91**,** 451-453.

KANNEL, W. B., ABBOTT, R. D., SAVAGE, D. D. & MCNAMARA, P. M. 1982. Epidemiologic features of chronic atrial fibrillation: the Framingham study. *N Engl J Med,* 306**,** 1018-22.

KANNEL, W. B., WOLF, P. A., BENJAMIN, E. J. & LEVY, D. 1998. Prevalence, incidence, prognosis, and predisposing conditions for atrial fibrillation: population-based estimates. *Am J Cardiol,* 82**,** 2N-9N.

KAPLAN, P., JURKOVICOVA, D., BABUSIKOVA, E., HUDECOVA, S., RACAY, P., SIROVA, M., LEHOTSKY, J., DRGOVA, A., DOBROTA, D. & KRIZANOVA, O. 2007. Effect of aging on the expression of intracellular Ca(2+) transport proteins in a rat heart. *Mol Cell Biochem,* 301**,** 219-26.

KATZ, A. M. 1993. Cardiac ion channels. *N Engl J Med,* 328**,** 1244-51.

KE, Y., LEI, M., COLLINS, T. P., RAKOVIC, S., MATTICK, P. A., YAMASAKI, M., BRODIE, M. S., TERRAR, D. A. & SOLARO, R. J. 2007. Regulation of L-type calcium channel and delayed rectifier potassium channel activity by p21-activated kinase-1 in guinea pig sinoatrial node pacemaker cells. *Circ Res,* 100**,** 1317-27.

KEATING, M. T. & SANGUINETTI, M. C. 2001. Molecular and cellular mechanisms of cardiac arrhythmias. *Cell,* 104**,** 569-80.

KEITH, A. & FLACK, M. 1907. The Form and Nature of the Muscular Connections between the Primary Divisions of the Vertebrate Heart. *J Anat Physiol,* 41**,** 172-89.

KIM, D. & FU, C. 1993. Activation of a nonselective cation channel by swelling in atrial cells. *J Membr Biol,* 135**,** 27-37.

KIMURA, J., NOMA, A. & IRISAWA, H. 1986. Na-Ca exchange current in mammalian heart cells. *Nature,* 319**,** 596-7.

KISTLER, P. M., SANDERS, P., FYNN, S. P., STEVENSON, I. H., SPENCE, S. J., VOHRA, J. K., SPARKS, P. B. & KALMAN, J. M. 2004. Electrophysiologic and electroanatomic changes in the human atrium associated with age. *J Am Coll Cardiol,* 44**,** 109-16.

KNOLLMANN, B. C., KATCHMAN, A. N. & FRANZ, M. R. 2001. Monophasic action potential recordings from intact mouse heart: validation, regional heterogeneity, and relation to refractoriness. *J Cardiovasc Electrophysiol,* 12**,** 1286-94.

KODAMA, I. & BOYETT, M. R. 1985. Regional differences in the electrical activity of the rabbit sinus node. *Pflugers Arch,* 404**,** 214-26.

KONDO, R. P., DEDERKO, D. A., TEUTSCH, C., CHRAST, J., CATALUCCI, D., CHIEN, K. R. & GILES, W. R. 2006. Comparison of contraction and calcium handling between right and left ventricular myocytes from adult mouse heart: a role for repolarization waveform. *J Physiol,* 571**,** 131-46.

KOSTIN, S., SCHOLZ, D., SHIMADA, T., MAENO, Y., MOLLNAU, H., HEIN, S. & SCHAPER, J. 1998. The internal and external protein scaffold of the T-tubular system in cardiomyocytes. *Cell Tissue Res,* 294**,** 449-60.

KURACHI, Y. 1985. Voltage-dependent activation of the inward-rectifier potassium channel in the ventricular cell membrane of guinea-pig heart. *J Physiol,* 366**,** 365-85.

KUROKAWA, J., ABRIEL, H. & KASS, R. S. 2001. Molecular basis of the delayed rectifier current I(ks)in heart. *J Mol Cell Cardiol,* 33**,** 873-82.

LAI, L. P., SU, M. J., LIN, J. L., LIN, F. Y., TSAI, C. H., CHEN, Y. S., HUANG, S. K., TSENG, Y. Z. & LIEN, W. P. 1999. Down-regulation of L-type calcium channel and sarcoplasmic reticular Ca(2+)-ATPase mRNA in human atrial fibrillation without significant change in the mRNA of ryanodine receptor, calsequestrin and phospholamban: an insight into the mechanism of atrial electrical remodeling. *J Am Coll Cardiol,* 33**,** 1231-7.

LAKATTA, E. G. 1987. Cardiac muscle changes in senescence. *Annu Rev Physiol,* 49**,** 519-31.

LAKATTA, E. G. 1993. Deficient neuroendocrine regulation of the cardiovascular system with advancing age in healthy humans. *Circulation,* 87**,** 631-6.

LAKATTA, E. G. & DIFRANCESCO, D. 2009. What keeps us ticking: a funny current, a calcium clock, or both? *Journal of Molecular and Cellular Cardiology,* 47**,** 157-170.

LAKATTA, E. G., MITCHELL, J. H., POMERANCE, A. & ROWE, G. G. 1987. Human aging: changes in structure and function. *J Am Coll Cardiol,* 10**,** 42A-47A.

LAKATTA, E. G. & SOLLOTT, S. J. 2002. Perspectives on mammalian cardiovascular aging: humans to molecules. *Comp Biochem Physiol A Mol Integr Physiol,* 132**,** 699-721.

LAKS, M. M., NISENSON, M. J. & SWAN, H. J. 1967. Myocardial cell and sarcomere lengths in the normal dog heart. *Circ Res,* 21**,** 671-8.

LALANI, G. G., SCHRICKER, A., GIBSON, M., ROSTAMIAN, A., KRUMMEN, D. E. & NARAYAN, S. M. 2012. Atrial conduction slows immediately before the onset of human atrial fibrillation: a bi-atrial contact mapping study of transitions to atrial fibrillation. *J Am Coll Cardiol,* 59**,** 595-606.

LASISI, G. T., ADEBOLA, A. P., OGAH, O. S. & DANIEL, F. A. 2012. Prevalence of ventricular arrhythmias and heart rate variability pattern in chronic heart failure. *Niger Postgrad Med J,* 19**,** 157-62.

LAURITA, K. R. & ROSENBAUM, D. S. 2008. Cellular mechanisms of arrhythmogenic cardiac alternans. *Prog Biophys Mol Biol,* 97**,** 332-47.

LEI, M., GODDARD, C., LIU, J., LEONI, A. L., ROYER, A., FUNG, S. S., XIAO, G., MA, A., ZHANG, H., CHARPENTIER, F., VANDENBERG, J. I., COLLEDGE, W. H., GRACE, A. A. & HUANG, C. L. 2005. Sinus node dysfunction following targeted disruption of the murine cardiac sodium channel gene Scn5a. *J Physiol,* 567**,** 387-400.

LEVINE, H. J. 1997. Rest heart rate and life expectancy. *J Am Coll Cardiol,* 30**,** 1104-6.

LI-JUN, J., XUE-YIN, L., CONG-XIN, H., BO, Y., SHA-NING, Y., GANG, W., QIANG, X. & HUANG-JUN, L. 2012. Electrophysiologic characteristics of the Crista terminalis and implications on atrial tachycardia in rabbits. *Cell Biochem Biophys,* 62**,** 267-71.

LI, J., QU, J. & NATHAN, R. D. 1997. Ionic basis of ryanodine's negative chronotropic effect on pacemaker cells isolated from the sinoatrial node. *Am J Physiol,* 273**,** H2481-9.

LI, Z., NICOLL, D. A., COLLINS, A., HILGEMANN, D. W., FILOTEO, A. G., PENNISTON, J. T., WEISS, J. N., TOMICH, J. M. & PHILIPSON, K. D. 1991. Identification of a peptide inhibitor of the cardiac sarcolemmal Na(+)-Ca2+ exchanger. *J Biol Chem,* 266**,** 1014-20.

LIM, C. C., APSTEIN, C. S., COLUCCI, W. S. & LIAO, R. 2000. Impaired cell shortening and relengthening with increased pacing frequency are intrinsic to the senescent mouse cardiomyocyte. *J Mol Cell Cardiol,* 32**,** 2075-82.

LIM, C. C., LIAO, R., VARMA, N. & APSTEIN, C. S. 1999. Impaired lusitropy-frequency in the aging mouse: role of Ca(2+)-handling proteins and effects of isoproterenol. *Am J Physiol,* 277**,** H2083-90.

LIPMAN, R. D., CHRISP, C. E., HAZZARD, D. G. & BRONSON, R. T. 1996. Pathologic characterization of brown Norway, brown Norway x Fischer 344, and Fischer 344 x brown Norway rats with relation to age. *J Gerontol A Biol Sci Med Sci,* 51**,** B54-9.

LIU, J., DOBRZYNSKI, H., YANNI, J., BOYETT, M. R. & LEI, M. 2007. Organisation of the mouse sinoatrial node: structure and expression of HCN channels. *Cardiovasc Res,* 73**,** 729-38.

LIU, J., SIRENKO, S., JUHASZOVA, M., ZIMAN, B., SHETTY, V., RAIN, S., SHUKLA, S., SPURGEON, H. A., VINOGRADOVA, T. M., MALTSEV, V. A. & LAKATTA, E. G. 2011. A full range of mouse sinoatrial node AP firing rates requires protein kinase A-dependent calcium signaling. *J Mol Cell Cardiol,* 51**,** 730-9.

LLACH, A., MOLINA, C. E., FERNANDES, J., PADRO, J., CINCA, J. & HOVE-MADSEN, L. 2011. Sarcoplasmic reticulum and L-type Ca(2)(+) channel activity regulate the beat-to-beat stability of calcium handling in human atrial myocytes. *J Physiol,* 589**,** 3247-62.

LLOYD-JONES, D. M., WANG, T. J., LEIP, E. P., LARSON, M. G., LEVY, D., VASAN, R. S., D'AGOSTINO, R. B., MASSARO, J. M., BEISER, A., WOLF, P. A. & BENJAMIN, E. J. 2004. Lifetime risk for development of atrial fibrillation: the Framingham Heart Study. *Circulation,* 110**,** 1042-6.

LO, H. M., LIN, F. Y., LIN, J. L., HSU, K. L., CHIANG, F. T., TSENG, C. D. & TSENG, Y. Z. 1999. Impaired cardiac performance relating to delayed left atrial activation after atrial compartment operation for chronic atrial fibrillation. *Pacing Clin Electrophysiol,* 22**,** 379-81.

LOMPRE, A. M., LAMBERT, F., LAKATTA, E. G. & SCHWARTZ, K. 1991a. Expression of sarcoplasmic reticulum Ca(2+)-ATPase and calsequestrin genes in rat heart during ontogenic development and aging. *Circ Res,* 69**,** 1380-8.

LOMPRE, A. M., MERCADIER, J. J. & SCHWARTZ, K. 1991b. Changes in gene expression during cardiac growth. *Int Rev Cytol,* 124**,** 137-86.

LOPATIN, A. N. & NICHOLS, C. G. 2001. Inward rectifiers in the heart: an update on I(K1). *J Mol Cell Cardiol,* 33**,** 625-38.

LOPEZ-LOPEZ, J. R., SHACKLOCK, P. S., BALKE, C. W. & WIER, W. G. 1995. Local calcium transients triggered by single L-type calcium channel currents in cardiac cells. *Science,* 268**,** 1042-5.

LOPSHIRE, J. C. & ZIPES, D. P. 2006. Sudden cardiac death: better understanding of risks, mechanisms, and treatment. *Circulation,* 114**,** 1134-6.

LUSS, I., BOKNIK, P., JONES, L. R., KIRCHHEFER, U., KNAPP, J., LINCK, B., LUSS, H., MEISSNER, A., MULLER, F. U., SCHMITZ, W., VAHLENSIECK, U. & NEUMANN, J. 1999. Expression of cardiac calcium regulatory proteins in atrium v ventricle in different species. *J Mol Cell Cardiol,* 31**,** 1299-314.

LUTTGAU, H. C. & NIEDERGERKE, R. 1958. The antagonism between Ca and Na ions on the frog's heart. *J Physiol,* 143**,** 486-505.

LYASHKOV, A. E., JUHASZOVA, M., DOBRZYNSKI, H., VINOGRADOVA, T. M., MALTSEV, V. A., JUHASZ, O., SPURGEON, H. A., SOLLOTT, S. J. & LAKATTA, E. G. 2007. Calcium cycling protein density and functional importance to automaticity of isolated sinoatrial nodal cells are independent of cell size. *Circulation Research,* 100**,** 1723-1731.

MACE, L. C., PALMER, B. M., BROWN, D. A., JEW, K. N., LYNCH, J. M., GLUNT, J. M., PARSONS, T. A., CHEUNG, J. Y. & MOORE, R. L. 2003. Influence of age and run training on cardiac Na+/Ca2+ exchange. *J Appl Physiol,* 95**,** 1994-2003.

MACIEL, L. M., POLIKAR, R., ROHRER, D., POPOVICH, B. K. & DILLMANN, W. H. 1990. Age-induced decreases in the messenger RNA coding for the sarcoplasmic reticulum Ca2(+)-ATPase of the rat heart. *Circ Res,* 67**,** 230-4.

MACKAAY, A. J., BLEEKER, W. K., HOF, T. O. & BOUMAN, L. N. 1980. Temperature dependence of the chronotropic actions of calcium: functional inhomogeneity of the rabbit sinus node. *J Mol Cell Cardiol,* 12**,** 433-43.

MACKENZIE, L., BOOTMAN, M. D., BERRIDGE, M. J. & LIPP, P. 2001. Predetermined recruitment of calcium release sites underlies excitation-contraction coupling in rat atrial myocytes. *J Physiol,* 530**,** 417-29.

MACKENZIE, L., BOOTMAN, M. D., LAINE, M., BERRIDGE, M. J., THURING, J., HOLMES, A., LI, W. H. & LIPP, P. 2002. The role of inositol 1,4,5-trisphosphate receptors in Ca(2+) signalling and the generation of arrhythmias in rat atrial myocytes. *J Physiol,* 541**,** 395-409.

MACLENNAN, D. H., BRANDL, C. J., KORCZAK, B. & GREEN, N. M. 1985. Amino-acid sequence of a Ca2+ + Mg2+-dependent ATPase from rabbit muscle sarcoplasmic reticulum, deduced from its complementary DNA sequence. *Nature,* 316**,** 696-700.

MACLENNAN, D. H. & KRANIAS, E. G. 2003. Phospholamban: A crucial regulator of cardiac contractility. *Nature Reviews Molecular Cell Biology,* 4**,** 566-577.

MACLENNAN, D. H. & WONG, P. T. 1971. Isolation of a calcium-sequestering protein from sarcoplasmic reticulum. *Proc Natl Acad Sci U S A,* 68**,** 1231-5.

MADLE, A., LINHARTOVA, K. & KOZA, J. 2001. Effects of the T-type calcium channel blockade with oral mibefradil on the electrophysiologic properties of the human heart. *Med Sci Monit,* 7**,** 74-7.

MAN, K. C., KNIGHT, B., TSE, H. F., PELOSI, F., MICHAUD, G. F., FLEMMING, M., STRICKBERGER, S. A. & MORADY, F. 2000. Radiofrequency catheter ablation of inappropriate sinus tachycardia guided by activation mapping. *J Am Coll Cardiol,* 35**,** 451-7.

MANI, S. K., EGAN, E. A., ADDY, B. K., GRIMM, M., KASIGANESAN, H., THIYAGARAJAN, T., RENAUD, L., BROWN, J. H., KERN, C. B. & MENICK, D. R. 2010. beta-Adrenergic receptor stimulated Ncx1 upregulation is mediated via a CaMKII/AP-1 signaling pathway in adult cardiomyocytes. *J Mol Cell Cardiol,* 48**,** 342-51.

MARINE, J. E., KORLEY, V. J., OBIOHA-NGWU, O., CHEN, J., ZIMETBAUM, P., PAPAGEORGIOU, P., MILLIEZ, P. & JOSEPHSON, M. E. 2001. Different patterns of interatrial conduction in clockwise and counterclockwise atrial flutter. *Circulation,* 104**,** 1153-7.

MARTINI, F., OBER, W. C. & WELCH, K. 2006. *Fundamentals of anatomy & physiology,* San Francisco ; London, Pearson/Benjamin Cummings.

MARX, S. O., REIKEN, S., HISAMATSU, Y., JAYARAMAN, T., BURKHOFF, D., ROSEMBLIT, N. & MARKS, A. R. 2000. PKA phosphorylation dissociates FKBP12.6 from the calcium release channel (ryanodine receptor): defective regulation in failing hearts. *Cell,* 101**,** 365-76.

MASSON-PEVET, M. A., BLEEKER, W. K., BESSELSEN, E., TREYTEL, B. W., JONGSMA, H. J. & BOUMAN, L. N. 1984. Pacemaker cell types in the rabbit sinus node: a correlative ultrastructural and electrophysiological study. *J Mol Cell Cardiol,* 16**,** 53-63.

MATSUDA, N., HAGIWARA, N., SHODA, M., KASANUKI, H. & HOSODA, S. 1996. Enhancement of the L-type Ca2+ current by mechanical stimulation in single rabbit cardiac myocytes. *Circ Res,* 78**,** 650-9.

MATSUYAMA, T. A., INOUE, S., KOBAYASHI, Y., SAKAI, T., SAITO, T., KATAGIRI, T. & OTA, H. 2004. Anatomical diversity and age-related histological changes in the human right atrial posterolateral wall. *Europace,* 6**,** 307-15.

MAXWELL, C. J., HOGAN, D. B., CAMPBELL, N. R. & EBLY, E. M. 2000. Nifedipine and mortality risk in the elderly: relevance of drug formulation, dose and duration. *Pharmacoepidemiol Drug Saf,* 9**,** 11-23.

MCDONALD, T. F., CAVALIE, A., TRAUTWEIN, W. & PELZER, D. 1986. Voltage-dependent properties of macroscopic and elementary calcium channel currents in guinea pig ventricular myocytes. *Pflugers Arch,* 406**,** 437-48.

MCNUTT, N. S. & FAWCETT, D. W. 1969. The ultrastructure of the cat myocardium. II. Atrial muscle. *J Cell Biol,* 42**,** 46-67.

MERCANDO, A. D., ARONOW, W. S., EPSTEIN, S. & FISHBACH, M. 1995. Signal-averaged electrocardiography and ventricular tachycardia as predictors of mortality after acute myocardial infarction in elderly patients. *Am J Cardiol,* 76**,** 436-40.

MINAMISAWA, S., WANG, Y., CHEN, J., ISHIKAWA, Y., CHIEN, K. R. & MATSUOKA, R. 2003. Atrial chamber-specific expression of sarcolipin is regulated during development and hypertrophic remodeling. *J Biol Chem,* 278**,** 9570-5.

MITCHELL, R. D., SIMMERMAN, H. K. & JONES, L. R. 1988. Ca2+ binding effects on protein conformation and protein interactions of canine cardiac calsequestrin. *J Biol Chem,* 263**,** 1376-81.

MORGAN, J. P., ERNY, R. E., ALLEN, P. D., GROSSMAN, W. & GWATHMEY, J. K. 1990. Abnormal intracellular calcium handling, a major cause of systolic and diastolic dysfunction in ventricular myocardium from patients with heart failure. *Circulation,* 81**,** III21-32.

NAIR, R. R. & NAIR, P. 2001. Age-dependent variation in contractility of adult cardiac myocytes. *Int J Biochem Cell Biol,* 33**,** 119-25.

NAKAYAMA, H., WILKIN, B. J., BODI, I. & MOLKENTIN, J. D. 2006. Calcineurin-dependent cardiomyopathy is activated by TRPC in the adult mouse heart. *FASEB J,* 20**,** 1660-70.

NICHOLL, P. A. & HOWLETT, S. E. 2006. Sarcoplasmic reticulum calcium release channels in ventricles of older adult hamsters. *Can J Aging,* 25**,** 107-13.

OLIVETTI, G., MELISSARI, M., CAPASSO, J. M. & ANVERSA, P. 1991. Cardiomyopathy of the aging human heart. Myocyte loss and reactive cellular hypertrophy. *Circ Res,* 68**,** 1560-8.

ONO, K., FOZZARD, H. A. & HANCK, D. A. 1993. Mechanism of cAMP-dependent modulation of cardiac sodium channel current kinetics. *Circ Res,* 72**,** 807-15.

OPTHOF, T. 1988. The mammalian sinoatrial node. *Cardiovasc Drugs Ther,* 1**,** 573-97.

OPTHOF, T. 1994. Gap junctions in the sinoatrial node: immunohistochemical localization and correlation with activation pattern. *J Cardiovasc Electrophysiol,* 5**,** 138-43.

OPTHOF, T., DE JONGE, B., MACKAAY, A. J., BLEEKER, W. K., MASSON-PEVET, M., JONGSMA, H. J. & BOUMAN, L. N. 1985. Functional and morphological organization of the guinea-pig sinoatrial node compared with the rabbit sinoatrial node. *J Mol Cell Cardiol,* 17**,** 549-64.

OPTHOF, T., DE JONGE, B., MASSON-PEVET, M., JONGSMA, H. J. & BOUMAN, L. N. 1986. Functional and morphological organization of the cat sinoatrial node. *J Mol Cell Cardiol,* 18**,** 1015-31.

OTSU, K., WILLARD, H. F., KHANNA, V. K., ZORZATO, F., GREEN, N. M. & MACLENNAN, D. H. 1990. Molecular cloning of cDNA encoding the Ca2+ release channel (ryanodine receptor) of rabbit cardiac muscle sarcoplasmic reticulum. *J Biol Chem,* 265**,** 13472-83.

PERIASAMY, M., BHUPATHY, P. & BABU, G. J. 2008. Regulation of sarcoplasmic reticulum Ca2+ ATPase pump expression and its relevance to cardiac muscle physiology and pathology. *Cardiovasc Res,* 77**,** 265-73.

PHILIPSON, K. D., NICOLL, D. A., OTTOLIA, M., QUEDNAU, B. D., REUTER, H., JOHN, S. & QIU, Z. 2002. The Na+/Ca2+ exchange molecule: an overview. *Ann N Y Acad Sci,* 976**,** 1-10.

PIEPHO, R. W. & FENDLER, K. J. 1991. Antihypertensive therapy in the aged patient. Clinical pharmacokinetic considerations. *Drugs Aging,* 1**,** 194-211.

PLENGE-TELLECHEA, F., SOLER, F. & FERNANDEZ-BELDA, F. 1997. On the inhibition mechanism of sarcoplasmic or endoplasmic reticulum Ca2+-ATPases by cyclopiazonic acid. *J Biol Chem,* 272**,** 2794-800.

PODRID, P. J. & KOWEY, P. R. 2001. *Cardiac arrhythmia : mechanisms, diagnosis, and management,* Philadelphia ; London, Lippincott William & Wilkins.

PRESTLE, J., DIETERICH, S., PREUSS, M., BIELIGK, U. & HASENFUSS, G. 1999. Heterogeneous transmural gene expression of calcium-handling proteins and natriuretic peptides in the failing human heart. *Cardiovasc Res,* 43**,** 323-31.

PROTAS, L., DIFRANCESCO, D. & ROBINSON, R. B. 2001. L-type but not T-type calcium current changes during postnatal development in rabbit sinoatrial node. *Am J Physiol Heart Circ Physiol,* 281**,** H1252-9.

PUMIR, A., ARUTUNYAN, A., KRINSKY, V. & SARVAZYAN, N. 2005. Genesis of ectopic waves: role of coupling, automaticity, and heterogeneity. *Biophys J,* 89**,** 2332-49.

QU, J., BARBUTI, A., PROTAS, L., SANTORO, B., COHEN, I. S. & ROBINSON, R. B. 2001. HCN2 overexpression in newborn and adult ventricular myocytes: distinct effects on gating and excitability. *Circ Res,* 89**,** E8-14.

QUINN, G. R. & FANG, M. C. 2012. Atrial fibrillation: stroke prevention in older adults. *Clin Geriatr Med,* 28**,** 617-34.

REDDY, L. G., JONES, L. R., PACE, R. C. & STOKES, D. L. 1996. Purified, reconstituted cardiac Ca2+-ATPase is regulated by phospholamban but not by direct phosphorylation with Ca2+/calmodulin-dependent protein kinase. *J Biol Chem,* 271**,** 14964-70.

REEVES, J. P. & HALE, C. C. 1984. The stoichiometry of the cardiac sodium-calcium exchange system. *J Biol Chem,* 259**,** 7733-9.

REUTER, H. & SEITZ, N. 1968. The dependence of calcium efflux from cardiac muscle on temperature and external ion composition. *J Physiol,* 195**,** 451-70.

RODEN, D. M. & GEORGE, A. L., JR. 1997. Structure and function of cardiac sodium and potassium channels. *Am J Physiol,* 273**,** H511-25.

ROTH, D. A., WHITE, C. D., PODOLIN, D. A. & MAZZEO, R. S. 1998. Alterations in myocardial signal transduction due to aging and chronic dynamic exercise. *J Appl Physiol,* 84**,** 177-84.

ROVETTI, R., CUI, X., GARFINKEL, A., WEISS, J. N. & QU, Z. 2010. Spark-induced sparks as a mechanism of intracellular calcium alternans in cardiac myocytes. *Circ Res,* 106**,** 1582-91.

RUBIO, M., BODI, I., FULLER-BICER, G. A., HAHN, H. S., PERIASAMY, M. & SCHWARTZ, A. 2005. Sarcoplasmic reticulum adenosine triphosphatase overexpression in the L-type Ca2+ channel mouse results in cardiomyopathy and Ca2+ -induced arrhythmogenesis. *J Cardiovasc Pharmacol Ther,* 10**,** 235-49.

SAITO, A., SEILER, S., CHU, A. & FLEISCHER, S. 1984. Preparation and morphology of sarcoplasmic reticulum terminal cisternae from rabbit skeletal muscle. *J Cell Biol,* 99**,** 875-85.

SAKAI, M., DANZIGER, R. S., XIAO, R. P., SPURGEON, H. A. & LAKATTA, E. G. 1992. Contractile response of individual cardiac myocytes to norepinephrine declines with senescence. *Am J Physiol,* 262**,** H184-9.

SANDERS, L., RAKOVIC, S., LOWE, M., MATTICK, P. A. & TERRAR, D. A. 2006. Fundamental importance of Na+-Ca2+ exchange for the pacemaking mechanism in guinea-pig sino-atrial node. *J Physiol,* 571**,** 639-49.

SANGUINETTI, M. C., JIANG, C., CURRAN, M. E. & KEATING, M. T. 1995. A mechanistic link between an inherited and an acquired cardiac arrhythmia: HERG encodes the IKr potassium channel. *Cell,* 81**,** 299-307.

SANGUINETTI, M. C. & JURKIEWICZ, N. K. 1991. Delayed rectifier outward K+ current is composed of two currents in guinea pig atrial cells. *Am J Physiol,* 260**,** H393-9.

SATOH, H. 1997. Electrophysiological actions of ryanodine on single rabbit sinoatrial nodal cells. *Gen Pharmacol,* 28**,** 31-8.

SCARPACE, P. J., MOORADIAN, A. D. & MORLEY, J. E. 1988. Age-associated decrease in beta-adrenergic receptors and adenylate cyclase activity in rat brown adipose tissue. *J Gerontol,* 43**,** B65-70.

SCHAPER, J., MEISER, E. & STAMMLER, G. 1985. Ultrastructural morphometric analysis of myocardium from dogs, rats, hamsters, mice, and from human hearts. *Circ Res,* 56**,** 377-91.

SCHIEFER, A., MEISSNER, G. & ISENBERG, G. 1995. Ca2+ activation and Ca2+ inactivation of canine reconstituted cardiac sarcoplasmic reticulum Ca(2+)-release channels. *J Physiol,* 489 (Pt 2)**,** 337-48.

SCHLEGEL, A., VOLONTE, D., ENGELMAN, J. A., GALBIATI, F., MEHTA, P., ZHANG, X. L., SCHERER, P. E. & LISANTI, M. P. 1998. Crowded little caves: structure and function of caveolae. *Cell Signal,* 10**,** 457-63.

SCHOTTEN, U., GREISER, M., BENKE, D., BUERKEL, K., EHRENTEIDT, B., STELLBRINK, C., VAZQUEZ-JIMENEZ, J. F., SCHOENDUBE, F., HANRATH, P. & ALLESSIE, M. 2002. Atrial fibrillation-induced atrial contractile dysfunction: a tachycardiomyopathy of a different sort. *Cardiovasc Res,* 53**,** 192-201.

SCHRAM, G., POURRIER, M., MELNYK, P. & NATTEL, S. 2002. Differential distribution of cardiac ion channel expression as a basis for regional specialization in electrical function. *Circ Res,* 90**,** 939-50.

SCHRODER, E., BYSE, M. & SATIN, J. 2009. L-Type Calcium Channel C Terminus Autoregulates Transcription. *Circulation Research,* 104**,** 1373-U238.

SCHUESSLER, R. B., BOINEAU, J. P. & BROMBERG, B. I. 1996. Origin of the sinus impulse. *J Cardiovasc Electrophysiol,* 7**,** 263-74.

SCHULMAN, S. P., LAKATTA, E. G., FLEG, J. L., LAKATTA, L., BECKER, L. C. & GERSTENBLITH, G. 1992. Age-related decline in left ventricular filling at rest and exercise. *Am J Physiol,* 263**,** H1932-8.

SEGAWA, I., KIKUCHI, M., TASHIRO, A., HIRAMORI, K., SATO, M. & SATODATE, R. 1996. Association of myotonic dystrophy and sick sinus syndrome, with special reference to electrophysiological and histological examinations. *Intern Med,* 35**,** 185-8.

SEGUCHI, H., RITTER, M., SHIZUKUISHI, M., ISHIDA, H., CHOKOH, G., NAKAZAWA, H., SPITZER, K. W. & BARRY, W. H. 2005. Propagation of Ca2+ release in cardiac myocytes: role of mitochondria. *Cell Calcium,* 38**,** 1-9.

SEISENBERGER, C., SPECHT, V., WELLING, A., PLATZER, J., PFEIFER, A., KUHBANDNER, S., STRIESSNIG, J., KLUGBAUER, N., FEIL, R. & HOFMANN, F. 2000. Functional embryonic cardiomyocytes after disruption of the L-type alpha1C (Cav1.2) calcium channel gene in the mouse. *J Biol Chem,* 275**,** 39193-9.

SETH, M., SUMBILLA, C., MULLEN, S. P., LEWIS, D., KLEIN, M. G., HUSSAIN, A., SOBOLOFF, J., GILL, D. L. & INESI, G. 2004. Sarco(endo)plasmic reticulum Ca2+ ATPase (SERCA) gene silencing and remodeling of the Ca2+ signaling mechanism in cardiac myocytes. *Proc Natl Acad Sci U S A,* 101**,** 16683-8.

SEVERS, N. J. 1990. The cardiac gap junction and intercalated disc. *Int J Cardiol,* 26**,** 137-73.

SHAM, J. S., JONES, L. R. & MORAD, M. 1991. Phospholamban mediates the beta-adrenergic-enhanced Ca2+ uptake in mammalian ventricular myocytes. *Am J Physiol,* 261**,** H1344-9.

SHER, A. A., NOBLE, P. J., HINCH, R., GAVAGHAN, D. J. & NOBLE, D. 2008. The role of the Na+/Ca2+ exchangers in Ca2+ dynamics in ventricular myocytes. *Prog Biophys Mol Biol,* 96**,** 377-98.

SHI, W., WYMORE, R., YU, H., WU, J., WYMORE, R. T., PAN, Z., ROBINSON, R. B., DIXON, J. E., MCKINNON, D. & COHEN, I. S. 1999. Distribution and prevalence of hyperpolarization-activated cation channel (HCN) mRNA expression in cardiac tissues. *Circ Res,* 85**,** e1-6.

SHINOHARA, T., JOUNG, B., KIM, D., MARUYAMA, M., LUK, H. N., CHEN, P. S. & LIN, S. F. 2010. Induction of atrial ectopic beats with calcium release inhibition: Local hierarchy of automaticity in the right atrium. *Heart Rhythm,* 7**,** 110-6.

SHREINER, D. P., WEISFELDT, M. L. & SHOCK, N. W. 1969. Effects of age, sex, and breeding status on the rat heart. *Am J Physiol,* 217**,** 176-80.

SHULL, G. E., SCHWARTZ, A. & LINGREL, J. B. 1985. Amino-acid sequence of the catalytic subunit of the (Na+ + K+)ATPase deduced from a complementary DNA. *Nature,* 316**,** 691-5.

SIMMERMAN, H. K., COLLINS, J. H., THEIBERT, J. L., WEGENER, A. D. & JONES, L. R. 1986. Sequence analysis of phospholamban. Identification of phosphorylation sites and two major structural domains. *J Biol Chem,* 261**,** 13333-41.

SMITH, J. M., CLANCY, E. A., VALERI, C. R., RUSKIN, J. N. & COHEN, R. J. 1988a. Electrical alternans and cardiac electrical instability. *Circulation,* 77**,** 110-21.

SMITH, J. S., IMAGAWA, T., MA, J., FILL, M., CAMPBELL, K. P. & CORONADO, R. 1988b. Purified ryanodine receptor from rabbit skeletal muscle is the calcium-release channel of sarcoplasmic reticulum. *J Gen Physiol,* 92**,** 1-26.

SMITH, P. K., KROHN, R. I., HERMANSON, G. T., MALLIA, A. K., GARTNER, F. H., PROVENZANO, M. D., FUJIMOTO, E. K., GOEKE, N. M., OLSON, B. J. & KLENK, D. C. 1985. Measurement of protein using bicinchoninic acid. *Anal Biochem,* 150**,** 76-85.

SMYRNIAS, I., MAIR, W., HARZHEIM, D., WALKER, S. A., RODERICK, H. L. & BOOTMAN, M. D. 2010. Comparison of the T-tubule system in adult rat ventricular and atrial myocytes, and its role in excitation-contraction coupling and inotropic stimulation. *Cell Calcium,* 47**,** 210-23.

SOELLER, C. & CANNELL, M. B. 1999. Examination of the transverse tubular system in living cardiac rat myocytes by 2-photon microscopy and digital image-processing techniques. *Circ Res,* 84**,** 266-75.

SOLARO, R. J. & RARICK, H. M. 1998. Troponin and tropomyosin: proteins that switch on and tune in the activity of cardiac myofilaments. *Circ Res,* 83**,** 471-80.

SONG, Y., YAO, Q., ZHU, J., LUO, B. & LIANG, S. 1999. Age-related variation in the interstitial tissues of the cardiac conduction system; and autopsy study of 230 Han Chinese. *Forensic Sci Int,* 104**,** 133-42.

SPACH, M. S. & DOLBER, P. C. 1986. Relating extracellular potentials and their derivatives to anisotropic propagation at a microscopic level in human cardiac muscle. Evidence for electrical uncoupling of side-to-side fiber connections with increasing age. *Circ Res,* 58**,** 356-71.

STEWART, P. S. & MACLENNAN, D. H. 1974. Surface particles of sarcoplasmic reticulum membranes. Structural features of the adenosine triphosphatase. *J Biol Chem,* 249**,** 985-93.

STIEBER, J., HERRMANN, S., FEIL, S., LOSTER, J., FEIL, R., BIEL, M., HOFMANN, F. & LUDWIG, A. 2003. The hyperpolarization-activated channel HCN4 is required for the generation of pacemaker action potentials in the embryonic heart. *Proc Natl Acad Sci U S A,* 100**,** 15235-40.

STREHLER, E. E., FILOTEO, A. G., PENNISTON, J. T. & CARIDE, A. J. 2007. Plasma-membrane Ca(2+) pumps: structural diversity as the basis for functional versatility. *Biochem Soc Trans,* 35**,** 919-22.

SUN, H., GASPO, R., LEBLANC, N. & NATTEL, S. 1998. Cellular mechanisms of atrial contractile dysfunction caused by sustained atrial tachycardia. *Circulation,* 98**,** 719-27.

SZENTESI, P., PIGNIER, C., EGGER, M., KRANIAS, E. G. & NIGGLI, E. 2004. Sarcoplasmic reticulum Ca2+ refilling controls recovery from Ca2+-induced Ca2+ release refractoriness in heart muscle. *Circ Res,* 95**,** 807-13.

TADA, M., YAMADA, M., KADOMA, M., INUI, M. & OHMORI, F. 1982. Calcium transport by cardiac sarcoplasmic reticulum and phosphorylation of phospholamban. *Mol Cell Biochem,* 46**,** 73-95.

TAFFET, G. E. & TATE, C. A. 1993. CaATPase content is lower in cardiac sarcoplasmic reticulum isolated from old rats. *Am J Physiol,* 264**,** H1609-14.

TAKASAGO, T., IMAGAWA, T., FURUKAWA, K., OGURUSU, T. & SHIGEKAWA, M. 1991. Regulation of the cardiac ryanodine receptor by protein kinase-dependent phosphorylation. *J Biochem,* 109**,** 163-70.

TANAAMI, T., ISHIDA, H., SEGUCHI, H., HIROTA, Y., KADONO, T., GENKA, C., NAKAZAWA, H. & BARRY, W. H. 2005. Difference in propagation of Ca2+ release in atrial and ventricular myocytes. *Jpn J Physiol,* 55**,** 81-91.

TATE, C. A., HELGASON, T., HYEK, M. F., MCBRIDE, R. P., CHEN, M., RICHARDSON, M. A. & TAFFET, G. E. 1996. SERCA2a and mitochondrial cytochrome oxidase expression are increased in hearts of exercise-trained old rats. *Am J Physiol,* 271**,** H68-72.

TELLEZ, J. O., MCZEWSKI, M., YANNI, J., SUTYAGIN, P., MACKIEWICZ, U., ATKINSON, A., INADA, S., BERESEWICZ, A., BILLETER, R., DOBRZYNSKI, H. & BOYETT, M. R. 2011. Ageing-dependent remodelling of ion channel and Ca2+ clock genes underlying sino-atrial node pacemaking. *Exp Physiol,* 96**,** 1163-78.

TRAFFORD, A. W., DIAZ, M. E., NEGRETTI, N. & EISNER, D. A. 1997. Enhanced Ca2+ current and decreased Ca2+ efflux restore sarcoplasmic reticulum Ca2+ content after depletion. *Circ Res,* 81**,** 477-84.

TSIEN, R. W., KASS, R. S. & WEINGART, R. 1979. Cellular and subcellular mechanisms of cardiac pacemaker oscillations. *J Exp Biol,* 81**,** 205-15.

TURNER, M. J., MIER, C. M., SPINA, R. J., SCHECHTMAN, K. B. & EHSANI, A. A. 1999. Effects of age and gender on the cardiovascular responses to isoproterenol. *J Gerontol A Biol Sci Med Sci,* 54**,** B393-400; discussion B401-3.

UEMURA, N., OHKUSA, T., HAMANO, K., NAKAGOME, M., HORI, H., SHIMIZU, M., MATSUZAKI, M., MOCHIZUKI, S., MINAMISAWA, S. & ISHIKAWA, Y. 2004. Down-regulation of sarcolipin mRNA expression in chronic atrial fibrillation. *Eur J Clin Invest,* 34**,** 723-30.

UEYAMA, T., OHKUSA, T., HISAMATSU, Y., NAKAMURA, Y., YAMAMOTO, T., YANO, M. & MATSUZAKI, M. 1998. Alterations in cardiac SR Ca(2+)-release channels during development of heart failure in cardiomyopathic hamsters. *Am J Physiol,* 274**,** H1-7.

ULLRICH, N. D., VALDIVIA, H. H. & NIGGLI, E. 2012. PKA phosphorylation of cardiac ryanodine receptor modulates SR luminal Ca2+ sensitivity. *J Mol Cell Cardiol,* 53**,** 33-42.

VAN WAGONER, D. R., POND, A. L., LAMORGESE, M., ROSSIE, S. S., MCCARTHY, P. M. & NERBONNE, J. M. 1999. Atrial L-type Ca2+ currents and human atrial fibrillation. *Circ Res,* 85**,** 428-36.

VANGHELUWE, P., RAEYMAEKERS, L., DODE, L. & WUYTACK, F. 2005. Modulating sarco(endo)plasmic reticulum Ca2+ ATPase 2 (SERCA2) activity: cell biological implications. *Cell Calcium,* 38**,** 291-302.

VANGHELUWE, P., SIPIDO, K. R., RAEYMAEKERS, L. & WUYTACK, F. 2006. New perspectives on the role of SERCA2's Ca2+ affinity in cardiac function. *Biochim Biophys Acta,* 1763**,** 1216-28.

VATNER, D. E., SATO, N., KIUCHI, K., SHANNON, R. P. & VATNER, S. F. 1994. Decrease in myocardial ryanodine receptors and altered excitation-contraction coupling early in the development of heart failure. *Circulation,* 90**,** 1423-30.

VENETUCCI, L. A., TRAFFORD, A. W., DIAZ, M. E., O'NEILL, S. C. & EISNER, D. A. 2006. Reducing ryanodine receptor open probability as a means to abolish spontaneous Ca2+ release and increase Ca2+ transient amplitude in adult ventricular myocytes. *Circ Res,* 98**,** 1299-305.

VENETUCCI, L. A., TRAFFORD, A. W. & EISNER, D. A. 2007. Increasing ryanodine receptor open probability alone does not produce arrhythmogenic calcium waves: threshold sarcoplasmic reticulum calcium content is required. *Circ Res,* 100**,** 105-11.

VERHEIJCK, E. E., VAN GINNEKEN, A. C., WILDERS, R. & BOUMAN, L. N. 1999. Contribution of L-type Ca2+ current to electrical activity in sinoatrial nodal myocytes of rabbits. *Am J Physiol,* 276**,** H1064-77.

VEST, J. A., WEHRENS, X. H., REIKEN, S. R., LEHNART, S. E., DOBREV, D., CHANDRA, P., DANILO, P., RAVENS, U., ROSEN, M. R. & MARKS, A. R.

2005. Defective cardiac ryanodine receptor regulation during atrial fibrillation. *Circulation,* 111**,** 2025-32.

VINOGRADOVA, T. M., BROCHET, D. X., SIRENKO, S., LI, Y., SPURGEON, H. & LAKATTA, E. G. 2010. Sarcoplasmic reticulum Ca2+ pumping kinetics regulates timing of local Ca2+ releases and spontaneous beating rate of rabbit sinoatrial node pacemaker cells. *Circ Res,* 107**,** 767-75.

VINOGRADOVA, T. M., LYASHKOV, A. E., ZHU, W., RUKNUDIN, A. M., SIRENKO, S., YANG, D., DEO, S., BARLOW, M., JOHNSON, S., CAFFREY, J. L., ZHOU, Y. Y., XIAO, R. P., CHENG, H., STERN, M. D., MALTSEV, V. A. & LAKATTA, E. G. 2006. High basal protein kinase A-dependent phosphorylation drives rhythmic internal Ca2+ store oscillations and spontaneous beating of cardiac pacemaker cells. *Circ Res,* 98**,** 505-14.

VINOGRADOVA, T. M., ZHOU, Y. Y., MALTSEV, V., LYASHKOV, A., STERN, M. & LAKATTA, E. G. 2004. Rhythmic ryanodine receptor Ca2+ releases during diastolic depolarization of sinoatrial pacemaker cells do not require membrane depolarization. *Circulation Research,* 94**,** 802-809.

WALDEN, A. P., DIBB, K. M. & TRAFFORD, A. W. 2009. Differences in intracellular calcium homeostasis between atrial and ventricular myocytes. *J Mol Cell Cardiol,* 46**,** 463-73.

WALKER, K. E., LAKATTA, E. G. & HOUSER, S. R. 1993. Age associated changes in membrane currents in rat ventricular myocytes. *Cardiovasc Res,* 27**,** 1968-77.

WALSH, K. B. & KASS, R. S. 1988. Regulation of a heart potassium channel by protein kinase A and C. *Science,* 242**,** 67-9.

WANG, T. J., LARSON, M. G., LEVY, D., VASAN, R. S., LEIP, E. P., WOLF, P. A., D'AGOSTINO, R. B., MURABITO, J. M., KANNEL, W. B. & BENJAMIN, E. J. 2003. Temporal relations of atrial fibrillation and congestive heart failure and their joint influence on mortality: the Framingham Heart Study. *Circulation,* 107**,** 2920-5.

WANG, Z., FERMINI, B. & NATTEL, S. 1993. Sustained depolarization-induced outward current in human atrial myocytes. Evidence for a novel delayed rectifier K+ current similar to Kv1.5 cloned channel currents. *Circ Res,* 73**,** 1061-76.

WARD, C. & WITHAM, M. 2009. *A practical guide to heart failure in older people,* Oxford, Wiley-Blackwell.

WEBER, C. R., GINSBURG, K. S., PHILIPSON, K. D., SHANNON, T. R. & BERS, D. M. 2001. Allosteric regulation of Na/Ca exchange current by cytosolic Ca in intact cardiac myocytes. *J Gen Physiol,* 117**,** 119-31.

WEBER, K. & OSBORN, M. 1969. The reliability of molecular weight determinations by dodecyl sulfate-polyacrylamide gel electrophoresis. *J Biol Chem,* 244**,** 4406-12.

WEI, J. Y., SPURGEON, H. A. & LAKATTA, E. G. 1984. Excitation-contraction in rat myocardium: alterations with adult aging. *Am J Physiol,* 246**,** H784-91.

WEISS, J. N., KARMA, A., SHIFERAW, Y., CHEN, P. S., GARFINKEL, A. & QU, Z. 2006. From pulsus to pulseless: the saga of cardiac alternans. *Circ Res,* 98**,** 1244-53.

WOLF, P. A., ABBOTT, R. D. & KANNEL, W. B. 1991. Atrial fibrillation as an independent risk factor for stroke: the Framingham Study. *Stroke,* 22**,** 983-8.

WONG, K., BOHELER, K. R., BISHOP, J., PETROU, M. & YACOUB, M. H. 1998. Clenbuterol induces cardiac hypertrophy with normal functional, morphological and molecular features. *Cardiovasc Res,* 37**,** 115-22.

WOOD, M. A. & ELLENBOGEN, K. A. 2002. Cardiology patient pages. Cardiac pacemakers from the patient's perspective. *Circulation,* 105**,** 2136-8.

WU, X., ZHANG, T., BOSSUYT, J., LI, X., MCKINSEY, T. A., DEDMAN, J. R., OLSON, E. N., CHEN, J., BROWN, J. H. & BERS, D. M. 2006. Local InsP3-dependent perinuclear Ca2+ signaling in cardiac myocyte excitation-transcription coupling. *J Clin Invest,* 116**,** 675-82.

XIANDA, C., BAIMING, Q., LIXUAN, W., XUELIE, H., JIANWU, Y. & ZHONGJIE, L. 2003. The initial study on the origin and reentrant mechanism of paroxysmal

atrial fibrillation arising from right atrium with non-contact mapping system. *Chinese Journal of Cardiac Pacing and Electrophysiology,* 17**,** 22-26.

XIAO, R. P., SPURGEON, H. A., O'CONNOR, F. & LAKATTA, E. G. 1994. Age-associated changes in beta-adrenergic modulation on rat cardiac excitation-contraction coupling. *J Clin Invest,* 94**,** 2051-9.

XIAO, R. P., TOMHAVE, E. D., WANG, D. J., JI, X., BOLUYT, M. O., CHENG, H., LAKATTA, E. G. & KOCH, W. J. 1998. Age-associated reductions in cardiac beta1- and beta2-adrenergic responses without changes in inhibitory G proteins or receptor kinases. *J Clin Invest,* 101**,** 1273-82.

XIONG, W., TIAN, Y., DISILVESTRE, D. & TOMASELLI, G. F. 2005. Transmural heterogeneity of Na+-Ca2+ exchange: evidence for differential expression in normal and failing hearts. *Circ Res,* 97**,** 207-9.

XU, A. & NARAYANAN, N. 1998. Effects of aging on sarcoplasmic reticulum Ca2+-cycling proteins and their phosphorylation in rat myocardium. *Am J Physiol,* 275**,** H2087-94.

XU, H., GUO, W. & NERBONNE, J. M. 1999. Four kinetically distinct depolarization-activated K+ currents in adult mouse ventricular myocytes. *J Gen Physiol,* 113**,** 661-78.

XU, L., CHEN, J., LI, X. Y., REN, S., HUANG, C. X., WU, G. & JIANG, X. J. 2012. Analysis of Na(+)/Ca (2+) exchanger (NCX) function and current in murine cardiac myocytes during heart failure. *Mol Biol Rep,* 39**,** 3847-52.

YAMAMOTO, M., HONJO, H., NIWA, R. & KODAMA, I. 1998. Low-frequency extracellular potentials recorded from the sinoatrial node. *Cardiovasc Res,* 39**,** 360-72.

YANIV, Y., MALTSEV, V. A., ZIMAN, B. D., SPURGEON, H. A. & LAKATTA, E. G. 2012a. The "funny" current (I(f)) inhibition by ivabradine at membrane potentials encompassing spontaneous depolarization in pacemaker cells. *Molecules,* 17**,** 8241-54.

YANIV, Y., SPURGEON, H. A., LYASHKOV, A. E., YANG, D., ZIMAN, B. D., MALTSEV, V. A. & LAKATTA, E. G. 2012b. Crosstalk between mitochondrial and sarcoplasmic reticulum Ca2+ cycling modulates cardiac pacemaker cell automaticity. *PLoS One,* 7**,** e37582.

YEAGER, M. & GILULA, N. B. 1992. Membrane topology and quaternary structure of cardiac gap junction ion channels. *J Mol Biol,* 223**,** 929-48.

YEH, Y. H., WAKILI, R., QI, X. Y., CHARTIER, D., BOKNIK, P., KAAB, S., RAVENS, U., COUTU, P., DOBREV, D. & NATTEL, S. 2008. Calcium-handling abnormalities underlying atrial arrhythmogenesis and contractile dysfunction in dogs with congestive heart failure. *Circ Arrhythm Electrophysiol,* 1**,** 93-102.

YIN, F. C., SPURGEON, H. A., RAKUSAN, K., WEISFELDT, M. L. & LAKATTA, E. G. 1982. Use of tibial length to quantify cardiac hypertrophy: application in the aging rat. *Am J Physiol,* 243**,** H941-7.

YIN, F. C., SPURGEON, H. A., WEISFELDT, M. L. & LAKATTA, E. G. 1980. Mechanical properties of myocardium from hypertrophied rat hearts. A comparison between hypertrophy induced by senescence and by aortic banding. *Circ Res,* 46**,** 292-300.

YUAN, W., GINSBURG, K. S. & BERS, D. M. 1996. Comparison of sarcolemmal calcium channel current in rabbit and rat ventricular myocytes. *J Physiol,* 493 (Pt 3)**,** 733-46.

ZAUN, H. C., SHRIER, A. & ORLOWSKI, J. 2012. N-Myristoylation and Ca2+ Binding of Calcineurin B Homologous Protein CHP3 Are Required to Enhance Na+/H+ Exchanger NHE1 Half-life and Activity at the Plasma Membrane. *J Biol Chem,* 287**,** 36883-95.

ZEMANCIKOVA, A. & TOROK, J. 2009. Effect of chronic nifedipine treatment on blood pressure and adrenergic responses of isolated mesenteric artery in young rats with developing spontaneous hypertension. *Physiol Res,* 58**,** 921-5.

ZENG, J. & RUDY, Y. 1995. Early afterdepolarizations in cardiac myocytes: mechanism and rate dependence. *Biophys J,* 68**,** 949-64.

ZHAI, J., SCHMIDT, A. G., HOIT, B. D., KIMURA, Y., MACLENNAN, D. H. & KRANIAS, E. G. 2000. Cardiac-specific overexpression of a superinhibitory pentameric phospholamban mutant enhances inhibition of cardiac function in vivo. *J Biol Chem,* 275**,** 10538-44.

ZHAO, Y., XU, J., GONG, J. & QIAN, L. 2009. L-type calcium channel current up-regulation by chronic stress is associated with increased alpha(1c) subunit expression in rat ventricular myocytes. *Cell Stress Chaperones,* 14**,** 33-41.

ZHOU, Z. & LIPSIUS, S. L. 1993. Na(+)-Ca2+ exchange current in latent pacemaker cells isolated from cat right atrium. *J Physiol,* 466**,** 263-85.

ZIPES, D. P. 2003. Mechanisms of clinical arrhythmias. *Pacing Clin Electrophysiol,* 26**,** 1778-92.